List of Contents

Summary

Neuronal death is induced by a series of pathogeneses in different neurodegenerative diseases, and one of them, which has been widely accepted previously, is the overload of intracellular calcium (Ca^{2+}) in neurones. This study has investigated ryanodine receptor (RyR) on the endoplasmic reticulum (ER) and several potassium (K^+) channels which might be neuroprotective, such as the large conductance Ca^{2+}-activated K^+ channel (BK) and adenosine-5'-triphosphate (ATP)-sensitive K^+ channel, in both neuronal and astrocytoma cell lines. The reverse transcription (RT)-polymerase chain react (PCR) results in this Thesis show that the messages of RyR, BK channel and ATP-sensitive K+ channel (K_{ATP}) exist at the messenger ribonucleic acid (RNA) level in those cell lines. And, the expression of RyRIII message was found being increased in SH-SY5Y cells but decreased in NTERA-2 cells after differentiation. The BK channel was confirmed as functional in SH-SY5Y cells with patch clamp recording. Cell insults which increase intracellular Ca^{2+} ($[Ca^{2+}]_i$), such as cobalt (II) chloride ($CoCl_2$), hydrogen peroxide (H_2O_2), beta-amyloid ($A\beta_{1-42}$) and glutamate, were found to reduce cell number in those cell lines in cell proliferation MTS [3-(4,5-dimethylthiazol-2-yl)-5-(3-carboxymethoxyphenyl)-2-(4-sulfophenyl)-2H-tetrazolium, inner salt] assays, and the cells with higher expression of RyRIII message were more sensitive to $CoCl_2$ and H_2O_2 insults. In cell proliferation assays testing RyR or K^+ channel modulators in the

presence of insults, it has been found that generic blockade of RyR or K^+ channel might be neuroprotective, and the activation of RyR or BK channel and the blockade of K_{ATP} channel may aggravate the insults. Selective blockade of RyRI and RyRII cannot protect the cells, which probably indicates that RyRIII is the key target in neuroprotection. Activators of the K_{ATP} channel cannot protect the cells at a low dose of $CoCl_2$ but might be protective at a high dose, although cromakalim was an exception. Hence, blockade of RyRIII and the BK channel, and activation of the K_{ATP} channel, could be possible neuroprotective strategies. Future study should measure $[Ca^{2+}]_i$ and cell apoptosis through Ca^{2+} imaging and fluorescence-activated cell sorting (FACS) respectively, and design selective a RyRIII blocker.

1. Introduction

1. Introduction

Neurodegeneration is the progressive loss of structure and/or function of neurones, including the death of neurones. Most of the neurodegenerative diseases are related to the damage or loss of brain tissues, or related to the dysfunction of neurones. For example, Parkinson's disease (PD), which is a movement disorder, is contributed by the loss of dopaminergic neurones in the substantial nigra and the degeneration of monoaminergic neurones in the brain stem and basal ganglia (Stutzmann and Mattson, 2011). Alzheimer's disease (AD), which is a progressive deterioration in a broad range of cognitive functions including language, personality, visual-spatial abilities, and characteristically, memory (Arispe et al., 2007, Kagan et al., 2002), is caused by the shrinkage and dysfunction of brain tissues, such as hippocampal neurones (Mattson and Kater, 1989). Huntington disease (HD), which is a genetic disease contributed by a disorder of gene, is also found with dysfunction of brain areas like striatum, cortical structures (Mattson and Magnus, 2006) and limbic system (Mattson, 2003). Stroke, which is caused by a clot formed in a cerebral blood vessel, has been found to cause dysfunction of neurones because of the high energy demand and results in neurone death (MacDonald et al., 2006). Finally amyotrophic lateral sclerosis (ALS) is also related to neurodegeneration linked to peripheral neuropathies (Fernyhough and Calcutt, 2010), although it is not a brain disorder.

Neurodegenerative diseases are widely spread nowadays. According to a report

from the World Health Organisation (WHO), the prevalence rate of stroke is ranging from 5 to 10 per 1,000 population and it is estimated that 5.5 million subjects die from stroke every year (Prilipko, 2004). In Europe, the number of persons with stroke, including extension, has been estimated as 8.2 million in 2010, the number in UK being estimated as 947 thousand by then (Gustavsson et al., 2011). The prevalence of dementia has been estimated as 18 – 25 million subjects in 2000 and 50% - 75% of them are AD cases which is the commonest pathology in dementia. The prevalence of dementia including AD is age-dependent and doubles with every five-year increment in age from 1% for 60 – 64 years old group to 45% for those aged 95 years or over (Prilipko, 2004). There were more than 6.3 million dementia subjects in Europe by 2010 and 738 thousand of them exist in the UK (Gustavsson et al., 2011). WHO has estimated the incidence of PD as between 16 – 19 per 100,000 people per year and the crude prevalence is 160 per 100,000 people per year (Prilipko, 2004). The prevalence of PD in Europe is estimated as 1.2 million subjects, while 110 thousand of them are in UK (Gustavsson et al., 2011).

The cost for neurodegenerative diseases cannot be neglected neither. The average cost of stroke was €7,775 per patient in Europe and was €8,967 in UK in 2010 (Gustavsson et al., 2011), which means the total cost was about 64 billion Euros all over the Europe including about 8.5 billion Euros in UK. The average cost for dementia was about 17 thousand Euros per patient in Europe and was about 30 thousand Euros in UK in 2010 (Gustavsson et al., 2011), which means the total cost was about 107 billion Euros all over Europe

including about 22 billion Euros in UK. The average cost of PD was about 11 thousand Euros per patient in Europe and was 21.5 thousand Euros in UK in 2010 (Gustavsson et al., 2011), which means the total cost was about 13 billion Euros all over Europe including about 2.4 billion Euros in UK. The total cost for stroke, PD and dementia, although not all of the neurodegenerative diseases are included, would be about 180 billion Euros over Europe. According to the WHO report on the primary method of financing neurological care, 59% are based on social insurance, 33% are tax-based, and 8% are out of pocket in Europe (Prilipko, 2004). That means, the burden on neurodegenerative diseases in Europe would be more than 165 billion Euros to the governments and society and would be nearly thousand Euros to each individual patient.

Considering the wide prevalence of neurodegenerative diseases and the huge cost to the government, society and patients themselves, it is essential to find a way to prevent or treat these diseases. Since most of the neurodegenerative diseases are related to the dysfunction of neurones or loss of brain tissues, which progresses to neuronal death, this Thesis is focussed on "the cellular basis of neurodegeneration" and establishes neuronal insult models to find possible targets for a neuroprotective purpose, such as the ryanodine receptor (RyR) and potassium (K^+) channels.

1.1 Cell death and calcium

Neurones are excitable cells that rapidly communicate electrical signals in a

precise spatio-temporal manner. Calcium (Ca^{2+}) is a major intracellular messenger that mediates many of the physiological responses to chemical and electrical stimulation. Hence, the influx of Ca^{2+} through channels is a critical signal for the release of neurotransmitters from presynaptic terminals and for the responses of the postsynaptic neurone (Mattson, 2007). Unfortunately such an influx, if excessive, may eventually cause cell death. Ca^{2+} activates calpains and caspases, which are forms of cysteine proteases that degrade a variety of substrates (Mattson, 2007, Nixon, 2003). They can also induce oxidative stress (Mattson, 2007, Lafon-Cazal et al., 1993), and finally can trigger apoptosis which is a form of programmed cell death (Ankarcrona et al., 1995, Mattson, 2007).

Intracellular Ca^{2+} ($[Ca^{2+}]_i$) overload caused by Ca^{2+} influx has been implicated in several neurodegenerative diseases, such as ischemic stroke, ALS, PD, AD (Stutzmann and Mattson, 2011) and HD (Mattson, 2007). In normal neurones, large amounts of energy need to be spent to maintain the homeostasis of ion gradients, and Ca^{2+}-ATPases on the cell membrane and the endoplasmic reticulum (ER) membrane are one of the major adenosine-5'-triphosphate (ATP) sinks (Mattson, 2007) and the ER is a large intracellular Ca^{2+} pool.

In stroke, compromised blood flow in vascular damage results in a massive release of glutamate which can activate the N-Methyl-D-aspartate (NMDA) receptor. The activation of the NMDA receptor can cause a rise in $[Ca^{2+}]_i$ (MacDonald et al., 2006). In addition, membrane associated oxidative stress

can impair the function of glutamate transporters, and promote membrane depolarization and Ca^{2+} influx through NMDA receptors (Mattson, 2007).

In ALS patients, the Ca^{2+} content in motor neurones is significantly increased (Mattson, 2007), and such an increase has been linked with a Copper (Cu)/Zinc (Zn)-superoxide dismutase (SOD) mutation and with the death of motor neurones (Kruman et al., 1999).

PD has been linked with the death of dopaminergic neurones (Stutzmann and Mattson, 2011) and dopamine is a widely accepted treatment for PD. Furthermore, previous studies have suggested that the death of dopaminergic neurones is contributed by mitochondrial stress, with a possible role of perturbed $[Ca^{2+}]_i$ homeostasis downstream of the mitochondrial alterations (Mattson et al., 2008). Previous experiments have also found that PD cybrids (mitochondrially transformed cells) recovered from a carbachol-induced increase in cytosolic Ca^{2+} 53% more slowly than controls (Sheehan et al., 1997).

For HD, it has been proposed in previous studies that a polyglutamine expansion would modify huntingtin to mutant huntingtin fragmentation, and the latter could be switched to huntingtin oligomers through polyglutamine expansion and/or the increasing of ferrous (Fe^{2+}), copper I (Cu^{+}) or hydrogen peroxide (H_2O_2). The huntingtin oligomers may then increase $[Ca^{2+}]_i$ and cause cell damage or death (Mattson and Magnus, 2006). Ca^{2+}-stabilizing agents

which can prevent $[Ca^{2+}]_i$ overload have therefore been proposed as a possible treatment for HD (Mattson and Magnus, 2006).

AD is a chronic, fatal, neurodegenerative disease which causes progressive deterioration in a broad range of cognitive functions including language, personality, visual-spatial abilities, and characteristically, memory (Arispe et al., 2007, Kagan et al., 2002). In the research on AD, a lot of attention has been paid to the role of Ca^{2+}. Some studies on brain tissue from AD patients have revealed that alterations in cellular Ca^{2+} homeostasis contribute to the cell death. Further, previous studies have reported that the amount of free and protein bound Ca^{2+}, and the activity of Ca^{2+}-independent proteases, are increased in neurones containing neurofibrillary tangles as compared with tangle-free neurones in brain tissue from AD patients (Mattson, 2007, Nixon, 2003). The Ca^{2+} entering through putative Ca^{2+} channels formed by β-amyloid (Aβ) stemming from amyoid precursor protein (APP) may be one possible pathogenesis of $[Ca^{2+}]_i$ overload (Alarcón et al., 2006), and, certainly a Ca^{2+} current through an Aβ channel has been recorded with electrophysiological techniques previously (Jang et al., 2010).

To summarise those studies mentioned above, it may be important to consider that $[Ca^{2+}]_i$ overload plays an important role in neuronal death and in most, if not all, of the neurodegenerative diseases. However, the source of the $[Ca^{2+}]_i$ rise might not be from solely the outside of the cell, but may also be derived from an intracellular store. As soon as Ca^{2+} has entered the cells, either through

an NMDA receptor channel or Aβ, the increased $[Ca^{2+}]_i$ binds with the receptors on the ER, which is known as an intracellular Ca^{2+} pool, and actives the Ca^{2+} channels on ER. This causes more Ca^{2+} to be released from ER and the $[Ca^{2+}]_i$ is further increased (Berridge, 2010). Importantly, this pathway is called Ca^{2+} induced Ca^{2+} release (CICR) path. In neurones, like many other cells, apoptosis would be activated by the increased $[Ca^{2+}]_i$ and cell death would follow. Fig. 1.1 outlines Ca^{2+} signalling and the CICR pathway on the ER.

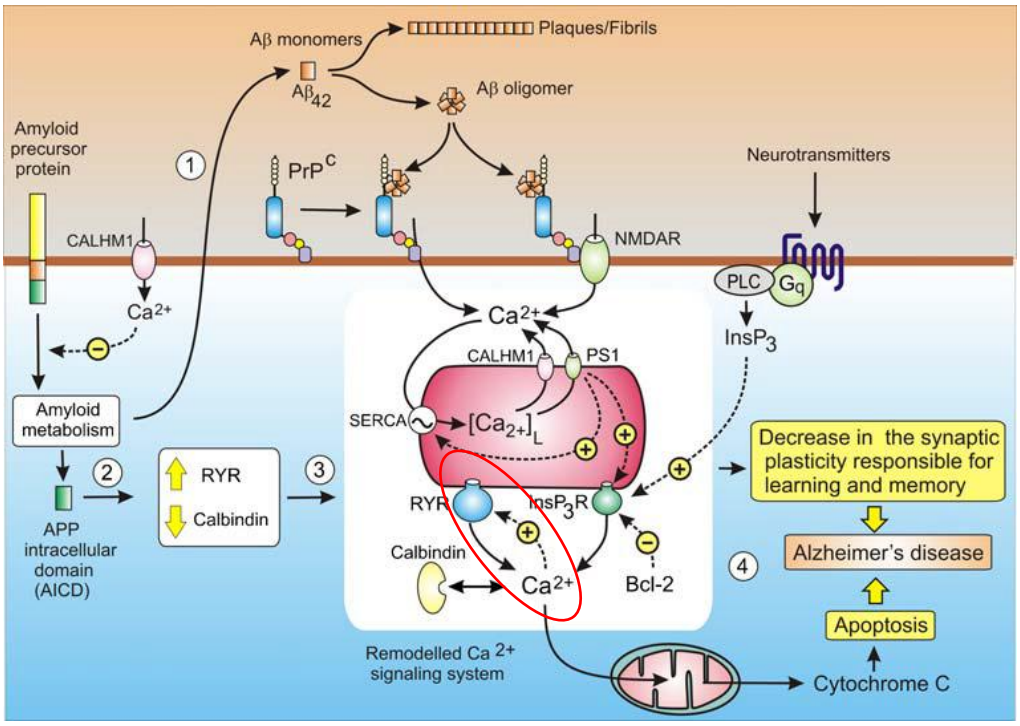

Figure 1.1 $[Ca^{2+}]_i$ signals and activation of cell death (Berridge, 2010)

The CICR system (see Fig. 1.1) has a key well understood physiological function also in skeletal muscle and cardiac muscle by triggering release of further Ca^{2+} from the muscle sarcoplasmic reticulum (Endo, 1977). In neurones, other studies have pointed out that any rise in $[Ca^{2+}]_i$ may not solely result in

inducing cell apoptosis, but might somehow be protective. Although it has been mentioned above that neuronal death in ischemic stroke is contributed by the Ca^{2+} release from ER, another study has claimed that when neurones are exposed to a mild brief ischemia they can be more resistant to a more severe ischemic stroke (Calabrese et al., 2007). However, this result does not fit well with a Ca^{2+} hypothesis of neuronal death. The possible reason is that ER Ca^{2+} release can stimulate NF-κB, which is a transcription factor. The activation of NF-κB can down-regulate NMDA current and inhibit Ca^{2+} release via inositol 1,4,5-trisphosphate (IP_3) receptor (Stutzmann and Mattson, 2011). That means, the brief ischemia, which can increase $[Ca^{2+}]_i$, might not necessarily be protective, but just temporally down-regulate NMDA receptor and prolong further increasing of $[Ca^{2+}]_i$.

1.2 Intracellular Ca^{2+} and ER

As introduced before, in most of the models of neurodegeneration mimicking stroke, PD, ALS, HD and AD, neuronal death or dysfunction is caused by, or related to an increase of $[Ca^{2+}]_i$, even if the pathologies of $[Ca^{2+}]_i$ increase are different. The ER plays an important role in $[Ca^{2+}]_i$ homeostasis. Thus, some ER Ca^{2+} release mechanisms are going to be briefly introduced here since ER is known as an important intracellular Ca^{2+} pool.

1.2.1 Inositol 1,4,5-trisphosphate receptor

IP_3 receptor (IP_3R) is a Ca^{2+} channel located on the ER membrane. There are 3 mammalian subtypes of IP_3R (Stutzmann and Mattson, 2011). IP_3R1 is a tetramer of four subunits, and, for each subunit, the amino terminal is the IP_3 binding domain, the carboxyl terminal is the channel-forming domain, and the middle part is a modulatory domain. The other two subtypes of IP_3R have similar amino acid sequence with IP_3R1 with a homology of 70.5% for IP_3R2 and a homology of 64.6% for IP_3R3 (Bezprozvanny, 2005).

IP_3R is a cation-selective channel gated by IP_3 (Bezprozvanny, 2005). When there is limited intracellular [IP_3], few receptors bind IP_3 and localized small Ca^{2+} signals are generated by Ca^{2+} released through a single IP_3R channel. When there is intermediate intracellular [IP_3], coordinated openings of several channels within a group is triggered by Ca^{2+} release from one channel stimulating gating of nearby channels through CICR process. When there is high intracellular [IP_3], global propagating Ca^{2+} signals can be evoked and the Ca^{2+} released at one cluster can trigger Ca^{2+} release at adjacent clusters by CICR (Parker et al., 1996). According to previous measurements of Ca^{2+} current magnitude through RyR [< 0.5 pico ampere (pA)], and considering that the relative magnitudes of Ca^{2+} currents through IP_3R and RyR can be estimated to be about 2.85, the Ca^{2+} current through an IP_3R channel under physiological ionic conditions is predicted to be 0.1 – 0.2 pA (Foskett et al., 2007).

The reason that the cycles of Ca^{2+} release exist is that IP_3R is a CICR channel,

and can be activated by not only IP_3, but also intracellular Ca^{2+}. Under low $[Ca^{2+}]_i$ [about 50 nano moles (nM)] in the environment, the activity of IP_3R channel is very low (Foskett et al., 2007). As the $[Ca^{2+}]_i$ is increased from 100 nM, the IP_3R channel activity can also be increased until $[Ca^{2+}]_i$ is 1 micro mole (μM), and the maximum opening probability (P_o) of IP_3R is estimated as about 0.8. Interestingly, channel P_o stays at the maximum level over a wide range of $[Ca^{2+}]_i$ until about 10 – 20 μM. When the $[Ca^{2+}]_i$ is further raised above 20 μM, the IP_3R channel is inhibited (Foskett et al., 2007, Mak et al., 1998). Hence, in the cycles of Ca^{2+} release mentioned above, high intracellular $[IP_3]$ stimulates the IP_3R channel and releases Ca^{2+}, and increased $[Ca^{2+}]_i$ actives the IP_3R and continues the Ca^{2+} release thereafter. Although Ca^{2+} can modulate the P_o of the IP_3R channel, Ca^{2+} cannot independently active IP_3R channel in the absence of IP_3 (Stutzmann and Mattson, 2011). Besides the intracellular Ca^{2+}, the IP_3R channel can be modulated by luminal Ca^{2+} also. IP_3R activity can be inhibited by luminal Ca^{2+}, and the channel can be rapidly inactivated by high luminal Ca^{2+} after it is activated by IP_3 (Foskett et al., 2007).

In addition to intracellular and luminal Ca^{2+}, IP_3R can be modulated by ATP and pharmacological modulators. ATP [< milli mole (mM)] can active IP_3R1, and adenophostin A (nM) actives IP_3R1 and IP_3R2. Heparin [microgram per millilitre (μg/mL)] and decavanadate (μM) also inhibit all 3 subtypes of IP_3R, while xestospongin C (μM) and caffeine (mM) can inhibit IP_3R1 only (Alexander et al., 2009).

Previous studies have linked IP_3R channel with some neurodegenerative diseases. In ischemic stroke, Ca^{2+} release through the IP_3R channel is enhanced (Stutzmann and Mattson, 2011). In AD, presenilin (PS) 1 actives IP_3R to release more luminal Ca^{2+} and increase $[Ca^{2+}]_i$ (Berridge, 2010).

1.2.2 Ryanodine receptor

RyR is another important Ca^{2+} release channel on the ER membrane (Stutzmann et al., 2006a). The name of "ryanodine receptor" is given because it is sensitive to a plant alkaloid ryanodine (Sorrentino, 1995), which is found in the South American plant Ryania speciosa (Flacourtiaceae) (Rogers et al., 1948). The chemical structure of ryanodine is shown in Fig. 1.2.

There are three isoforms of RyR found so far: RyRI, RyRII and RyRIII. They are distributed in many different organs, tissues or cells (Giannini et al., 1995). However, generally speaking, RyRI is mostly found in skeletal muscle, RyRII is usually found in cardiac muscle, and RyRIII is widely found in neurones (Vanterpool et al., 2006, Manunta, 2000). Thus, they are named skeletal type (sRyR), cardiac type (cRyR) and brain type (bRyR) respectively in some papers (Hakamata et al., 1992, Furuichi et al., 1994). The amino acid and mRNA sequences of human RyRs have been studied before (Bhat and Ma, 2002, Yamaguchi et al., 2004, Tilgen et al., 2001, Pugh et al., 2005), and the degree of homology on amino acid is quite high. It is 67% between RyRI and RyRII, is 66% between RyRI and RyRIII and is 70% between RyRII and

RyRIII (Manunta, 2000).

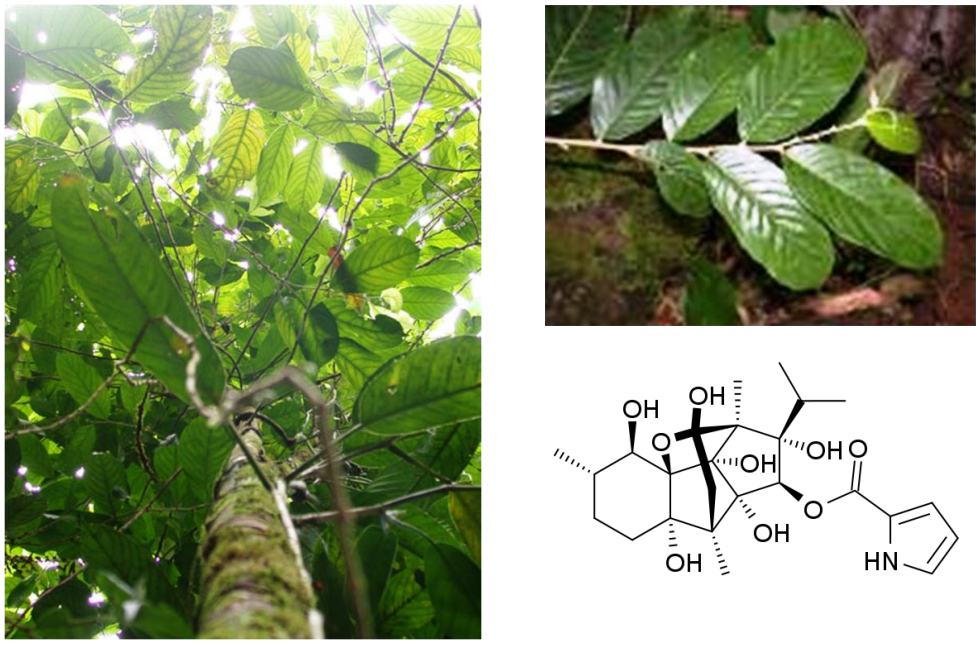

Fig. 1.2 Ryania speciosa and ryanodine. Left hand panel: ryania speciosa; right top: ryania speciosa; and right bottom: chemical structure of ryanodine.

The three-dimensional of RyRIII is shown in Fig. 1.3.

Previous work with the RyRI has shown that the three-dimensional structure of RyRI is similar to that of RyRIII shown above (Samsó et al., 2005). The differences between RyRI and RyRII, and even the selective RyRII binding areas, have been studied and described in 1990s (Manunta, 2000, Sorrentino, 1995). But, the differences between RyRIII and the other two isoforms have not been completely revealed yet.

RyR, like the IP_3R, is a CICR channel on the ER. It is a high-conductance but relatively nonspecific cation channel [about 100 – 150 pico siemens (pS) for

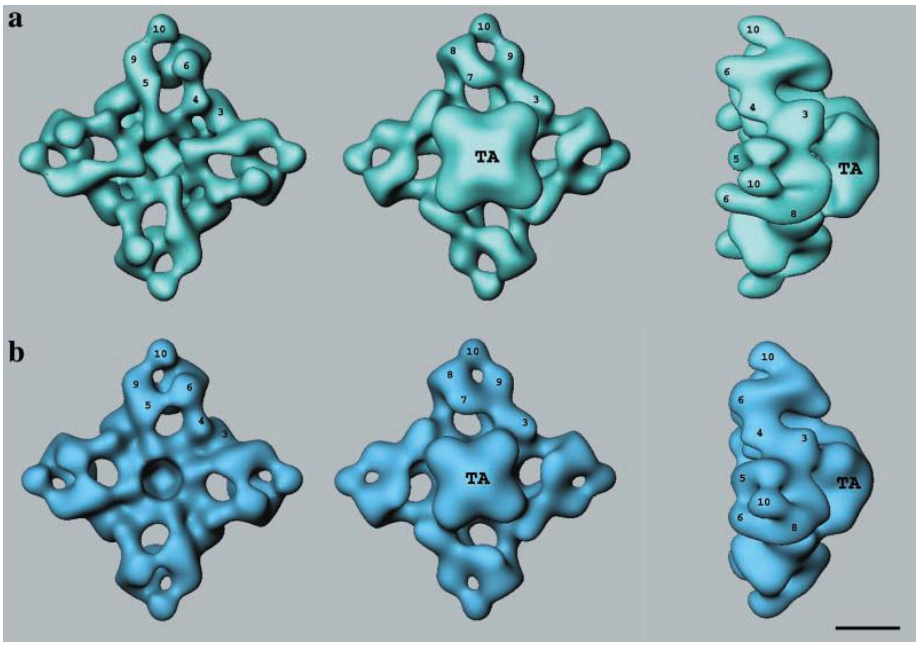

Fig. 1.3 Three-dimensional structure of RyRIII (Sharma et al., 2000). a: RyRIII in open buffer. Open buffer favours the open state of RyR channel and contains 400 mM sodium chloride (NaCl), 20 mM 1,4-piperazinediethanesulfonic acid (PIPES) (pH = 7.2), 5 mM Na_2AMP, 2 mM dithiothreitol, 0.2 mM calcium chloride ($CaCl_2$), 0.1 mM ethylene glycol tetraacetic acid (EGTA), 0.6% 3-[(3-cholamidoprophl)dimethylammonio]-1-propanesulfonic acid [CHAPS, weight to volume (w/v)], 0.3% soybean phospholipid and 1 μg/mL leupeptin. And b: RyRIII in closed buffer. Closed buffer contains 400 mM NaCl, 20 mM PIPES, 2 mM dithiothreitol, 0.1 mM EGTA, 1% CHAPS (w/v) and 1 μg/mL leupeptin. This buffer favours the closed state of RyR channel. Scale bar is 100 angstrom (Å). The left panel shows the cytoplasmic view, the central panel shows the face interacting with junctional face membrane, and the right panel shows the interaction of transmembrane assembly (TA) with the cytoplasmic assembly. All the numbers show the domains which have been studied previously.

Ca^{2+}], which is therefore quite different from IP_3R (Stutzmann and Mattson, 2011). The three isoforms of RyR have different sensitivities to intracellular Ca^{2+} (RyRI > RyRII > RyRIII). All of the three isoforms can be activated by low concentrations of intracellular Ca^{2+} (μM) to release luminal Ca^{2+} and can be inhibited by high $[Ca^{2+}]_i$ (Alexander et al., 2009). Ca^{2+} release through RyRI

can achieve maximal release at about 5 μM $[Ca^{2+}]_i$ and can be inhibited by intracellular Ca^{2+} at several hundred μM (Alexander et al., 2009) to low mM range (Stutzmann and Mattson, 2011). The RyRII and RyRIII require higher $[Ca^{2+}]_i$ for inhibition, requiring about 1 mM (Alexander et al., 2009) to 10 mM (Stutzmann and Mattson, 2011) or above. The RyR can also be modulated by luminal Ca^{2+} and high luminal Ca^{2+} levels increase its responsiveness to some cytosolic agonists (Stutzmann and Mattson, 2011). In addition, in a transgenic (KM670/671NL + V717F) mouse model, importantly, enhanced expression of RyR and increased $[Ca^{2+}]_i$ have been reported, but the $[Ca^{2+}]_i$ is similar to control in the transgenic model with silenced RyRIII (Supnet et al., 2006). This result suggests that $[Ca^{2+}]_i$ cannot be markedly increased without the existence of RyR, even in the transgenic AD model.

In addition to both intracellular and luminal Ca^{2+}, RyR can also be modulated by ATP, calmodulin, cytosolic magnesium (Mg^{2+}) and some pharmacological modulators. Cytosolic ATP (mM) can active RyR while Mg^{2+} (mM) can inhibit it (Stutzmann and Mattson, 2011). Calmodulin at low $[Ca^{2+}]_i$ level actives RyRI and RyRIII. Ryanodine (nM – μM) and caffeine (mM) can active all the three isoforms of RyR, and suramin (μM) can active RyRI and RyRII. Ruthenium red inhibits all the three isoforms of RyR, ryanodine (> 100 μM) and procaine block RyRI and RyRII only, and dantrolene blocks RyRI and RyRIII only (Alexander et al., 2009).

Intriguingly, previous studies have related the dysfunction of RyR to several

neurodegenerative diseases. Ca^{2+} release through RyR is enhanced in ischemic stroke (Stutzmann and Mattson, 2011), and the study on a transgenic AD mouse model (KM670/671NL + V717F), which has been mentioned above, has revealed that both RyR expression and Ca^{2+} release are enhanced in the transgenic model comparing with the control (Supnet et al., 2006). Some studies even claim that RyR induced Ca^{2+} release in the ER may be crucially involved in the formation of the pathological hallmarks of AD (Kelliher et al., 1999).

1.2.3 Other considerations

Besides IP_3R and RyR, there are other relevant targets on the ER which could either modulate Ca^{2+} release from ER directly, or modulate IP_3R or RyR. These include PS, Ca^{2+} homeostasis modulator 1 (CALHM1) and the sarcoplasmic-endoplasmic reticulum Ca^{2+} ATPase (SERCA).

There are two types of PS, PS1 and PS2. PS has been widely studied in AD research since it can cleave APP to generate Aβ (Stutzmann and Mattson, 2011). Previous studies have also found that PS, either wild type or mutant, can increase the intracellular Ca^{2+} level and can enhance IP_3-evoked Ca^{2+} responses. PS can also increase the open probability of (EC_{50} = 7 nM) and the Ca^{2+} release current from the RyR channel (Rybalchenko et al., 2008). In addition, PS itself may constitute a Ca^{2+} leak channel to release luminal Ca^{2+} (Berridge, 2010, Stutzmann and Mattson, 2011, Tu et al., 2006). Besides the release from

luminal Ca^{2+}, PS can also increase $[Ca^{2+}]_i$ by enhancing Ca^{2+} entry from extracellular sources (Lessard et al., 2005). In addition to modulating intracellular Ca^{2+}, PS increases potassium (K^+) current in hippocampal neurones, an action which may be related to neuronal apoptosis (Zhang et al., 2004).

CALHM1 is a novel Ca^{2+} channel localised to both the ER and plasma membrane (Stutzmann and Mattson, 2011). A previous study has proposed that CALHM1 is an essential component of a previously uncharacterised Ca^{2+} channel that controls both Aβ level and $[Ca^{2+}]_i$, both of which are related to AD (Dreses-Werringloer et al., 2008), and, luminal Ca^{2+} can be released from CALHM1 (Berridge, 2010). However, the link between CALHM1 and AD is still arguable and some other studies have shown no support for CALHM1's role in AD. This is reviewed in Stutzmann and Mattson (2011).

In addition to those luminal Ca^{2+} release channels mentioned above, IP_3R, RyR, PS and CALHM1, there is a Ca^{2+} influx pump, SERCA, on the ER membrane. It pumps cytosolic Ca^{2+} into the ER using energy derived from ATP hydrolysis. There are three (SERCA1, SERCA2 and SERCA3) different proteins, and they can be further divided to 7 isoforms (SERCA1a, SERCA1b, SERCA2a, SERCA2b, SERCA3a, SERCA3b and SERCA3c). SERCA2b and SERCA3 are expressed in nomuscle tissues, SERCA2b particularly is expressed in brain (Stutzmann and Mattson, 2011). Previously it has been shown that the activity of SERCA2b to pump Ca^{2+} into ER can be enhanced by higher expression of

PS1, which means that high expression of PS1 would accelerate cytosolic Ca^{2+} clearance (Green et al., 2008). This result does not suggest a neuroprotective effect of PS1, since the enhanced activity of SERCA may not balance the increased activity of IP_3R and the Ca^{2+} leak through PS1 itself (Berridge, 2010).

1.3 Neuronal insult

Since this thesis is focused on the cellular basis of neurodegeneration, several cell insult models, which can result in neuronal death and may be highly relevant to neuronal degenerative diseases, have been considered. These are now described in turn.

1.3.1 β-amyloid

Aβ is thought to be the main pathogenesis of AD (Zahradníková and Palade, 1993). Some studies of the channel hypothesis claim that the Aβ peptides are the major constituents of senile plaques found in the brain (Plant et al., 2003), especially in the hippocampal regions (Mattson and Kater, 1989), of AD patients. They accumulate in plaques in the brain, form ion channels, and actually damage and/or kill neurones (Alarcón et al., 2006, Kagan et al., 2002, Kelliher et al., 1999, Lin et al., 2001). Such a channel forming ability of Aβ peptides was first demonstrated in lipid bilayers in 1993 (Arispe et al., 2007, Kagan et al., 2002) and the 3D structure of the Aβ ion channel was reviewed in 2007 (Lal et al., 2007). Other studies have shown that Aβ peptides can insert

into the plasma membranes of target cells, transport ions such as Ca^{2+}, and mediate cytotoxicity in a manner consistent with channel formation (Kagan et al., 2002). Further, patch clamping has also confirmed that the Aβ channel is existent and functional (Jang et al., 2010).

However, neurones must maintain ionic gradients and membrane potential to function properly in their signalling role, and even small decrements in membrane potential can alter firing properties and lead to significant brain dysfunction. In particular, neurones need to maintain $[Ca^{2+}]_i$ low (~ 100 nM), hence the Ca^{2+} entering into neurones from Aβ channels will potentially trigger apoptosis or at least modify signalling function (Kagan et al., 2002).

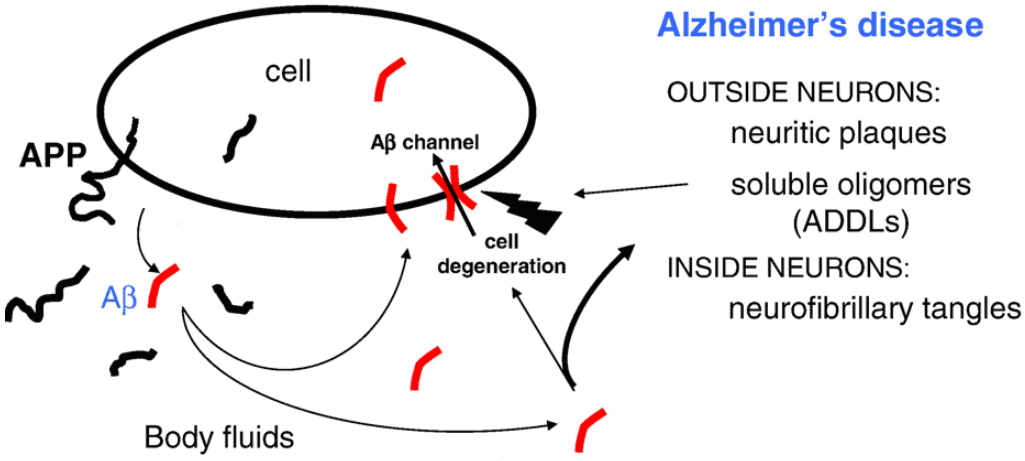

Fig. 1.4 Aβ peptides and its actions on cells (Arispe et al., 2007)

Fig. 1.4 shows the principal of Aβ channel. The APP is a form of transmembrane protein, and can generate Aβ following the activity of a specific enzyme (Kelliher et al., 1999). Most Aβ remains in the medium in a non-toxic and non-aggregated state. But, in the AD brain, the Aβ plaques can

form neuritic plaques, soluble oligomers and ion channels in cells. Such a channel will allow ions, such as Ca^{2+}, and neurotoxins to enter into, and will cause neurofibrillary tangles (Arispe et al., 2007).

In addition to the Ca^{2+} channel formation approach, Aβ can also modulate acetylcholine (ACh) release in brain neurones. ACh dysregulation has been linked to AD and other dementias in previous studies. The activity of the ACh synthesizing enzyme choline acetyltransferase is reduced in the neocortex of AD brain, and reduced ACh release and loss of cholinergic neurones occurs in the basal forebrain region in AD brains (Kar, 2002). Importantly, a fluorescence test on SK-N-MC cells (a human neuroepithelioma cell line) has found that $A\beta_{1-42}$ can bind with the α7 nicotinic ACh receptor with high affinity and can reduce cell viability at a concentration of nM (Wang et al., 2000). Another in vitro study with rat hippocampal slices has shown that 10 nM Aβ can inhibit ACh release in 2 hours (h) (Kar et al., 1998), and, such an inhibitory effect is more significant in the aged cognitively-impaired rats than it is in the aged cognitively-unimpaired rats or young adult rats (Vaucher et al., 2001). These effects may also underlie the toxic effect of Aβ in neurones, however whether intracellular Ca^{2+} changes are involved in these actions is still unknown.

1.3.2 Hypoxia mimicked by cobalt (II) chloride

Hypoxia is a widely used model in cardiac disease studies and it has a major role in the pathogenesis of cardiac dysfunction (Bautista et al., 2009). Hypoxia

has also been found to promote chondrogenesis in stem cells (Kanichai et al., 2008). In those models, hypoxia is linked with ischemia, and hypoxia/ischemia can lead to the modulation of some bioactive lipid messengers such as eicosanoids whose synthesis is highly regulated in reperfusion as well (Bazan et al., 2002). Clearly, ischemia is a key pathogenesis of ischemic stroke and, besides stroke, hypoxia has been implicated in several other brain disorders or neurodegenerative diseases too, or even has been used as a model for those studies. For example, hypoxia has been used as a model to induce generalized seizure to study the role of potassium channels (Yamada et al., 2001). And, hypoxia is also an important contributor to the onset and progression of AD (Bazan et al., 2002).

In addition to having been considered as a model of a range of diseases, hypoxia directly modulates $[Ca^{2+}]_i$. Previous work believes that the modulation of Ca^{2+} by IP_3R is based on hypoxia preconditioning in hippocampal neurones (Bickler et al., 2009).

Cobalt (II) chloride ($CoCl_2$) has been used as a hypoxia mimetic model in previous studies (Gasperi et al., 2010, Bautista et al., 2009), and in neurones, $CoCl_2$ can increase the generation of Aβ by up-regulating the expression of APP as well as the expression of β-secretase and γ-secretase (Zhu et al., 2009). As described above, Aβ is the key pathogenesis factor for neurones in AD and is an obvious neuronal insult model.

1.3.3 Oxidative stress induced by hydrogen peroxide

Oxidative stress has been found to be increased in the aged brain, and aging is obviously related to a range of neurodegenerative diseases or brain disorders such as stroke and AD (Floyd and Hensley, 2002). Besides, oxidative stress is allegedly involved in ALS as well since an increased level of Ca^{2+}, and oxyradicals are found in spinal cord motor neurones in ALS patients (Kruman et al., 1999). Furthermore, some other studies believe that oxidative stress is also involved in PD (Egea et al., 2007). In cells oxidative stress is essentially an insult to mitochondria and causes mitochondrial dysfunction (Lin and Beal, 2006).

H_2O_2 has been utilised effectively as an oxidative stress insult model for cellular based studies before. Hence, the cell death with H_2O_2 has been tested with a mouse hippocampal cell line (Ishimura et al., 2008), and, there is evidence to suggest that H_2O_2 is not an oxidative stress insult only in neurodegeneration, but also can modulate $[Ca^{2+}]_i$ directly (Krebs et al., 2007). A similar study has been done with cardiac cell lines to investigate the effect of H_2O_2 on gating Ca^{2+} release channel and to link this release with the function of the RyR (Boraso and Williams, 1994).

1.3.4 Glutamate

Glutamate has often been studied in previous studies researching of

neurodegeneration since it can bind with, and activate the NMDA receptor, which is a Ca^{2+} influx channel.

Glutamate has therefore been used as an insult in neuronal cell lines, and glutamate induces neurodegeneration for example in hippocampal neurones (Mattson, 1989). It can directly induce neuronal death and direct the cells to apoptosis based on the modification of mitochondrial functions (Ankarcrona et al., 1995), and can also induce neuronal death by deregulation of $[Ca^{2+}]_i$ and has been used as an ischemia model (Dolga et al., 2011). This effect could be due in part to the activation of NMDA receptor since the latter can induce Ca^{2+} signals (Alford et al., 1993, Makarewicz et al., 2003). In addition, stimulation of the NMDA receptor can produce superoxide ($O^{\cdot -}$) which is toxic to cells, and is linked with ALS (Lafon-Cazal et al., 1993). Amazingly experimental results have shown that 1 mM glutamate can induce APP secretion in 30 minutes (Jolly-Tornetta et al., 1998).

In addition, glutamate is involved in, and linked with the other insults. Previous studies conclude that glutamate (1 mM) and the activation of NMDA receptor are essential in the cell death in a hypoxia mimetic model, although this same study has also indicated that 1 mM glutamate alone is not toxic to neurones if hypoxia is absent (Rootwelt et al., 1998). There are even some studies that have challenged the idea of a toxic effect of glutamate by suggesting that the activation of CICR channel, such as IP_3R, can be inhibited by glutamate (Kato and Rubel, 1999).

1.4 Possible neuroprotective targets studied in this thesis

As introduced above, the CICR channel plays an important role in luminal Ca^{2+} release and in $[Ca^{2+}]_i$ homeostasis. Hence, the CICR channels could be selected as a potential target for research on neuroprotection. As will be seen, this thesis focuses on RyR, which is a CICR channel on the ER. In addition, dysfunction of the K^+ channel and involvement of ATP has been mentioned above in some cases of neurodegeneration and neuronal death. Hence several types of K^+ channels are also considered here, given their possible roles in neuroprotection.

1.4.1 Ryanodine receptor

As introduced above, earlier studies have pointed out that RyR is implicated in luminal Ca^{2+} release (Stutzmann et al., 2006a), and it is well known as a Ca^{2+}-regulating protein on the ER membrane. Hence its blockade could potentially protect neurones against excitotoxic injury (Mattson, 2007).

But why the RyR rather than the other important CICR channel IP_3R? This is based on a consideration of selectivity. $[Ca^{2+}]_i$ overload and CICR are likely factors in neurodegeneration, but do play a physiological role in skeletal and cardiac muscles. Hence, if selected for a neuroprotective strategy, possible side effects on other targets or tissues other than neurones are expected. In this case, it is preferred to pick a target located in neurones only, rather than one widely spread in other organs or tissues. The distributions of three isoforms of RyR

have been investigated in previous studies, and RyRIII is the only isoform which is mainly located in brain neurones (Sorrentino, 1995). However importantly there is little difference in the distribution of the three IP_3R subtypes.

Equally the RyRIII target is a better target than the SERCA. Although the distribution of different subtypes of SERCA are different, and only SERCA2b is mainly distributed in brain, there are few pharmacology modulators available for SERCA thus far. In addition, the effect of SERCA on $[Ca^{2+}]_i$ modulation is smaller than the effects of RyR or IP_3R, although SERCA does play a positive role in reducing $[Ca^{2+}]_i$. (Green et al., 2008, Berridge, 2010).

As introduced in Section 1.2.2, there are several pharmacological RyR modulators available. This study proposes to test the effect of those modulators on models of neuronal insult to see whether RyR blockade, particularly the blockade of RyRIII rather than the other two isoforms, would be neuroprotective or not.

1.4.2 Potassium channel

As introduced above, there are three potential cell insults to be used in this study, Aβ, hypoxia and oxidative stress. All of these can increase $[Ca^{2+}]_i$ and induce neuronal death. However, besides the issue of $[Ca^{2+}]_i$, K^+ channel activity may play a role in those cell insults. A previous study has found that

platelets from AD patients have a modified activity in a K^+ channel (Silva et al., 1998), and, a mathematical model has also shown that any Aβ-mediated block of the K^+ current could result in increased intracellular Ca^{2+} levels and hence increased membrane excitability (Good and Murphy, 1996). However, there are some other contrasting studies claiming the opposite. For example, one study in 1998 has shown that tetraethylammonium (TEA), which is a K^+ channel blocker, can reduce the neuronal death from a Aβ insult (Yu et al., 1998).

So, there remains the big question whether activation or blockade of K^+ channels would be neuroprotective. Several K^+ channels which have been studied before, such as the large conductance Ca^{2+} activated K^+ channel (BK), ATP-sensitive K^+ channel (K_{ATP}) and the voltage-gated K^+ channel (K_v), are therefore introduced here.

1.4.2.1 Large conductance Ca^{2+}-activated K^+ channel

Some studies have claimed that the activation of BK channel is neuroprotective. In an in vivo $BK^{-/-}$ mouse model (homozygous mice lacking the BKα subunit), transient focal cerebral ischemia induced by middle cerebral artery occlusion produced larger infarct volume and higher post-ischemia mortality than the wild type counterpart, and NMDA-induced neurotoxicity was found to be larger than in the wild type counterpart when NMDA is injected intracerebrally (Liao et al., 2010). In an in vitro model of rat hippocampal tissue, electrically-

induced glutamate release was reduced by a selective BK opener (Gribkoff et al., 2001). For the possible neuroprotective function of the BK channel, one review in 2006 has proposed that the activation of BK channel results in hyperpolarization of membrane potential which will close voltage-gated Ca^{2+} channels, reduce Ca^{2+} entry and diminish Ca^{2+} (Burg et al., 2006). In addition to consideration at the cell membrane, one study on guinea pig ventricular cells has suggested that the activation of mitochondrial BK channels can cause mitochondrial K^+ uptake, and that such an uptake can protect the heart against ischemic injury and infarction (Xu et al., 2002).

In contrast, some other studies have highlighted the opposite effect of BK channel activation. The review mentioned above (Burg et al., 2006) has also pointed out that the activation of BK channels can enhance transmembrane K^+ efflux which can cause cell shrinkage, $[Ca^{2+}]_i$ increase and finally cell apoptosis. One study on cardiomyocytes has claimed that the interference of the BK β1 subunit mRNA increases cardiomyocyte resistance to ischemia (Bautista et al., 2009).

So whether BK channel activation is neuroprotective, or not, is still uncertain. Therefore, the BK channel is investigated in this Thesis to ascertain its role, if any.

The BK is a channel with an α subunit and four similar or different β subunits. The α subunit is the main and essential part of BK and its silence would render

the whole channel nonfunctional. The expression of different β subunits is variable in different areas. β1 is primarily expressed in smooth muscle, hair cells, and some neurones, β2 is found in ovary and endocrine tissue, β3 is found in testis, and β4 is the most abundant β subunit in the brain. The BK channel with different β subunits may have different properties and processes different functions. (Orio et al., 2002).

The topography of the BK channel is shown in Fig. 1.5.

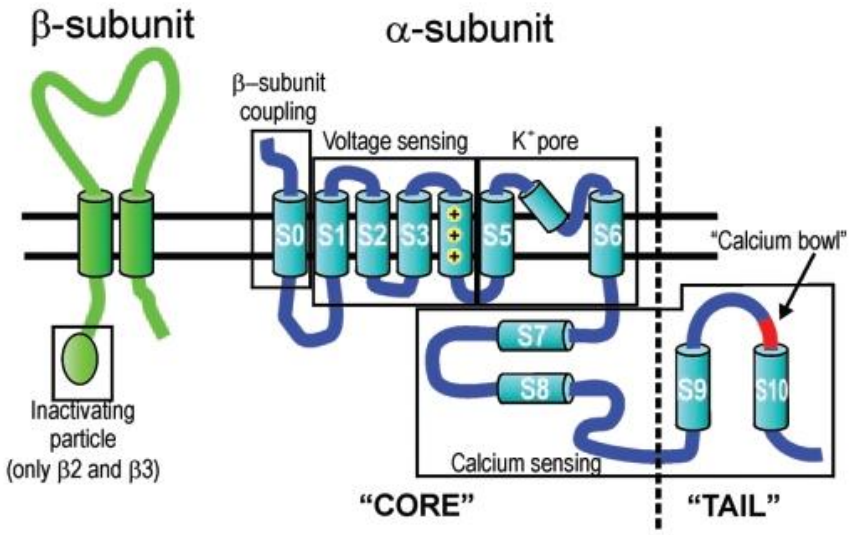

Fig. 1.5 BK α and β subunit topography (Orio et al., 2002).

1.4.2.2 ATP-sensitive K^+ channel

Some previous studies have proposed that the activation of K_{ATP} channel can protect neurones. One in vivo study on the $K_{ir}6.2$ knocked out mouse model has found that the neurones were severely damaged after focal cerebral ischemia induced by middle cerebral artery occlusion, whereas few injured

neurones were found in the wild type counterparts (Sun et al., 2006). Another study on a $K_{ir}6.2$ mutant mouse model has also found that the activity of substantia nigra pars reticulate neurones, which plays an important role in the control of seizures, was enhanced during hypoxia, while the activity of the same neurones in normal mice was inactivated by the opening of the postsynaptic K_{ATP} channel (Yamada et al., 2001). Similar neuronal activity has been found in the normal mice when tolbutamide, which is a K_{ATP} channel blocker, was applied (Yamada and Inagaki, 2005). In addition, another study on rat hippocampal cells has found that diazoxide (a K_{ATP} opener) treatment of neurones reduces neuronal death from insults of $A\beta_{25-35}$ or hypoxia induced by ferrous sulphate ($FeSO_4$) (Goodman and Mattson, 1996). Also, data from mice administrated diazoxide has shown that the infarct volume in the brain under cerebral ischemia was reduced (Liu et al., 2002).

In contrast, other studies have claimed the opposite. One study on mammalian central neurones has shown cell apoptosis induced by cromakalim, a K_{ATP} opener, in electron micrographs (Yu et al., 1997), and another study in rat hippocampal neurones has found that 5-hydroxydecanoate, a mitochondrial K_{ATP} blocker, can increase cell survival from glutamate or staurosporine insult (Liu et al., 2003). In addition to neurones, another study on rat preadipocytes has found that diazoxide can reduce the relative cell number, while the K_{ATP} channel blocker glibenclamide can increase cell number, in MTT assays (Wang et al., 2007). For a possible mechanism, it was believed that K^+ efflux from mitochondria can cause mitochondrial membrane depolarization, cyt c release,

and induce subsequent extrusion of cytosolic K^+ via a K^+ channel on the cell membrane (Burg et al., 2006).

Since it is still unclear what the role of K_{ATP} is in neuronal death, it is also investigated here in those cellular insult models introduced above (see Section 1.3).

A functional K_{ATP} channel is constructed from four inward rectifier (K_{ir}) subunits and four sulphonylurea receptor (SUR) subunits (Burg et al., 2006). Although the ion-conducting structure of K_{ATP} channel exists in the K_{ir} subunits (Ho et al., 1993), SUR subunits are also essential for K_{ATP} channel function, since SUR subunits represent the ATP binding area. There are several inward rectifier K^+ channels found so far ($K_{ir}1$ to $K_{ir}7$), but only $K_{ir}6$ is found to be ATP sensitive (Alexander et al., 2009), hence it is named the K_{ATP} channel. There are two subtypes of K_{ATP} channel, $K_{ir}6.1$ and $K_{ir}6.2$, and there are three different SUR thus far, SUR1, SUR2A and SUR2B (Alexander et al., 2009). The proposed topography of the K_{ATP} channel is shown in Fig. 1.6.

1.4.2.3 Voltage-gated K^+ channel

Besides the BK and K_{ATP} channels, attention has also been paid to voltage-gated K^+ channels in studies on neurodegeneration. One previous study has found that there are two missense mutations on the 19q13 gene which is the causative gene in a Filipino adult-onset ataxia pedigree and a French

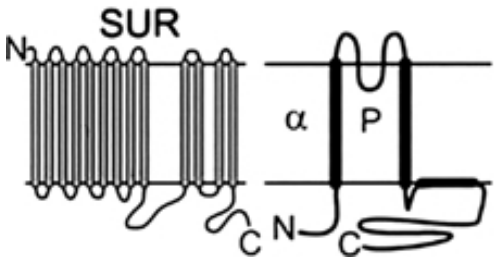

Fig. 1.6 Membrane topography of K_{ir} channel. "α" shows the pore-forming subunit, and "P" shows the area of the pore. (Burg et al., 2006)

childhood-onset ataxia pedigree, and both of them can alter K_v3.3 channel (KCNC3) function (Waters et al., 2006). It has also been found that the K_v3.4 (KCNC4) channel subunit is up-regulated in the early stages of AD (Angulo et al., 2004).

The K_v channel is composed by homo- or hetero-tetramers of α subunits with regulatory β subunits. The pore is located in the α subunit which has six transmembrane domains (Burg et al., 2006). There are 12 subfamilies of K_v channel found so far (Alexander et al., 2009). This study concentrates on the two subtypes mentioned above, i.e. K_v3.3 and K_v3.4, which belong to the K_v3 subfamily. The topography of the K_v channel is shown in Fig. 1.7.

1.5 Models of Neurodegeneration

To study neurodegenerative disease, different sorts of models have been used in previous research work, including in vivo animal models, animal tissue slice, primary cultures, cell lines and some other models such as bilayer or liposome to mimic the cell membrane. Some of these examples are discussed below.

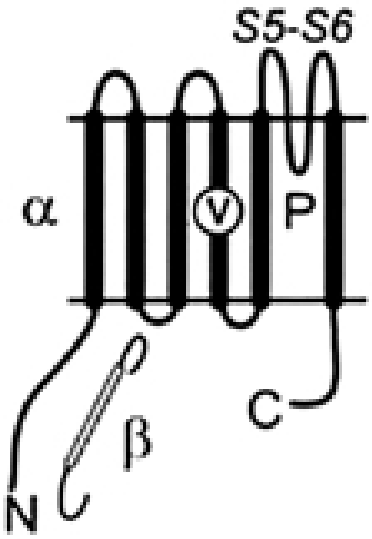

Fig. 1.7 K_v channel topography. "P" shows the region of the pore and "V" shows the voltage sensor area. (Burg et al., 2006)

1.5.1 In vivo animal models

Animal models are widely used in the studies of neurodegeneration. A transgenic (KM670/671NL + V717F) mouse model was used to investigate the expression of RyRIII, Ca^{2+} signalling and K^+ channel expression (Supnet et al., 2006, Coles et al., 2008). APP transgenic mice (V717F or APP_{sw}) have been used to investigate the deposition of Aβ and local toxicity in brain parenchyma and cerebral blood vessels (Holtzman, 2004). A YAC128 HD transgenic mouse model was employed to test the possible neuroprotective effect of dantrolene and improved performance in both beam-walking and gait-walking assays were observed (Chen et al., 2011). As introduced above, a $BK^{-/-}$ mouse model with middle cerebral artery occlusion or NMDA-induced neurotoxicity treatment was used to study the BK channel function by measuring the infarct volume and post-ischemia mortality (Liao et al., 2010). Finally a $K_{ir}6.2$ mutant mouse

model with middle cerebral artery occlusion and/or a hypoxia mimetic or tolbutamide treatment was used to check the neuronal damage or substantia nigra pars reticulate activity (Sun et al., 2006, Yamada et al., 2001, Yamada and Inagaki, 2005).

1.5.2 Animal organs, tissues or primary cells

Besides the in vivo experiments undertaken on animal models, in vitro models with animal organs or tissues are also widely used in previous studies.

Mouse cortical tissue was used for PCR and western blot studies in an investigation of the function of cytosolic N-terminal of PS1 (Rybalchenko et al., 2008). Cortical slices and neurones were used for a 2-photon Ca^{2+} imaging test to distinguish the IP_3R- and RyR-mediated Ca^{2+} components (Stutzmann et al., 2006b).

Bullfrog sympathetic ganglion cells were used to test the role of RyR and BK channel in modulation of the action potential (Akita and Kuba, 2000). Primary cortical neurones from a triple transgenic mouse model of AD (PS1 mutant knock-in mouse with two additional transgenes, APP_{SWE} and tau_{P301L}) were selected to study the caffeine induced Ca^{2+} release from intracellular stores (Smith et al., 2005). Striatal medium spiny neurones from a YAC128 HD mouse model were used to investigate the intracellular Ca^{2+} release triggered by caffeine and glutamate (Chen et al., 2011). Finally, astrocytes from RyRIII

knock out mice were used to study the RyRIII function in astrocyte migration (Matyash et al., 2002).

1.5.3 Cell lines

Cell lines have also been used extensively to study cell death, dysfunction or dysregulation of $[Ca^{2+}]_i$.

For example, SH-SY5Y is a human neuroblastoma cell line, and it has been used to study cell proliferation and the effects of insults such as $CoCl_2$ and Aβ (Chong et al., 2007, Hunya et al., 2008).

The NTERA-2 clone D1 (NTERA-2) is a cell line of human Caucasian pluripotent embryonal carcinoma. In previous studies, NTERA-2 has been used as a cell line to represent "genuine" human neurones, to test the glutamatergic regulation of APP (Jolly-Tornetta et al., 1998), to investigate the production of $Aβ_{1-40/42}$ from APP by β-site APP cleaving enzyme (Lee et al., 2003), and to study the expression of the mutations in the presenilin (PS) 1 gene, PS1 being possibly the major cause of early onset familial AD (Tokuhiro et al., 1998). The inhibition and inducement of its proliferation has also been studied (Yao et al., 2007), and the properties of the BK channel in this cell line have also been studied (Chapman et al., 2007).

MOG-G-UVW is a human brain astrocytoma cell line. Astrocytes were used to

study anti-inflammation function and their relevant role in neuronal protection (Spillantini, 2011).

In addition to human cell lines, animal cell lines have been used in studies of neurodegeneration. For example, rat hippocampal neurones were used to study the Ca^{2+} release and sequestration by ryanodine-sensitive stores (Garaschuk et al., 1997).

1.5.4 Other models

Most studies previously were performed on either in vivo animal models or in vitro organs, isolated tissues, isolated cells or cell lines. Some research has utilised other models, such as electrophysiological work on bilayers or liposomes. One such study has recorded the activity of the Aβ channel in the bilayer (Jang et al., 2010).

The work in the thesis is particularly concerned with neuronal death and possible neuroprotective targets in human cells. Therefore, human cell lines were preferred rather than in vivo animal models, although the latter sometimes can mimic the neurodegenerative disease better than cell lines. The cell lines used in this thesis are introduced in Section 2.2.

1.6 Hypotheses

Based on previous studies, two hypotheses are proposed here and will be tested in the following studies:

a. That there is a role for the RyR channel in paradigms that mimic neurodegeneration, and that the blockade of the RyR, especially the selective blockade of RyRIII, is neuroprotective.

b. That there are K^+ channels, such as the BK channel and K_{ATP} channel, which are functional in neuronal cell lines, and are involved in neuronal protection.

The main objectives of the work presented here are

- To determine whether there is expression of a RyR message and K^+ channels in the model cell lines and to determine whether the expression of RyRIII message is changed during cell differentiation.
- To establish a robust and relevant method of inducing cell death using oxidative stress, hypoxia, or Aβ.
- To determine whether there is modified sensitivity to stressors during differentiation.
- To determine whether there is any neuronal protective effect by blocking or otherwise modulating RyR, particularly the RyRIII; and
- To assess whether K^+ channel activation or blockade can protect or exacerbate respectively the effects of stressors.

2. Methods and Materials

2. Methods and Materials

In this section, those general methods and materials which are used in many parts of this study are introduced. For more specific details, please refer to the relevant sections.

2.1 Cell culture

All cells are cultured in culture medium (relevant medium compositions will be described below) in 25 square centimetre (cm^2) or 75 cm^2 flasks (from Fisher Scientific) and incubated in a sterilised incubator (from Sanyo) at 37 centigrade (°C) with 5% of carbon dioxide (CO_2). Sterilised copper sulphate ($CuSO_4 \cdot 5H_2O$) water (H_2O) solution was kept in the incubator to maintain the humidity and a sterilisation status, and, everything placed in the incubator was previously sterilised. Cells are checked under the microscope (Nikon TMS) every day, and the contaminated or dead cells (if any) removed from the incubator as soon as they were identified. Usually, 3 millilitres (mL) of medium was the culture volume in each 25 cm^2 flask and 9 mL of medium was the volume in each 75 cm^2 flask. The medium was changed every 3 – 4 days, or at any other time when the pH was considered too low (the colour of medium was turning orange or even yellow). When the cells in the flask were 80% to 100% confluent, they were split or used for any further experiments such as ribonucleic acid (RNA) extraction or cell proliferation assays. Any experimental manoeuvres related to cell culture or living cells were performed

in a sterilised cabinet (Faster ultrasafe 48 model, from Bioquell) with sterilised tools. For sterilisation, all the plastics were autoclaved, all the metal or glass utensils were incubated in the oven (from Status) at 180 °C for at least 2 h, all the solutions were filtered through 0.2 micrometer (μm) filter membrane (from Corning), and all the other items were sprayed with 70% [volume to volume (v/v)] ethanol (C_2H_5OH).

To split the cells in a 25 cm^2 flask, the first step is to warm the medium, phosphate-buffered saline (PBS, pH = 7.4) and ethylenediaminetetraacetic acid [EDTA, $(HOOCCH_2)_2NCH_2CH_2N(CH_2COOH)_2$] / trypsin (0.2% / 0.025%, w/v, PBS solution, pH was adjusted to 7.4 – 7.6) in a water bath at 37°C for about 15 minutes (min) until the EDTA/trypsin has thawed. Then, the working area such as the cabinet (ventilated area) was sprayed and all objects which were going to be placed in this area were also sprayed with 70% C_2H_5OH to maintain sterile conditions. Following this, the medium was aspirated from the flask containing the cells and 1 mL of 1 × PBS was added into the flask to wash the cells. The solution in the flask was swirled to make sure all the cells were washed and then the PBS was aspirated from the flask. 500 micro litres (μL) of EDTA/trypsin was now added to the flask and the solution gently agitated in the flask to make sure every cell might detach, and then the flask was placed in the incubator for 3 – 5 min. After the incubation, the flask was tapped gently to make sure all the cells would detach, and the cells checked under the microscope to see if they were both round and floating. Then, 1 mL of culture medium was added to the flask to stop the digestion and the medium

containing the cells was thereafter transferred into a 1.5 mL centrifuge tube. It was centrifuged at 1,000 revs / minute (r/min) for 3 min (centrifuge is 545C model from Eppendorf). The supernatant was aspirated carefully without damaging the pellet of cells, and the pellet was resuspended in 1 mL of culture medium. If cells are split from a confluent 75 cm^2 flask, three times the volume of PBS, EDTA/trypsin and culture medium were applied. Then, the medium containing cells was split into several new flasks according to need. Finally, each new flask had medium made up to 3 mL, and was stored in the incubator.

To keep a large stock of living cells, these were frozen at -80 °C (ultra low temperature freezer from New Brunswick Scientific) or liquid nitrogen (N_2). To freeze the cells, a confluent 75 cm^2 flask of healthy cells was taken and the above splitting protocol was followed, until the cell pellet was obtained and the supernatant was removed. Then, the cells were resuspended in 4.5 mL of freezing medium. Finally, the medium containing the cells was allocated into 9 freezing tubes by placing 500 μL of the cell suspension into each tube. The composition of the freezing medium was foetal bovine serum (FBS) with 15% (v/v) of dimethyl sulfoxide (DMSO) and 100 u of penicillin-streptomycin mixture (P/S). The cells usually could be kept for roughly 1 month at -80 °C and would live for a longer period in the liquid N_2 environment (< -196 °C).

All the containers or facilities which were used for living cells were treated with Virkon before being discarded. All the pipettes, pipette tips (5 mL, 1 mL,

200 μL and 10 μL) and tubes (1.5 mL, 500 μL and 200 μL) used in this work are from Eppendorf. The water bath is 750 watt (W) from Grant.

$CuSO_4 \cdot 5H_2O$, C_2H_5OH and virkon are from Fisher Scientific. PBS (1 ×), P/S [10,000 units (u)] and FBS are from Invitrogen. EDTA, trypsin (from bovine pancreas), DMSO and sodium hydroxide (NaOH) are from Sigma-Aldrich. EDTA is dissolved in 1 mole (M) NaOH (a little 10 M NaOH could be applied to make the EDTA to be completely dissolved) as 20% (w/v) for stock. EDTA stock, trypsin, FBS, P/S and EDTA/trypsin mixture are stored at -20 °C (freezer is from Blomberg). PBS and medium are stored at 4 °C (fridge is from Blomberg). The DMSO is light sensitive.

2.2 Cell lines

The following human cell lines are used in this study.

2.2.1 SH-SY5Y

SH-SY5Y is a cell line derived from a human neuroblastoma. It responds to, and can be differentiated with retinoic acid (see Section 2.3). It is used here to test the existence of BK subunit and the avtivity of the BK channel, to test whether there is any change in RyRIII expression during differentiation, and it is also used to investigate the response to various insults (before and after differentiation), and to BK channel or RyR modulators.

The composition of the culture medium is minimum essential medium Eagles (EMEM) & nutrient mixture F12 ham (F12) (1 : 1, v/v) with 15% (v/v) of FBS, 2 mM L-glutamine, 1 × of MEM non-essential amino acid solution (NEAA), and 100 u of P/S. The neuronal characteristics are lost with increasing passage number (Ross et al., 1983), hence only the SH-SY5Y cells with a passage number lower than 22 were used in this study. Thus, a large stock of SH-SY5Y cells with lower passage numbers were prepared and stored at either -80 °C or in liquid N_2.

2.2.2 NTERA-2 clone D1

NTERA-2 clone D1 (NTERA-2) is a cell line of human Caucasian pluripotent embryonal carcinoma. It also responds to retinoic acid-induced differentiation (Andrews, 1984) (see Section 2.3). The NTERA-2 cell line is used here to test for changes in the RyRIII expression during differentiation, and to test its response to insults and the RyR modulator ruthenium red. The composition of the culture medium is Dulbeceo's modified Eagle medium (DMEM) with 10% (v/v) of FBS and 100 u of P/S.

2.2.3 MOG-G-UVW

MOG-G-UVW is a human astrocytoma cell line. It is used in this thesis to see whether there is any K^+ channel and/or RyRs expression at the mRNA level, and to test its response to insult models and BK and RyR modulators. The

composition for the culture medium was DMEM & nutrient mixture F10 ham (F10) (1 : 1, v/v) with 10% (v/v) of FBS and 100 u of P/S.

2.2.4 N2102Ep clone 2/A6

N2102Ep cell line is a human embryonal carcinoma. It does not response to retinoic acid-induced differentiation. So, in this study, the cell line N2102Ep was used as the negative control for NTERA-2 differentiation. The composition of the culture medium is DMEM with 10% (v/v) of FBS and 100 u of P/S.

2.2.5 MG-63

MG-63 is a cell line from a human osteosarcoma. In this study, MG-63 cells served as a negative control for RyRIII expression. Since it is believed that the RyRIII is mainly expressed in brain neurones (see Section 1.2.2), MG63 has been used as a negative control to see whether RyRIII message is absent, or is at least present at a much lower level than the counterpart neurone. The composition of the MG-63 culture medium is DMEM with 5% (v/v) of FBS and 100 u of P/S.

All the cells above are from Sigma-Aldrich. DMEM is from Invitrogen. EMEM, F10, F12 and NEAA (100 ×) are from Sigma-Aldrich. All the media, nutrient mixtures and NEAA were stored at 4 °C. L-glutamine (200 mM) is

from PAA Laboratories GmbH and is stored at -20 °C.

2.3 Cell differentiation

The differentiation of SH-SY5Y and NTERA-2 cells is induced by retinoic acid. The differentiation medium for each cell line is simply the relevant culture medium with 10 μM retinoic acid added. The differentiation period is 1 week for SH-SY5Y cells (Jämsä et al., 2004), and is 4 weeks for NTERA-2 cells (Andrews, 1984). Since N2102Ep cells were the negative control for NTERA-2 cells differentiation, N2102Ep cells were also treated with 10 μM retinoic acid for 4 weeks.

Retinoic acid is light sensitive. Thus, minimum essential checking and medium changing was undertaken with cells during the differentiation period. Equally, splitting was avoided during the differentiation process. Retinoic acid is from Sigma-Aldrich. It was dissolved in DMSO at 10 mM as the stock, and was diluted to 10 μM in relevant medium in order to differentiate the cells. Retinoic acid stock was stored at -20 °C. The structure of retinoic acid is shown below:

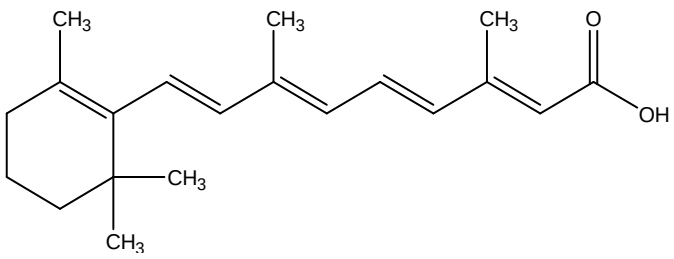

2.4 RNA extraction

RNA was extracted from cells in a confluent 75 cm^2 flask. The medium was aspirated and 3 mL of PBS was added to the flask to wash the cells. The PBS was then in turn aspirated, 2.5 mL of TRIzol reagent was added to the flask and spread over the entire surface to maximise the RNA return. After all the cells had detached from the bottom of the flask, the TRIzol solution containing RNA was transferred into two of 2 mL tubes by placing 1.25 mL of the TRIzol sample into each tube. Then, 250 μL of chloroform ($CHCl_3$) was added into each tube, and the tubes were turned over a couple of times. Following this the tubes were centrifuged at 14,000 r/min for 10 min at room temperature. The pink bottom solution was the $CHCl_3$ phase containing the organic contents from TRIzol but without any RNA, and the colourless supernatant was the aqueous phase containing the RNA. The colourless supernatant from each tube was then transferred into a 1.5 mL tube.

The next step is RNA precipitation. 500 μL of isopropyl alcohol [$(CH_3)_2CHOH$] was added into each 1.5 mL tube and both tubes were incubated at room temperature for about 10 min. Then, the tubes were once again centrifuged at 14,000 r/min for 10 min at room temperature, whereupon the RNA should form visible pellets in the bottom of the tubes. The supernatant was then removed carefully without any damage to the RNA pellets, and 500 μL of C_2H_5OH (75%, v/v) was added to each tube. The mixture was vortexed and centrifuged at 14,000 r/min at room temperature for 5 min, then, the supernatant was

removed carefully again and the tubes were left open at room temperature for the remaining C_2H_5OH to evaporate. Attention should be paid here to prevent the samples completely drying out. Finally, 25 μL of nuclease free H_2O was added to each tube, and the tubes were stored at -80 °C overnight for the RNA sample to be rehydrated. All of the above steps were carried in a fume cupboard except when washing the cells with PBS and centrifuging.

The third step is the DNAse treatment. This step removes the remaining deoxyribonucleic acid (DNA) (Szewczyk et al.) in the RNA sample. The RNA sample from both tubes was removed from the -80 °C freezer and combined in a 500 μL tube. 5 μL of 10 × DNAseI buffer and 1 μL of rDNAse 1 were added to the 50 μL RNA sample. The mixture was then incubated in a thermal cycler at 37 °C for 30 min. Following that, 5 μL of DNAse inactivation reagent is added to the mixture after a strong vortex. Thereafter, the mixture was incubated at room temperature for 2 min and vortexed after each minute. Finally, the tube was centrifuged at 10,000 r/min for 2 min at room temperature. The RNA sample needed was contained in the supernatant, thus the supernatant was transferred into a 200 μL tube for storage. All the reagents were kept in ice until required in this step.

The last step is RNA quantification. The RNA sample was diluted 50 times by placing 2 μL of it in 98 μL of nuclease free H_2O. The concentration of diluted RNA sample was then measured with a spectrophotometer, with H_2O being the blank. Finally, two results were obtained. One was the ratio of absorbance

between 260 nano metre (nm) and 280 nm, which represents the level of protein contamination. The ratio should be higher than 1.5 for a successful RNA extraction. The other reading obtained is the concentration of RNA (w/v) in the 50 times diluted sample. It was used to estimate the RNA concentration in the original stock, which should be 50 times higher. After preparation, the RNA was stored at -80 °C.

TRIzol is from Invitrogen and is stored at 4 °C. $CHCl_3$ and nuclease free H_2O are from Sigma-Aldrich. $(CH_3)_2CHOH$ is from Fisher Scientific. The DNAse treatment kit (DNAseI buffer, rDNAse 1 and DNAse inactivation reagent) is from Ambion and was stored at -20 °C. The PCR workstation (fume cupboard) is from Labcaire. The vortex is from Rotamixer.

2.5 Reverse transcription

Reverse transcription (RT) was carried out for those qualifying RNA samples in order to prepare the cDNA for future polymerase chain reaction (PCR) or quantitative PCR (Q-PCR). To make sure that the PCR or Q-PCR result is comparable, the same amount of RNA sample was added in each reaction of reverse transcription. Additionally, to test the purity of RNA and to see whether there is any possible DNA contamination, a counterpart of no-RT was performed for each reaction as a negative control. There was no reverse transcriptase, the essential enzyme to transcript the mRNA into cDNA, in the no-RT control, and that was essentially the only difference between the no-RT

control and the normal reverse transcription reaction mixture. The details of the reverse transcription protocol are given below:

Firstly, the same reaction mixtures were prepared in two of 500 μL tubes with the following reagents:

Table 2.1 Reagents of RNA mixture

Reagents	Amount to add
Nuclease free H_2O	Up to 5.0 μL
Relevant RNA sample	1 micro gram (μg)
Random primers (500 μg/mL)	1.0 μL

After preparing the RNA mixtures, they were incubated at 70 °C for 5 min. Then, they were chilled in ice immediately for at least 5 min after incubation. Thereafter, the following mixtures were prepared for reverse transcription in another two 500 μL tubes.

Table 2.2 Reaction mixture for reverse transcription

Reagents	Volume to add (μL)	
	No-RT	Sample
Nuclease free H_2O	7.1	6.1
RNA mixture	5.0	5.0
Reaction buffer (5 ×)	4.0	4.0
Magnesium (II) chloride ($MgCl_2$, 25 mM)	2.4	2.4
dNTP mix (10 mM each)	1.0	1.0
Reverse transcriptase	-	1.0
rRNAsin, RNAse inhibitor (40 u/μL)	0.5	0.5

After both the no-RT control and the sample were prepared, they were

incubated in a thermocycler (from Perkin Elmer Catus) following the programme: 25 °C × 5 min + 42 °C × 1 h + 70 °C × 15 min. The no-RT and cDNA products were then stored at -20 °C.

The reverse transcription kit (reaction buffer, $MgCl_2$, dNTPs, reverse transcriptase, random primer and RNAsin) and dNTP mix were from Promega and were stored at -20 °C. The centrifuge is from MSE Micro Centaur.

2.6 Primer design

As soon as the cDNA was prepared, PCR was performed with relevant primers. Before the PCR protocol is introduced below (see Section 2.7), how the primers were designed in this study is discussed here.

The appropriate primers should be ideally located in different exons of the whole DNA sequence, should contain about 40% of adenine (A) or thymine (T) and about 60% of cytosine (C) or guanine (G), and should not match each other closely which may result in primer-dimer formation. In this project, the primers were designed online on the webpage of Primer III.

Firstly, the whole mRNA sequences of the relevant targets were searched in PubMed (http://www.ncbi.nlm.nih.gov/pubmed). The sequences were also double checked with blast on PubMed (http://blast.ncbi.nlm.nih.gov/blast.cgi) to see whether the mRNA sequences were exactly what were required. The

confirmed whole mRNA sequence was then copied and pasted into the website of Primer III (http://frodo.wi.mit.edu/primer3). Then certain requirements were set for the primer design. In this project, primer size was set around 20 base pairs (bp), the annealing temperature was set between 55 °C and 60 °C, and the percentage of C and G (GC%) was set at about 60% as mentioned before. The primer design programme was run and the suggested primers were listed in order of how they match the criteria set. The pair of primers with highest priority was selected and examined once more with blast to see whether they matched perfectly the sequence to be amplified. The required similarity was set as higher than 80% in this work. Finally, the pair of primers was examined on the website of Ensembl (http://www.ensembl.org) to see whether they were actually located in different exons.

Primers are from Invitrogen. Primers were dissolved in TE buffer (Tris base and EDTA, pH = 8.0) at 100 μM for stock and were diluted to 10 μM in nuclease free H_2O for PCR. Primers were stored at -20 °C. Tris-base [Tris (hydroxymethyl) aminomethane, $C_4H_{11}NO_3$] is from Fisher Scientific.

2.7 PCR

PCR was used to amplify a certain DNA sequence with the cDNA product gained from the reverse transcription reaction. If the target DNA can be successfully amplified, it means that there is the relevant message in the original mRNA derived from the RNA extraction, and this means in turn that

there is the relevant message in the donor cells.

In each PCR reaction, there was always a negative and a positive control. The positive control was the amplification of a house keeping gene on the cDNA. The purpose of the positive control was a guarantee that all the reagents including the cDNA and the PCR conditions were of good quality. In this project, β-actin, which is a house keeping gene and expressed in almost all cell lines, was selected as a positive control. The negative control was the amplification of the house keeping gene in the no-RT sample (see Section 2.5). Since no-RT generates no cDNA, this should not respond to any PCR amplification, and the PCR result of the negative control should yield no band. The purpose of the negative control was a guarantee that all the reagents including the cDNA were still purified without any genomic DNA contamination. For each PCR reaction, the following mixture (see Table 2.3) was prepared in 200 μL tubes.

As soon as the PCR mixtures were prepared, the tubes were placed in the PCR thermocycler (from Biometra) and the following PCR amplification programme was run: 95 °C × 2min + [95 °C × 30 seconds (s) + annealing temperature × 45 s + 72 °C × 1 min] × 30 to 50 cycles + 72 °C × 5 min. The annealing temperature and the number of cycles were determined according to different target DNA and different primers. A higher annealing temperature and/or a larger number of cycles would result in a stronger reaction but less specific amplification. The volume of $MgCl_2$ was also optimised. Higher Mg^{2+}

concentration would cause a stronger reaction but again less specific amplification. These details were optimised in a PCR condition optimisation step. The details for PCR condition optimisation is discussed later (see PCR condition optimization in Section 3.2.1). The PCR results and products were examined using gel electrophoresis (see Section 2.9).

Table 2.3 Reaction mixture for PCR amplification

Reagents	Volume to add (μL)		
	Negative control	Positive control	Sample
Nuclease free H_2O	Up to 12.5	Up to 12.5	Up to 12.5
Green Go Taq flexi buffer	2.5	2.5	2.5
$MgCl_2$ (25 mM)	0.25 – 2	0.25 – 2	0.25 – 2
β-actin primer forward (10 μM)	0.5	0.5	-
β-actin primer reverse (10 μM)	0.5	0.5	-
Target primer forward (10 μM)	-	-	0.5
Target primer reverse (10 μM)	-	-	0.5
No-RT	0.5	-	-
cDNA	-	0.5	0.5
dNTP mix (10 mM each)	0.25	0.25	0.25
Go Taq DNA polymerase (5 u/μL)	0.0625	0.0625	0.0625

In this thesis, PCR was also performed to amplify a large quantity of those target DNA fragments which were already known to exist. The large quantity amplification was performed to get a large amount of target DNA fragment for sequencing or for Q-PCR. For the large quantity amplification, 4 times the volume of each reagent was used for each reaction.

The PCR kit (Green Go Taq flexi buffer, $MgCl_2$ and Go Taq DNA polymerase)

is from Promega and is stored at -20 °C.

2.8 Gel electrophoresis

In this project, electrophoresis was used to examine the results of PCR amplification, or to separate the large amount of target DNA fragment.

The gel used in this project was 10 milligrams per milliliter (mg/mL) of agarose. To prepare a gel, 700 milligrams (mg) [balance: maximum = 400 grams (g), d = 0.1 g, AND HL-400 model, from Sartorius] of agarose was mixed within 70 mL of 1 × TAE buffer in a 100 mL conical flask. 1 × TAE buffer is a water solution of 40 mM Tris [$(HOCH_2)_3CNH_2$] base, 20 mM acetic acid (CH_3COOH) and 1 mM EDTA. The agarose was not soluble in TAE at room temperature, hence, the mixture was heated to boiling with a microwave (800 W, E, from LG) and swirled a few times, until the agarose was completely dissolved and the mixture was transparent and clear. Then, the flask containing boiled agarose solution was cooled down in tap water to about 60 °C before 2.1 μL of ethidium bromide (EB, 0.003%, v/v) was added. The boiled agarose solution containing EB was then poured into an electrophoresis tank which was sealed on all four sides. The relevant comb (10 μL one for the testing the purified DNA, 20 μL one for normal PCR and 50 μL one for the large amount amplification) was loaded on the gel and any visible bubble was removed. The comb should go deep into the gel but should not break through it.

When the gel was completely cooled, it was solid. The comb was then removed gently without damaging the wells on the gel, and the gel placed in the electrophoresis tank where the wells were close to the negative electrode. The ladder (hyperladder II for 50 – 2,000 bp) and the samples were then added into each well respectively. For the 10 μL or 20 μL wells, 5 μL of ladder and 10 μL of each sample were added. For the 50 μL wells, 10 μL of ladder and 50 μL of each sample were added. Finally, the electrophoresis was run at 100 millvolt (mV) for 50 min.

For normal PCR, a photo was taken on the gel in ultraviolet (UV) light. Ideally there should be no band for the negative control, and only one band for the positive control. Usually, there should be only one band also for the sample DNA fragment and the size of it was estimated by comparing it with the ladder. If there was more than one band present, the PCR condition was further optimised or another pair of primers used.

For the large quantity amplification, the gel was moved onto a UV light to see whether the two controls were clean and clear, and to see whether the size of target DNA had a correct size of base pairs by comparing the band position against the ladder. If the amplification result was acceptable, the band of target DNA was cut off and stored in 500 μL tube for DNA purification and future sequencing or Q-PCR.

Agarose [gelation temperature 32 – 40 °C and gel strength > 950 gram per

square centimetre (g/cm^2)] and CH_3COOH are from Fisher Scientific. EB (10 mg/mL) was from Bio-Rad and is light sensitive.

2.9 Gel purification

The purified DNA fragment was needed for sequencing and for possible Q-PCR. In this work, the purpose of the gel purification was to get a high concentration of purified target DNA fragment and it was performed after the gel slice had been cut from the large quantity PCR amplification. The gel extraction kit from Qiagen was applied and the relevant "MinElute gel extraction kit protocol" was adopted in this project.

The first step was to dissolve the gel slice. The gel slice was cut under UV light with a scalpel which had been sterilised with C_2H_5OH (70%, v/v). As much as possible of the part of gel slice which did not contain DNA and was not bright under UV light was removed, but the entire DNA band was left in the cut gel slice. The gel slice was weighed and dissolved in 3 volumes [volume to weight (v/w)] of buffer QG. Here, 3 volumes means 3 μL for a 1 mg gel slice. Then, the mixture was incubated at 50 °C for 10 min or until the gel slice was dissolved completely. To help dissolve the gel slice, the tube was vortexed every 2 – 3 min during the incubation. When the gel slice was dissolved completely, the pH of the solution was checked for its colour. It should be yellow like the colour of buffer QG without dissolved agarose. If it was orange or violet, up to 10 μL of sodium acetate (CH_3COONa) (pH was adjusted to 5.0

with CH_3COOH) was added to turn the colour yellow. The reason to adjust the pH was that the absorption of DNA to the membrane of MinElute column was efficient only at pH $\leqslant$ 7.5. After that, 1 volume of $(CH_3)_2CHOH$ was added to the solution, and the tube was swirled for a few seconds. Then, the sample was transferred into a MinElute spin column which was placed in a 2 mL collection tube. Thereafter, the tube containing the column was centrifuged at 13,000 r/min for 1 min, and the flow-through was discarded. The column was placed back into the same collection tube and 500 μL of Buffer QG was added again into the spin column. The collection tube containing the spin column was centrifuged for 1 min at 13,000 r/min again and the flow-through was discarded as well. Finally, the spin column was placed back into the same collection tube again.

The following washing procedure step was adopted. 750 μL of buffer PE was added into the column and the sample was incubated at room temperature for 5 min. Then the tube containing the column was centrifuged at 13,000 r/min for 1 min and the flow-through was discarded. Following that, the spin column was placed back into the same collection tube and the tube was centrifuged for 1 min at 13,000 r/min once again to remove all the buffers. The flow-through was then discarded.

The last step was required to elute the DNA. The MinElute spin column was transferred into a 1.5 mL tube and 10 μL of buffer EB with C_2H_5OH was added to the centre of the membrane in the spin column. The tube containing the

column was incubated at room temperature for 1 min and centrifuged at 13,000 r/min for 1 min thereafter. The flow-through in the 1.5 mL tube was the purified DNA and it was stored at -20 °C.

The purity and quality of the purified DNA was tested with electrophoresis. 3 μL of the DNA sample was mixed with 1 μL of DNA loading buffer, and the 4 μL of mixture was run through a gel electrophoresis process as mentioned above. If the band was visible, clear and specific under the UV light, the purity and quality of the purified DNA was deemed acceptable for future sequencing or Q-PCR.

Gel purification kit (buffer QG, PE and EB) was from Qiagen. The scalpel was from Swann-Morton.

2.10 Sequencing

Sequencing was used to confirm that the DNA fragment which had been amplified by PCR was exactly the one expected. Although the sample is a purified DNA fragment, it was still necessary to further amplify it for sequencing purposes. To prepare for the PCR amplification, the mixture with the following composition (see Table 2.4) was prepared in a 500 μL tube:

Since the highest temperature during the amplification was 96 °C, the purpose of adding mineral oil was to avoid any water evaporation during amplification.

The volume needed for the purified DNA sample was dependent on its concentration. The higher its concentration, the less volume was needed, and the volume of H_2O was up to the volume used for the purified DNA sample. The primers here should be the ones which have been used in previous PCR, but either the forward or reverse one can be used in sequencing.

Table 2.4 DNA amplification composition for sequencing

Reagents	Volume to add (μL)
Mineral oil	40.0
Nuclease free H_2O	Up to 50, (~ 3.2)
Purified DNA fragment	~ 3.0
Sequencing buffer	1.0
Primer (4 μM)	0.8
R R Premix (Big dye)	2.0

After the mixture was prepared, the tube was placed in the thermocycler which had been preheated to 96 °C. Then, the following programme was performed: 96 °C × 2 min + (96 °C × 30 s + 50 °C × 15 s + 60 °C × 4 min) × 25 cycles.

After the amplification programme was finished, all the contents in the tube were transferred on a piece of parafilm (from American National Can^{TM}). The reaction mix, which was the aqueous part, should stay as a bubble distinct from the mineral oil, hence, the reaction can be removed from the oil and transferred into another 500 μL tube containing 50 μL of 95% (v/v) C_2H_5OH and 2 μL of CH_3COONa (pH was adjusted to 4.6 with CH_3COOH). The tube was then vortexed and incubated at room temperature for 15 min. Following that, it was centrifuged at full speed (15,000 r/min) for 20 min and the supernatant which

did not contain DNA was carefully aspirated. The pellet might be very small and even almost invisible. In such circumstances, a little volume of supernatant was left in the tube to avoid any possible damage to the pellet. Subsequently, the pellet was washed with 250 μL of 70% C_2H_5OH, vortexed and centrifuged at the same speed again for another 5 min, and the supernatant was discarded in the same way. Thereafter, the pellet was rinsed again with another 250 μL of 70% C_2H_5OH, and was vortexed and centrifuged at the same speed for 5 min. Most of the supernatant was then removed but about 10 μL of it was left at the bottom of the tube to cover the pellet. Finally, the sample was sent to the sequencing lab to obtain the sequence. This final step was done by the sequencing lab in Central Biotechnology Services, School of Medicine, Cardiff University.

Since the R R Premix (a dye to make DNA base testable) is light sensitive, the R R Premix and any mixture containing it should be covered with foil when they were not in the thermocycler or centrifuge. R R Premix was a gift given by Dr. Bronwen Evans in School of Medicine, Cardiff University.

CH_3COONa buffer was 3 M CH_3COONa with pH being adjusted to 4.6 – 5.0 with CH_3COOH. The pH meter was a pH211 model microprocessor pH meter and is from Hanna Instruments. Aluminium foil was from Hygex.

2.11 Cell proliferation and assays

Cell proliferation was carried out in 96 well plates (from Corning) in the cell insult experiments and in studies to test the effect of channel modulators. To evaluate the relative cell numbers, MTS assays were used since the reagent can combine with the enzyme from living cells and causes absorbance at 490 nm. MTS is 3-(4,5-dimethythiazol-2-yl)-5-(3-carboxymethoxyphenyl)-2-(4-sulfophenyl)-2H-tetrazolium, inner salt. The absorbance is proportional to the cell number, and so the relative cell number to control reflects, in effect, the cell viability in the presence of treatment.

MTS is bioreduced by cells into a formazan product that is soluble in tissue culture medium. The conversion of MTS into aqueous, soluble formazan is accomplished by dehydrogenase enzymes found in metabolically active cells. The quantity of formazan product as measured by the amount of 490 nm absorbance is directly proportional to the number of living cells in culture. (Barltrop et al., 1991)

Cells were taken out from a flask with EDTA/trypsin (see Section 2.1) and seeded in the 96 well plate at a density of 15,000 per well in 100 μL per well of relevant culture medium without any drug treatment. After the cells were incubated at 37 °C overnight, the medium was aspirated and 100 μL of any insult medium, with or without testing drugs was added into each relevant well. The insult medium was the culture medium for the relevant cells without FBS. Since FBS is essential in cell proliferation, the cells cannot proliferate without FBS. Thus, any reduction on cell number here means that the drug tested is

killing cells rather than the drug slows down the cell proliferation process. The cell sample treated with the insult medium without any test drugs was the control and the relative cell number was set as 1. Then the cells were incubated at 37 °C for 24 h before 20 μL of MTS & phenazine methosulfate (PMS) (20 : 1, v/v) mixture was added into each well. The plates were then incubated at 37 °C for another 2 – 4 hours and the absorbance was read at 490 nm (laser plate reader is Sunrise Touchscreen model, from Tecan).

In each experiment there were blank wells prepared for each sample. The blank wells were the wells with the same solution mix but with no cells present. The absorbance of the blank was subtracted from the absorbance of each relevant sample for data analysis. The net absorbance (where the absorbance of the relevant blank was subtracted) of each sample was thereafter compared with that of control, where the relative cell number was set at 1, and the final ratio was the relative cell number of each sample.

Each experiment was repeated in triplicate at least for statistical purposes. For the comparison between 2 groups, a t test was performed; and for the comparison amongst 3 or more groups, one way analysis of variance (ANOVA) with post-hoc test was performed. The confidence interval was set at $p < 0.05$.

The Cell Titer 96® Aqueous MTS Reagent Powder was from Promega. MTS powder is dissolved in PBS as 2 mg/mL. The pH of the MTS solution was adjusted to 6.0 – 6.5 and MTS solution was filtered for sterilization. PMS was

from Sigma. PMS powder is dissolved in PBS. Both MTS and PMS are light sensitive. They were covered with foil and stored at -20 °C.

2.12 Electrophysiology

For the single channel patch clamp recording, about 2,000 cells were seeded on the cover slips [diameter = 26 millimetre (mm), from Fisher Scientific] within 100 µL of culture medium. The cover slips were placed in a 12 well plate (from Corning) with 1 cover slip in each well. The plate with cover slips containing cells was incubated at 37 ºC for at least 4 h for the cells to be completely seeded on the cover slips. Thereafter, 1 mL of culture medium was added into each well containing cover slip, and the plate was placed in the incubator until ready to be used.

For patching, the cover slip containing cells was removed from the plate and as much medium on the cover slip removed as possible. Then, the cover slip was fixed in a chamber, topped up with reference buffer, and placed on the microscope stage (from Nikon) with 40 × as the objective. The reference electrode was filled with the same solution as the bath solution, and the recording electrodes were prepared from borosilicate glass capillaries (1.5 mm outside diameter and 0.86 mm inside diameter, from Harvard Apparatus) using a microelectrode puller (DMZ universal puller from Zeitz-Instruments GmbH) and were filled with a relevant patching solution. To prepare the electrode, one capillary is pulled and heat-polished to two equal length parts and the outside

diameter at the tip is about 1 micrometre (μm). For the patch-clamp recording here, sodium (Na^+) Locke was used as the bath solution and the filling solution for the reference electrode, and a high K^+ solution filled the recording electrode.

A cell with a clean membrane and separated from other cells was selected for patching, then the recording electrode was moved into the bath solution. A square wave voltage signal was obvious on the oscilloscope screen (OX 722 model from Metrix) when the recording electrode is in the reference solution. Positive pressure was applied as soon as the recording electrode has contacted the bath buffer. Then, the recording electrode was advanced gently and slowly with a manipulator (from Narishige) until it touched the cell membrane. Attention should be paid to this step since the tip of recording electrode is extremely easy to break if it touches the cover slip. When the electrode touches the cell membrane, the resistance increased and the voltage signal reduced correspondingly on the oscilloscope screen. As soon as the recording electrode touched the cell membrane, negative pressure was applied to achieve a seal with high resistance (giga ohm, GΩ).

Three different configurations of recording were used: cell attached, inside-out, and outside-out cell recording. In this project, cell attached was adopted first as soon as a good seal was achieved. For a cell attached patching, the electrode is attached to the membrane with minimum disturbance to the cell. Any electrical current recorded was due to the movement of the ions through the ion channel in the “isolated” patch of cell membrane under the pipette. A range of voltages

were applied to record the current, and compute the conductance, opening probability etc. of channels in the patch.

In addition to cell attached recording, inside-out recording was also performed. Hence, the patch of membrane under the electrode was pulled away and removed from the rest of the cell membrane. The inside part of the cell membrane was then facing the reference solution in the bath. A range of voltages was once again applied to record the current, compute the conductance, opening probability and so on, from the channel in this configuration.

Current data were acquired at different voltages. To acquire the data, a current-voltage (I-V) converting amplifier headstage (CV 4, from Axon Instruments) was fixed on the manipulator holding the recording electrode, and was connected to an amplifier. The output signals were amplified by an Axopatch -1D amplifier and AC-DC AMP (from Axon Instruments and NeuroLog System, Digitimer respectively), and then digitised (BNC2110 from National Instruments). Then, the data obtained were analysed using WinEDR software and two plots were constructed principally to characterise the features of the channel being patched. One was the I-V curve, and the slope of the linear portion of any trend line gives the conductance, which is an important hallmark of any channel. The other plot was the open probability – voltage curve, which illustrates whether the opening of the channel is voltage dependent or not.

2.13 Drugs solutions

DMEM, EMEM, F10, F12, NEAA and all media were stored at 4 °C, and FBS, glutamine, P/S and retinoic acid stock were stored at -20 °C. Retinoic acid is light sensitive and was dissolved in DMSO at 10 mM for stock. The compositions of media for cell freezing and culture are listed here (see Table 2.5)

Primers were dissolved in TE buffer at 100 μM for stock and were diluted to 10 μM in H_2O for PCR. Primers were stored at -20 °C. Agarose was dissolved in TAE (1×) buffer for electrophoresis. TAE (50 ×) buffer was prepared for stock, and was diluted to 1 × in H_2O until use. The compositions of TE and TAE (50 ×) buffer are listed in Table 2.6.

Table 2.5 Compositions of media (v/v)

	DMEM	DMSO	EMEM	F10	F12	FBS	Glutamine (200 mM)	NEAA (100 ×)	P/S (10,000 u)	Retinoic acid (10 mM)
Freezing	-	15%	-	-	-	84%	-	-	1%	-
MG-63	94%	-	-	-	-	5%	-	-	1%	-
MOG-G-UVW	44.5%	-	-	44.5%	-	10%	-	-	1%	-
N2102Ep	89%	-	-	-	-	10%	-	-	1%	-
NTERA-2	89%	-	-	-	-	10%	-	-	1%	-
NTERA-2 differentiation	88.9%	-	-	-	-	10%	-	-	1%	0.1%
SH-SY5Y	-	-	41%	-	41%	15%	1%	1%	1%	-
SH-SY5Y differentiation	-	-	40.95%	-	40.95%	15%	1%	1%	1%	0.1%

Table 2.6 Compositions of TE and TAE (50 ×) buffer

Chemicals	TE buffer	TAE (50 ×) buffer
Tris base	-	2 M
Tris hydrogen acid (HCl)	10 mM	-
EDTA	1 mM	50 mM
CH_3COOH	-	1 M
pH	8.0	-

The compositions of Na^+ Locke and high K^+ solution for patch-clamp recording are listed in Table 2.7.

Table 2.7 Compositions of Na^+ Locke and high K^+ solution

Contents	Na^+ Locke (for reference)	High K^+ solution (for recording)
sodium chloride (NaCl)	150 mM	10 mM
potassium chloride (KCl)	3 mM	140 mM
EGTA	-	11 mM
HEPES	10 mM	10 mM
D-Glucose	10 mM	-
$CaCl_2$	2 mM	1 mM
$MgCl_2$	2 mM	1 mM
pH	7.4	7.2

Calcium chloride dehydrate ($CaCl_2 \cdot 2H_2O$), magnesium chloride ($MgCl_2 \cdot 6H_2O$), NaCl and KCl are from Fisher Scientific, and D-(+)-glucose ($C_6H_{12}O_6$), EGTA and HEPES ($C_8H_{18}N_2O_4S$) are from Sigma-Aldrich.

3. RyR Expression Determined by PCR and Quantitative PCR

3. RyR Expression Determined by PCR and Quantitative PCR

3.1 Introduction

Since previous studies have suggested that RyRIII is the brain type RyR and therefore mainly located in the brain and neuronal cells (Furuichi et al., 1994, Hakamata et al., 1992), the PCR work in this thesis was undertaken to test the presence of the relevant mRNA in the selected neuronal cell model. Furthermore, since two of the above cell lines can be differentiated to human neurones, Q-PCR was performed to see what the change, if any, in mRNA levels is during differentiation.

PCR for RyRs has been carried out previously (Hosoi et al., 2001, Shoshan-Barmatz et al., 2005, Grievink and Stowell, 2008) and these data have provided a starting point for the studies described here. Most of those previous PCR experiments have used primers which require annealing temperatures at 54 – 62 centigrade (°C) for 30 – 40 cycles. Some have used a decreasing annealing temperature (Burgos et al., 2005, Hosoi et al., 2001, Shoshan-Barmatz et al., 2005, Grievink and Stowell, 2008). The extension temperature was different in those experiments: 68 °C has been used in some, whereas 72 °C was used in the others.

3.2 Materials and methods

NTERA-2 and SH-SY5Y cells were differentiated with 10 μM retinoic acid treatment for 28 days or 7 days respectively (see Section 2.3). PCR amplification of RyRs was performed on the following cell lines: undifferentiated SH-SY5Y, differentiated SH-SY5Y, undifferentiated NTERA-2, differentiated NTERA-2, MOG-G-UVW, N2102Ep and MG-63. The lengths of PCR products, the three isoforms of RyR, are based on the primers designed and are between 200 bp and 300 bp in this study (see Section 3.3.2). Since the main target in this thesis is RyRIII, some of the experiments, such as the optimisation of PCR condition and Q-PCR, focused on RyRIII.

3.2.1 Optimisation of PCR conditions

As discussed before (see Section 2.7), the annealing temperature, number of cycles and Mg^{2+} concentration ($[Mg^{2+}]$) dictate the quality of PCR and should therefore be optimised. Higher annealing temperature, more PCR cycles and higher $[Mg^{2+}]$ result in a stronger activity but a less specific amplification. So, all of these 3 issues have been considered, and optimised for the PCR. In the study here, only the PCR condition for RyR amplification was optimised, the ones for BK, K_v or K_{ATP} channels were following the optimised conditions from previous studies in this laboratory (Henney, 2008, Reviriego, 2009, Henney et al., 2009). The way to optimise the PCR condition, in this project, was to run the PCR and electrophoresis under different conditions and select the best one which gives a specific and clear band.

The annealing temperature was varied between 55 °C and 60 °C and the [Mg^{2+}] was varied between 0.75 mM and 1.5 mM for PCR optimisation. These PCRs were run with cDNA from N2102Ep cells. The details of the PCR conditions which have been trialed are listed below:

Table 3.1 PCR condition optimisation

Tests	Factors and levels		
	Annealing temperature (°C)	Number of cycles	[Mg^{2+}] (mM)
1	55	30	1.5
2	55	40	1.5
3	55	50	1.5
4	58	30	0.75
5	58	30	1.0
6	58	30	1.25
7	58	30	1.5
8	58	40	1.5
9	60	30	1.5

3.2.2 Q-PCR

Q-PCR is a technique to test the DNA concentration based on the fluorescence, and the result can quantitatively reflect the expression of the target DNA. In theory, it is to be expected that the DNA amount should double after each cycle of PCR. Hence, the principle of Q-PCR is testing the number of cycles needed for the amount of target DNA to be amplified to a set amount, and the number of cycles needed is defined as the C_t value. The more cycles needed, if the efficiency is always the same, the smaller amount of target DNA in the sample, and the lower mRNA expression in the original cell line.

For the fluorescence, SYBR green was used here and it was contained in the SuperMix in the Q-PCR kit. The SuperMix contains Platinum® Taq DNA polymerase, SYBR® green I dye, Tris-HCl, KCl, $MgCl_2$ (6mM), deoxyguanosine triphosphate (dGTP, 400 μM), deoxyadenosine triphosphate (dATP, 400 μM), deoxycytidine triphosphate (dCTP, 400 μM), deoxyuridine triphosphate (dUTP, 800 μM), uracil DNA glycosylase (UDG), and stabilizers. The composition for the Q-PCR reaction is listed below:

Table 3.2 Q-PCR composition

Reagents	Volume to add (μL)
Platinum® SYBR® green qPCR SuperMix-UDG	12.5
Nuclease free H_2O	Up to 25
cDNA	< 5
Forward primer (10 μM)	0.5
Reverse primer (10 μM)	0.5
ROX reference dye	Optional, 0.05

The volume of cDNA was computed as follows. Since the florescence in Q-PCR is directly proportioned to the concentration of DNA product in a certain range, which is called “linearity range”, the volume of cDNA added should make the amount of the target DNA in the mix above sit in the linearity range. As described above, the cDNA was obtained from the reverse transcription of 1 μg of RNA, hence, 100 pico grams (pg) to 1 μg of cDNA sample is usually used here. The ROX reference dye is optional. It is used to normalize the fluorescent reporter signal, and is only used to accompany certain Q-PCR instruments. For the primers, since the target DNA for Q-PCR in this work was RyRIII, the pair of RyRIII primers, referred to previously, was used here (see

Section 3.3.2).

After the above mixture was prepared, they were placed in the Q-PCR thermocycler and the following programme was run: 50 °C × 2 min + 95 °C × 2 min + (95 °C × 15 s + annealing temperature × 30 s + reading) ×40 cycles + melting curve. The annealing temperature here was the one which had been optimised for the amplified target. The number of cycles was flexible between 30 to 50 cycles, and the melting curve was applied to find out the melting temperature (T_m) of the DNA product. To get the melting curve, the sample was heated from 49 °C to 96 °C, which was the whole temperature range of the Q-PCR programme (see above). After each 0.2 °C increase of temperature, there was 1 s stop for a fluorescence reading. Since every DNA fragment would have a specific T_m, the melting curve and T_m result could be used to exam the purity of the product. T_m is the peak temperature in melting curve. In theory, there should be only one product amplified, and only one T_m obtained in each sample. If more than one T_m was obtained in one sample, it was possible that the cDNA or the reagents were contaminated.

Besides T_m in the melting curve, efficiency is also an important parameter in Q-PCR. As mentioned above, the DNA amount should double after each cycle in theory. Efficiency is an indicator of much target DNA has been amplified, and a value of 1 means the DNA amount doubles after each cycle. To calculate this, the target DNA sample is diluted by different amounts to get a series of target DNA samples. The Q-PCR programme is then run on this series of

samples and a group of C_t values obtained. Finally, a trend line of C_t value against Lg dilution times can be plotted out and the slope of this trend line calculated. The Efficiency can then be calculated according to the following equation:

$$\text{Efficiency} = 10^{\left(\frac{1}{\text{slope}}\right)} - 1.$$

Usually the higher the efficiency, the better. For any Q-PCR test, the efficiency is acceptable if it is higher than 0.8. More importantly, the efficiency of the endogenous control should be comparable with the one of the sample tested.

For quantitative purposes, to compare the RyRIII expression before and after differentiation, $\Delta\Delta C_t$ method was used for the result analysis and β-actin, which is a house keeping gene, was selected as the endogenous control. Therefore, in each Q-PCR reaction, the C_t value for β-actin in both undifferentiated and differentiated cells was obtained and was defined as $C_{t,\beta u}$ and $C_{t,\beta d}$ respectively. At the same time, the C_t value for RyRIII, which was the target gene, could be obtained also and was defined as $C_{t,Ru}$ and $C_{t,Rd}$ respectively. As soon as the four Ct values were obtained, the calculation was carried out in the following way. Firstly, to make sure that the results were able to be used for quantitative calculation, the efficiency of the four amplifications, both endogenous controls and target DNA in both undifferentiated and differentiated cells, should be the same. Besides, the C_t values of endogenous control in both undifferentiated and differentiated cells, $C_{t,\beta u}$ and $C_{t,\beta d}$, should be the same also. Secondly, if $C_{t,\beta u}$ and $C_{t,\beta d}$ are similar and comparable, two ΔC_t values, which represent the difference of C_t values between endogenous

control and target gene in the same cell line, can be obtained. The ΔC_t for undifferentiated cells was defined as $\Delta C_{t,u} = C_{t,Ru} - C_{t,\beta u}$, and the ΔC_t for different cells was $\Delta C_{t,d} = C_{t,Rd} - C_{t,\beta d}$. Thirdly, the $\Delta\Delta C_t$ value, which was defined as $\Delta C_{t,d} - \Delta C_{t,u}$, can be calculated. Finally, the final result $2^{-\Delta\Delta C_t}$ can be calculated to determine what fold increase of RyRIII expression in the differentiated cells there is, compared with the undifferentiated counterpart.

3.2.3 Materials and facilities

For RNA extraction, the DNAse kit, including DNAseI buffer (10 ×), rDNAse 1 and DNAse inactivation reagent, was from Bioline and stored at -20 °C. DNAse RNAse free H_2O was from Invitrogen. The spectrophotometer (DU730) was from Beckman Coulter.

For the RT-PCR and electrophoresis, reverse transcription kit [including random primer (500 μg/mL), reaction buffer (5 ×), $MgCl_2$ (25 mM), reverse transcriptase and rRNAsin® RNAse inhibitor (40 u/μL)], dNTPs mix (10 mM each) and PCR kit [including green Go Taq flexi buffer (5 ×), $MgCl_2$ (25 mM) and Go Taq DNA polymerase (5 u/μL)] were from Promega. All primers were from Invitrogen. They were dissolved in Tris-EDTA buffer (TE, 10 mM Tris and 1 mM EDTA, pH was adjusted to 8.0) as 100 μM for stock and the stocks were diluted in nuclease free H_2O to 10 μM or 4 μM for PCR or sequencing respectively. All the reverse transcription kit, dNTPs mix, PCR kit and primers were stored at -20 °C. HyperLadder II (100 lanes, for 50 – 2,000 bp) was from

Bioline and was stored at 4 °C. The thermocycler for reverse transcription was from Perkin Elmer Cetus, the one for PCR was UNO-Thermoblock from Biometra. The electrophoresis tank was from Fisher Scientific and electrophoresis power supply was from Apelex. The UV system is a Dual-Intensity Transilluminator from Genetic Research Instrumentation Ltd, and the photography system is an Olympus camera with AlphaDigDoc RT software.

For Q-PCR, the kit, including Platinum® SYBR® Green qPCR SuperMix-UDG, ROX reference dye, $MgCl_2$ (50 mM) and bovine serum albumin (20 ×), is from Invitrogen and was stored at -20 °C. The thermocycler was an Opticon 2 DNA engine from MJ Research, GRII.

For gel purification and sequencing, the Gel purification kit, including Buffer QG for solubilisation, Buffer PE for washing and Buffer EB for elution, was from Qiangen. DNA loading buffer (5 ×) was from Bioline and was stored at 4 °C. Both R R Premix (Big Dye) and sequencing buffer were gifts from Dr. Bronwen Evans in School of Medicine, Cardiff University, and were stored at -20 °C. The R R Premix is light sensitive.

3.3 Results

3.3.1 Cell differentiation

NTERA-2 cells were treated with 10 μM retinoic acid for 4 weeks to

differentiate to human neurones, and SH-SY5Y cells were treated for 7 days for differentiation. The undifferentiated and differentiated cells are shown in Fig. 3.1 and Fig. 3.2 respectively.

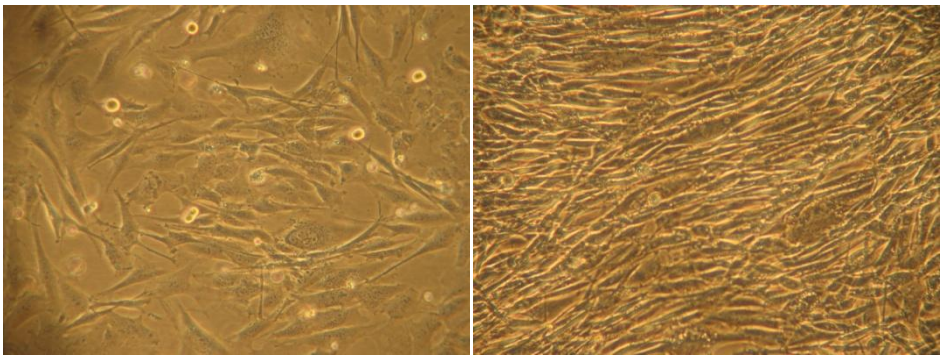

Fig. 3.1 NTERA-2 cell differentiation induced by 10 μM retinoic acid for 4 weeks (100 ×). The left hand panel shows what the NTERA-2 cells look like before differentiation, and the right hand one shows the morphology of the NTERA-2 cells after 4 weeks differentiation.

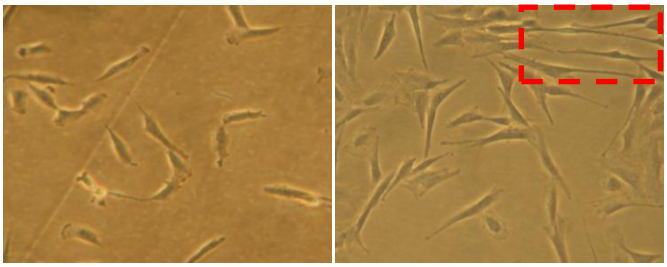

Fig. 3.2 SH-SY5Y cell differentiation induced by 10 μM retinoic acid for 7 days (100 ×). The left hand panel shows how the SH-SY5Y cells look before differentiation, and the right hand one shows the morphology of the SH-SY5Y cells after 1 week differentiation.

In this study, only the morphology of the cells has been used to evaluate the success of cell differentiation. From Figs 3.1 and 3.2, it can be seen that the both the differentiated NTERA-2 cells and the differentiated SH-SY5Y cells are more spindly than their undifferentiated counterparts respectively. A

previous study which has used morphology as the differentiation indicator has measured the neurite length (median). It was 4.7 for undifferentiated SH-SY5Y cells and was 5.4 after 5 days differentiation (Lovat et al., 1997). The difference in neurite length between undifferentiated and differentiated SH-SY5Y cells in this study is actually more obvious, especially in those cells shown in the red square (see Fig. 3.2). Thus, it can be surmised that the cells had been differentiated successfully.

3.3.2 Primer design

The primers were designed online as outlined above (see Section 2.5). Among those candidate primers, the one expected to produce a product with the higher percentage, i.e. closest similarity to the target gene, was selected.

The sequence of primers, as well as relevant information for β-actin, RyRI, RyRII and RyRIII are listed below in Table 3.3:

3.3.3 PCR condition optimisation

The results of those experiments are shown in Figs. 3.3 - 3.9.

Comparing Figs. 3.3, 3.4 and 3.6, it can be seen that 40 or 50 cycles are too much for the RyRIII amplification. There were multiple bands after 40 or 50 cycles, whereas the PCR amplification was expected to generate a clear and

Table 3.3 Primers for β-actin, RyRI, RyRII and RyRIII (Homo sapiens)

Primers		Gene description	Primer sequence	Product size	PCR conditions recommended by Primer III
β-actin	Forward	Actin, beta (ACTB), mRNA. 1,852 bases	5'-cccagccatgtacgttgcta	126 bp	55 °C, 40 cycles
	Reverse		5'-agggcataccctcgtagatg		
RyRI	Forward	Ryanodine receptor 1 (skeletal) (RyR1), transcript variant 1, mRNA. 15,391 bases	5'-catcagcacgacatgagctt	241 bp	58 °C, 30 cycles
	Reverse		5'-tgttgctctctttgccattg		
RyRII	Forward	Ryanodine receptor 2 (cardiac) (RyR2), mRNA. 16,365 bases	5'-caaccggactcgtcgtattt	249 bp	58 °C, 30 cycles
	Reverse		5'-ttggctttctctttggctgt		
RyRIII	Forward	Ryanodine receptor 3 (RyR3), mRNA. 15,563 bases	5'-gaaagtgtgaaacgcagcaa	211 bp	58 °C, 30 cycles
	Reverse		5'-gcaggaagactgctggaaac		

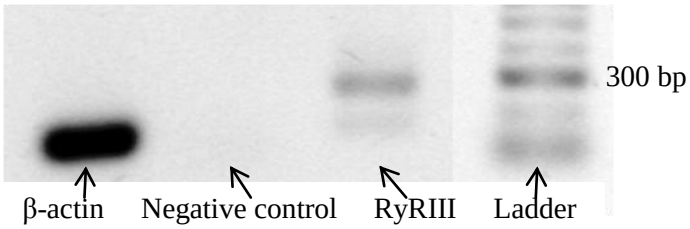

Fig. 3.3 RyRIII in N2102Ep, 55 °C, 30 cycles, 1.5 mM Mg^{2+}. The negative control is clear and clean and the positive control (β-actin) is shown as a single clear band, which means the cDNA sample qualifies. The RyRIII band is not sufficiently clear.

specific band. 30 cycles were deemed to be the optimum number of cycles for RyRIII amplification. Comparing Figs. 3.5 and 3.7, it can be seen that the optimum [Mg^{2+}] is 1.5 mM, rather than any other concentration. When the

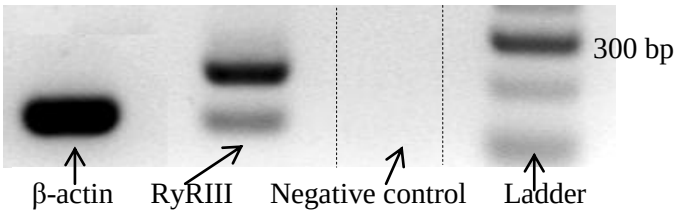

Fig. 3.4 RyRIII in N2102Ep, 55 °C, 40 cycles, 1.5 mM Mg^{2+}. The RyRIII band is clear, but the band is not specific.

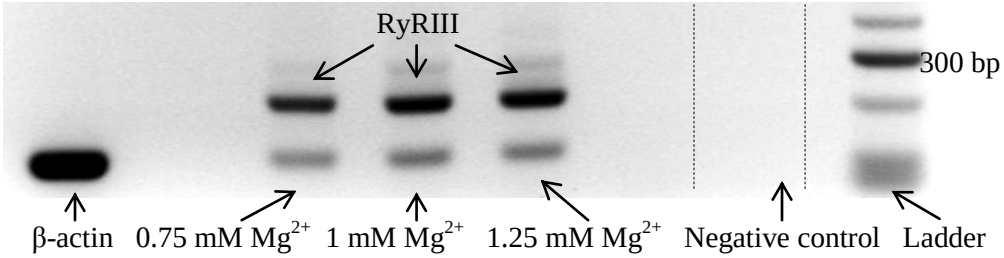

Fig. 3.5 RyRIII in N2102Ep, 58 °C, 30 cycles. The RyRIII band is clear but unspecific.

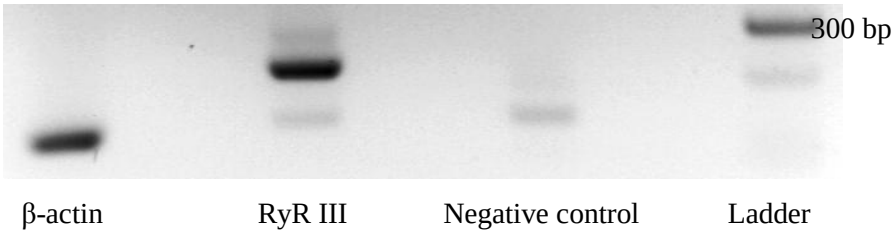

Fig. 3.6 RyRIII in N2102Ep, 55 °C, 50 cycles, 1.5 mM Mg^{2+}. The RyRIII band is clear but unspecific. There is also a weak band in the negative control, suggesting that 50 cycles are too many.

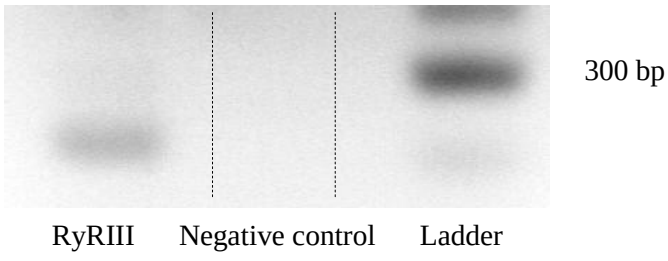

Fig. 3.7 RyRIII in N2102Ep, 58 °C, 30 cycles, 1.5 mM Mg^{2+}. The RyRIII band is clear and specific, just a little weak.

[Mg^{2+}] was 1.25 mM, 1.0 mM or 0.75 mM, there were unexpected bands in the

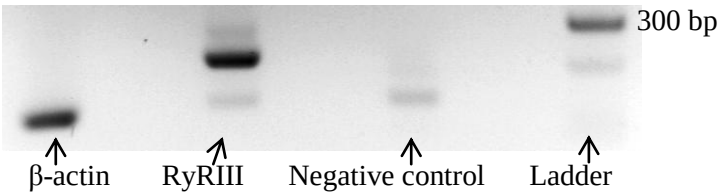

Fig. 3.8 RyRIII in N2102Ep, 58 °C, 40 cycles, 1.5 mM Mg^{2+}. The RyRIII band is clear but unspecific. There are bands in the negative control

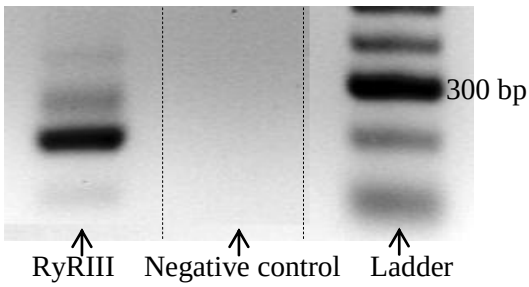

Fig. 3.9 RyRIII in N2102Ep, 60 °C, 30 cycles, 1.5 mM Mg^{2+}. The RyRIII band is clear but unspecific. There are multiple bands in the amplification of RyRIII.

RyRIII amplification as shown in Fig. 3.5. Thus, the optimum [Mg^{2+}] after the PCR condition optimisation was found to be 1.5 mM. Comparing Figs. 3.3, 3.7 and 3.9, it is clear that 55 °C was too low an annealing temperature since the RyRIII band was not clear, but 60 °C was too high since unspecific amplification products were produced. Comparing Figs. 3.7 and 3.8, it can be further confirmed that 40 cycles were too many for RyRIII amplification since extra bands appeared. Thus, the optimised PCR condition for the RyRIII amplification was 58 °C as the annealing temperature, 30 cycles as the number of cycles, and 1.5 mM as the [Mg^{2+}].

3.3.4 PCR

After the PCR conditions were optimised, the PCR was performed on those cell lines above. The following PCR results show the RyRs amplification in the following cell lines: MG-63, MOG-G-UVW, N2102Ep, undifferentiated NTERA-2, differentiated NTERA-2, undifferentiated SH-SY5Y and differentiated SH-SY5Y.

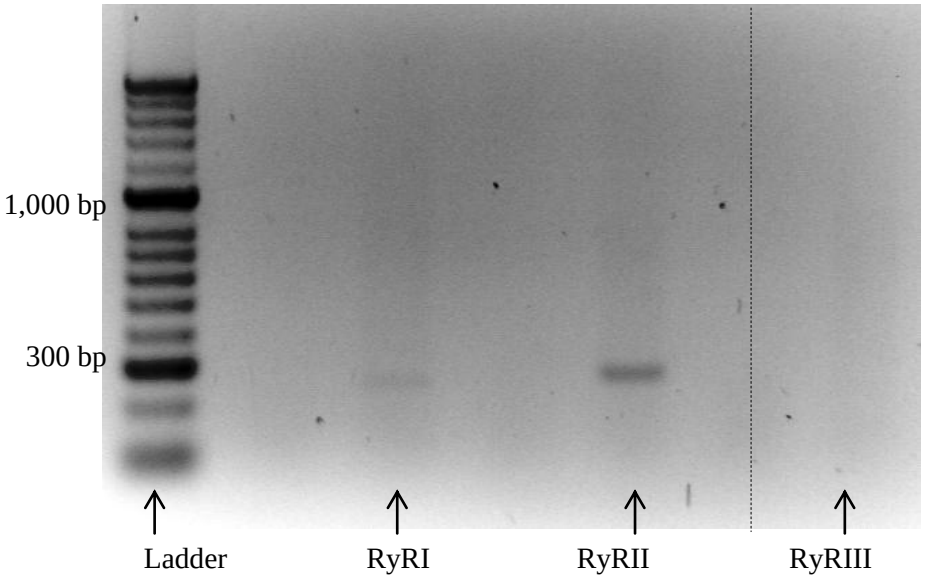

Fig 3.10 RyR isoforms in the MG-63 cell line.

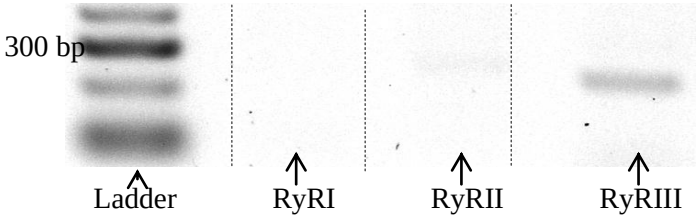

Fig. 3.11 RyR isoforms in the MOG-G-UVW cell line

Fig. 3.12 RyR isoforms in the N2102Ep cell line.

Fig. 3.13 RyR isoforms in the undifferentiated NTERA-2 cell line

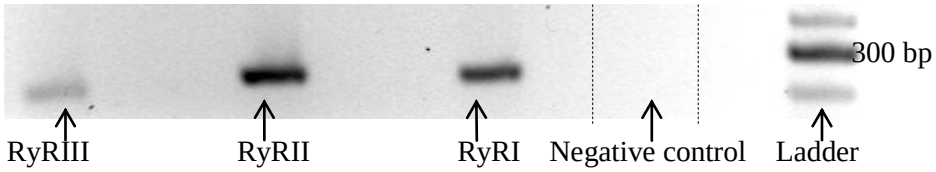

Fig. 3.14 RyR isoforms in the differentiated NTERA-2 cell line.

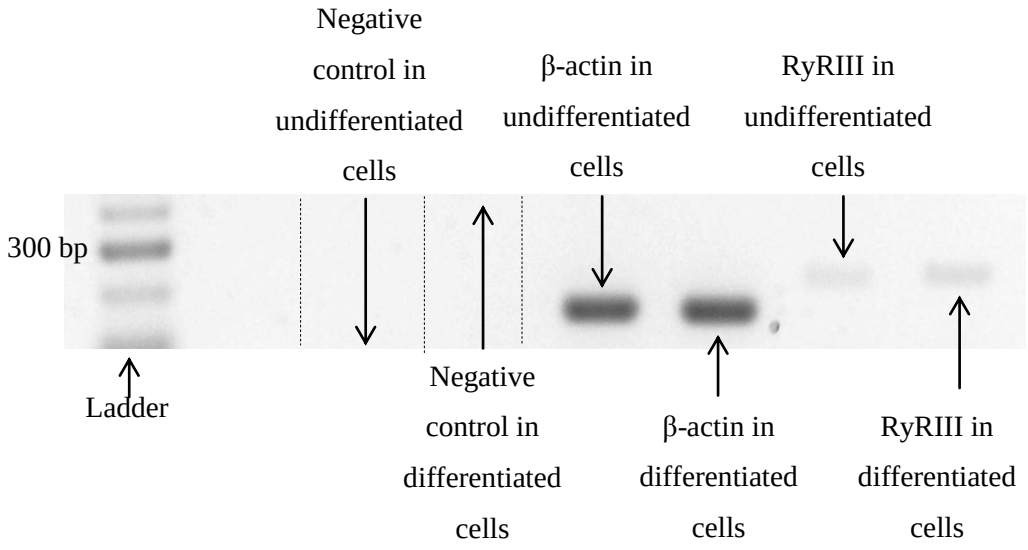

Fig. 3.15 RyRIII in SH-SY5Y cell line.

From the data above, it can be seen that there was little RyRIII message in MG-63 cells. However, there is RyRIII message in astrocytes, such as MOG-G-UVW, and the RyRIII band was stronger than for the other two isoforms. In NTERA-2 cells, the RyRIII expression was quite strong before the differentiation but was weaker after the differentiation. Conversely, the opposite was true during the differentiation of SH-SY5Y, since the RyRIII expression was stronger in the differentiated ones. The result of PCR indicates

the existence of certain messages, but does not measure the expression quantitatively. So, Q-PCR was carried out after the band from PCR had been confirmed with sequencing.

3.3.5 Sequencing

As soon as the PCR condition had been optimised for RyRIII, large amount amplification was performed to generate the high concentration of the DNA fragment of RyRIII, in order to check that the sequence of the DNA fragment generated could be confirmed as RyRIII. Fig. 3.16 shows a PCR of large amount amplification of RyRIII. The cDNA used here was the sample obtained from the undifferentiated NTERA-2 cells.

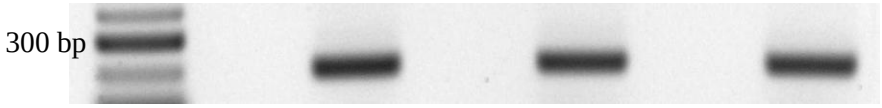

Fig. 3.16 Large amount amplification of RyRIII from the undifferentiated NTERA-2 cell line.

After the bands were cut down under UV light and the gel slices were purified, the sequencing process was performed. The result from Central Biotechnology Services, School of Medicine, Cardiff University is shown in Fig. 3.17.

From these data, the sequence of this sample is:

TGAGGGATTGGAACTTTACTCTTCTCCATGGCTATCAGAGATTTTGG

ATAGAAACAGAGGAGTATTCCTTTGAAGAGAAACTAGTACAGGATT

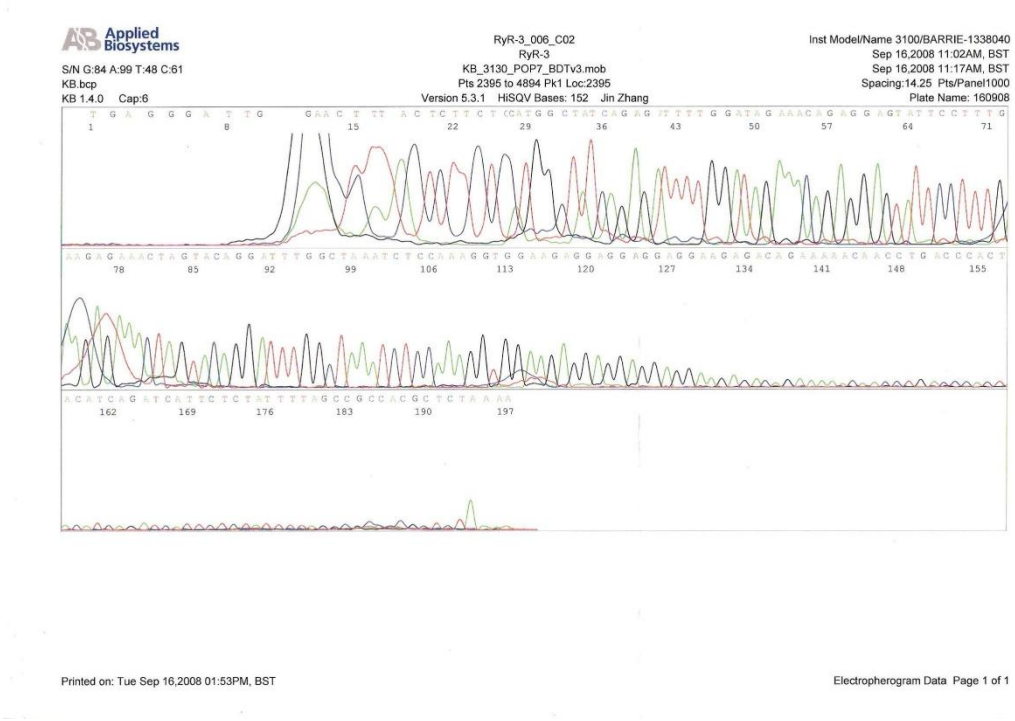

Fig. 3.17 Sequencing result of RyRIII

TGGCTAAATCTCCAAAGGTGGAAGAGGAGGAGGAGGAAGAGACAG
AAAAACAACCTGACCCACTACATCAGATCATTCTCTATTTTAGCCGC
CACGCTCTAAAA.

The blast test was run afterwards, and the percentage of the sequence above is 88% homologous to RyRIII. Thus, it can be confirmed that the product from the PCR was RyRIII, and the PCR conditions and primers were legitimate for use for Q-PCR, which is a quantitative test of the expression.

3.3.6 Q-PCR

Q-PCR was first performed to test the RyRIII expression during the

differentiation of NTERA-2 cells. Fig. 3.18 below shows the fluorescence graph of the negative controls and Figs. 3.19, 3.20 show the melting curve of negative controls to demonstrate the purity of the cDNA sample.

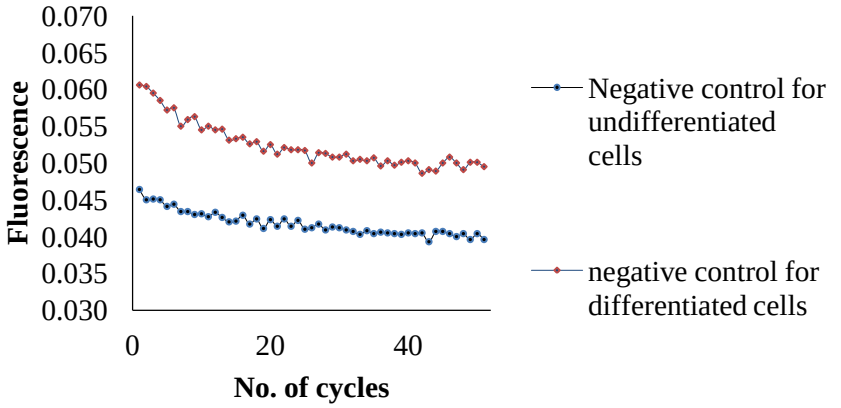

Fig. 3.18 Fluorescence of the negative controls in Q-PCR in the NTERA-2 cell line. Note that both two lines are flat and the fluorescence has not increased even after 50 cycles.

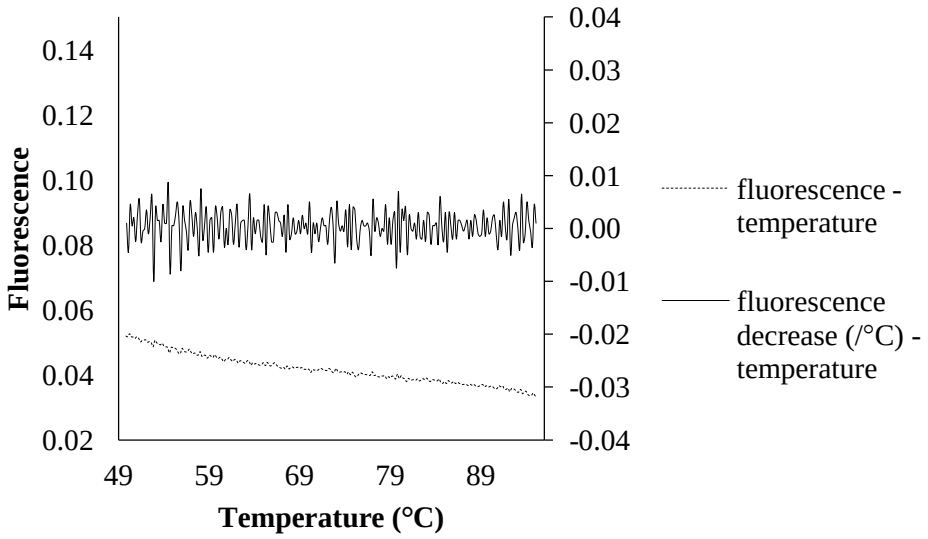

Fig. 3.19 The melting curve of negative control in undifferentiated NTERA-2 cells. There is no peak appearing in the fluorescence decrease curve, which means that the sample is not contaminated.

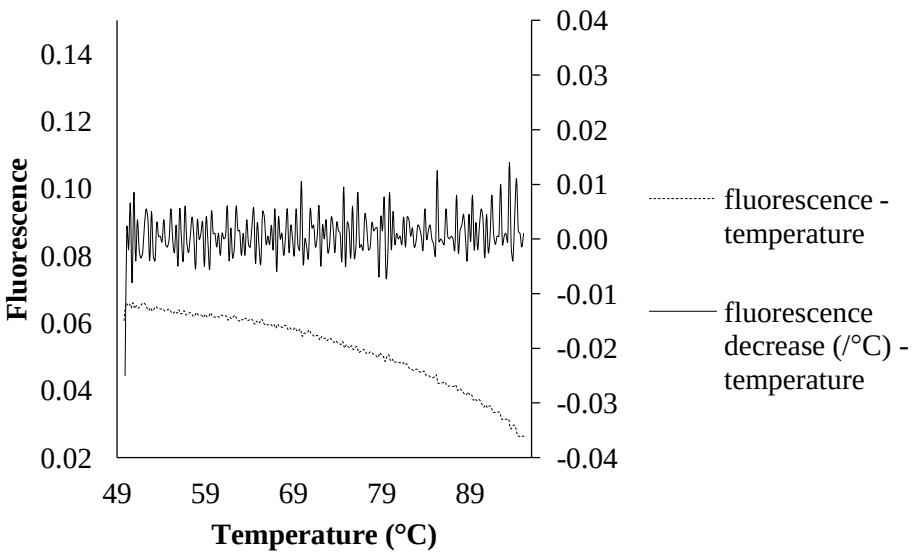

Fig. 3.20 The melting curve of the negative control in differentiated NTERA-2 cells. There is no peak in the fluorescence decrease curve, which means that the sample is not contaminated.

From Figs. 3.18 – 3.20, it can be concluded that the samples and reagents were clean enough and no nuclease contamination existed in the samples. Figs. 3.21 and 3.22 show the melting curve of the positive control, β-actin which is an endogenous control, in both undifferentiated and differentiated NTERA-2 cells to demonstrate the purity.

From the Figs. 3.21 and 3.22, it can be concluded that the samples were clean and purified, and the PCR conditions were fit for the endogenous control, β-actin, since only one single product was amplified. Figs. 3.23 and 3.24 demonstrates the melting curve of RyRIII in both undifferentiated and differentiated cells.

From Figs. 3.23 and 3.24, it can be concluded that the samples were clean and

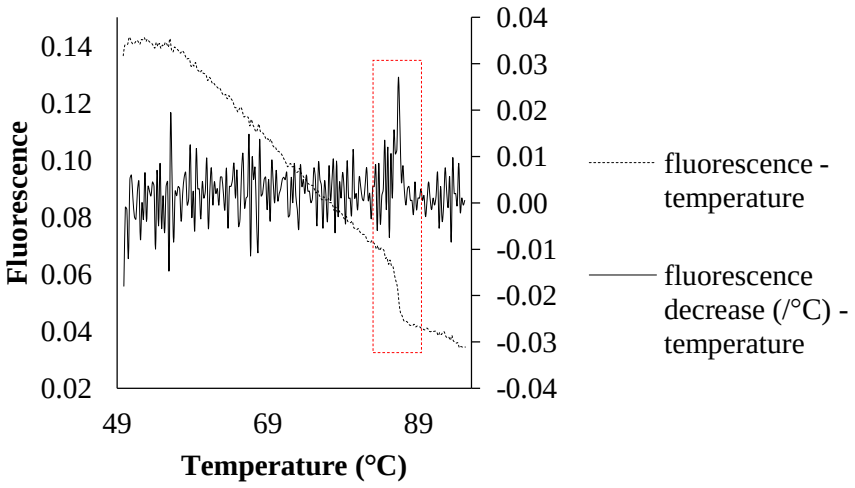

Fig. 3.21 The melting curve of the endogenous control in undifferentiated NTERA-2 cells. There is only a single peak in the fluorescence decrease – temperature curve, which means that the purity is acceptable.

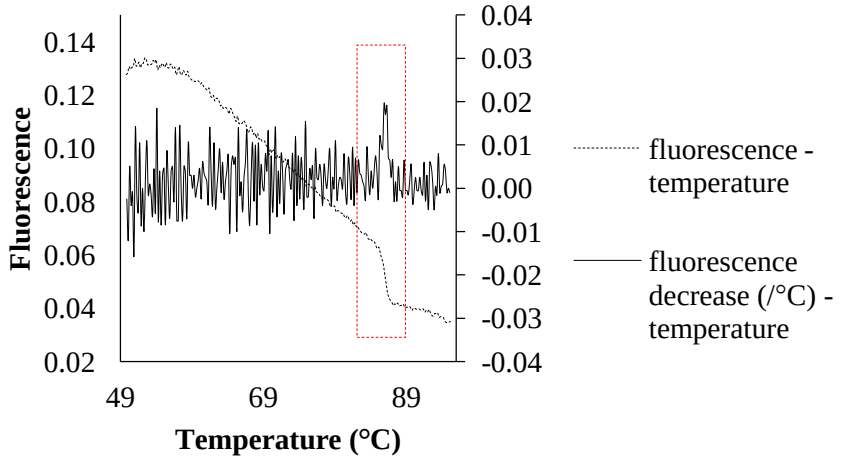

Fig. 3.22 The melting curve of the endogenous control in differentiated NTERA-2 cells. There is only a single peak in the fluorescence decrease – temperature curve, which means that the purity is acceptable.

purified, and the PCR conditions were fit for the target gene fragment, RyRIII, since only one product was amplified.

Before running the Q-PCR to measure RyRIII quantitatively, efficiency of

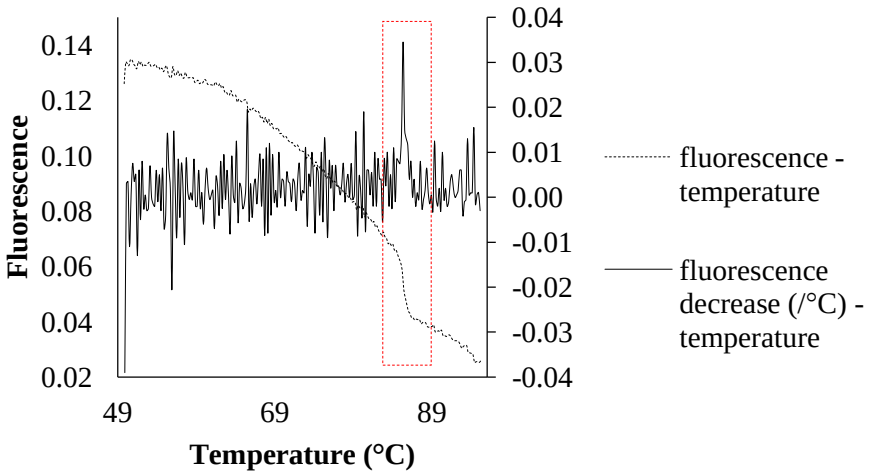

Fig. 3.23 The melting curve of RyRIII in undifferentiated NTERA-2 cells. There is only a single peak in the fluorescence decrease – temperature curve, which means that the purity is acceptable.

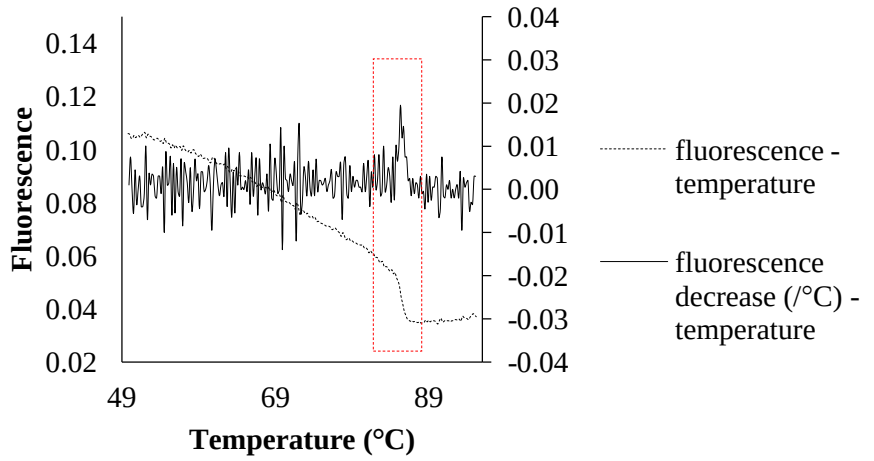

Fig. 3.24 The melting curve of RyRIII in differentiated NTERA-2 cells. There is only a single peak in the fluorescence decrease – temperature curve, which means that the purity is acceptable.

amplification of both endogenous control (β-actin) and target gene (RyRIII) was tested.

The slope in Fig. 3.25 for β-actin is 3.024. Efficiency (E) is:

Table 3.4 C_t values in β-actin standard curve

Times of dilution	1	10	10^2	10^3	10^4	10^5	10^6	10^7	10^8	10^9
C_t value	9	18	16	21	23	24	27	31	36	40

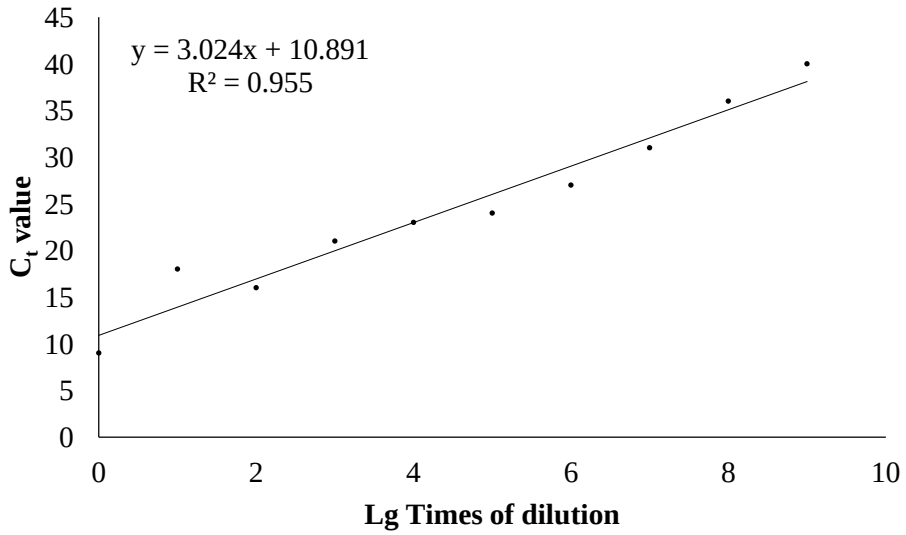

Fig. 3.25 Standard curve of β-actin

$$E = 10^{(\frac{1}{\text{slope}})} - 1,$$

so

$$E_{\beta\text{-actin}} = 10^{(\frac{1}{3.024})} - 1 = 1.1$$

Table 3.5 C_t values in RyRIII standard curve

Times of dilution	1	10	10^2	10^3	10^4	10^5	10^6	10^7	10^8	10^9
C_t	7	12	15	20	23	28	38	36	38	41

The slope in Fig. 3.26 for RyRIII is 3.952. Efficiency is:

$$E_{\text{RyRIII}} = 10^{(\frac{1}{3.952})} - 1 = 0.8$$

Both of the efficiencies are close to 1 and are acceptable for Q-PCR

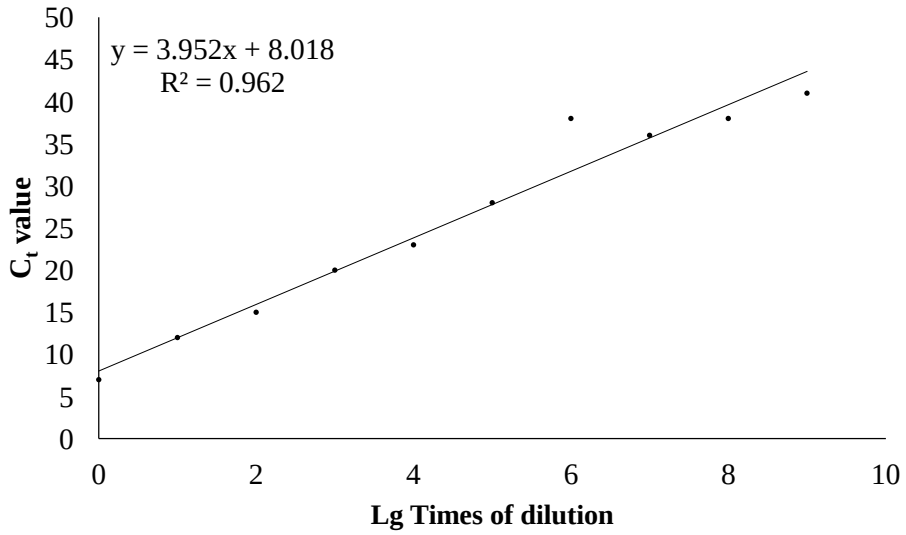

Fig. 3.26 Standard curve of RyRIII

comparison.

Hence, the results, ΔC_t, generated from different groups of Q-PCR could be used for analysis. The results and analysis are tabulated in Table 3.6, and the results are presented in Fig. 3.27.

Table 3.6 Q-PCR results of RyRIII in NTERA-2 cell line

Duplicate	Samples	Ct	ΔCt	ΔΔCt	Average, p, $2^{-\Delta\Delta C_t}$
Experiment 1	β-actin, undifferentiated	20.41	11.61	5.90	Average: 5.11 p < 0.05 $2^{-\Delta\Delta C_t}$ = 0.0290
	RyRIII, undifferentiated	32.02			
	β-actin, differentiated	19.49	17.51		
	RyRIII, differentiated	37.00			
Experiment 2	β-actin, undifferentiated	20.74	14.60	4.32	
	RyRIII, undifferentiated	35.34			
	β-actin, differentiated	25.88	18.92		
	RyRIII, differentiated	44.80			

From these tables and figures in this section, it may be concluded that the

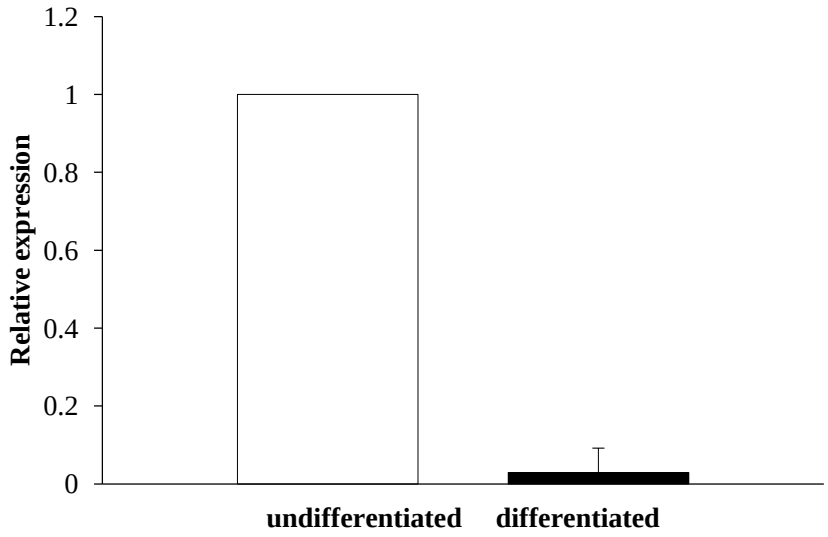

Fig. 3.27 Q-PCR result of RyRIII expression during the differentiation of NTERA-2 cells. It is clear that the relative expression of RyRIII was reduced after differentiation, compared with the undifferentiated counterpart.

RyRIII expression was "turned down" during the retinoic acid induced differentiation in NTERA-2 cells.

In addition to the NTERA-2 cell line, another neuroblastoma cell line, SH-SY5Y was also selected for Q-PCR tests of the RyRIII expression change during differentiation.

Firstly, the purity of the samples was tested from the Q-PCR of the negative control.

From the Figs. 3.28 – 3.30, it can be seen that nothing was amplified in the negative control samples of both undifferentiated and differentiated SH-SY5Y cells during the Q-PCR, hence, it can be concluded that the sample is clean and

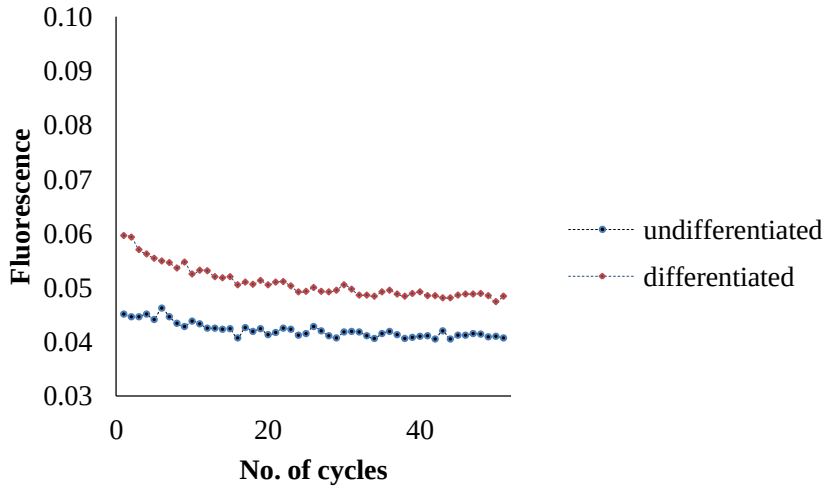

Fig. 3.28 Negative control in both undifferentiated and differentiated SH-SY5Y cells. It is suggested by the fluorescence curve that nothing was amplified.

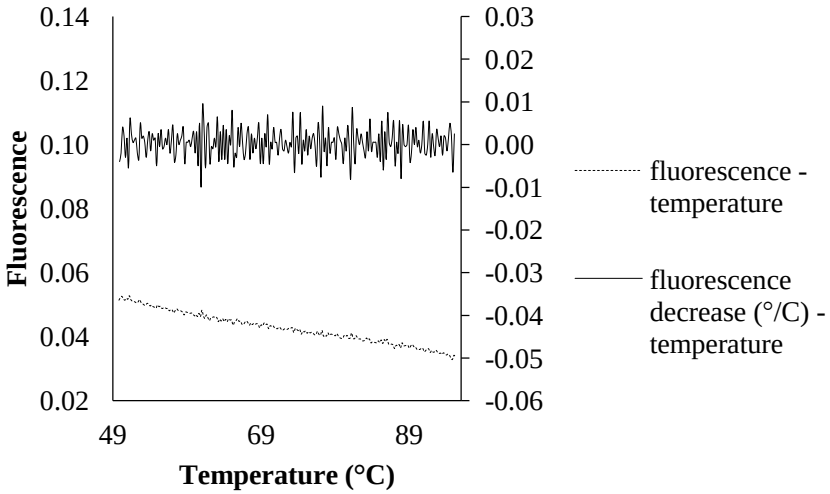

Fig. 3.29 The melting curve of the negative control in undifferentiated SH-SY5Y cells. No peak was observed.

pure enough for further experiments.

In the Figs. 3.31 and 3.32, only one single peak was observed in each graph, which means the endogenous control is pure and clean. Two melting curve figures for the RyRIII amplification in both undifferentiated and differentiated

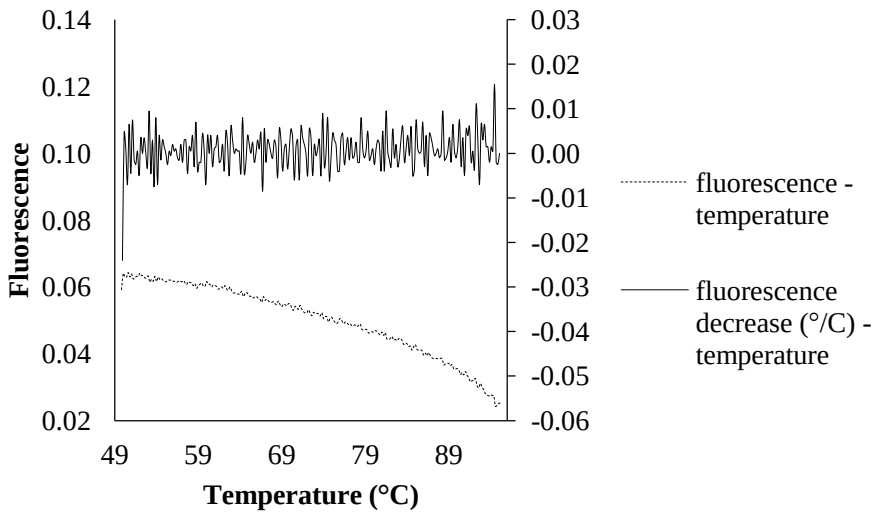

Fig. 3.30 The melting curve of the negative control in differentiated SH-SY5Y cells. No peak was observed.

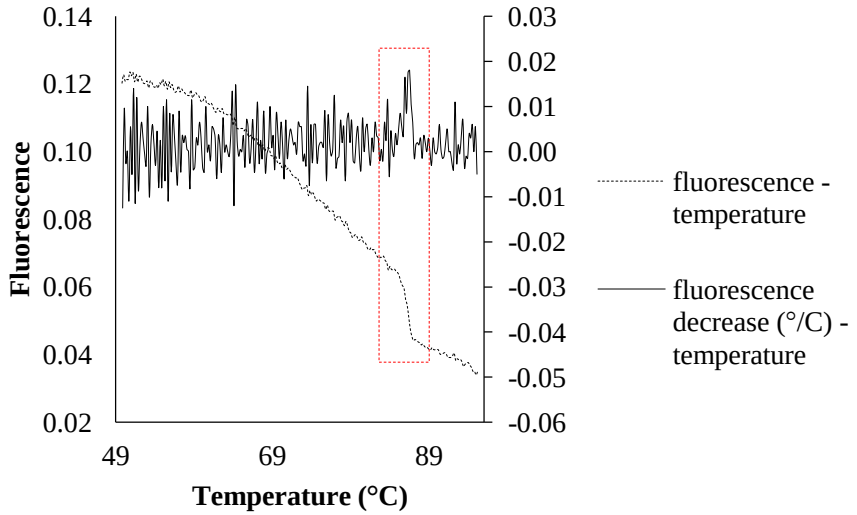

Fig. 3.31 The melting curve of endogenous control, β-actin, in undifferentiated SH-SY5Y cells. Only one single peak was observed in the curve.

SH-SY5Y cell are shown in Figs. 3.33 and 3.34.

Based on the confirmation of the purity of the samples, Q-PCR was performed and repeated in triplicate. The results are tabulated below in Table 3.7 and Fig.

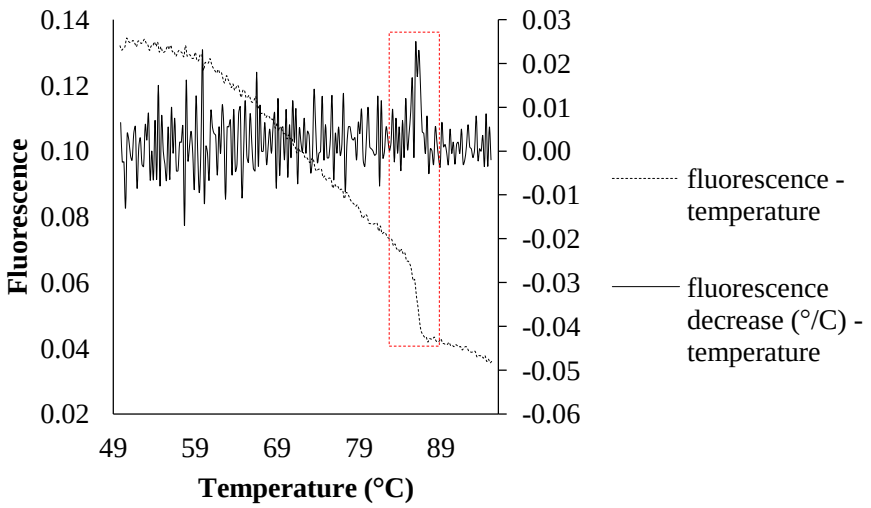

Fig. 3.32 The melting curve of endogenous control, β-actin, in differentiated SH-SY5Y cells. Only one single peak was obtained in the curve.

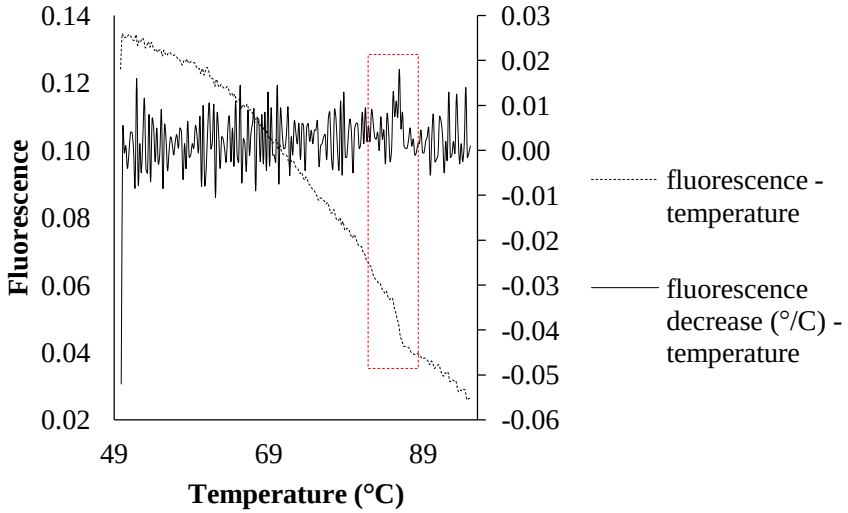

Fig. 3.33 The melting curve of RyRIII in undifferentiated SH-SY5Y cells. Only one single peak was observed in the curve.

3.35.

From the Table 3.7 and Fig. 3.35 in this section, it can be observed that the RyRIII expression in SH-SY5Y cells was increased after the differentiation

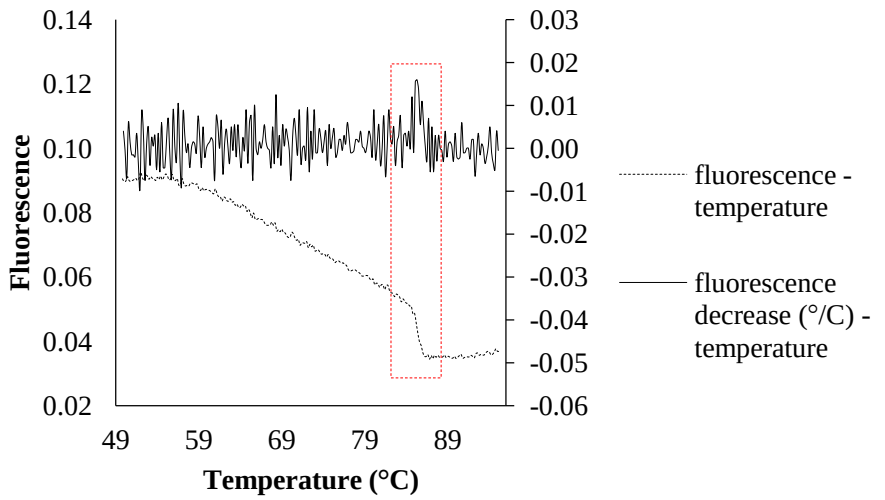

Fig. 3.34 The melting curve of RyRIII in differentiated SH-SY5Y cells. Only one single peak was observed in the curve.

Table 3.7 Q-PCR results of RyRIII expression in SH-SY5Y cell line

Triplicate	Samples	C_t	ΔC_t	$\Delta\Delta C_t$	Average (standard error), $2^{-\Delta\Delta C_t}$
Experiment 1	β-actin, undifferentiated	22.51	15.96	-3.88	Average: -2.68 (0.735) $2^{-\Delta\Delta C_t} = 6.41$ $p < 0.05$ (t test)
	RyRIII, undifferentiated	38.47			
	β-actin, differentiated	23.89	12.08		
	RyRIII, differentiated	35.97			
Experiment 2	β-actin, undifferentiated	26.07	20.76	-2.06	
	RyRIII, undifferentiated	46.83			
	β-actin, differentiated	22.08	18.70		
	RyRIII, differentiated	40.78			
Experiment 3	β-actin, undifferentiated	23.14	15.64	-2.01	
	RyRIII, undifferentiated	38.78			
	β-actin, differentiated	24.51	13.54		
	RyRIII, differentiated	38.05			

induced by retinoic acid.

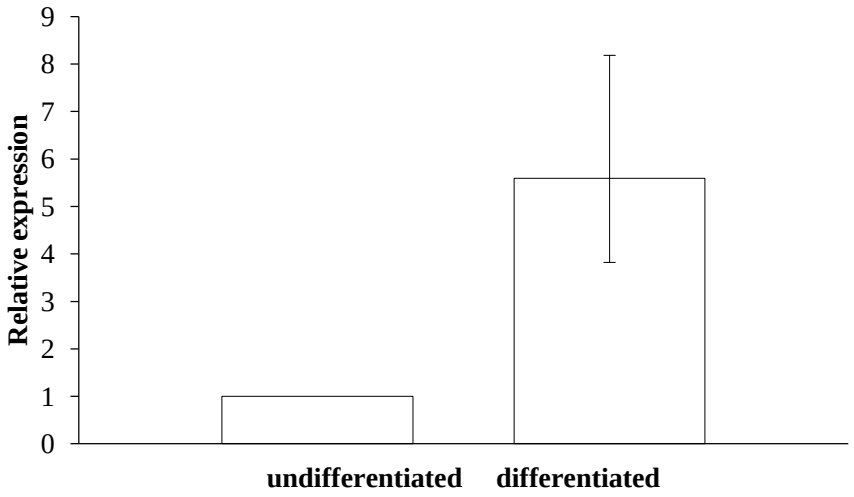

Fig. 3.35 The relative expression of RyRIII in SH-SY5Y cells before and after retinoic acid induced differentiation.

3.4 Discussion

The principal result here is that in SH-SY5Y cells, which are presumed differentiated, there is a significantly higher expression of RyRIII (the opposite results in NTERA-2 cells are discussed later on p99-100). It is worth considering first the evidence that these cells have become differentiated.

Cell differentiation can be tracked using neuronal markers, however, how successful an approach this is, remains arguable. For example, PCR for growth-associated-protein 43 (GAP-43) was used as a neuronal marker in norepinephrine induced SH-SY5Y differentiation (Laifenfeld et al., 2002). A western blot study however has failed to demonstrated any difference of GAP-43 expression in SH-SY5Y cells before and after retinoic acid induced differentiation (Joshi et al., 2007).

Besides neuronal markers, other studies accept confirmation of differentiation from the morphology of the cells (Lovat et al., 1997). Since cells which differentiate to human neurones should have budding synapses, successfully differentiated cells should be spindly, while undifferentiated ones remain round. Figure 3.36 shows a sample of differentiated SH-SY5Y cells in a previous study (Lovat et al., 1997).

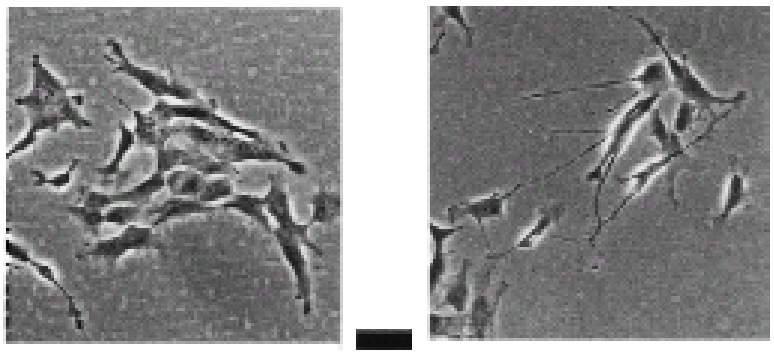

Fig. 3.36 Retinoic acid induced differentiation of SH-SY5Y cells (Lovat et al., 1997). The left hand panel shows the undifferentiated SH-SY5Y cells, and the right hand one shows the differentiated ones. The bar is 10 μm.

Some studies use no evaluation, simply following the standard differentiation protocol and assumed that the cells were differentiated after the standard protocol has been adopted (Tieu et al., 1999).

In this study, a change in morphology was assessed to evaluate whether the cells were differentiated or not, although morphology is a subjective indicator and is not always easy to accept. For example, in the study above which has used morphology to evaluate the differentiation (Lovat et al., 1997), there was limited difference in morphology observed between the undifferentiated and

differentiated SH-SY5Y cells. But in this study, it was noticed that both the differentiated NTERA-2 and the differentiated SH-SY5Y cells were characterised by elongated processes in comparison to the undifferentiated counterparts. These processes are perhaps indicative of budding synapses.

In the PCR results, it was clear that RyRIII is almost non existent in MG-63 cells, which are a human osteosarcoma cell line, but exists in MOG-G-UVW, N2102Ep, NTERA-2 and SH-SY5Y cells, which are astrocytoma, neuronal cells or cells with the potential to be differentiated to neurones. These results were consistent with previous studies which suggested that RyRIII is the prevalent RyR in the brain.

If RyRIII is believed to be the brain type of ryanodine receptor, the expectation might be that there would be a higher expression in the differentiated neurones, rather than the undifferentiated or any other cells. However, according to the Q-PCR results from NTERA-2 cells reported here, the RyRIII expression was decreased after the differentiation, although the morphology suggested that the NTERA-2 cells had more processes. The differentiated PCR figures also confirmed this finding (see Fig. 3.13 and 3.14). The possible explanation for this is that RyRIII does not exist in neurones only, but is also present in some other organs and tissues, for example epithelial lung cells (mink) (Sorrentino, 1995) and germ cells (Giannini et al., 1995). The latter was confirmed in PCR investigating RyRs in N2102Ep cell line, which is a non seminomatous germ cell carcinoma derived cell line. Fig. 3.12 has shown that RyRIII was highly

expressed in the N2102Ep cells. That may be consistent with RyRIII presenting a high expression in undifferentiated NTERA-2 cells since both N2102Ep and undifferentiated NTERA-2 cells are human embryonal carcinoma.

Nevertheless in contrast, the differentiation of SH-SY5Y cell line was accompanied by an increased RyRIII expression. The RT-PCR results from SH-SY5Y cell line suggested that the RyRIII expression was increased after retinoic acid induced differentiation (see Fig. 3.15). Importantly, the difference was confirmed and was significant in Q-PCR as well.

But, the increase of RyRIII expression does not necessarily mean an increase of the total RyR present, since the expression of the other two isoforms have not been tested. The increase of RyRIII expression only means the cells are more "neuronal" since RyRIII is the brain type ryanodine receptor. Nevertheless, what the difference is amongst three isoforms of RyR in terms of function, and why brain neurones require more RyRIII than the other types of cells do, has seldom been discussed previously. In this study, the expression of RyRIII in SH-SY5Y cell line has been linked with the resistance to insults and the response to RyR modulators. The relevant data are now presented in Chapter 4 and Chapter 5.

3.5 Conclusion

To summarise the results above, it is suggested that RyRIII may have a higher

expression in a neuronal cell line than it has in most other organs, but germ or embryonal carcinoma might be an exception. Therefore, the SH-SY5Y cell line was selected as the primary cell model in future work, although MOG-G-UVW and NTERA-2 cells were not overlooked.

The main purpose or aim of this thesis was not solely to find out where RyRIII was expressed, but to assay its role in neurodegeneration, and to ascertain whether it could be a potential target for the neurodegeneration treatment. If RyRIII is believed to play an important role in neurodegeneration, especially in neuronal death, the cell line which has a higher RyRIII expression (i.e. differentiated SH-SY5Y) should be more sensitive to the counterpart which has a lower RyRIII expression (i.e. undifferentiated SH-SY5Y). Hence, cell insult models were established next. In order to test the relative sensitivities of differentiated SH-SY5Y cells and undifferentiated ones, modulators, including RyR modulators, were then tested in those models.

4. Cell Insult Models

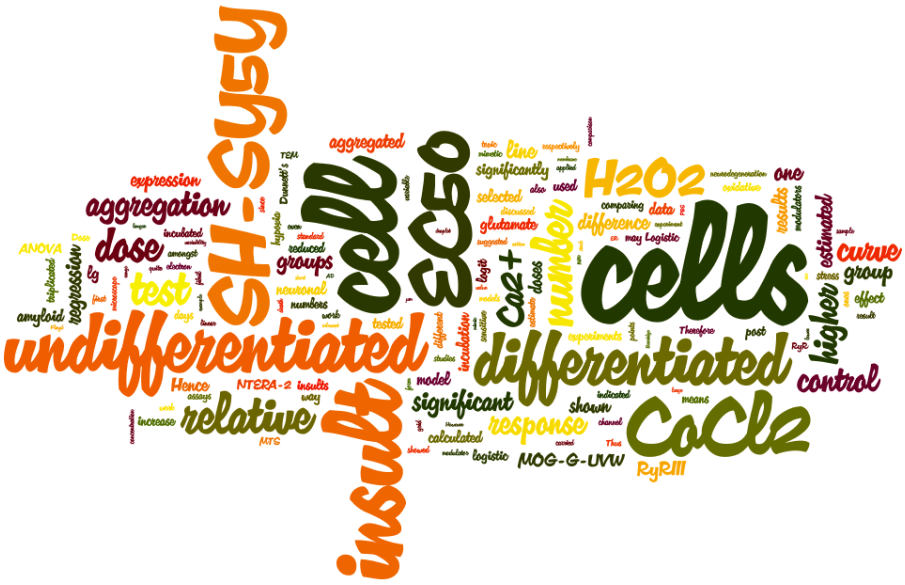

4. Cell Insult Models

4.1 Introduction

A number of cell insults can mimic or trigger neurodegeneration or cell death. The cell insult models used here were tested in cell proliferation and MTS assays, and were established to find the kind of insults which could be deployed to mimic neurodegeneration.

Obviously, since one proposed hypothesis of AD is the deposition of Aβ on the cell membrane, Aβ is the insult which is closest to AD. $A\beta_{1-42}$ was therefore selected as an insult in this work and has been proved to be toxic to neuronal cells in previous cell proliferation and assays studies (Tweedie et al., 2006, Mulder et al., 2003, Folin et al., 2005).

$A\beta_{1-42}$ is however expensive, is not easy to use since it has to be aggregated to fibrils to cause insult to cells (Ueda et al., 2002), hence some alternative models were adopted also. As discussed in the introduction, the toxic function of $A\beta_{1-42}$ may be via formation of a Ca^{2+} channel on the cell membrane with a resultant increase in $[Ca^{2+}]_i$ (Arispe et al., 2007, Berridge, 2010). An alternative model should thus mimic neurodegeneration by reducing cell viability through increasing the $[Ca^{2+}]_i$.

To achieve this, hypoxia induced by $CoCl_2$ was selected as another neuronal

insult in this project. Hypoxia was studied as a model of neurodegeneration of relevance to Alzheimer's disease (Bazan et al., 2002, Gasperi et al., 2010). $CoCl_2$ has been used as a hypoxia mimetic (Gasperi et al., 2010), and was found to increase the generation of Aβ via up-regulating the expression of APP as well as the expression of β-secretase and γ-secretase (Zhu et al., 2009). Hence, it is reasonable to propose that $CoCl_2$ induced hypoxia can be used as a neuronal insult to challenge cells and to test modulators.

Besides the hypoxia mimetic challenge, oxidative stress induced by H_2O_2 was selected as a cell insult model. Previous studies have suggested a link between oxidative stress and neurodegeneration, such as AD (Lin and Beal, 2006, Floyd, 1999, Floyd and Hensley, 2002). H_2O_2 is a freely diffusible form of reactive oxygen species and has been used as oxidative stress model (Ishimura et al., 2008), and can increase $[Ca^{2+}]_i$ (Krebs et al., 2007). Therefore, H_2O_2 was selected as a second neuronal insult model here to challenge the cells and test modulators.

In addition to $CoCl_2$ and H_2O_2 insults, glutamate is another insult model which has been previously studied and linked with neurodegeneration. Glutamate can increase $[Ca^{2+}]_i$ and induce neurodegeneration and such an effect can be prevented by the blockade of muscarnic receptor (Mattson, 1989). One other study also believed that glutamate-induced stimulation of NMDA receptors mediates toxic increases in $[Ca^{2+}]_i$ (Dolga et al., 2011)

4.2 Methods and materials

The cell insult model was based on the methods of cell proliferation and MTS assay described in section 2.11.

In the $A\beta_{1-42}$ insult model, amyloid can be incubated and aggregated, and its aggregation viewed by electron microscope. This method is going to be discussed in section 4.2.1 under $A\beta_{1-42}$ aggregation.

For all the three insults, especially in the case of the $CoCl_2$ and H_2O_2 insult, a range of dosages of "insult" (100 nM – 1 mM) were selected to estimate the relevant EC_{50} (half maximal effective concentration), i.e. a dosage to kill 50% of cells reducing the relative cell number to be 0.5. The EC_{50} of $CoCl_2$ or H_2O_2 of each cell line was then set as standard insult for further test of modulators. This chapter discusses how the EC_{50} was estimated for each insult and each cell line.

4.2.1 $A\beta_{1-42}$ aggregation

As discussed in the introduction (see Chapter 1), soluble APP does not induce cell apoptosis directly, it generates the Aβ which is deposited on the cell membrane as plaques and putative Ca^{2+} channels may be formed. The toxic effect of aggregated $A\beta_{1-42}$ has previously been studied on both dog (Torp et al., 2000) and human (Roher et al., 1993) tissues. The $A\beta_{1-42}$ sample was incubated

to induce aggregation and examined under the electron microscope before being adopted as an insult to the cells.

To form aggregates and fibres, the $A\beta_{1-42}$ sample was dissolved in PBS at 100 μM and incubated at 37 °C for a few days. The incubation duration was variable from 3 days (Qahwash et al., 2007) to 6 days (Fülöp et al., 2004). In this work, the longest incubation period, 1 week, was selected.

The incubated $A\beta_{1-42}$ solution was sampled and diluted for transmission electron microscope (TEM) study. A 50 μL droplet of 1 μM solution was laid on a clean surface and the droplet was incubated on the surface of the grid. After passing the grid from droplet to droplet, the suspension of specimen was incubated on the grid for about 15 min. Then, the sample was treated with 1% glutaraldehyde in buffer for about 10 min. Thereafter, it was washed 3 times with buffer with 1 min washing each time and 6 times with H_2O. Finally, it was treated with 2% aqueous uranyl acetate $[UO_2(CH_3COO)_2 \cdot 2H_2O]$ for about 5 min. The grid was picked up on tweezers and dried at room temperature. The sample was then viewed through TEM.

For each TEM experiment, the negative control, which was the grid without any $A\beta_{1-42}$ sample, was prepared. Ideally, there should not be any amyloid viewed in the negative control. Then, the comparison between the figures of $A\beta_{1-42}$ before and after incubation indicates whether the amyloid had grown longer and was aggregated or not.

Photography under the electron microscope was done by the Central Biotechnology Services, School of Medicine, Cardiff University. Visual comparison and photographs was suffice to determine whether the amyloid was aggregated.

4.2.2 EC_{50} estimation

In this study, the EC_{50} of either H_2O_2 or $CoCl_2$ was estimated in three groups of triplicated MTS assays. The doses selected in each group were based on logarithmic steps.

Taking the $CoCl_2$ insult to NTERA-2 cells as an example, 5 different doses, 100 nM, 1 μM, 10 μM, 100 μM and 1 mM, were tested in the first triplicated group. According to the relative cell number result from the first group, it can be seen for example that 100 nM or 1 μM had little effect on cell numbers. Hence, 100 nM and 1 μM were not subsequently tested. Another two doses were included in the second triplicated test, such that the second 5 different doses were 10 μM, 30 μM, 100 μM, 300 μM and 1 mM. If with the new result, 300 μM and 1 mM were deemed too high, they were not subsequently tested, and, another two doses were included in the third triplicated test. So, the 5 doses in the last triplicated experiment would be 10 μM, 20 μM, 30 μM, 50 μM and 100 μM.

Finally, after the 3 groups of triplicated experiments, all the relative cell

number results collected from the dosages between 100 nM and 1 mM were analysed. The logarithmic dose (lg dose) – effect (relative cell number) curve was constructed and a cumulative logistic distribution trend line fitted to the data. Therefore, according to the logistic regression, the dose which reduced the relative cell number (effect) to 0.5 was taken as the EC_{50}.

The details of logistic regression are explained here. If the relative cell number is P at the dose of C, then the cumulative logistic distribution trend line is a line showing P against lg C. Here, "lg" means log based 10, and $\lg x = \log_{10} x$. To estimate the EC_{50}, following calculations were undertaken. Firstly, the logit (P) value was calculated.

$$\text{logit}(P) = \ln \frac{1 - P}{P}$$

Here "ln" means log based e, and $\ln x = \log_e x$. The logit (P) value should be a linear relation with lg C. Thus, the linear trend line of logit (P) against lg C was constructed, and, a linear function between logit (P) and lg C was plotted, namely:

$$\text{logit}(P) = a \times \lg C + b$$

Here, both "a" and "b" are constant numbers. According to the definition of EC_{50}, P should be 0.5 at EC_{50} dose and logit (P) should be 0. Hence, the lg C value which makes logit (P) to be 0 is the one needed, and the C value here is EC_{50}.

$$\lg C = \frac{\text{logit}(P) - b}{a}$$

$$\lg EC_{50} = \frac{-b}{a}$$

$$EC_{50} = 10^{\frac{-b}{a}}$$

The EC_{50} of $A\beta_{1-42}$ was estimated from only one group of triplicated MTS assay since the amyloid was expensive and was less convenient to use than the other two models. The dose range for $A\beta_{1-42}$ was much narrower, since previous studies have pointed out that 10 μM can induce neuronal cell apoptosis (Kajkowski et al., 2001). Thus, the dose range tested for $A\beta_{1-42}$ insult model was between 625 nM and 40 μM.

4.2.3 Drug solutions

All $A\beta_{1-42}$, $CoCl_2$ and H_2O_2 are from Sigma-Aldrich. $A\beta_{1-42}$ was dissolved in PBS at 100 μM and was incubated at 37 °C for 7 days before being applied to cells (see Section 4.2.1). $CoCl_2$ is dissolved in H_2O at 10 mM for stock. H_2O_2 is diluted in PBS at 1 M for stock. Both $CoCl_2$ and H_2O_2 are light sensitive and both stocks are stored at 4 °C. Glutamate is from Fisher Scientific and was dissolved in PBS at 1 M for stock. The glutamate stock was also stored at 4 °C. The haemocytometer for counting cell number is from Mrienfeld.

4.3 Results

4.3.1 $CoCl_2$ insult

The $CoCl_2$ insult was applied to the MOG-G-UVW cells first, and the data in

the form of a dose – response curve is shown in Fig. 4.1.

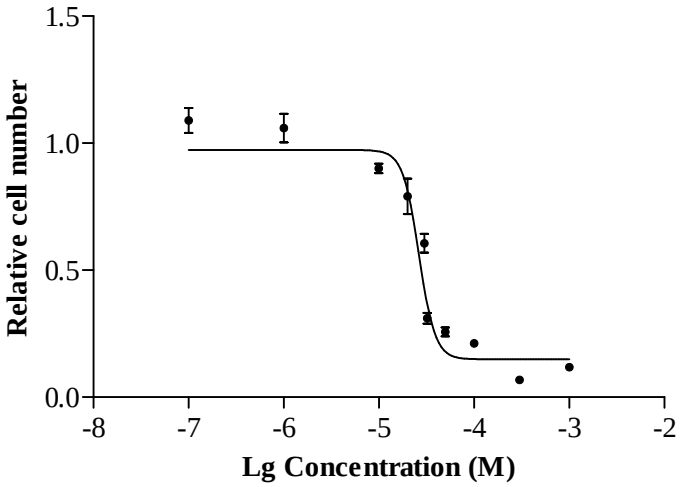

Fig. 4.1 Dose – response curve of $CoCl_2$ insult in MOG-G-UVW cell line. The points are the means of 3 for 100 nM, 1 μM, 20 μM, 50 μM and 300 μM, 6 for 30 μM, 100 μM and 1 mM, and 9 for 10 μM.

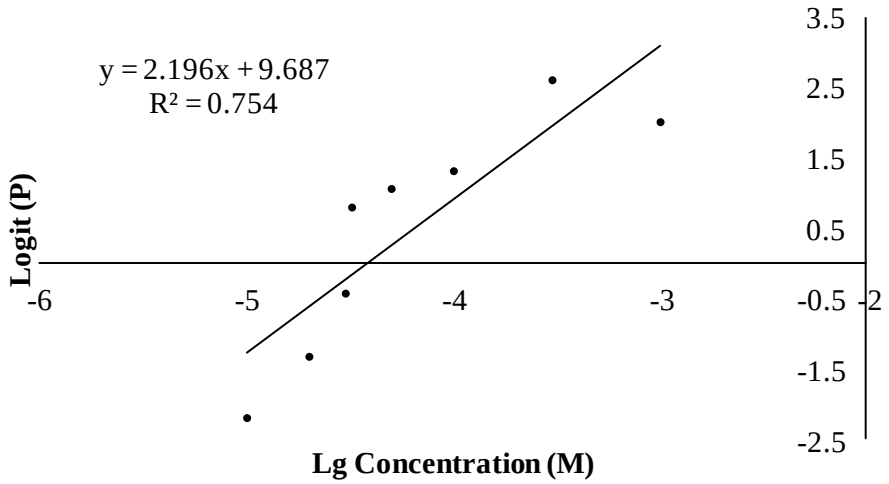

Fig. 4.2 Logistic regression of the dose – response curve of $CoCl_2$ insult in the MOG-G-UVW cell line.

A one way ANOVA test for all the groups in Fig. 4.1 suggested $p < 0.001$, and the Dunnett's post test (comparing each group to control) suggested that 10 μM

or above caused a significant reduction in the relative cell number from control ($p < 0.01$ for 10 μM group, and $p < 0.001$ for 20 μM to 1 mM groups). Logistic regression is shown in Fig. 4.2 and the EC_{50} is then calculated.

$$EC_{50} = 10^{\frac{-9.687}{2.196}}$$

So, the EC_{50} of $CoCl_2$ to MOG-G-UVW was estimated as between 30 and 40 μM. This was the concentration for the $CoCl_2$ experiments which was used in further modulator tests with these cells.

In comparison, the action of $CoCl_2$ in the SH-SY5Y cells is shown in the dose – response curve of Fig. 4.3

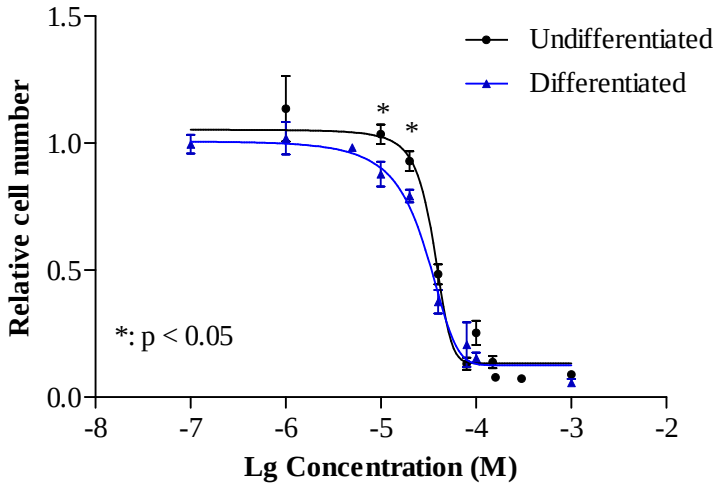

Fig. 4.3 Dose – response curve for $CoCl_2$ in both undifferentiated and differentiated SH-SY5Y cells

For the undifferentiated cells, data points were the means of 3 for 20 μM, 40

μM, 80 μM, 150 μM and 160 μM, 6 for 1 μM and 300 μM, and 9 for 10 μM, 100 μM, 1 mM and the control. For the differentiated cells, data points were the means of 3 for 100 nM, 1 μM, 5 μM, 20 μM, 40 μM, 80 μM, 100 μM and 1 mM groups, 6 for 10 μM and the control.

A one way ANOVA test for the $CoCl_2$ effects in the undifferentiated SH-SY5Y cells suggested that the difference amongst those groups was significant ($p < 0.001$), and the Dunnett's post test (comparing each group with the control) indicated that 40 μM or higher dose of $CoCl_2$ had a significant effect on the relative cell number from the control group ($p < 0.001$). The one way ANOVA test for the insults in the differentiated cells showed that the difference amongst the groups was significant also ($p < 0.001$), and the Dunnett's post test (comparing each group with the control) showed that 20 μM $CoCl_2$ or higher has significantly reduced the cell number. The significances were $p < 0.01$ for 20 μM and $p < 0.001$ for 40 μM and above.

To estimate the EC_{50} doses of $CoCl_2$ in undifferentiated and differentiated SH-SY5Y cells, logistic regressions were carried out and EC_{50} doses were calculated (see Fig. 4.4 & Fig. 4.5).

Hence the EC_{50} of $CoCl_2$ in undifferentiated SH-SY5Y cells was calculated as:

$$EC_{50} = 10^{\frac{-11.82}{2.711}} = 0.0000437 \text{ M} = 43.7 \text{ μM}$$

The EC_{50} of $CoCl_2$ in differentiated SH-SY5Y cells was calculated as:

$$EC_{50} = 10^{\frac{-10.66}{2.372}} = 0.0000321 \text{ M} = 32.1 \text{ μM}$$

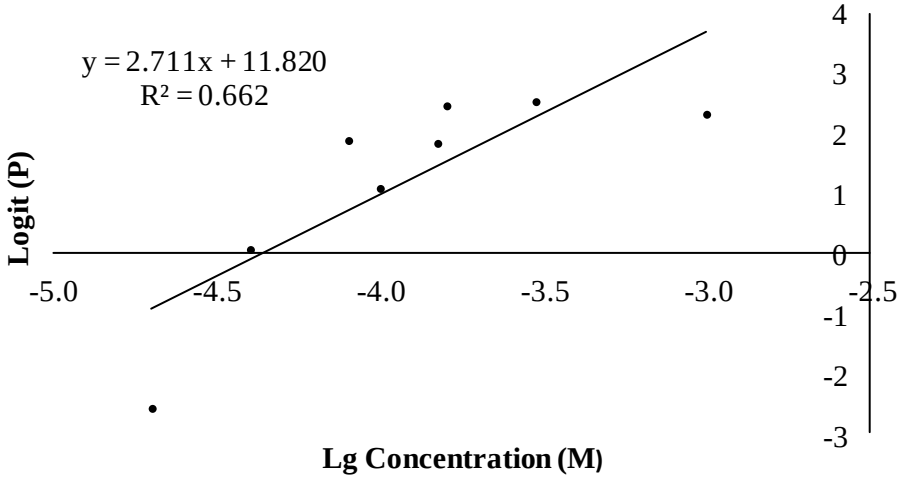

Fig.4.4 Logistic regression of the dose – response curve of $CoCl_2$ insult in undifferentiated SH-SY5Y cell line

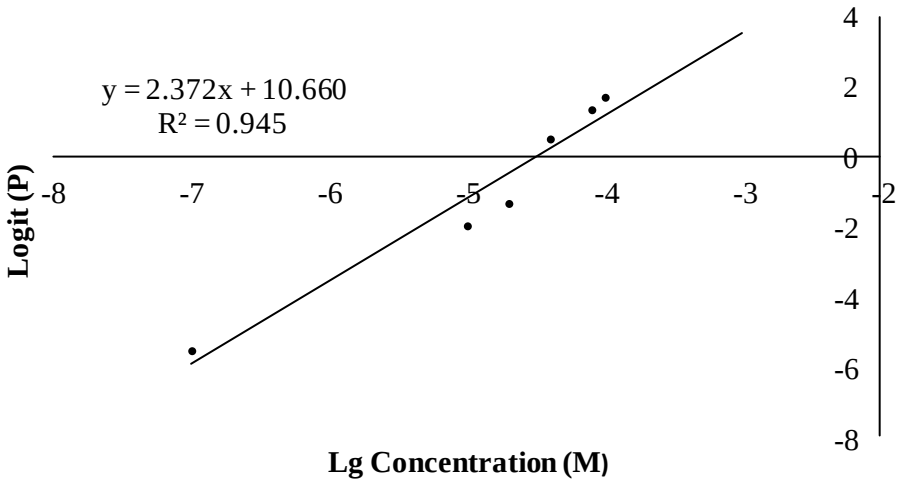

Fig.4.5 Logistic regression of the dose – response curve of $CoCl_2$ insult in differentiated SH-SY5Y cell line

Thus, the EC_{50} doses for $CoCl_2$ in undifferentiated and differentiated SH-SY5Y cells were estimated as about 44 μM and 32 μM respectively. These are the

$CoCl_2$ concentrations used in future modulator test experiments in SH-SY5Y cells.

In addition, the relative cell number for undifferentiated and differentiated cells were 0.930 (± 0.0473) and 0.878 (±0.0529) respectively ($p < 0.05$, t test) at 10 μM, and were 0.484 (± 0.0489) and 0.379 (± 0.0565) respectively ($p < 0.05$, t test) at 20 μM. The relative cell numbers in differentiated SH-SY5Y cells were consistently lower than the counterparts in undifferentiated cells under 10 μM and 20 μM $CoCl_2$.

Finally, the action of $CoCl_2$ was tested on undifferentiated NTERA-2 cells. The dose – response curve for these experiments is shown in Fig. 4.6.

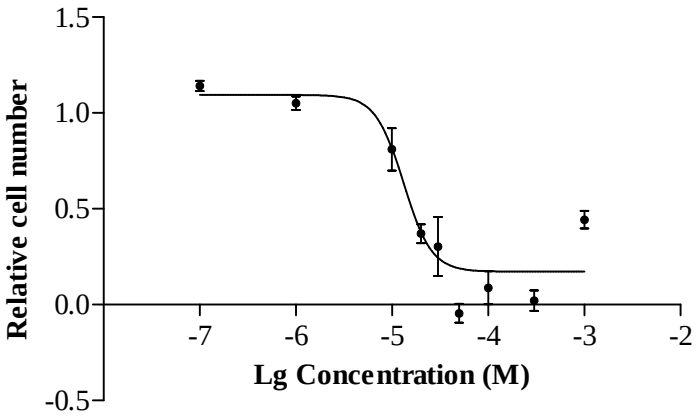

Fig. 4.6 Dose - response curve for $CoCl_2$ in undifferentiated NTERA-2 cells. The data points were the means of 3 for 100 nM, 1 μM, 20 μM, 50 μM and 300 μM, 6 for 30 μM and 1 mM, and 9 for 10 μM, 100 μM and the control.

A one way ANOVA test for $CoCl_2$ against undifferentiated NTERA-2 cells indicated that the difference amongst those groups was significant ($p < 0.001$),

and the Dunnett's post test (comparing each group with the control) indicated that $CoCl_2$ at 20 μM or higher significantly reduced cell number from the control ($p < 0.01$ at 20 μM, and $p < 0.001$ at 30 μM and above).

To estimate the EC_{50} of $CoCl_2$ in undifferentiated NTERA-2, the logistic regression is shown in Fig. 4.7.

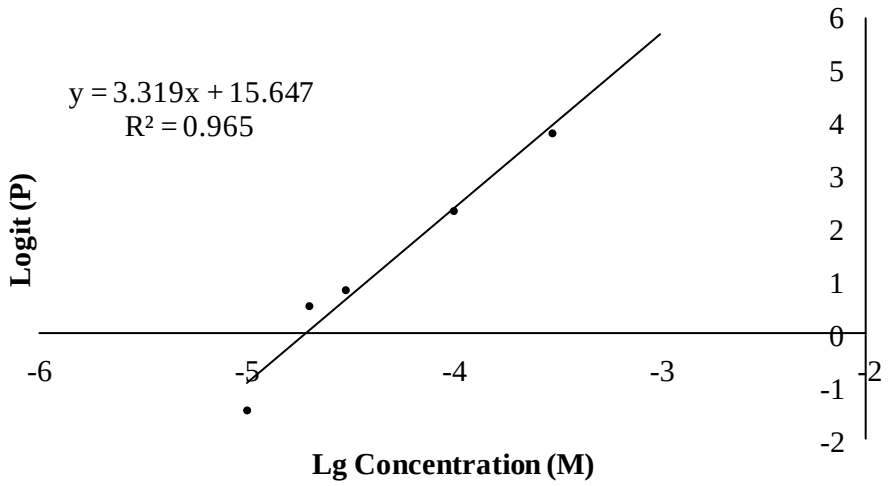

Fig. 4.7 Logistic regression of the dose – response curve of $CoCl_2$ in undifferentiated NETA-2 cells

Thus, EC_{50} is calculated as:

$$EC_{50} = 10^{\frac{-15.6}{3.32}}$$

The EC_{50} for $CoCl_2$ in undifferentiated NTERA-2 cells was estimated between 10 and 20 μM. Hence, 15 μM is the $CoCl_2$ concentration used in future modulator test experiments in undifferentiated NTERA-2 cells.

4.3.2 H_2O_2 insult

The action of H_2O_2 was tested on both undifferentiated and differentiated SH-SY5Y cells. The dose – response curves for these experiments are shown in Fig 4.8:

A one way ANOVA test for the H_2O_2 effects in undifferentiated SH-SY5Y cells suggested that the difference amongst those groups was significant ($p < 0.001$), and the Dunnett's post test (comparing each group with the control) indicated that 300 μM or higher dose of H_2O_2 had a significant effect on the relative cell number from the control group ($p < 0.01$at 300 μM and $p < 0.001$ for 450 μM or above).

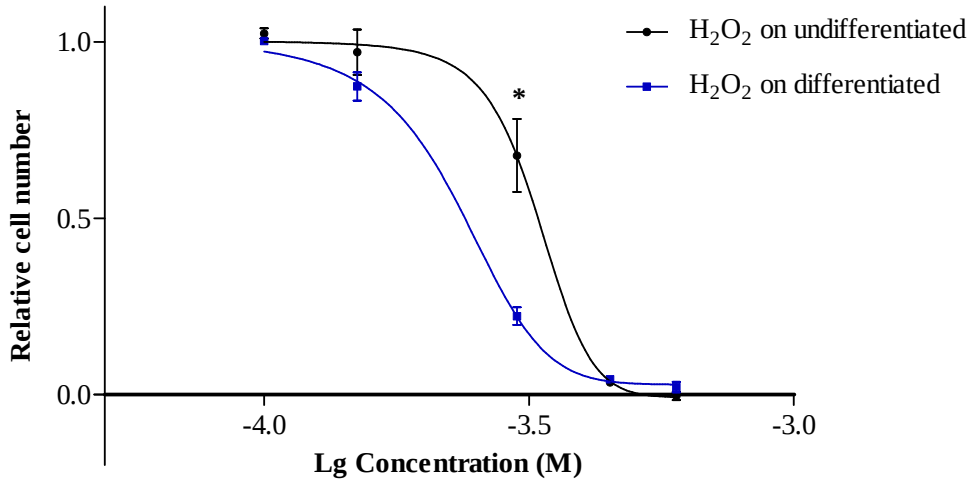

Fig. 4.8 Dose – response curve for H_2O_2 in both undifferentiated and differentiated SH-SY5Y cells.

A one way ANOVA test for the insults in differentiated cells showed that the

difference amongst the groups was also significant ($p < 0.001$), and the Dunnett's post test (comparing each group with the control) showed that 150 μM H_2O_2 or higher would significantly reduce the cell number. The significances were $p < 0.01$ for 150 μM, and $p < 0.001$ for 300 μM and above.

A one way ANOVA test with Tukey's post test (comparing every two groups) for the comparison of the action of H_2O_2 in both undifferentiated and differentiated cells indicated that the relative cell numbers were significantly different ($p < 0.001$) between the undifferentiated group and differentiated group at 300 μM.

To estimate the EC_{50}, a linear logistic regression was carried out.

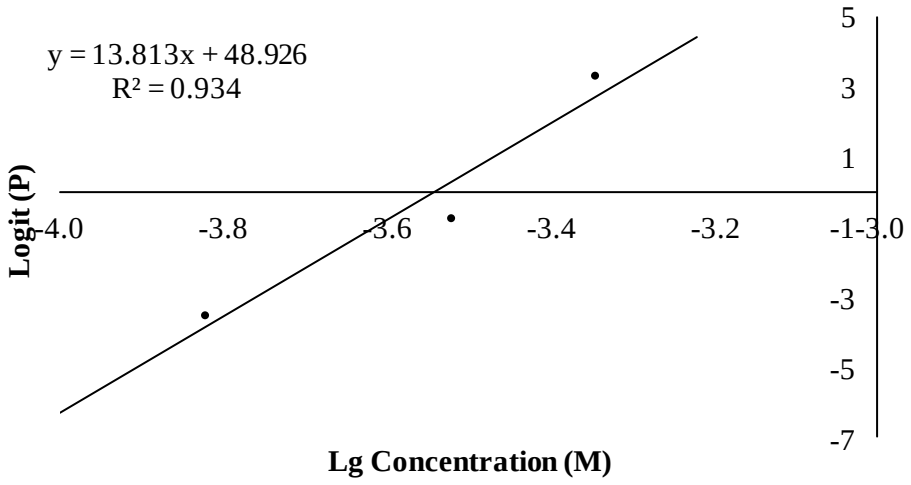

Fig. 4.9 Logistic regression of the dose – response curve of H_2O_2 in undifferentiated SH-SY5Y cells

The EC_{50} of H_2O_2 in undifferentiated SH-SY5Y cells is calculated as:

$$EC_{50} = 10^{\frac{-48.9}{13.8}} = 0.000286\ M = 286\ \mu M$$

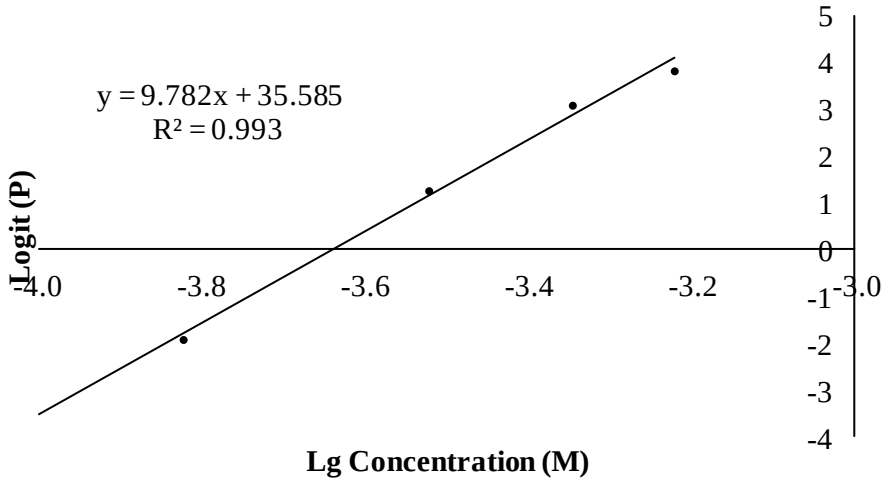

Fig. 4.10 Logistic regression of the dose – response curve of H_2O_2 in differentiated SH-SY5Y cells

The EC_{50} of H_2O_2 in differentiated SH-SY5Y cells is calculated as:

$$EC_{50} = 10^{\frac{-35.6}{9.78}} = 0.000230\ M = 230\ \mu M$$

Hence, the EC_{50} concentration of H_2O_2 was estimated around 286 μM in undifferentiated SH-SY5Y cells and around 230 μM in differentiated SH-SY5Y cells. Therefore these are the H_2O_2 concentrations used in further modulator test experiments in SH-SY5Y cells.

4.3.3 $A\beta_{1-42}$ aggregation and fibril

Before Aβ is applied in cell proliferation assays, it should be incubated and aggregated first. TEM photos were taken for $A\beta_{1-42}$ before and after the 1 week

incubation. These figures are shown in Fig. 4.11.

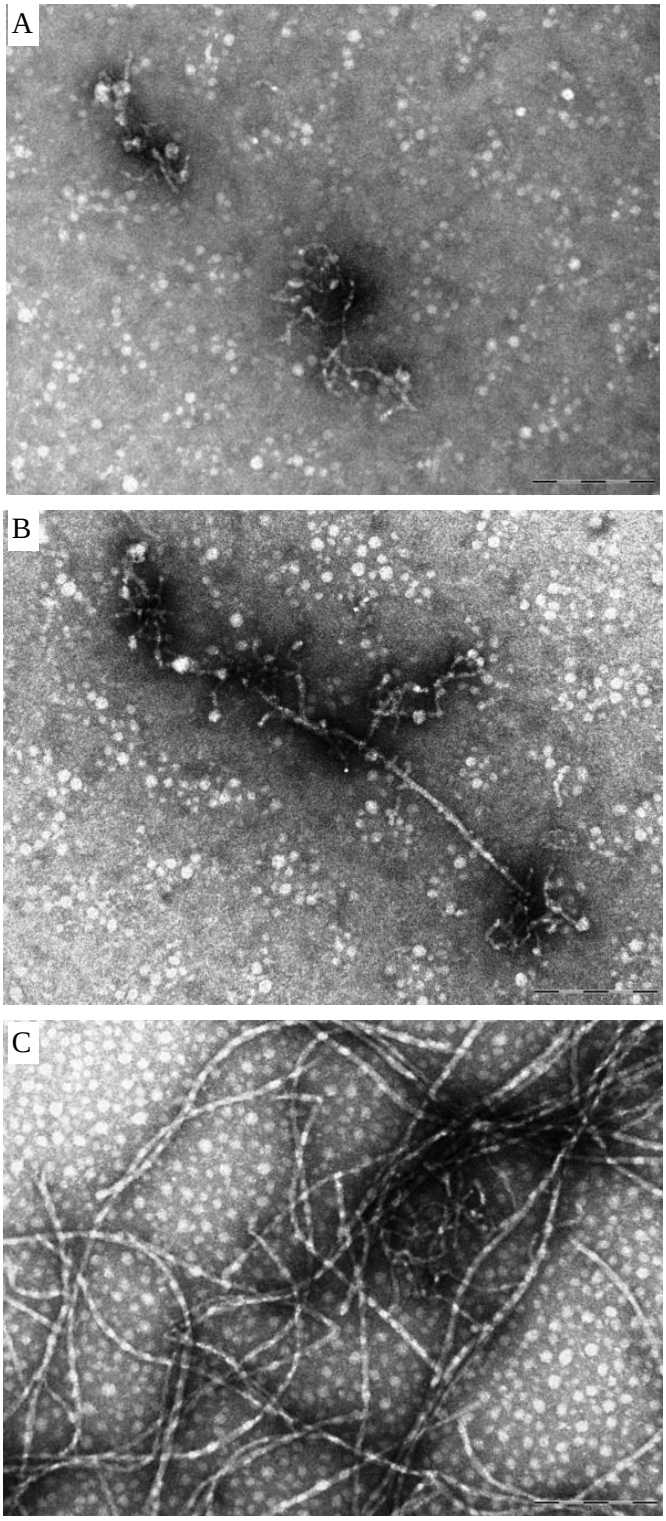

Fig. 4.11 TEM graph of $A\beta_{1-42}$ aggregation. A: negative control, B: $A\beta_{1-42}$ before incubation, and C: $A\beta_{1-42}$ after 1 week aggregation. Scale bar is 200 nM.

$A\beta_{1-42}$ aggregation and fibril formation are obvious in Fig. 4.11C. Compared with the negative control (Fig. 4.11A), the non-aggregated $A\beta_{1-42}$ (Fig. 4.11B) is a short peptide of about 400 – 600 nm length. After 7 days incubation and aggregation, the aggregated $A\beta_{1-42}$ was longer than 1 – 2 μm in length (Fig. 4.11C). This confirms that the $A\beta_{1-42}$ is aggregated after 7 days incubation.

4.3.4 $A\beta_{1-42}$ insult

The $A\beta_{1-42}$ insult was carried on the undifferentiated SH-SY5Y cells first, and the relevant dose – response curve is shown in Fig. 4.12.

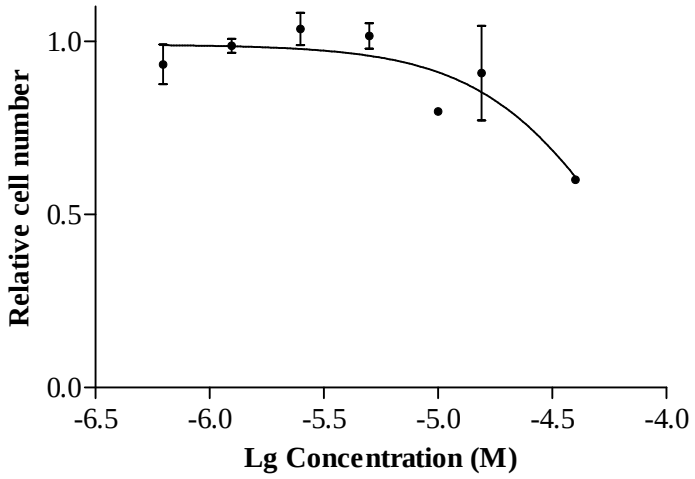

Fig. 4.12 Dose – response curve for $A\beta_{1-42}$ insult in undifferentiated SH-SY5Y cells. The data points were the means of 3 for 1 – 15 μM $A\beta_{1-42}$ insult and the control, and 1 for 40 μM $A\beta_{1-42}$.

From the figure, it can be seen that above 10 μM $A\beta_{1-42}$ may cause cell death in undifferentiated SH-SY5Y cells, the relative cell number at 10 μM being 0.797 ± 0.00849. However, the standard errors in several groups are very large. A

one way ANOVA test for all the groups showed that the difference amongst the groups was not significant, but a t test between the 10 μM insult and the control showed a significant difference in the relative cell number ($p < 0.01$).

The highest concentration of $A\beta_{1-42}$ in this experiment only reduced the relative cell number to be 0.600, therefore, the EC_{50} could not be estimated from these data.

The $A\beta_{1-42}$ insult was then tested on differentiated SH-SY5Y cells for comparison. The relevant dose – response curve is shown in Fig. 4.13.

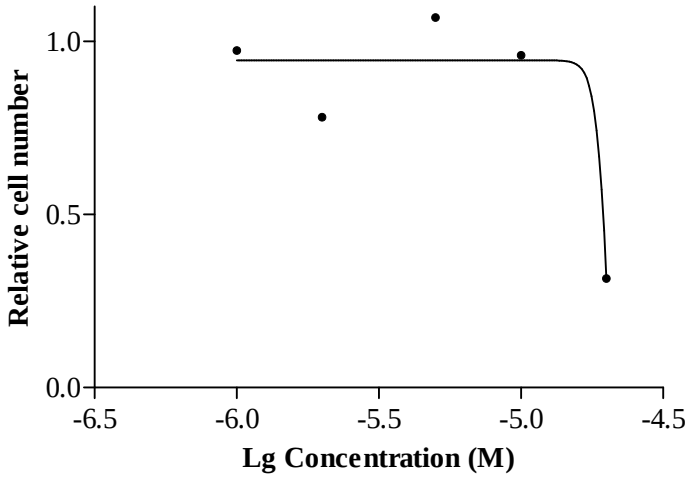

Fig. 4.13 Dose – response curve for $A\beta_{1-42}$ insult in differentiated SH-SY5Y cells

This experiment was carried out in only one 96 well plate, but measurements were made in triplicate. The relative cell number was calculated from the average of the 3 wells.

To estimate the EC_{50} of $A\beta_{1-42}$ on differentiated SH-SY5Y cell line, a linear logistic regression was carried out. The trend line is shown in Fig. 4.14.

Hence, the EC_{50} was calculated as:

$$EC_{50} = 10^{-\frac{8.841}{1.990}} = 0.0000361 \text{ M} = 36.1 \text{ } \mu\text{M}$$

This EC_{50} is out of the dose range selected in the insult experiment, thus, it cannot be considered an acceptable EC_{50}.

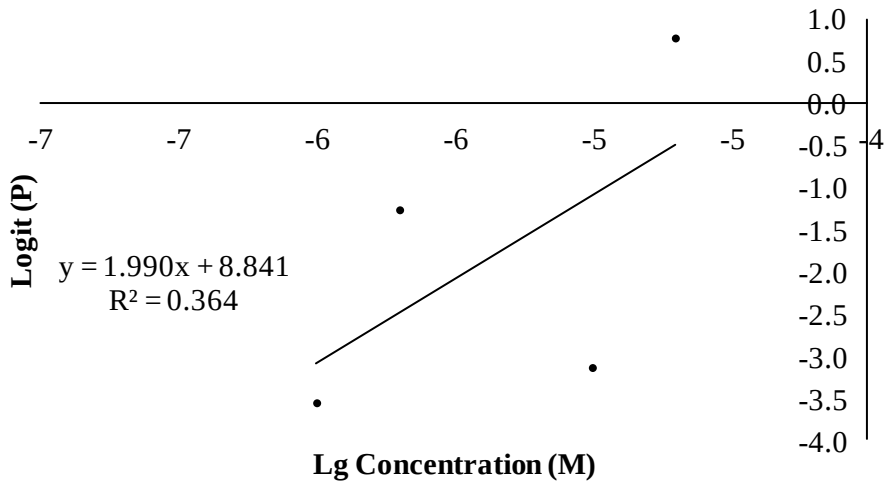

Fig. 4.14 Logistic regression to the dose – response curve of $A\beta_{1-42}$ insult in differentiated SH-SY5Y cell line.

4.3.5 Glutamate insult

The glutamate insult was applied to the MOG-G-UVW cells and the data in the form of a dose – response curve is shown in Fig. 4.15.

A one way ANOVA test for all the groups suggested that the difference

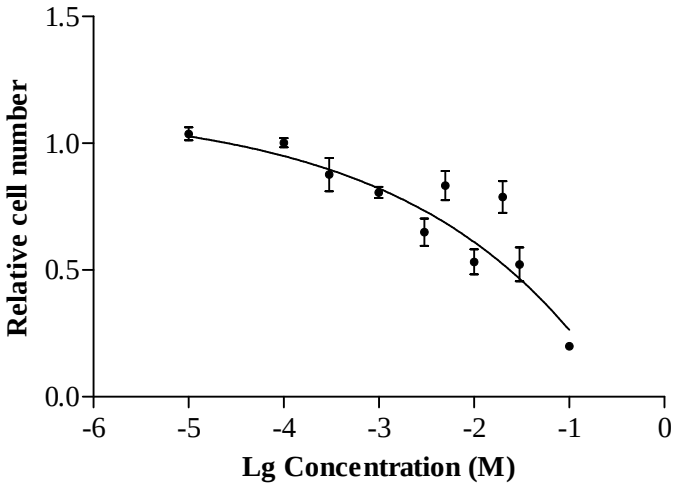

Fig. 4.15 Dose – response curve of glutamate insult in MOG-G-UVW cells. The data points are the means of 12 for 10 mM and the control, 9 for 300 μM, 1 mM and 30 mM, 6 for 100 μM, 3 mM and 100 mM, and 3 for 10 μM, 5 mM and 20 mM.

amongst those groups was significant ($p < 0.001$), and the Dunnett's post test (comparing each group with the control) indicated that 1 mM, 3 mM, 10 mM, 30 mM or higher dose of glutamate caused a significant reduction in the relative cell number from the control ($p < 0.05$ for 1 mM and $p < 0.001$ for the others). To estimate the EC_{50} of glutamate in MOG-G-UVW cells, the logistic regression is shown in Fig. 4. 16.

$$EC_{50} = 10^{\frac{-1.638}{1.074}} = 0.0298 \text{ M} = 29.8 \text{ mM}$$

So, the EC_{50} of glutamate to MOG-G-UVW cells was estimated as 29.8 mM.

4.4 Discussion

Based on the results above, the following ideas can be summarised.

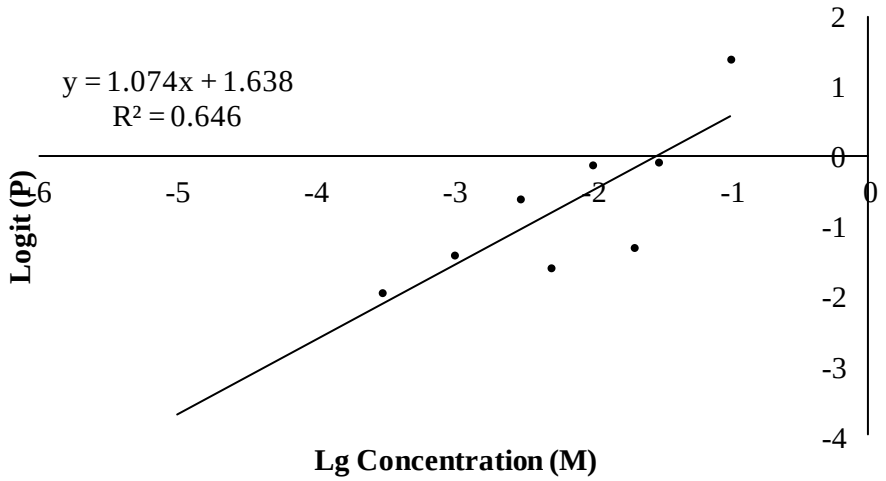

Fig. 4.16 Logistic regression of the dose – response curve of glutamate insult in the MOG-G-UVW cell line.

4.4.1 $CoCl_2$ insult

The "threshold" $CoCl_2$ doses were 40 μM and 20 μM for undifferentiated and differentiated SH-SY5Y cells respectively, and the EC_{50} doses for $CoCl_2$ were 44 μM and 32 μM for undifferentiated and differentiated SH-SY5Y cells respectively. In addition, the relative cell number in differentiated SH-SY5Y cells was lower than the counterparts in undifferentiated cells under 10 μM and 20 μM $CoCl_2$. It would seem clear that the differentiated SH-SY5Y cells are more sensitive than the undifferentiated ones. It is tempting to suggest that this difference between undifferentiated and differentiated SH-SY5Y cells in sensitivities to $CoCl_2$ insult could be linked to the difference on RyRIII expression in Q-PCR.

From the Q-PCR results described in Chapter 3, it was shown that the

differentiated SH-SY5Y cells had a potentially higher expression RyRIII than the undifferentiated ones (about 6 fold). Hence we can tentatively propose that the cells with a higher RyRIII expression are more sensitive to $CoCl_2$ insult.

Why might this be the case? As mentioned in Section 4.1, $CoCl_2$ is a hypoxia mimetic which may induce neuronal death (Gasperi et al., 2010), and also upregulates the expression of APP so increasing the generation of Aβ (Zhu et al., 2009). Further, as discussed in the introduction (see Chapter 1), Aβ plaque deposited on the neuronal membrane may form a Ca^{2+} channel and so potentially increase $[Ca^{2+}]_i$ (Arispe et al., 2007, Berridge, 2010, Jang et al., 2010). The end result is that $CoCl_2$ may increase the $[Ca^{2+}]_i$ in neurones. Also the RyR is a CICR channel on the ER and if activated would further increase $[Ca^{2+}]_i$ finally precipitating cell death (Berridge, 2010, Manunta, 2000). This may then be the basis that the cells with higher RyRIII expression would be more sensitive to the $[Ca^{2+}]_i$ increase induced by those insult models.

Thus, when the same dose of $CoCl_2$ was applied to both undifferentiated and differentiated SH-SY5Y cells, the same change in $[Ca^{2+}]_i$ would occur initially and the RyR would be activated. Nevertheless, since there are more RyRIII expressed in the differentiated cells, more Ca^{2+} channels would be opened on the ER when they are activated, more Ca^{2+} would then be released from the ER in the differentiated cells. Consequently the $[Ca^{2+}]_i$ increase would be greater in the differentiated cells than in the undifferentiated ones leading to more cell apoptosis or cell death.

However, this conclusion is debatable. The RyRIII expression in differentiated SH-SY5Y cells was 6 fold more than it in the undifferentiated cells, but the differences in EC_{50} in respect of relative cell numbers in the presence of 10 μM or 20 μM $CoCl_2$ were not so markedly different, although significant. The possible reason to explain this is that $[Ca^{2+}]_i$ homeostasis is maintained by a number of interacting systems, rather than RyR only. For example, IP_3R (another Ca^{2+} release channel on the ER) can be blocked by Bcl-2 when the $[Ca^{2+}]_i$ is increased (Berridge, 2010, Rong et al., 2008). Hence, the increase in $[Ca^{2+}]_i$ caused by RyR activation would be possibly balanced by some other receptor or modulator so influencing Ca^{2+} levels.

4.4.2 H_2O_2 insult

From the H_2O_2 insult to both undifferentiated and differentiated SH-SY5Y cells, a similar difference was noticed. Differentiated cells could be compromised by H_2O_2 at a dose of 150 μM or higher, but the undifferentiated ones were not affected until the dose was increased to 300 μM. The relative cell numbers of the differentiated cells were lower than those of undifferentiated cells below 300 μM H_2O_2 insult, the relative cell numbers being 0.678 (± 0.127) and 0.223 (± 0.0310) respectively. In addition, the EC_{50} in the undifferentiated cells (about 286 μM) was higher than the one in differentiated ones (230 μM). This difference between undifferentiated and differentiated SH-SY5Y cells in sensitivities to H_2O_2 insult can also be linked to the difference in RyRIII expression in Q-PCR, the differentiated SH-SY5Y

cells with a higher RyRIII expression being more sensitive to H_2O_2 insult.

As discussed, previously oxidative stress has been linked with neurodegeneration, such as occurs in AD (Lin and Beal, 2006, Floyd, 1999, Floyd and Hensley, 2002), and H_2O_2 application, a model for oxidative stress (Ishimura et al., 2008), increases $[Ca^{2+}]_i$ (Krebs et al., 2007). Therefore, the difference in susceptibility to H_2O_2 insult between undifferentiated and differentiated SH-SY5Y cells would possibly be contributed by the different expression of RyRIII.

4.4.3 $A\beta_{1-42}$ aggregation

A number of previous studies have reported aggregation results. Reviews of the literature indicated that the aggregation of amyloid was quite variable in different samples or labs. In some of the studies, the aggregation was quite successful and the aggregated fibril of $A\beta_{1-42}$ was even longer than 1 μm (see Fig. 4.17), while some others have failed to demonstrate such a long fibril after aggregation (see Fig. 4.18).

Fig. 4.17 Aggregation of Aβ after 0 h, 12 h, 24 h, 48 h and 72 h of incubation (scale bar: 50 nm). It can be clearly observed that the amyloid fibril was aggregated and much longer than it was at the beginning. (Qahwash et al., 2007)

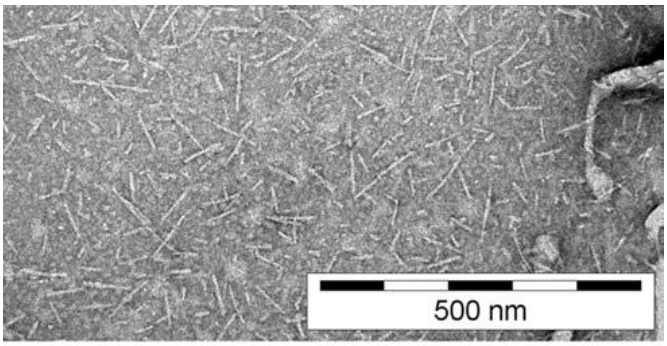

Fig. 4.18 Aggregation of $A\beta_{25\text{-}35a}$ after 6 days. They were short, rod-like aggregates with an average length in the interval 20 – 120 nm. (Fülöp et al., 2004)

In the work reported here, the aggregation results of $A\beta_{1\text{-}42}$ were also quite variable. Some of the successful aggregation results, and where long fibrils were present were comparable with data above (see Fig. 4.1), however, there were also some short aggregates even after 1 week incubation at 37 °C (see Fig. 4.19).

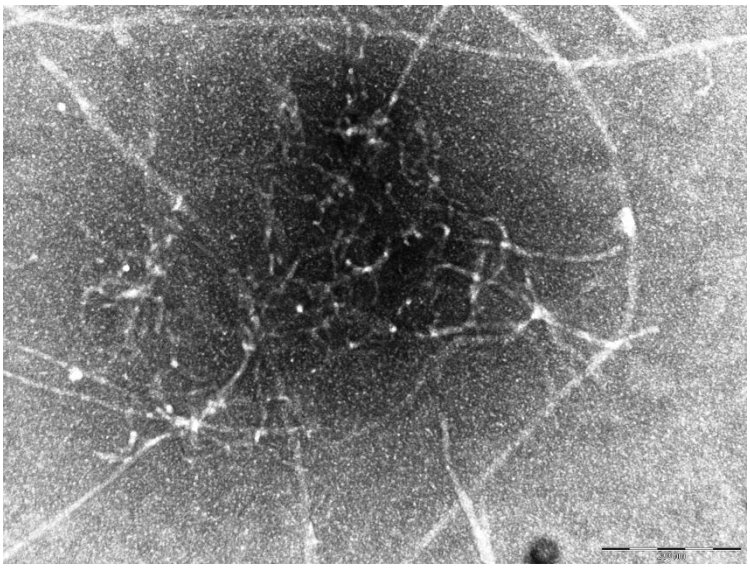

Fig. 4.19 TEM of $A\beta_{1\text{-}42}$ after 1 week aggregation. It sould be noticed that some of the fibrils were still as short as 200 nm or less. Scale bar is 200 nm.

4.4.4 $A\beta_{1-42}$ insult

It was clear that the standard errors in the MTS assays of the challenge presented by $A\beta_{1-42}$ were very large. Given the results of $A\beta_{1-42}$ aggregation, it could be argued that the variable aggregation of the amyloid had resulted at least in part of the variation of the insult result.

As discussed before, the non-aggregated $A\beta_{1-42}$ has a limited toxic effect. Hence, one would expect that the cells treated with the non-aggregated $A\beta_{1-42}$ would show a higher relative cell number to the ones treated with the aggregated long fibrils. Therefore, the triplicated samples with the "same" treatment would produce quite different results and this would result in the large standard error. Thus, it may be reasonable that the mean of cell numbers under 20 μM $A\beta_{1-42}$ insult is higher than the counterpart under 10 μM $A\beta_{1-42}$ insult in undifferentiated SH-SY5Y cells. Obviously, the standard error was significant in the Aβ insult results.

Therefore, large variability of amyloid aggregation and the variable effect of $A\beta_{1-42}$ were the reasons that $A\beta_{1-42}$ was not selected as the primary cell insult in the future tests with modulators. However, even if there was significant variability, it still could be seen that the cell numbers, in both undifferentiated and differentiated SH-SY5Y cells, were reduced by the $A\beta_{1-42}$ insult at 10 – 20 μM or higher. Those results confirm at least that $A\beta_{1-42}$ reduce the cell numbers in neuronal cell line.

4.4.5 Glutamate insult

The EC_{50} of glutamate insult in MOG-G-UVW cells was very high (29.8 mM), in comparison with previous studies. The relative cell number results in glutamate were unstable in this work, for example 20 mM and 50 mM glutamate insult did not have any significant effect on the relative cell number in the Dunnett's post test. This dose is much higher than the glutamate-receptor affinity requires (K_m), it might be argued whether glutamate would induce neuronal death through binding with NMDA receptor. In addition, glutamate is easily switched into glutamine, which is non-toxic to most cells, in H_2O solution. Hence, glutamate was not selected as an insult model to test the possible effects of RyR and K^+ channel modulators.

4.5 Conclusions

4.5.1 $A\beta_{1-42}$ aggregation

$A\beta_{1-42}$ is aggregated after 7 days incubation at 37 °C. The length of the amyloid is increased from about 400 nm to more than 1 μm or even 2 μm.

The result of aggregation was however quite variable with some amyloid not been aggregated even after 1 week incubation. This has led to significant variability in the cell insult and MTS assays results with the peptide.

4.5.2 Cell insults

Since the aim of this section of work was to try to establish the cell insult models in different cell lines, the first consideration is about the validity of these insult models.

$A\beta_{1-42}$ was toxic to both undifferentiated and differentiated SH-SY5Y cells, 10 μM $A\beta_{1-42}$ significantly reducing the relative cell number of undifferentiated SH-SY5Y cells, but the relative cell number was still higher than 0.5 even at 40 μM. For the differentiated SH-SY5Y cells however, the relative cell number at 20 μM is lower than 0.5. However, since the variability in respect of $A\beta_{1-42}$ aggregation was significant and the standard errors in the MTS assays were high also, $A\beta_{1-42}$ was not selected as the principle cell insult model, but was used once to test the RyR modulators.

$CoCl_2$ as a hypoxia mimetic was established in both neuronal cell lines and the astrocytoma cell line used in this work. For the MOG-G-UVW cells, 10 μM or higher significantly reduced relative cell number, and the EC_{50} was estimated between 30 μM and 40 μM. For the undifferentiated SH-SY5Y cells, 40 μM or higher significantly reduced the relative cell number, and the EC_{50} was estimated at about 44 μM. For the differentiated SH-SY5Y cells, 20 μM or higher significantly reduced the relative cell number, and the EC_{50} was estimated at about 32 μM. And finally, for the undifferentiated NTERA-2 cells, 20 μM or higher significantly reduced the relative cell number, and the EC_{50}

was estimated at about 15 μM.

H_2O_2, as a mimic of oxidative stress, was established in both undifferentiated and differentiated SH-SY5Y cells. For the undifferentiated SH-SY5Y cells, 300 μM or higher significantly decreased the relative cell number, and the EC_{50} was estimated at about 286 μM. For the differentiated SH-SY5Y cells, 150 μM or higher significantly decreased the relative cell number, and the EC_{50} was estimated at about 230 μM.

The relevant data for the EC_{50} doses which were chosen for further experiments are listed in Table 4.1.

Table 4.1 EC_{50} of each insult

	MOG-G-UVW	Undifferentiated NTERA-2	Undifferentiated SH-SY5Y	Differentiated SH-SY5Y
$CoCl_2$	32.2 μM	15 μM	40 μM	33 μM
H_2O_2	-	-	286 μM	230 μM

4.5.3 Cell sensitivities to the insults

As reported in the results and discussed above, it has been concluded that differentiated SH-SY5Y cells, which had a higher RyRIII expression than the undifferentiated ones, were more sensitive to both $CoCl_2$ and H_2O_2 insults.

Since it was presumed that a hypoxia mimetic, like $CoCl_2$, and oxidative stress, like H_2O_2, reduced the cell viability by increasing the $[Ca^{2+}]_i$, and that RyRIII,

is a CICR channel in the neuronal cells, it is reasonable to propose that a higher expression of RyRIII could make the cells more sensitive to those insults. A corollary then is that RyRIII blockers, or other modulators which maintain the $[Ca^{2+}]_i$ homeostasis, would potentially have a neuronal protective effect, at least against a hypoxia mimetic or an oxidative stress insult. Therefore, RyR modulators were tested subsequently in this thesis and this part of the work is presented in Chapter 5.

5. The Action of RyR Modulators on the Cell Insult Models

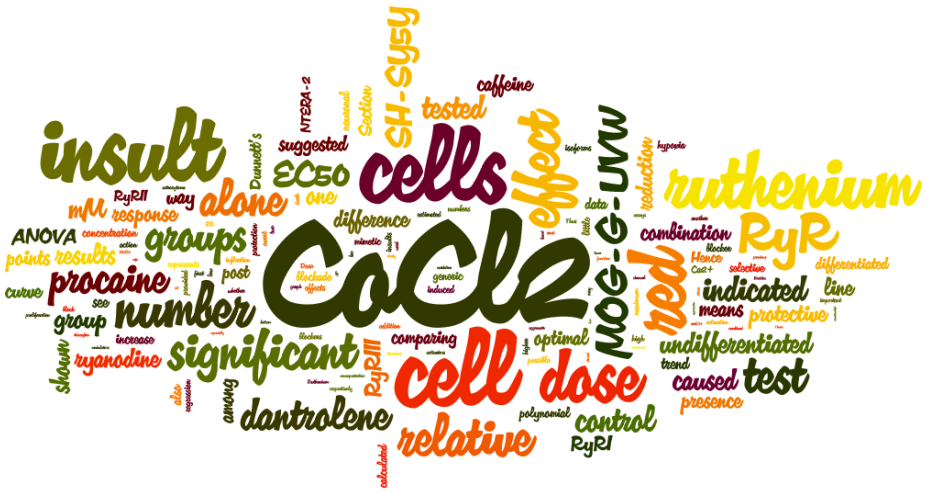

5. The Action of RyR Modulators on the Cell Insult Models

5.1 Introduction

As soon as the $A\beta_{1-42}$, hypoxia mimetic and oxidative stress insult models were established, the next step was to test whether the RyR blockers would have any neuroprotective effect or not, and whether RyRIII was more important than the other two isoforms of RyR.

In the introduction (see Chapter 1), the point was made that the key problem in AD is the deposition of Aβ on the neuronal cell membrane and the forming of putative Ca^{2+} channels by Aβ plaque (Arispe et al., 2007, Berridge, 2010). As discussed in the previous section (see Section 4.1), both the hypoxia mimetic state induced by $CoCl_2$ and oxidative stress caused by H_2O_2 may underpin neurodegeneration, such as occurs in AD (Gasperi et al., 2010, Lin and Beal, 2006, Floyd and Hensley, 2002). Further, $CoCl_2$ was found to increase the generation of Aβ via up-regulation of the expression of APP (Zhu et al., 2009) and H_2O_2 was found to increase the $[Ca^{2+}]_i$ also (Krebs et al., 2007). As soon as $[Ca^{2+}]_i$ is increased, the RyR, which is a Ca^{2+} release channel on ER, would be activated and could potentially further increase the $[Ca^{2+}]_i$. The large increase $[Ca^{2+}]_i$ would stimulate and/or start cell apoptosis (Berridge, 2010). Therefore, in principle blocking of the RyR might present a neuroprotective strategy and hence it was considered worthwhile to test RyR modulators to see whether they could demonstrate any protective effect against the established cell insult

models.

As discussed previously in Section 1.2.2 and Section 1.4.1, 3 isoforms of RyR have been identified with RyRI, RyRII and RyRIII mainly located in skeletal muscle, cardiac muscle and brain tissue respectively (Hakamata et al., 1992, Furuichi et al., 1994). This means, if a generic RyR blocker was applied, it would most likely have skeletal and/or cardiac side effects, even if there is any neuroprotective benefit. RyRIII is suggested to be the primary brain type of RyR, and was found to have a higher expression in the differentiated SH-SY5Y cells, human neurones which have been shown above to be more sensitive to both $CoCl_2$ and H_2O_2 insults, than undifferentiated SH-SY5Y cells, RyRIII was therefore proposed to be the more likely putative target, rather than the other 2 isoforms, for neuroprotection. Hence, the blockers for the RyRIII were tested in this section in the insults.

However, there is no selective RyRIII blocker so far identified. The only proven RyRIII channel blockers are ruthenium red and dantrolene, but ruthenium red has been shown to block the other 2 isoforms of RyR and dantrolene blocks RyRI also (Alexander et al., 2009). Thus, it is impossible to test whether blocking RyRIII alone would protect the neurones against Aβ, hypoxia or oxidative insults. To deal with this problem, the idea adopted here was to use ruthenium red, dantrolene and the selective blockers for the RyRI and RyRII only, to see which, if any, would demonstrate any neuroprotective effect. There are two proven “selective” RyRI and RyRII blockers, ryanodine (>

100 μM) and procaine (Alexander et al., 2009). Ryanodine has a two-way effect on RyR, and not only blocks RyRI and RyRII but also activates all 3 isoforms of RyR at low concentration (nM – μM). In addition, if it is believed that the activation to RyR, especially RyRIII, is an important pathogenesis in neuronal death, RyRIII activators should further induce the cell death when they are applied in combination with the cell insults. So, to test this hypothesis, RyR activators were also tested in this study. But, there is no selective RyRIII activator so far identified. The two available activators, which have been tested in this study, are generic RyR activators, caffeine and ryanodine (nM – μM) (Alexander et al., 2009).

To summarise, the aims in this part of work were:

a. to test whether RyR blockers, especially ruthenium red and dantrolene, protect the neuronal cells against the insults established;
b. to test whether RyR activators, such as caffeine and ryanodine (nM – μM), further induce cell death in combination with the insults established; and
c. to determine whether RyRIII is more important than the other 2 isoforms of RyR in neuroprotection.

5.2 Methods and materials

5.2.1 Methods

The modulators were tested in the cell proliferation MTS assays, with the $CoCl_2$ or $A\beta_{1-42}$ tested against MOG-G-UVW, undifferentiated NTERA-2, undifferentiated SH-SY5Y and/or differentiated SH-SY5Y cells. The means were calculated from at least 3 plates and each plate was in triplicate wells.

For ruthenium red, it has been suggested by previous studies that 1 – 500 μM blocks the RyR channel (Mori et al., 2005, Rosa et al., 1997). Hence, 1 – 500 μM ruthenium red was tested in cell proliferation assays first to ascertain the dose effects which would result in little overt changes in cell numbers. Then, if this was the case, 1 – 500 μM ruthenium red was combined with the cell insults where the EC_{50} of each insult for each cell line was used. Then polynomial fits of cell number of ruthenium red and the respective insult were constructed and the optimal dose of ruthenium red, i.e. the dose which provided maximum protection, was estimated.

For dantrolene, it has been suggested by previous studies that 100 nM – 100 μM would block the RyR channel (Chen et al., 2011, Egea et al., 2007). Hence, 100 nM – 100 μM dantrolene was tested in cell proliferation assays first to ascertain the doses which would result in little overt changes in cell numbers. Then, 100 nM – 100 μM dantrolene was combined with the $CoCl_2$ insult where the EC_{50} dose for each cell line was used. The logistic regression was used to estimate, if possible, the EC_{50} of dantrolene alone, and the polynomial fit of cell number of dantrolene and $CoCl_2$ insult was constructed and the optimal dose of dantrolene, i.e. the dose which provided maximum protection, was

estimated.

For procaine, it was reported previously that 100 μM – 5 mM procaine blocks the RyRI or RyRII receptor (Rosa et al., 1997, Kimball et al., 1996, Usachev et al., 1993). Hence, 100 μM – 5 mM procaine alone was tested in cell proliferation assays first to find out the dose range which was safe for the cells. Then, 100 μM – 5 mM procaine was combined with the cell insult, where the EC_{50} of each insult for each cell line was used.

For caffeine, it was reported previously that about 20 mM caffeine would active the RyR and 100 μM – 100 mM caffeine can increase the intracellular Ca^{2+} (Kato and Rubel, 1999, Parri and Crunelli, 2003). Hence, 100 μM – 100 mM caffeine alone was tested in cell proliferation assays first to construct the dose – response curve and to ascertain the dose which would result in little overt changes in cell numbers. Then, 100 μM – 100 mM caffeine was combined with $CoCl_2$ insult (EC_{50}) to see its effect, if any, on cell numbers.

For ryanodine, it has been suggested by previous studies that 10 nM – 2.5 μM can active the RyR channel (Hohenegger et al., 2002, Humerickhouse et al., 1993), and higher concentrations at about hundred μM can block RyRI and RyRII (Humerickhouse et al., 1994). Considering the cost of ryanodine, only 10 nM – 100 μM ryanodine was tested in cell proliferation assays first to construct the dose – response. Then, 10 nM – 100 μM ryanodine was combined with $CoCl_2$ insult (EC_{50}) to see its effects, if any, on cell numbers.

5.2.2 Polynomial regression

Polynomial trend line was constructed to estimate the optimal dose of each drug, if protective. Polynomial regression can be a mimetic of any other functions, since any function can be expanded into a polynomial expansion according to Taylor series. For example, when x = a, function f(x) can be expanded as:

$$f(x) = f(a) + \frac{f'(a)}{1} \cdot x + \frac{f''(a)}{1\times2} \cdot x^2 + \cdots + \frac{f^n(a)}{n!} \cdot x^n$$

Here, n is a positive integer and n → positive infinity.

The order of the polynomial regression should be 2 less than the population of data points. The optimal dose, i.e. the dose which provided maximum protection, is one of the inflection points of the polynomial trend line. Derivtisation was used to find the inflection points since, for any function, the first derivative should be 0 at the extrema.

5.2.3 Drug preparation

The five test compounds used are described below:

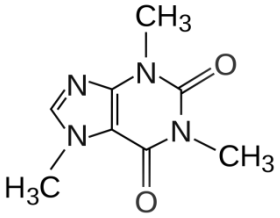

Caffeine: $C_8H_{10}N_4O_2$, was from Sigma-Aldrich, was dissolved in PBS as 100

mM for stock and stored at 4 °C.

Dantrolene: $C_{14}H_{10}N_4O_5$, sodium salt, was from Sigma-Aldrich, was dissolved in PBS as 10 mM for stock and stored at 4 °C. Dantrolene is light sensitive.

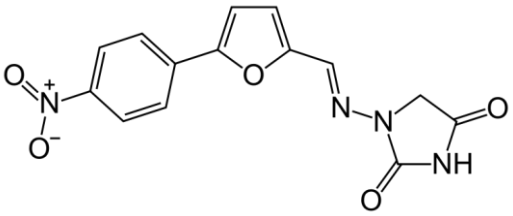

Procaine hydrochloride: $C_{13}H_{20}N_2O_2 \cdot HCl$, > 97%, was from Sigma-Aldrich, was dissolved in PBS as 100 mM for stock and stored at 4 °C.

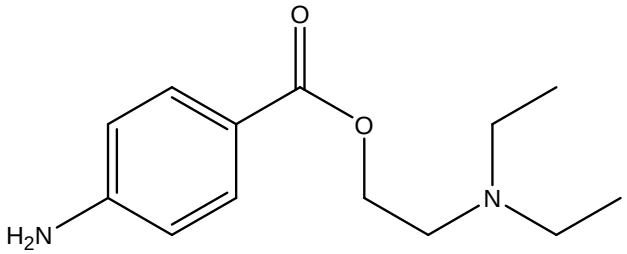

Ruthenium red: Ruthenium oxychloride ammoniated, dye content approx. 40%, was from Sigma-Aldrich, was dissolved in H_2O as 10 mM for stock and stored at 4 °C. Ruthenium red is light sensitive.

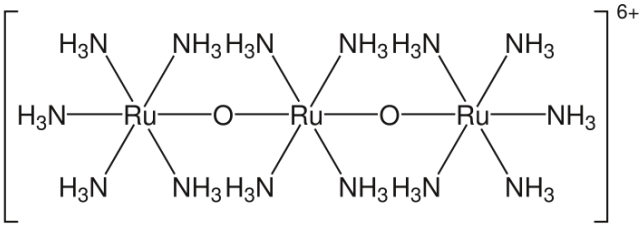

Ryanodine: $C_{25}H_{35}NO_9$, was from Tocris, was dissolved in PBS as 10 mM for stock and stored at -20 °C. Its structure is shown in Section 1.2.2.

5.3 Results

5.3.1 Ruthenium red against $CoCl_2$ insult

5.3.1.1 On MOG-G-UVW cells

The dose – response curve for ruthenium red in MOG-UVW cells is shown in Fig. 5.1:

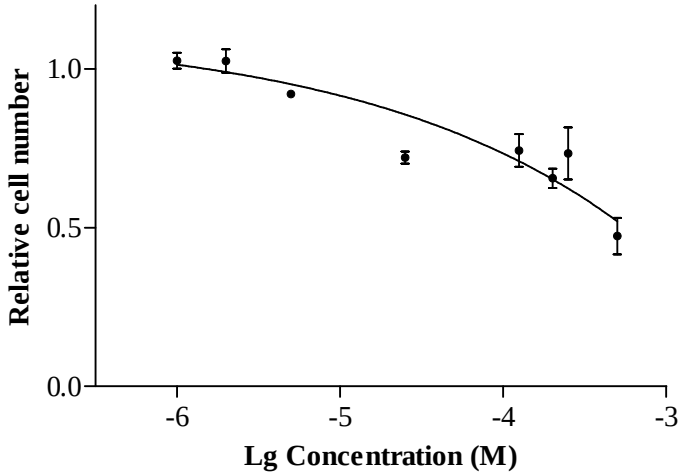

Fig. 5.1 Dose-response curve of ruthenium red action in MOG-G-UVW cells. The points were the means of 3 for 2 μM, 5 μM, 25 μM and 250 μM, and were 6 for 1 μM, 125 μM, 500 μM and the control.

The one way ANOVA test for all the groups indicated that the difference among all the groups was significant ($p < 0.001$), and the Dunnett's post test (comparing each group with the control) indicated that 25 μM or higher dose had a significant effect on the relative cell number from the control group ($p < 0.01$ at 25 μM). Thus, it can be ascertained that the highest dose of ruthenium

red which would result in little overt change in cell number in MOG-G-UVW cells was 5 μM. Logistic regression is shown in Fig 5.2 and the EC_{50} is calculated thereafter.

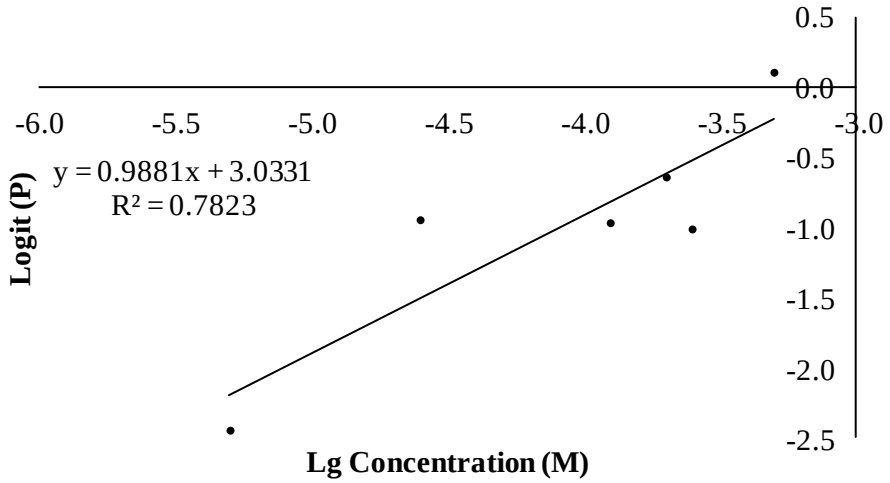

Fig. 5.2 Logistic regression to the dose – response curve of ruthenium red action in MOG-G-UVW cells

Hence, the EC_{50} of ruthenium red in MOG-G-UVW cells was calculated as:

$$EC_{50} = 10^{\frac{-3.033}{0.9881}} = 0.000852 \text{ M} = 852 \text{ μM}$$

However, this concentration, 852 μM, is higher than the highest dose which has been tested, so, it is not good enough to be considered as the EC_{50} of ruthenium red in MOG-G-UVW cells.

Then, ruthenium was tested on $CoCl_2$ insult in MOG-G-UVW cells, and the dose – response curve is shown in Fig. 5.3.

The one way ANOVA test for all the groups indicated that the difference

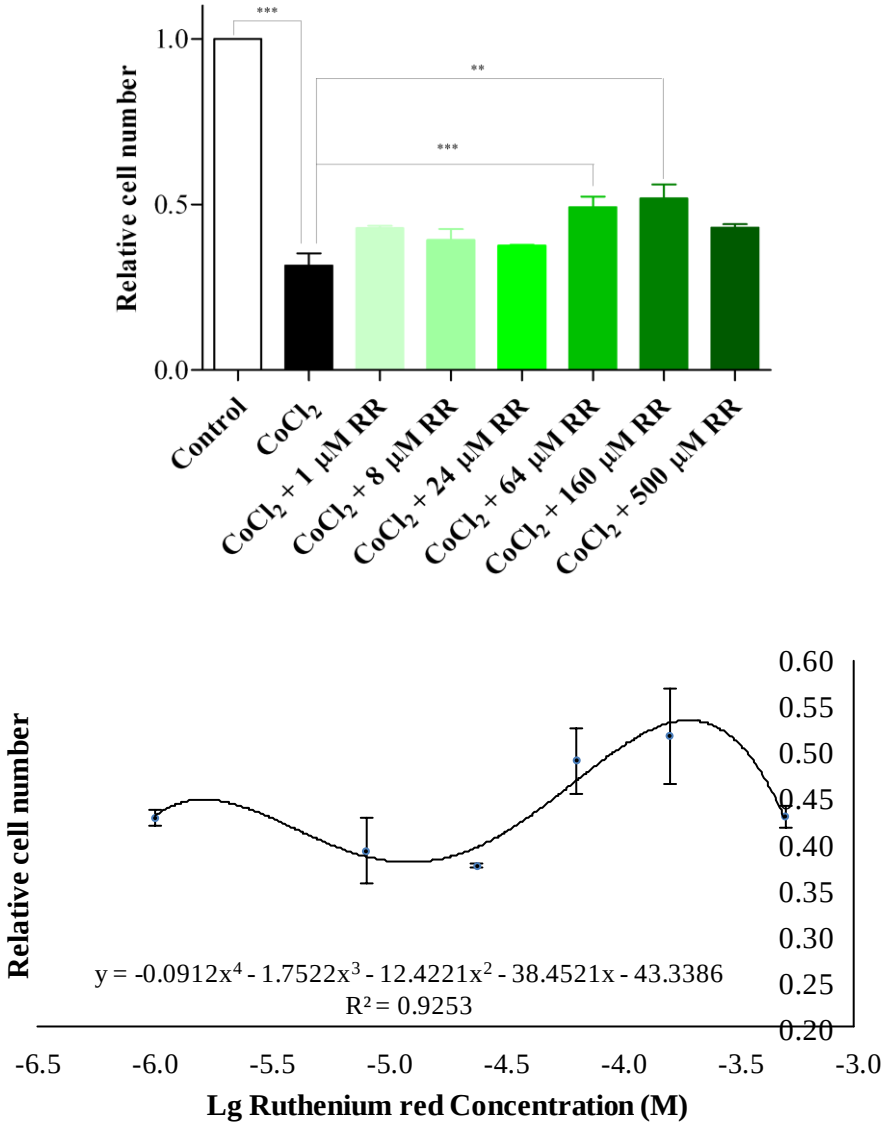

Fig. 5.3 The effect of Ruthenium red (RR) in combination with an EC_{50} of $CoCl_2$ (32.2 µM) in MOG-G-UVW cells. Above: bar graph showing the significant protective effect, and bottom: dose – response curve of ruthenium red in the presence of an EC_{50} of $CoCl_2$. The data points are the means of 3 for $CoCl_2$ + 1 µM ruthenium red, $CoCl_2$ + 24 µM ruthenium red, $CoCl_2$ + 160 µM ruthenium red, and $CoCl_2$ + 500 µM ruthenium red, and 6 for $CoCl_2$ + 8 µM ruthenium red, $CoCl_2$ + 64 µM ruthenium red, $CoCl_2$ alone and the control.

amongst the groups was significant ($p < 0.001$), and the Dunnett's post test (comparing each group with $CoCl_2$ insult) indicated that EC_{50} dose of $CoCl_2$

had a significant effect on the relative cell number from the control group ($p < 0.001$) and indicated that 64 μM or 160 μM ruthenium red in combination with an EC_{50} of $CoCl_2$ had a significant effect on the relative cell numbers compared with the $CoCl_2$ insult group ($p < 0.001$ and $p < 0.01$ respectively).

The optimal dose of ruthenium red against $CoCl_2$ insult in MOG-G-UVW cells was then calculated according to the polynomial trend line shown in Fig. 5.3.

$$y = -0.0912\ x^4 + 0.437\ x^3 - 0.587\ x^2 + 0.193\ x + 0.429$$

Here, y represents the relative cell number and x represents the lg concentration of ruthenium red (M), and $R^2 = 0.925$.

To calculate the optimal dose, which is one of the inflection points in the function above, the first derivative of it should be 0.

$$y' = 0, \text{ so}$$

$$y' = 4 \times (-0.0912) \times x^3 + 3 \times 0.437 \times x^2 - 2 \times 0.587 \times x + 0.193 = 0$$

$$\text{thus, } x = 0.000201 = 201\ \mu M$$

Hence, the optimal dose of ruthenium red against $CoCl_2$ insult in MOG-G-UVW cells, which provided maximum protection, was estimated as 201 μM.

5.3.1.2 Undifferentiated NTERA-2 cells

Besides the astrocytoma cell line, the action of ruthenium red was also tested on neuronal cells. The dose – response curve of ruthenium red action in

undifferentiated NTERA-2 cells is shown in Fig. 5.4.

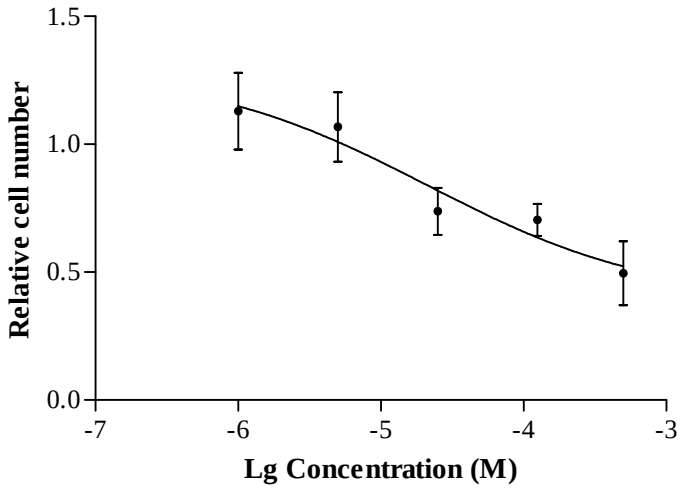

Fig. 5.4 Dose – response curve of ruthenium red action in undifferentiated NTERA-2 cells. The data points are the means of 3 in each group.

The one way ANOVA test for all the groups indicated that the difference amongst the groups was significant ($p < 0.01$), and the Dunnett's post test indicated that 500 μM ruthenium red had a significant effect on the relative cell number from the control group ($p < 0.05$). Hence, 125 μM or lower dose of ruthenium red did not cause an overt reduction in cell number from the control in undifferentiated NTERA-2 cells.

Ruthenium red was then tested on the $CoCl_2$ insult (15 μM) in undifferentiated NTERA-2 cells, and the results are shown in Fig. 5.5.

The one way ANOVA test for all the groups indicated that the difference amongst the groups was not significant. That was because of the large standard

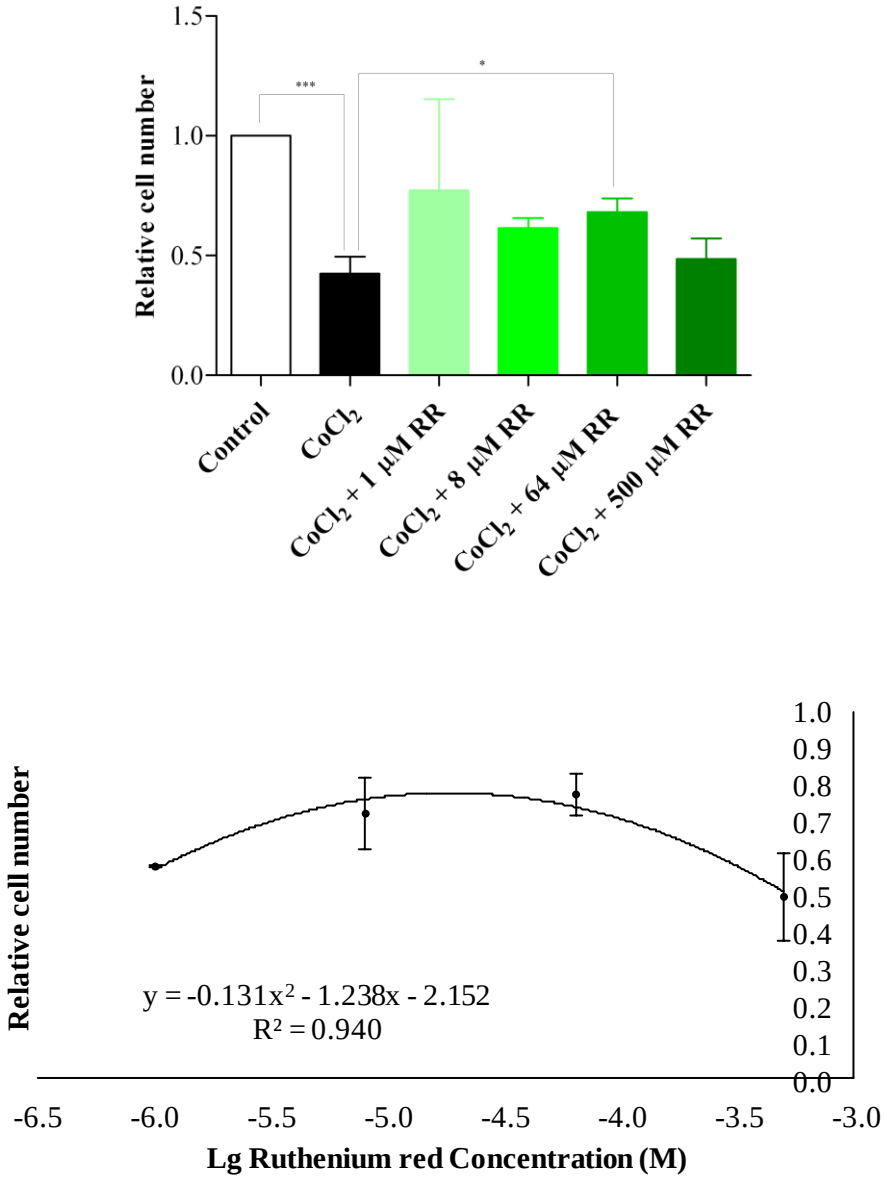

Fig. 5.5 The effect of ruthenium red (RR) in combination with an EC_{50} of $CoCl_2$ (15 µM) in undifferentiated NTERA-2 cells. Above: bar graph, and bottom: dose – response curve of ruthenium red effect. The points are the means of 3.

error in the $CoCl_2$ + 1 µM ruthenium red group. After this group was removed from the statistical test, the one way ANOVA test indicated that the difference amongst the rest of the groups was significant ($p < 0.001$), and the Dunnett's

post test (comparing each group with the $CoCl_2$ group) indicated that 64 μM ruthenium red in the presence of an EC_{50} of $CoCl_2$ caused a significant increase in the relative cell number from the $CoCl_2$ insult ($p < 0.05$).

The optimal dose of ruthenium red against $CoCl_2$ insult was then calculated based on the polynomial trend line in Fig. 5.5.

$$y = -0.131\ x^2 - 1.24\ x + 2.15$$

Here, y represents the relative cell number, and x represents the lg concentration of ruthenium red (M).

To calculate the optimal does, which is the inflection point of the polynomial trend line above:

$$y' = 2 \times (-0.131) \times x - 1.24 = 0$$

Hence, the optimal dose of ruthenium red, which provided maximum protection, was estimated as 18.8 μM.

5.3.1.3 Undifferentiated SH-SY5Y cells

In addition to NTERA-2 cell line, another neuronal cell line, SH-SY5Y, was also selected to test the action of ruthenium red in this study. Firstly, the dose – response curve of ruthenium red alone in undifferentiated SH-SY5Y cells is shown in Fig. 5.6.

The one way ANOVA test for all the groups indicated that the difference

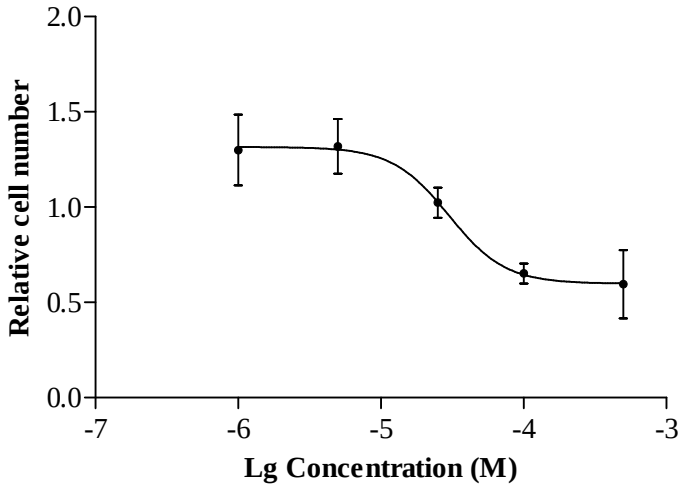

Fig. 5.6 Dose – response curve of ruthenium red action in undifferentiated SH-SY5Y cells. The data points are the means of 6.

amongst the groups was significant ($p < 0.001$), but the Dunnett's post test (comparing each group with the control) did not indicate any significant difference in relative cell numbers in ruthenium red treatment comparing with the control group. That means ruthenium red is safe for undifferentiated SH-SY5Y cells in this dose range (1 – 500 μM).

Then, ruthenium red was tested on $CoCl_2$ insult in undifferentiated SH-SY5Y cells, and the results are shown in Fig. 5.7.

The one way ANOVA test for all the groups indicated that the difference among those groups was significant ($p < 0.001$), and the Dunnett's post test (comparing each group with $CoCl_2$ alone) suggested that 40 μM $CoCl_2$ had a significant effect on the relative cell number from the control ($p < 0.001$), 10 μM ruthenium red in presence of $CoCl_2$ insult caused an increase in the relative

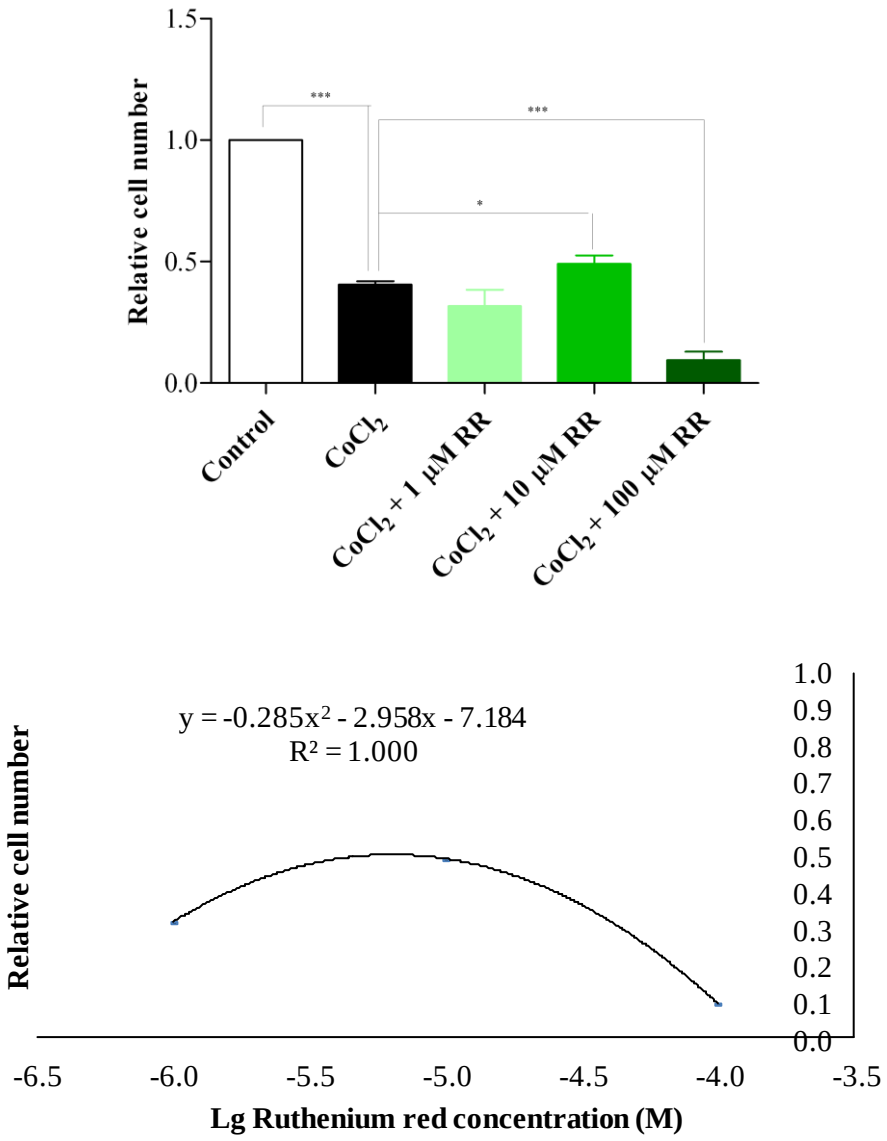

Fig. 5.7 The effect of ruthenium red (RR) in combination with an EC_{50} of $CoCl_2$ (40 μM) in undifferentiated SH-SY5Y cells. The data points are the means of 9 for $CoCl_2$ + 10 μM RR, $CoCl_2$ alone and the control, and 3 for $CoCl_2$ + 1 μM RR and $CoCl_2$ + 100 μM RR.

cell number from $CoCl_2$ alone ($p < 0.05$), and 100 μM ruthenium red in presence of $CoCl_2$ insult caused a reduction from $CoCl_2$ alone ($p < 0.001$).

Then, the optimal dose of ruthenium red against $CoCl_2$ insult was calculated based on the polynomial trend line in Fig. 5.7:

$$y = -0.285x^2 – 2.96x -7.18$$

Here, "y" represents the relative cell number, and "x" represents the lg concentration of ruthenium red. To calculate the optimal dose, which is the inflection point of the above function, following calculation was done thereafter:

$$y' = 2 \times (-0.285) \times x – 2.96 = 0$$

Hence, the optimal dose of ruthenium red against $CoCl_2$ insult in undifferentiated SH-SY5Y cells, which provided the maximum protection, was estimated as 6.46 μM.

5.3.1.4 Differentiated SH-SY5Y cells

Further to the undifferentiated SH-SY5Y cells, the effect of ruthenium red was also tested on the differentiated counterpart. The dose – response curve of ruthenium red in differentiated SH-SY5Y is shown in Fig. 5.8.

The one way ANOVA test for all the groups indicated that the difference among those groups was significant ($p < 0.01$), and the Dunnett's post test (comparing each group with the control) suggested that 5 μM ruthenium red caused a significant increase in the relative cell number from the control group ($p < 0.05$). That means ruthenium red is safe for differentiated SH-SY5Y cells in this range of dose (1 – 500 μM).

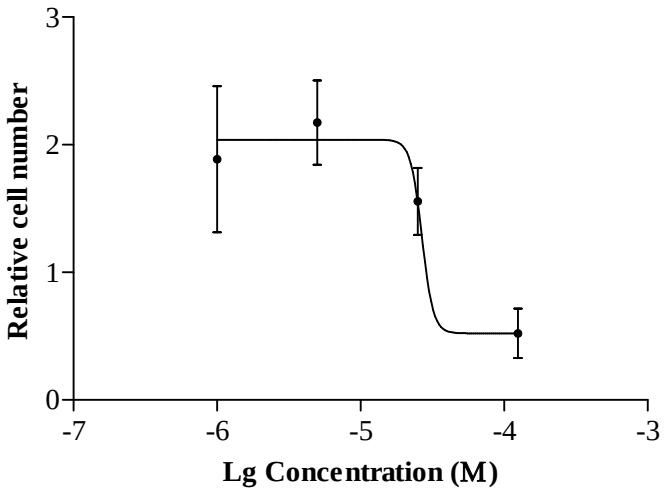

Fig. 5.8 Dose – response curve of ruthenium red in differentiated SH-SY5Y cells. The data points are the means of 9.

Then, ruthenium red was tested on the $CoCl_2$ insult in differentiated SH-SY5Y cells. The results are shown in Fig. 5.9.

The one way ANOVA test for all the groups indicated that the difference among those groups was significant ($p < 0.001$), and the Dunnett's post test (comparing each group with the $CoCl_2$ alone) indicated that 30 μM $CoCl_2$ alone caused a significant reduction in the relative cell number from the control, and 20 μM ruthenium red in the presence of $CoCl_2$ insult had a significant effect on the relative cell number from $CoCl_2$ alone ($p < 0.05$).

Then, the optimal dose of ruthenium red in differentiated SH-SY5Y cells was calculated based on the polynomial trend line in Fig. 5.9:

$$y = -1.587x^2 – 14.62x – 32.77$$

Hence, the optimal dose, which is the inflection point of the trend line above,

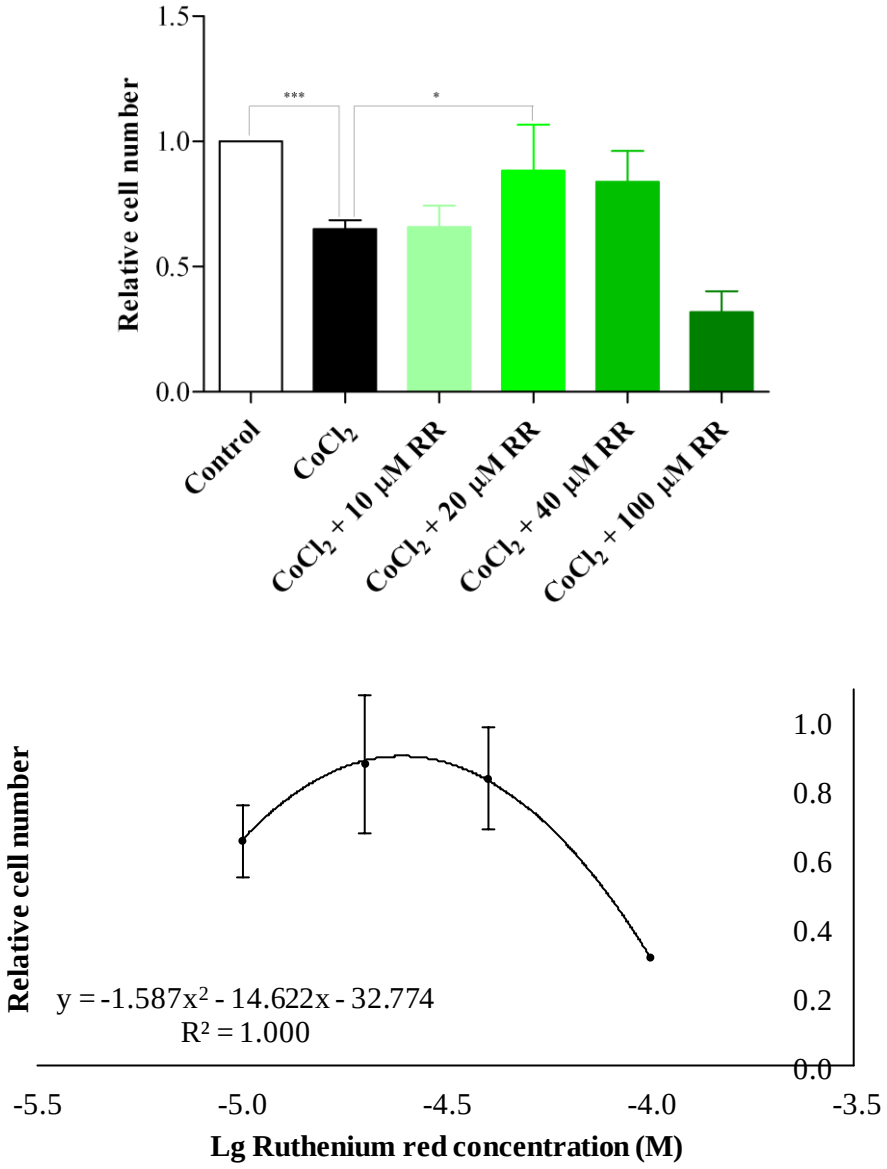

Fig. 5.9 The effect of ruthenium red (RR) in combination with $CoCl_2$ insult (30 μM) in differentiated SH-SY5Y cells. The data points are the means of 6 for $CoCl_2$ + 20 μM ruthenium red, and 3 for all the other groups.

was calculated.

$$y' = 2 \times (-1.587) \times x - 14.62 = 0$$

Thus, the optimal dose, which provided the maximum protection, against $CoCl_2$ insult in differentiated SH-SY5Y was estimated as 24.8 μM.

5.3.2 Dantrolene against $CoCl_2$ insult

Besides ruthenium red which is a generic RyR blocker, another RyR blocker, dantrolene, was also tested in the presence of $CoCl_2$ insult. As introduced before, dantrolene can "selectively" block RyRI and RyRIII (see Section 5.1).

5.3.2.1 On MOG-G-UVW cells

The dose-response curve for dantrolene in MOG-G-UVW cells is shown in Fig. 5.10.

The one way ANOVA test for all the groups in Fig. 5.10 indicated that the difference among those groups was significant ($p < 0.001$), and the Dunnett's post test (comparing each group with the control) indicated that 100 μM dantrolene caused a significant reduction in the relative cell number ($p < 0.001$), but the 1% vehicle, DMSO, did not have any overt effect on relative cell number. That means dantrolene is ineffective in MOG-G-UVW cells at 10 μM or lower concentration.

Dantrolene was then tested on $CoCl_2$ insult in MOG-G-UVW cells, and the results are shown in Fig. 5.11.

The one way ANOVA test for all the groups in Fig. 5.11 suggested that the difference among those groups was significant ($p < 0.001$), and the Dunnett's

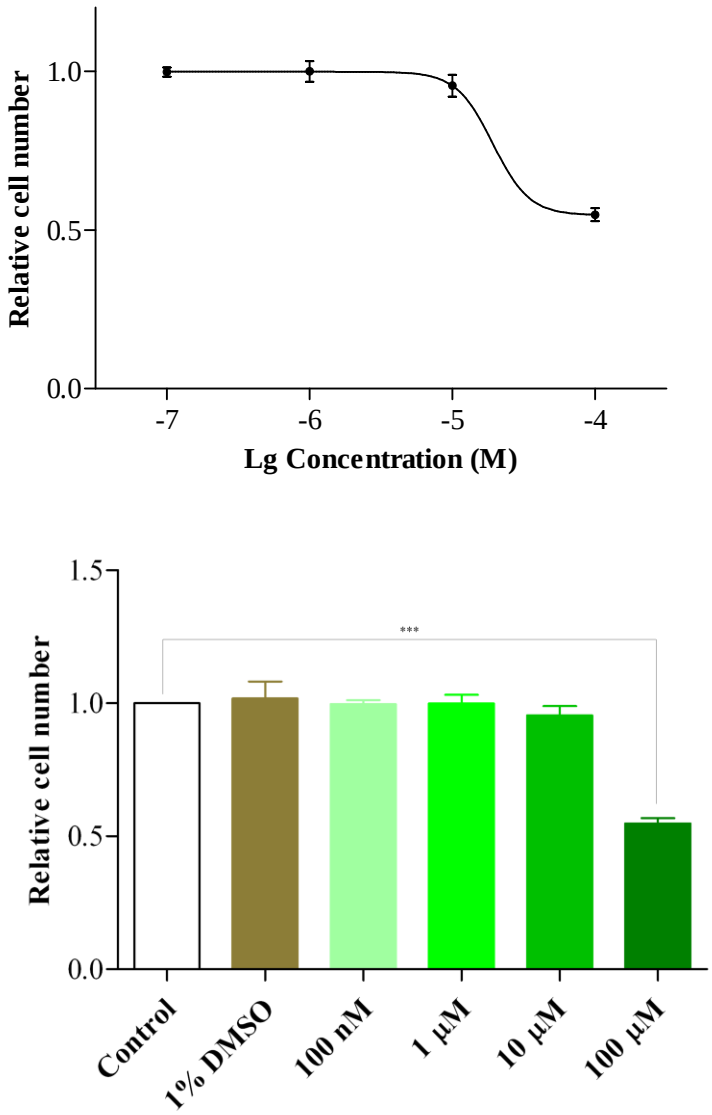

Fig. 5.10 Dose – response of dantrolene in MOG-G-UVW cells. Above: dose – response curve of dantrolene alone, and bottom: bar graph showing the vehicle, DMSO. The data points are the means of 3.

post test (comparing each group with $CoCl_2$ alone) indicated that $CoCl_2$ insult caused a significant reduction in the relative cell number from the control ($p < 0.001$), and 100 nM, 300 nM and 1 μM dantrolene in the presence of $CoCl_2$ had significant effects on the relative cell number from $CoCl_2$ alone ($p < 0.001$, $p < 0.05$ and $p < 0.001$ respectively).

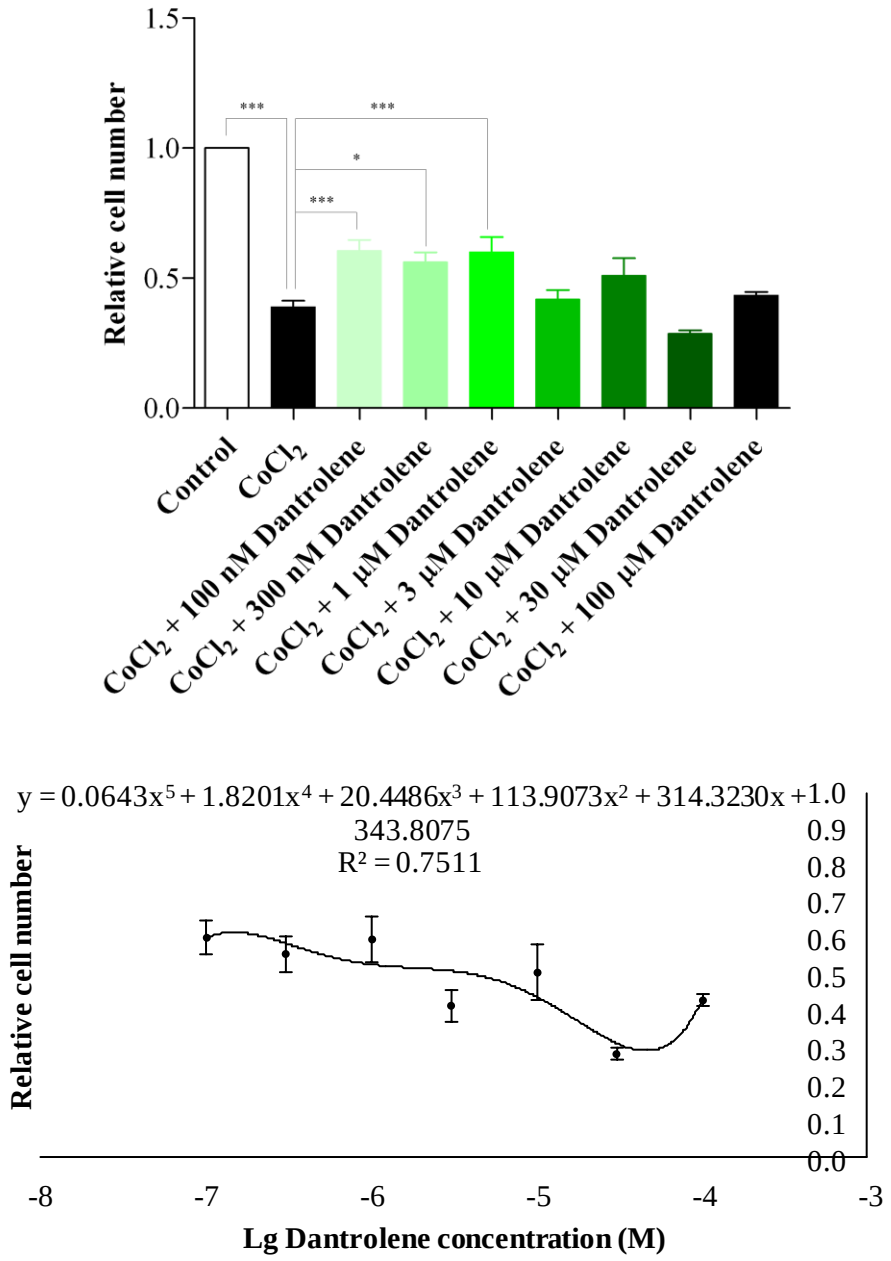

Fig. 5.11 The effect of dantrolene in combination with an EC_{50} of $CoCl_2$ (32.2 µM). Above: bar graph, and bottom: polynomial trend line. The data points are the means of 30 for $CoCl_2$ alone and the control, 6 for $CoCl_2$ + 100 nM dantrolene, $CoCl_2$ + 1 µM dantrolene and $CoCl_2$ + 10 µM dantrolene, and 3 for all the rest groups.

Then, the optimal dose of dantrolene against $CoCl_2$ insult in MOG-G-UVW cells, which provided the maximum protection, was calculated based on the

polynomial trend line in Fig. 5.11, which is:

$$y = 0.0643x^5 + 1.820x^4 + 20.45x^3 + 113.9x^2 + 314.3x + 343.8$$

Here, "y" represents the relative cell number, and "x" represents the lg concentration of dantrolene. The optimal dose, which should be one of the inflection points, was calculated thereafter.

$$y' = 5 \times 0.0643 \times x^4 + 4 \times 1.820 \times x^3 + 3 \times 20.45 \times x^2 + 2 \times 113.9 \times x + 314.3$$

$$= 0$$

Hence, the optimal dose of dantrolene against $CoCl_2$ insult in MOG-G-UVW cells was estimated as 200 nM.

5.3.2.2 On undifferentiated SH-SY5Y cells

In addition to the astrocytoma cell line, the effect of dantrolene was also tested on the neuronal cell line, SH-SY5Y. The dose – response curve for dantrolene in undifferentiated SH-SY5Y cells is shown in Fig. 5.12.

The one way ANOVA test for all the groups in Fig. 5.12 indicated that the difference among those groups was significant ($p < 0.001$), and Dunnett's post test (comparing each group with the control) indicated that 10 μM and 100 μM dantrolene alone caused a significant reduction in the relative cell number from the control ($p < 0.05$ and $p < 0.001$) respectively, but the vehicle, DMSO, did not have any overt effect on the relative cell number from the control group.

Dantrolene was then tested on a $CoCl_2$ insult in undifferentiated SH-SY5Y

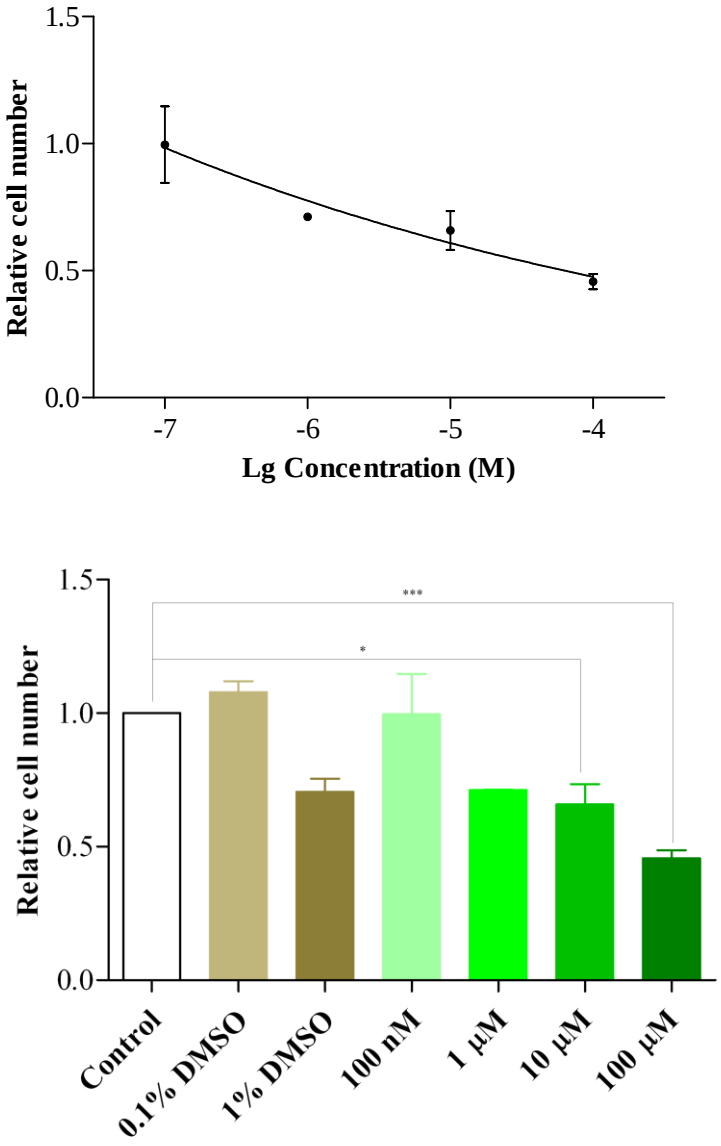

Fig. 5.12 Dose - response of dantrolene alone in undifferentiated SH-SY5Y cells. Above: dose – response curve, and bottom: bar graph showing the vehicle, DMSO. The data points are the means for 3.

cells. The results are shown in Fig. 5.13.

The one way ANOVA test for all the groups in Fig. 5.13 showed that the difference among those groups was significant ($p < 0.001$), and the Dunnett's post test (comparing each group with the $CoCl_2$ insult) indicated that 40 μM

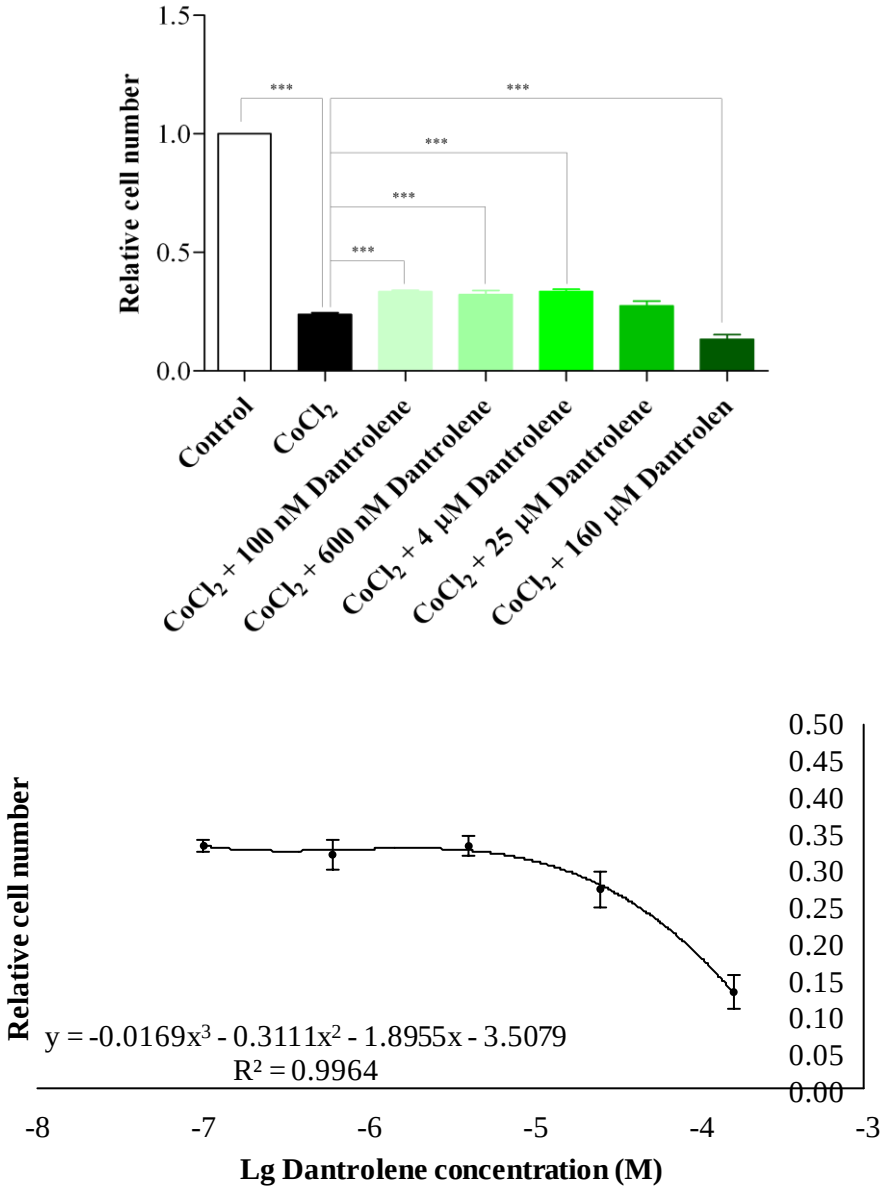

Fig. 5.13 The effect of dantrolene in combination with an EC_{50} of $CoCl_2$ (40 µM). Above: bar graph, and bottom: polynomial trend line of dantrolene effect in presence of $CoCl_2$ insult. The data points are the means of 3.

$CoCl_2$ caused a significant reduction in the relative cell number from the control ($p < 0.001$), 100 nM, 600 nM and 4 µM dantrolene in presence of $CoCl_2$ insult caused a significant increase in the relative cell numbers from the $CoCl_2$ insult ($p < 0.001$, $p < 0.01$ and $p < 0.001$ respectively), but 160 µM

dantrolene in presence of $CoCl_2$ insult caused a further reduction in the relative cell number from the $CoCl_2$ insult ($p < 0.001$).

Thereafter, the optimal dose of dantrolene against $CoCl_2$ insult in undifferentiated SH-SY5Y cells, which provided the maximum protection, was calculated based on the polynomial trend line in Fig. 5.13.

$$y = -0.0169x^3 – 0.3111x^2 – 1.896x – 3.508$$

Here, "y" represents the relative cell number, and "x" represents the lg concentration of dantrolene. The optimal dose, which is one of the inflection points of the above trend line, is therefore calculated.

$$y' = 3 \times (-0.0169) \times x^2 – 2 \times 0.3111 \times x - 1.896 = 0$$

The optimal dose of dantrolene against $CoCl_2$ insult in undifferentiated SH-SY5Y cells was then estimated as 2.34 μM.

5.3.3 Procaine effect on $CoCl_2$ insult

Besides the generic RyR blocker (ruthenium red) and a "selective" RyRI & RyRIII blocker (dantrolene), a third RyR blocker, procaine, has also been tested in this Thesis. As introduced above (see Section 5.1), procaine is a "selective" blocker for RyRI and RyRII.

5.3.3.1 On MOG-G-UVW cells

The dose – response curve of procaine in MOG-G-UVW cells is shown in Fig.

5.14

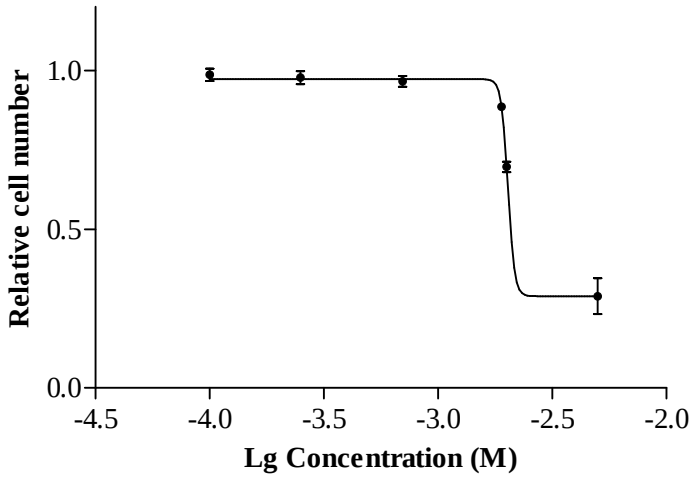

Fig. 5.14 Dose – response curve of procaine in MOG-G-UVW cells. The data points are the means of 15 for 700 μM and the control, 6 for 100 μM, 250 μM and 2 mM, and 3 for 1.9 mM and 5 mM.

The one way ANOVA tested for all the groups in Fig. 5.14 showed that the difference among those groups was significant ($p < 0.001$), and the Dunnett's post test (comparing each group with the control) indicated that 1.9 mM or higher dose of procaine caused significant reduction in the relative cell number from the control ($p < 0.01$ for 1.9 mM, and $p < 0.001$ for 2 mM and 5 mM). That means 700 μM or lower dose of procaine had little effect on the relative cell number in MOG-G-UVW cells.

To estimate the EC_{50} of procaine in MOG-G-UVW cells, a logistic regression was done and the trend line is shown in Fig. 5.15.

Then, the EC_{50} of procaine is calculated below:

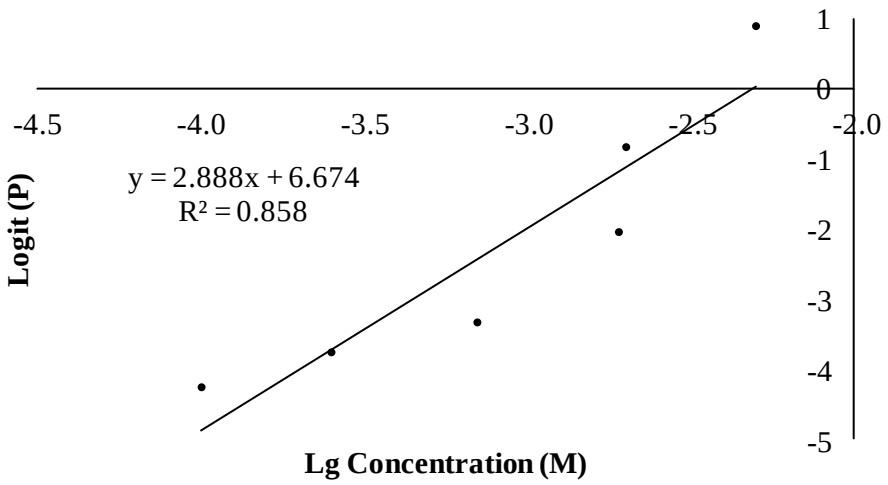

Fig. 5.15 Logistic regression of procaine action in MOG-G-UVW cells

$$EC_{50} = 10^{\frac{-6.674}{2.888}} = 0.004887 \text{ M} = 4.89 \text{ mM}.$$

Procaine was then tested on a $CoCl_2$ insult in MOG-G-UVW cells and the results are shown in Fig. 5.16.

The one way ANOVA test for all the groups in Fig. 5.16 indicated that the difference among those groups was significant ($p < 0.001$), and the Dunnett's post test (comparing each group with $CoCl_2$ insult) indicated that $CoCl_2$ insult caused a significant reduction in the relative cell number from the control ($p < 0.001$), and 5 mM procaine in presence of $CoCl_2$ had a significant effect on the relative cell number from $CoCl_2$ alone ($p < 0.01$). The results suggested that procaine did not protect the MOG-G-UVW cells from an EC_{50} dose of $CoCl_2$ insult.

5.3.3.2 On undifferentiated NTERA-2 cells

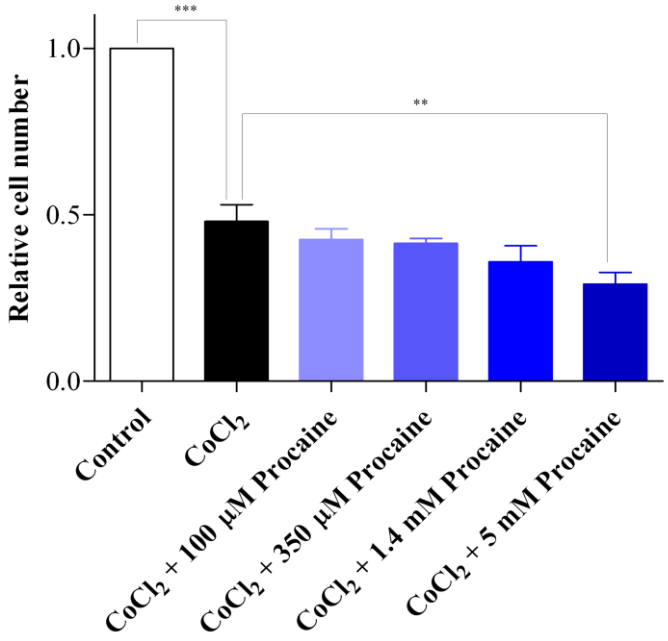

Fig. 5.16 The effect of procaine in combination with an EC_{50} of $CoCl_2$ (32.2 µM) in MOG-G-UVW cells. The data points are the means of 3.

In addition to the astrocytoma cell line, the possible effect of procaine, if any, has also been tested on neuronal cell lines. The results in undifferentiated NTERA-2 cells are presented here in Fig. 5.17.

The one way ANOVA test for all the groups in Fig. 5.17 indicated that the difference among those groups was significant ($p < 0.001$), and the Dunnett's post test (comparing each group with the $CoCl_2$ alone) indicated that $CoCl_2$ insult caused a significant reduction in the relative cell number from the control ($p < 0.001$), but procaine in the presence of $CoCl_2$ insult did not have any significant effect on the relative cell number from $CoCl_2$ alone. The results suggested that procaine has not protected the NTERA-2 cells from an EC_{50} of $CoCl_2$ insult.

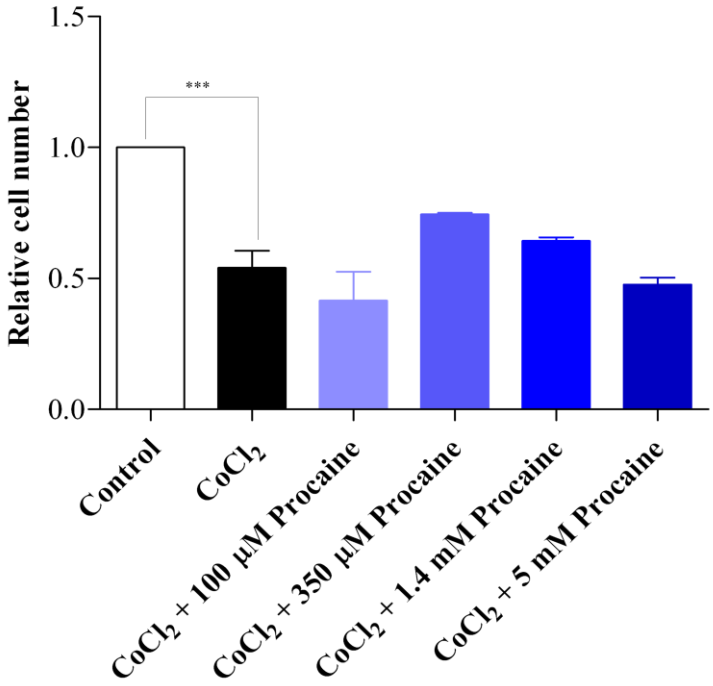

Fig. 5.17 The effect of procaine in combination with an EC_{50} of $CoCl_2$ (15 µM) in undifferentiated NTERA-2 cells. The data points are the means of 6 for $CoCl_2$ alone and the control, and 3 for procaine in combination with $CoCl_2$ insult.

5.3.3.3 Differentiated SH-SY5Y cells

Besides the NTERA-2 cells, another neuronal cell line, differentiated SH-SY5Y cells, was also selected to test the possible effect, if any, of procaine. One dose of procaine (5 mM) has been tested in combination with an EC_{50} dose of $CoCl_2$ insult (30 µM) in differentiated SH-SY5Y cells. The results are shown in Fig. 5.18.

The one way ANOVA test for all the groups in Fig. 5.18 indicated that the difference among those groups was significant ($p < 0.001$), and the Bonferroni's post test (comparing every two groups) indicated that $CoCl_2$ insult

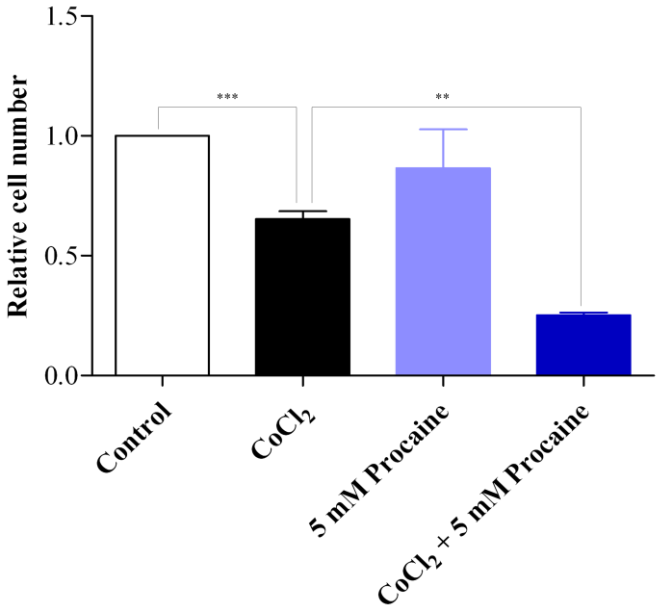

Fig. 5.18 The effect of procaine (5 mM) in combination with $CoCl_2$ insult (30 μM) in differentiated SH-SY5Y cells. The data points are the mean of 21 for the $CoCl_2$ alone and the control, 6 for 5 mM procaine alone, and 3 for procaine in combination with $CoCl_2$ insult.

caused a significant reduction in the relative cell number from the control ($p < 0.001$), and procaine in the presence of $CoCl_2$ insult had a significant effect on the relative cell number from the $CoCl_2$ alone ($p < 0.01$), but procaine alone did not cause any overt reduction in the relative cell number from the control. The results suggested that procaine aggravates the insult of $CoCl_2$ in differentiated SH-SY5Y cells.

5.3.4 Ryanodine effect on $CoCl_2$ insult

Besides procaine, ryanodine is another "selective" RyRI and RyRII blocker. But, ryanodine has a two-way effect on the RyR, as introduced above (see

Section 5.1): it can be a generic RyR activator at low concentrations (nM – μM), and can block RyRI and RyRII at a high concentration (about hundred μM). Thus, the possible effect, if any, of ryanodine in the presence of hypoxia mimetic has been tested in MOG-G-UVW cells. The dose - response of ryanodine alone is shown in Fig. 5.19.

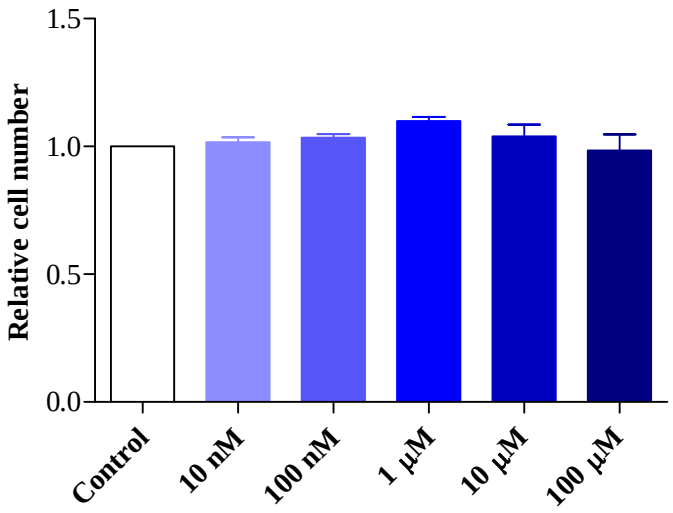

Fig. 5.19 Dose - response of ryanodine in MOG-G-UVW cells. The results are the means of 3.

The one way ANOVA test for all the groups in Fig. 5.19 indicated that the difference among those groups was not significant. That shows ryanodine has little effect on the relative cell number in MOG-G-UVW cells in this dose range (10 nM – 100 μM). The effect of ryanodine was then tested in combination with $CoCl_2$ insult in MOG-G-UVW cells, and the results are shown in Fig. 5.20.

The one way ANOVA test for all the groups in Fig. 5.20 suggested that the

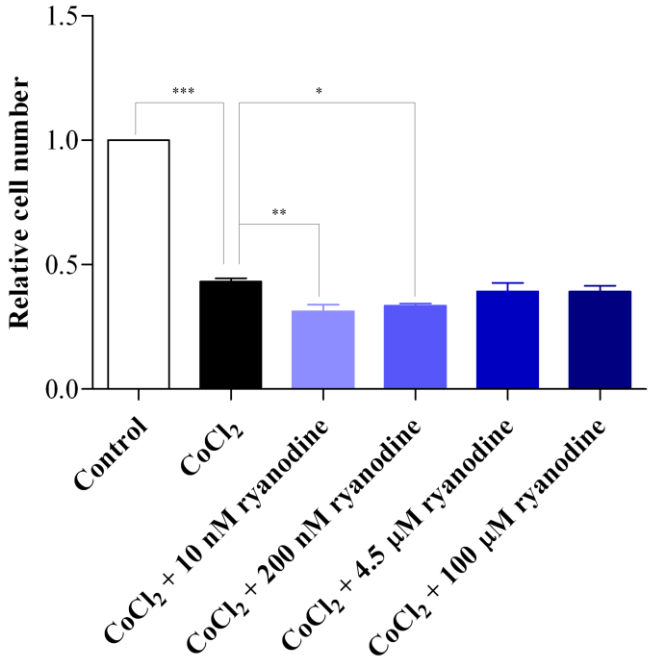

Fig. 5.20 The effect of ryanodine in combination with an EC_{50} of $CoCl_2$ insult (32.2 µM). The results are the mean of 3.

difference among those groups was significant ($p < 0.001$), and the Dunnett's post test (comparing each group with the $CoCl_2$ alone) indicated that $CoCl_2$ insult caused a significant reduction in the relative cell number from the control ($p < 0.001$), 10 µM and 200 µM ryanodine in presence of $CoCl_2$ insult had significant effects on the relative number from the $CoCl_2$ insult ($p < 0.01$ and $p < 0.05$ respectively), but 4.5 µM or higher dose of ryanodine in presence of $CoCl_2$ did not have any significant effect on the relative cell number from the $CoCl_2$ insult. The results suggested that ryanodine aggravates the insult of $CoCl_2$ at a low concentration which actives all the three isoforms of RyR, but has little effect on the relative cell number at a high concentration, which blocks both RyRI and RyRII.

5.3.5 Caffeine effect on $CoCl_2$ insult

In addition to a high dose of ryanodine, another generic RyR activator, caffeine, has also been tested in this Thesis. The dose – response curve of caffeine alone in MOG-G-UVW cells is shown in Fig. 5.21.

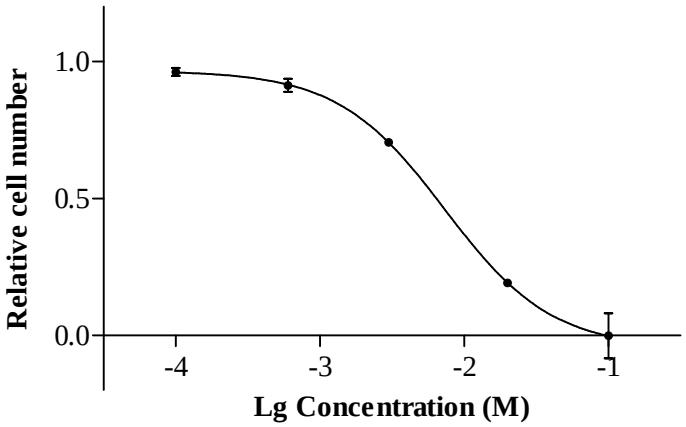

Fig. 5.21 Dose – response curve of caffeine in MOG-G-UVW cells. The data points are the means of 3.

The one way ANOVA test for all the groups in Fig. 5.21 indicated that the difference among those groups was significant ($p < 0.001$), and the Dunnett's post test (comparing each group with the control) indicated that 3 mM or higher dose of caffeine caused a significant reduction in the relative cell number from the control ($p < 0.001$).

To estimate the EC_{50} of caffeine in MOG-G-UVW cells, the logistic regression has been constructed in Fig. 5.22.

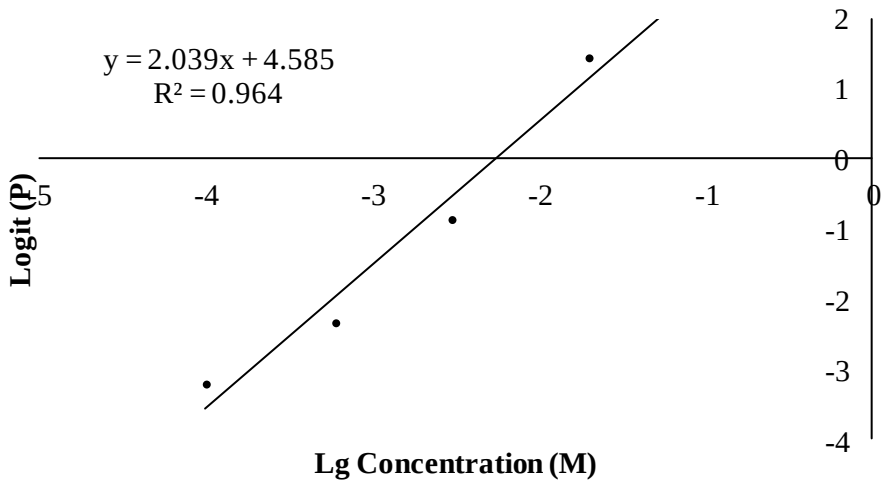

Fig. 5.22 Logistic regression of the effect of caffeine alone in MOG-G-UVW cells

Hence, the EC_{50} of caffeine in MOG-G-UVW is:

$$EC_{50} = 10^{\frac{-4.585}{2.039}} = 0.00564 \text{ M} = 5.64 \text{ mM}$$

Caffeine was then tested on $CoCl_2$ insult in MOG-G-UVW cells, and the results are shown in Fig. 5.23.

The one way ANOVA test for all the groups in Fig. 5.23 indicated that the difference among those groups was significant ($p < 0.001$), and the Dunnett's post test (comparing each group with the $CoCl_2$ alone) indicated that $CoCl_2$ insult caused a significant reduction in the relative cell number from the control ($p < 0.001$), and 10 mM – 100 mM caffeine in the presence of $CoCl_2$ insult had significant effects on the relative cell number from the $CoCl_2$ alone ($p < 0.001$). The results suggested that caffeine cannot protect MOG-G-UVW cells from $CoCl_2$ insult.

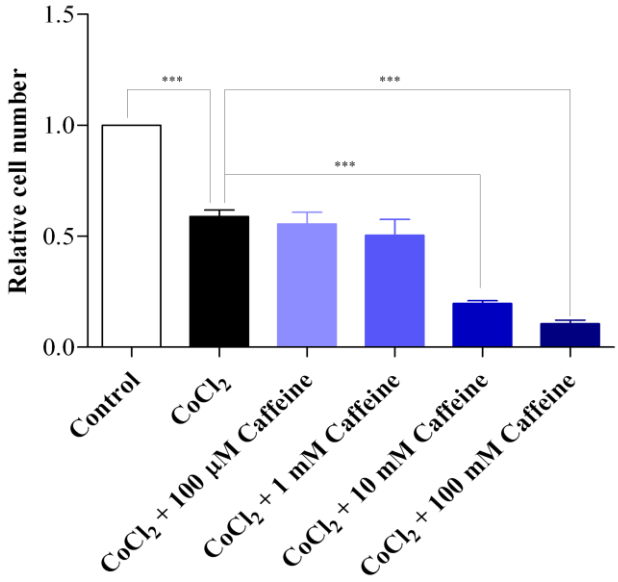

Fig. 5.23 The effect of caffeine in combination with an EC_{50} of $CoCl_2$ insult (32.2 µM) in MOG-G-UVW cells. The results are the means of 3.

5.3.6 Ruthenium red and procaine effect on $A\beta_{1-42}$ insult

In addition to the hypoxia mimetic effect induced by $CoCl_2$, another insult, $A\beta_{1-42}$, has also been selected to test for a possible effect, if any, of the RyR blockers, such as ruthenium red and procaine. The results are shown in Fig. 5.24.

The one way ANOVA test for all the groups indicated that the difference among those groups was significant ($p < 0.001$), and the Tukey's post test (comparing every two groups) indicated that 5 mM procaine in the presence of $A\beta_{1-42}$ had a significant effect on the relative cell number from the $A\beta_{1-42}$ alone. The results suggested that procaine is not protective in presence of $A\beta_{1-42}$, and ruthenium red has a trend to be protective, although not significant.

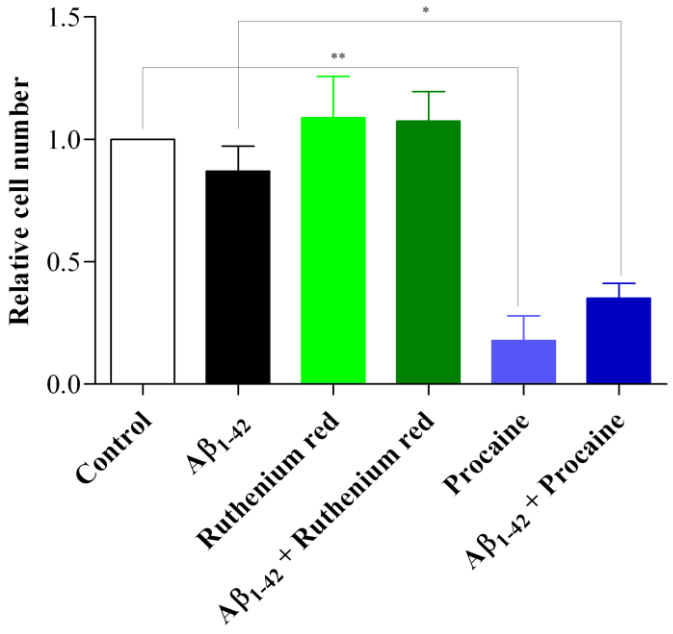

Fig. 5.24 The action of ruthenium red (10 μM) or procaine (5 mM) on $A\beta_{1-42}$ insult (15.5 μM) in undifferentiated SH-SY5Y cells. The results are the mean of 3.

5.4 Discussion

From all those results above, the effects of RyR modulators can be summarised as below:

5.4.1 RyR blockade

As introduced before (see Section 1.2.2 and 1.4.1), the RyR activation induced by the overload of $[Ca^{2+}]_i$ stress in cells, can release more Ca^{2+} from ER and further increase the $[Ca^{2+}]_i$ which can induce cell death. And, according to the Q-PCR results in Section 3 and the cell insult results in Section 4, the cells with higher RyRIII expression (i.e. differentiated SH-SY5Y) are more sensitive

to the cell insults which may increase the $[Ca^{2+}]_i$, including the hypoxia mimetic effect induced by $CoCl_2$ and oxidative stress induced by H_2O_2, than those with lower expression (i.e. undifferentiated SH-SY5Y). If it is the case that the RyR is partly responsible to the cell death, the blockade of RyR should be protective. Hence, RyR blockers ruthenium red and dantrolene have been tested here.

According to the results above, ruthenium red, a generic RyR blocker, is protective. In MOG-G-UVW cells, ruthenium red in combination with an EC_{50} dose of $CoCl_2$ insult caused an increase in the relative cell number from the $CoCl_2$ alone, although ruthenium red alone caused a reduction in the cell number from the control (see Section 5.3.1.1). In undifferentiated NTERA-2 cells, ruthenium red in the presence of $CoCl_2$ insult caused an increase in the relative cell number at a dose where ruthenium red alone had little effect on the cell number (see Section 5.3.1.2). In both undifferentiated and differentiated SH-SY5Y cells, ruthenium red alone did not cause any overt reduction in the cell number, but ruthenium red in combination with $CoCl_2$ insult caused an increase in the relative cell number from the $CoCl_2$ alone (see Section 5.3.1.3 and 5.3.1.4). In addition to the $CoCl_2$ insult, ruthenium red has also shown a trend to be protective in the presence of $A\beta_{1-42}$ insult in MOG-G-UVW cells, although not significantly (see Section 5.3.6). All of those results suggested that generic blockade of the RyR by ruthenium red is protective in the cells.

Furthermore, dantrolene, which is a “selective” RyRI and RyRIII blocker, is

also protective. In both MOG-G-UVW and undifferentiated SH-SY5Y cells, dantrolene in combination with the EC_{50} of $CoCl_2$ insult caused an increase in the relative cell number from the $CoCl_2$ alone at low concentration (100 nM – μM) where dantrolene alone has little effect on the cell numbers (see Section 5.3.2).

Thus, it can be suggested that generic blockade is protective, at least against the hypoxia mimetic effect induced by $CoCl_2$, in both astrocytoma and neuronal cell lines. And, as for the selectivity amongst all the three isoforms of RyR, it is possible that RyRI and/or RyRIII are/is playing an important role rather than RyRII because of the protective effect demonstrated by dantrolene.

5.4.2 RyR activation

In addition to the blockade, the opposite modulation was also considered and tested in this Thesis. If it is believed that blockade of the RyR is protective in the presence of the insult, the activation to RyR should aggravate the effect of insult, or at least cannot be protective. Hence, two generic RyR activators, caffeine and ryanodine (10 nM – 1 μM) were tested in this Thesis.

Caffeine is not protective. In MOG-G-UVW cells, caffeine in combination with an EC_{50} of $CoCl_2$ insult caused a reduction in the relative cell number from the $CoCl_2$ alone. This effect of caffeine appeared at a high dose where caffeine alone caused a reduction in the relative cell number (see Section 5.3.5).

Nevertheless, ryanodine has aggravated the $CoCl_2$ insult. In MOG-G-UVW cells, with an EC_{50} of $CoCl_2$ challenge, a low concentration of ryanodine, which is an active dose for RyR, caused a reduction in the relative cell number from $CoCl_2$ alone. The dose of ryanodine alone had little effect on the relative cell number (see Section 5.3.4).

Therefore, it can be suggested that the blockade of the RyR, especially RyRI and/or RyRIII can be protective in these cells, but the activation of RyR is not protective, or even may aggravate the insult.

5.4.3 RyRIII as a selective target

Although the blockade of the RyR is suggested to be protective, there is still one concern left: generic blockade of the RyR can cause side effects on tissues or organs other than brain neurones. So, it is important to know which isoform of RyR is more important in neuronal death, if there is any selectivity among the three isoforms.

Thus, procaine and ryanodine (high dose), which are "selective" RyRI and RyRII blockers, were also tested in this study.

Procaine is not protective. In MOG-G-UVW cells, procaine in combination with an EC_{50} of $CoCl_2$ insult caused a reduction in the relative cell number from the $CoCl_2$ alone. This effect appeared at a high dose of procaine which

alone had caused a reduction in the cell number (see Section 5.3.3.1). In undifferentiated NTERA-2 cells, procaine in the presence of $CoCl_2$ insult did not have any effect on the relative cell number from the $CoCl_2$ alone. And, in differentiated SH-SY5Y cells, in the face of an EC_{50} dose of $CoCl_2$, procaine has aggravated the insult at a dose where procaine alone has little effect on the cell number.

Ryanodine at a high dose (> 10 μM) is not protective either. In MOG-G-UVW cells, ryanodine in combination with $CoCl_2$ insult did not have any effect on the relative cell number at a high dose, although it has caused a reduction at low doses which can activate RyR.

Hence, it can be suggested that the blockade of the RyRI and RyRII is not protective against the hypoxia mimetic effect induced by $CoCl_2$. It is then possible that another isoform of RyR, RyRIII, is more important in neuronal death than RyRI and RyRII. This is consistent with previous studies which suggest that RyRIII is the brain type of RyR (see Section 1.2.2), and is consistent with the results in Chapter 3 and 4. However, whether RyRIII may possibly be expressed in other tissues or organs is still unsure. Therefore, PCR or western blot work to test the expression of RyRIII in the tissues or organs other than neurones is also needed. If the results might be negative, it would be more solid to suggest that RyRIII is a good neuroprotective target for future drug development.

5.5 Conclusions

Summarising all the results and discussion in this chapter, it may be concluded that:

a. generic activation of RyR, with caffeine or a low dose of ryanodine is not protective in cells against a hypoxia mimetic effect induced by $CoCl_2$, and may even aggravate the insult by further reducing the relative cell number;
b. generic blockade of the RyR with ruthenium red, or blockade of the RyRI and RyRIII with dantrolene, is protective in both astrocytoma and neuronal cells on the hypoxia mimetic effect induced by $CoCl_2$, and may even tend to be protective against the $A\beta_{1-42}$ insult;
c. selective blockade of the RyRI and RyRII, with procaine or high dose of ryanodine, is not protective in either astrocytoma or neuronal cells on the hypoxia mimetic effect induced by $CoCl_2$.

Therefore, it is possible that selective blockade of the RyRIII could be neuroprotective. If this is the case, RyRIII could be a good target for neuronal protection which could avoid the side effects on the other tissues or organs. Thus, possible future work can be:

a. to test the modulators above on other insults, such as oxidative stress induced by H_2O_2;
b. to test other RyR modulators if available, such as suramin, which is an

activator of RyRI and RyRII; and

c. to study the modulator binding domains on RyR, especially the differences in binding domains between RyRIII and the other two isoforms of RyR.

6. The Action of BK Modulators on the Cell Insult Models

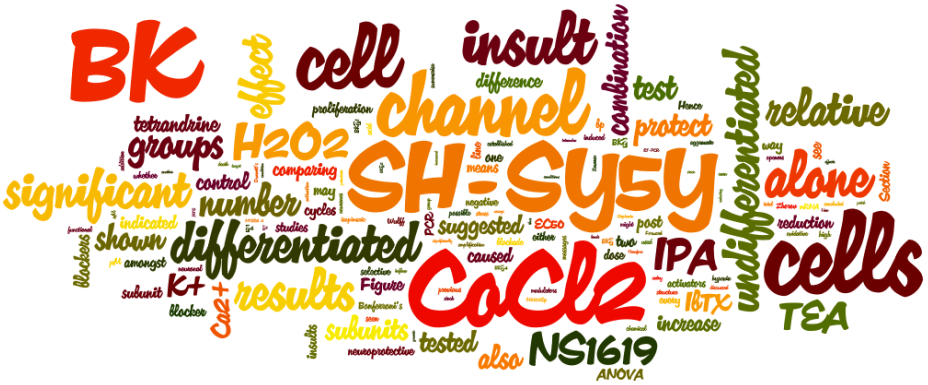

6. The Action of BK Modulators on the Cell Insult Models

6.1 Introduction

In addition to RyRIII, a K^+ channel, such as the BK, has been demonstrated as being neuroprotective. As discussed in the introduction (see Section 1.4.2.1), previous studies have found that BK channel prevalence was increased in hippocampal neurones from a transgenic AD mouse model (Tg2576, KM670/671NL) (Coles et al., 2008) and the activation of BK channel can protect neurones from glutamate insult (Liao et al., 2010). Since a selective RyRIII blocker is still unavailable, K^+ channel modulators were tested in this Thesis to determine some other possible targets to protect the neurones. The work on the BK channel is introduced in this chapter.

It has been proposed that neuronal death is mediated by an increase of $[Ca^{2+}]_i$, for example via the Ca^{2+} influx channel formed by Aβ plaque, and the possible neuroprotective effect presented by BK channel activation is related to the reduction of Ca^{2+} influx. It was suggested that neurones can be hyperpolarized by K^+ leaving the cells and driving the membrane potential towards the K^+ equilibrium potential. Such a repolarisation, or even hyperpolarisation, would cause a negative feed-back-regulation of Ca^{2+} influx and neurotransmitter release, and may thus constitute a powerful stop on cell excitation, Ca^{2+} accumulation and excitotoxicity (Liao et al., 2010). For the details about the "negative feed-back-regulation of Ca^{2+} influx", some other studies have shown

that BK channel in the presynaptic terminal membrane can cause spike narrowing and thus limit Ca^{2+} entry (Robitaille and Charlton, 1992). Other studies also suggest that BK activation can block Ca^{2+} entry through Ca_v channels and NMDA receptors by hyperpolarizing neurones and thus preventing neurotransmitter release and Ca^{2+}-overload (Wulff and Zhorov, 2008, Gribkoff et al., 2001).

Previous studies on homozygous mice lacking the BK channel α subunit have found that neuronal cell death, brain tissue infarct volume and area, animal mortality percentage and neurological deficit score were significantly increased compared with the wild type counterparts (Liao et al., 2010). A Ca^{2+} fluorescence study on nerve terminals has also found that the entry of Ca^{2+} into nerve terminals was increased after blockade of Ca^{2+} activated K^+ channel with charybdotoxin (CTX) (Robitaille and Charlton, 1992). The results of previous studies are shown below in Fig. 6.1 and Fig. 6.2:

Therefore, this chapter tests whether the BK channel exists and is functional in the neuronal cells used and whether its activation would protect the cells from those established insults.

6.2 Methods and materials

Whether the BK channel exists and is functional in SH-SY5Y cells was tested by RT-PCR and single channel patch clamp, and the possible effects of BK

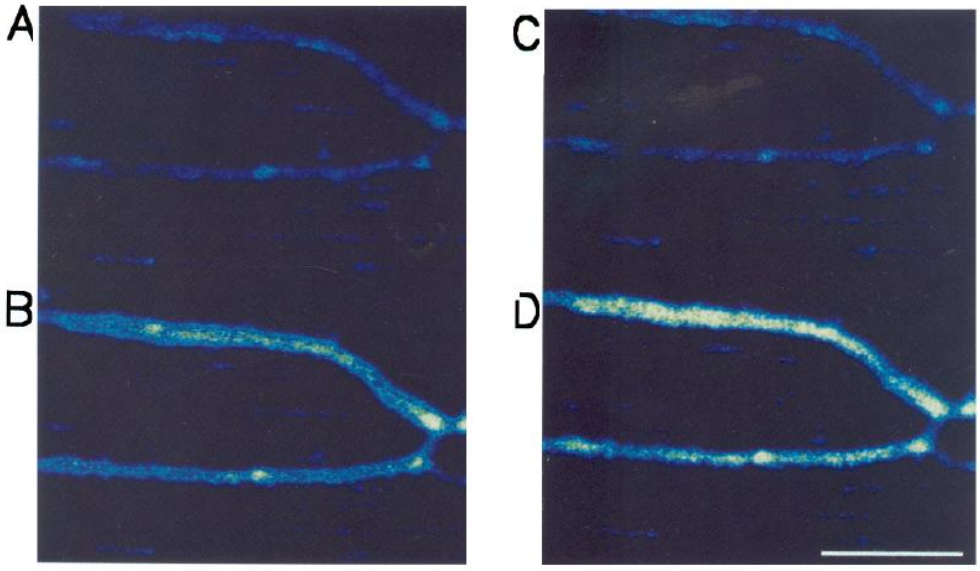

Figure 6.1 CTX increases Ca^{2+} entry in nerve terminals. A and B: Ca^{2+} signal before and 1 s after beginning of a train of stimuli [200 hertz (Hz)]. C and D: Ca^{2+} signal before and 1 s after the beginning of stimulation at 200 Hz, 15 min after application of CTX (10 nM) to block BK channel. (Robitaille and Charlton, 1992)

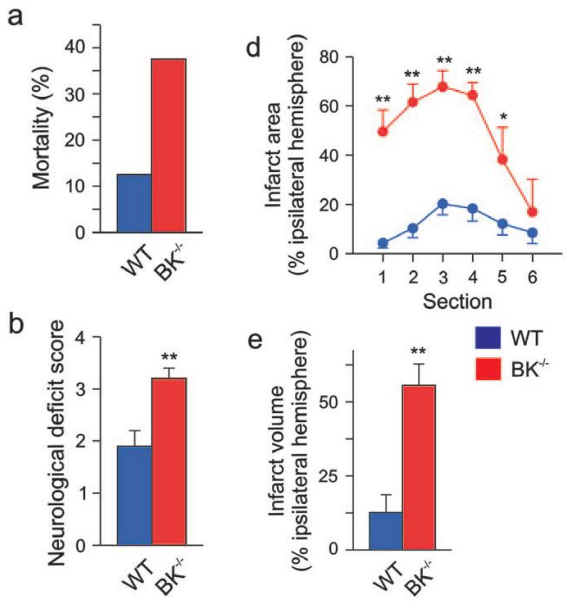

Figure 6.2 Deletion of BK channel increases mortality and severity of brain infarction after transient middle cerebral artery occlusion. a: Mortality within 7 h after reperfusion; b: the neurological deficit score evaluated 7 h after reperfusion; d: the infarction area of different brain sections; and e: the resulting infarction volume of the ipsilateral hemisphere. (Liao et al., 2010)

modulators were tested in cell proliferation MTS assays.

6.2.1 PCR

The PCR condition was optimised for the amplification of BK subunits in N2102Ep cells. The recommended annealing temperatures were 55 °C and 58 °C on Primer III website. So, the PCR condition optimisation was started from 55 °C, 40 cycles and 1.5 mM Mg^{2+}. Following that, another two PCR conditions were tried to make the target band more specific. The other two PCR conditions were: 58 °C, 40 cycles with 1.5 mM Mg^{2+}, and 58 °C, 30 cycles with 1.5 mM Mg^{2+}. The optimisation details are shown in the results section (Section 6.3.2).

After the PCR conditions were optimised, the PCR amplification of BK channel was carried out with MOG-G-UVW, N2102Ep, undifferentiated NTERA-2, differentiated NTERA-2, undifferentiated SH-SY5Y and differentiated SH-SY5Y cells to see whether the messages of BK subunits existed in the mRNA of those cell lines.

6.2.2 Electrophysiology

Patch recording was carried out on undifferentiated SH-SY5Y cells. The target channel for patching was BK. Hence, Na^{+} Locke was both the bath solution and the reference electrode, and a high K^{+} solution filled the recording

electrode. The compositions of Na^+ Locke and high K^+ solution are listed in Section 2.13.

6.2.3 Cell proliferation and MTS assays

The cell proliferation MTS assays were carried out on both undifferentiated and differentiated SH-SY5Y cells to test the possible effect, if any, of BK activators or blockers in combination with the established insults, such as oxidative stress and hypoxia.

The BK activators used here were NS1619 and isopimaric acid (IPA).

NS1619 [1-(2'-hydroxy-5'-trifluoromethylphenyl)-5-trifluoromethyl-2(3H)benzimidazolone], was the first synthetic BK activator identified in 1992 and was widely used as a pharmacological tool (Wulff and Zhorov, 2008). NS1619 was reported to directly activate the α subunit (Papassotiriou et al., 2000, Gribkoff et al., 1996) which means it can activate all of the BK channel isoforms regardless which β subunit(s) there is/are. It was reported that 3 – 30 μM NS1619 can increase the BK current and shift the I-V relationship toward more negative membrane potentials (Olesen et al., 1994). The chemical structure of NS1619 is:

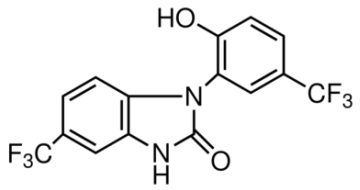

In previous studies, pimaric acid has been identified as another BK channel activator and it also can target the α subunit to activate BK channel ($EC_{50} \approx 3$ μM), regardless which β subunit(s) there is/are (Wulff and Zhorov, 2008). The chemical structure of IPA is:

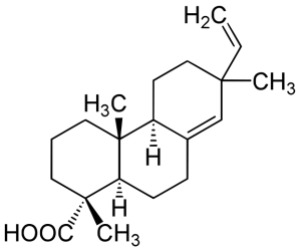

The three blockers which have been tested in this Thesis were tetraethylammonium (TEA), tetrandrine and iberiotoxin (IbTX).

TEA is not a selective BK blocker, but a generic K^+ channel blocker. TEA was used, in previous studies, to inhibit many K^+ channels at a high concentration range (μM – mM), and it has little or no effect on sodium (Na^+) or chloride (Cl^-) channel. To block the K^+ channel, TEA binds to an open channel from the cytoplasmic side (Wulff and Zhorov, 2008). The chemical structure of TEA is:

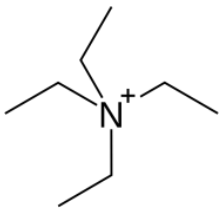

Tetrandrine is an alkaloid from the root of the creeper *Stephania tetrandra* S. Moore, which has been used as a traditional herb in the far east, such as China, for centuries as an analgesic and antipyretic agents (Wang and Lemos, 1995). It

induces a flickery blockade in the BK channel, and such a blockade was quasi selective compared to its blockade of the L-type Ca^{2+} channel (50 times more potent) (Wang and Lemos, 1995). But, studies on its blockade of the BK channel are quite limited, and its therapeutic value from blocking the BK channel was only investigated in skeletal or cardiac muscle, and tumors in recent years (Wang et al., 2004). The herb *Stephania tetrandra* S. Moore and the chemical structure of tetrandrine are shown in Fig. 6.3.

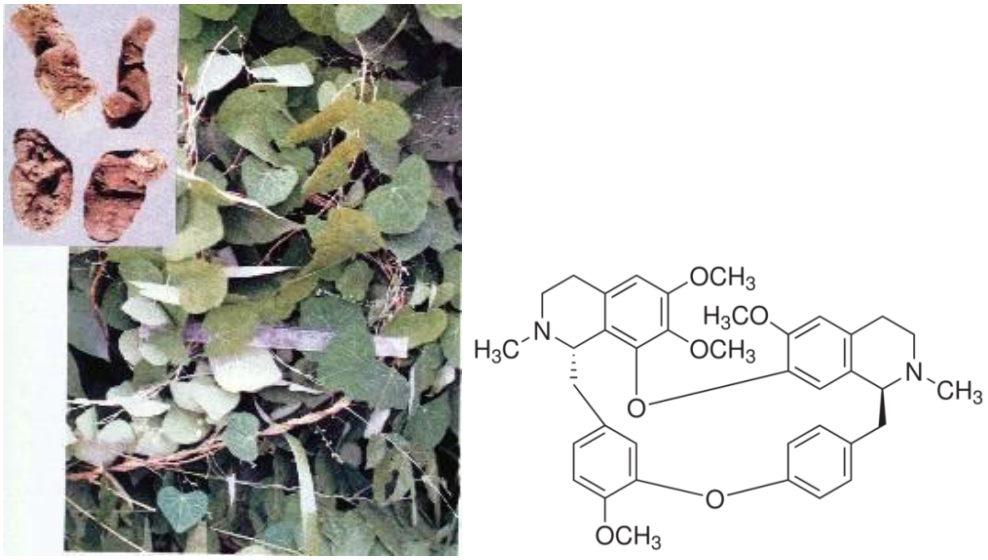

Fig. 6.3 *Stephania tetrandra* S. Moore and tetrandrine. Left hand panel: leaves and root of *Stephania tetrandra* S. Moore (picture from the webpage of Guiyang Medical Institute: http://210.40.160.21/zybbg/ffj.html), and right hand panel: chemical structure of tetrandrine.

Previous studies have suggested that IbTX is a BK blocker with an EC_{50} at about 10 nM (Wulff and Zhorov, 2008), and its blockade of the BK channel is β subunit dependent. The BK channel with β4 subunit could for example be resistant to IbTX (Meera et al., 2000). The chemical structure of IbTX is:

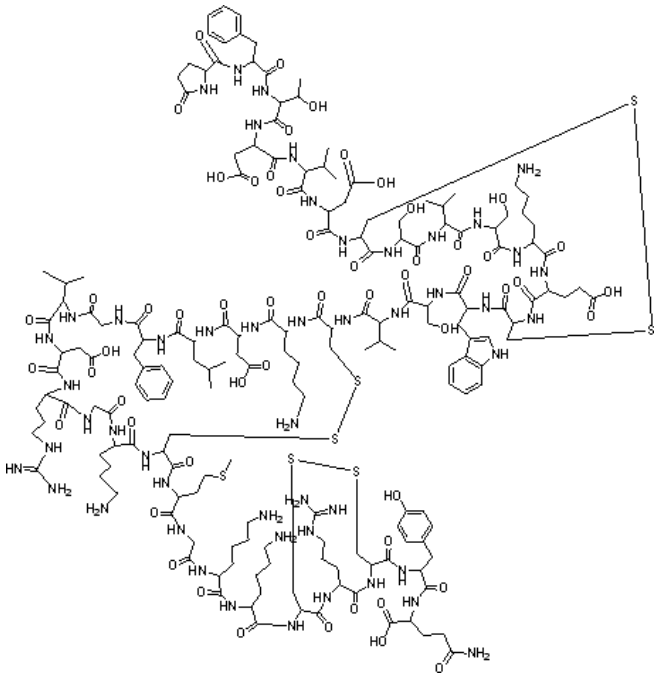

NS1619, IPA, TEA, tetrandrine and IbTX were tested on either H_2O_2 or $CoCl_2$ insults in SH-SY5Y cell line to see whether they would protect the cells or not.

6.2.4 Drug solutions

NS1619, IPA, tetrandrine and IbTX are from Sigma-Aldrich, and TEA is from Fisher Scientific. NS1619 was dissolved in C_2H_5OH, IPA and tetrandrine were dissolved in DMSO, IbTX and TEA were dissolved in PBS. 100 mM NS1619 stock, 100 mM TEA stock and 10 mM tetrandrine stock were stored at 4 °C, and 100 μM IbTX stock and 100 mM IPA stock were stored at -20 °C.

6.3 Results

6.3.1 Primer design

The primers for BK channel subunits are listed in the table below:

Table 6.1 Primers for BK subunits

Subunits	Description		Primer	Location
α	KCNMA1, mRNA, 3,537 bp in total	Forward	5'-ACGCAATCTGCCTCGCAGAGTTG	1,639 – 2,047 bp
		Reverse	5'-CATCATGACAGGCCTTGCAG	
β1	KCNMB1, mRNA, 1,518 bp in total	Forward	5'-CTGTACCACACGGAGGACACT	668 – 865 bp
		Reverse	5'-GTAGAGGCGCTGGAATAGGAC	
β2	KCNMB2, transcript variant 1, mRNA, 2,543 bp in total	Forward	5'-CATGTCCCTGGTGAATGTTG	808 – 1,044 bp
		Reverse	5'-TTGATCCGTTGGATCCTCTC	
β3	KCNMB3, transcript variant 3, mRNA, 1,835 bp in total	Forward	5'-AACCCCCTTTTCATGCTTCT	1,404 – 1,680 bp
		Reverse	5'-TCTTCCTTTGCTCCTCCTCA	
β4	KCNMB4, mRNA, 1,631 bp in total	Forward	5'-GTTCGAGTGCACCTTCACCT	648 – 892 bp
		Reverse	5'-TAAATGGCTGGGAACCAATC	

(Henney, 2008, Reviriego, 2009, Henney et al., 2009)

6.3.2 PCR condition optimisation

According to the results in Fig. 6.4 – 6.6, it can be seen that 55 °C, as an annealing temperature, was not ideal to prevent extra bands, and 40 cycles were too many for the amplification of BK subunits. Hence, the optimised PCR condition for BK subunits, with those primers above, was set at 58 °C for annealing temperature and 30 cycles for amplification.

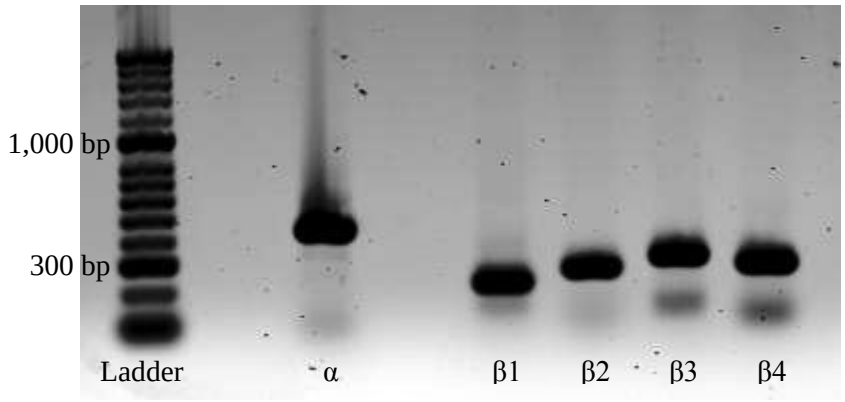

Figure 6.4 BK subunits in N2102Ep, 55 °C, 40 cycles. The bands of β subunits were clear but unspecific.

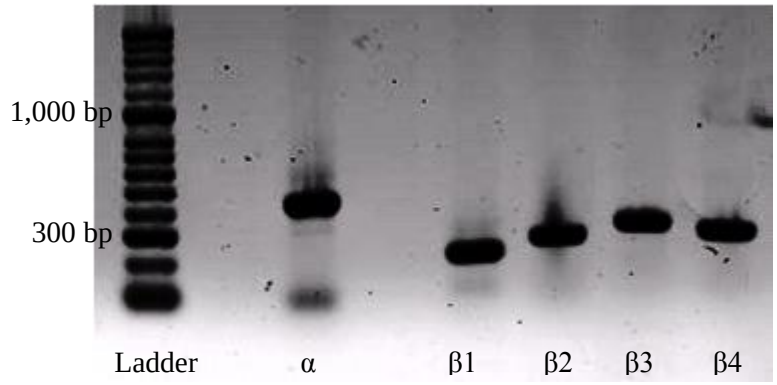

Figure 6.5 BK subunits in N2102Ep, 58 °C, 40 cycles. The bands were clear but there was primer dimer band in the α subunit amplification.

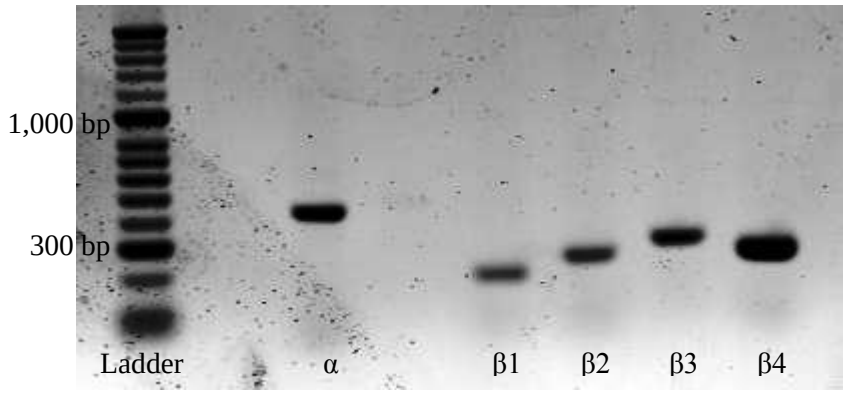

Figure 6.6 BK subunits in N2102Ep, 58 °C, 30 cycles. The bands were clear and specific.

6.3.3 RT-PCR

The RT-PCR results for BK channel subunits in the cell lines used are shown in Figs. 6.7 to 6.10.

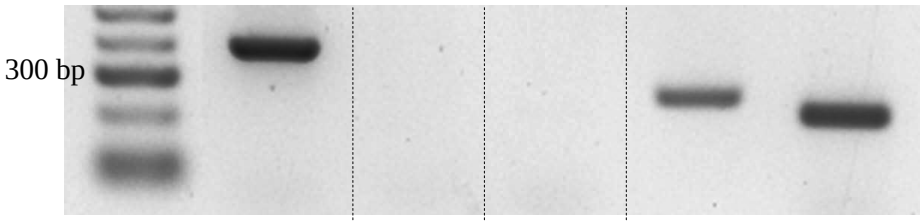

Fig. 6.7 BK channel subunits in MOG-G-UVW cells. There were messages for BKα, β3 and β4 subunits, but no message for BKβ1 or BKβ2.

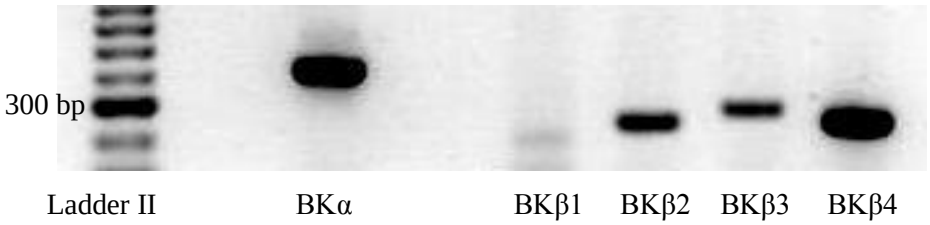

Fig. 6.8 BK channel subunits in undifferentiated NTERA-2 cells. There were messages for BKα, β2, β3 and β4 subunits, but was only a tiny message for BKβ1 subunits.

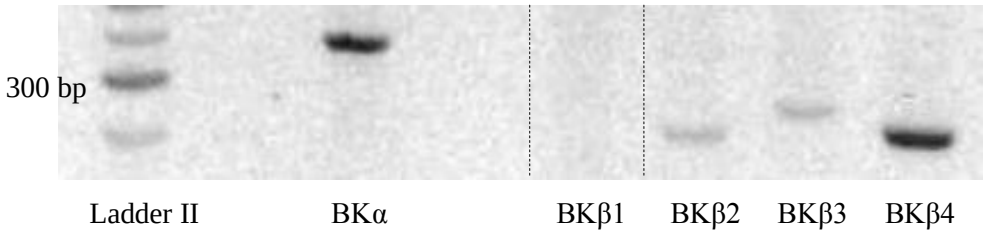

Fig. 6.9 BK channel subunits in differentiated NTERA-2 cells. There were messages for BKα, β2, β3 and β4 subunits, but any band for BKβ1 subunit was absent.

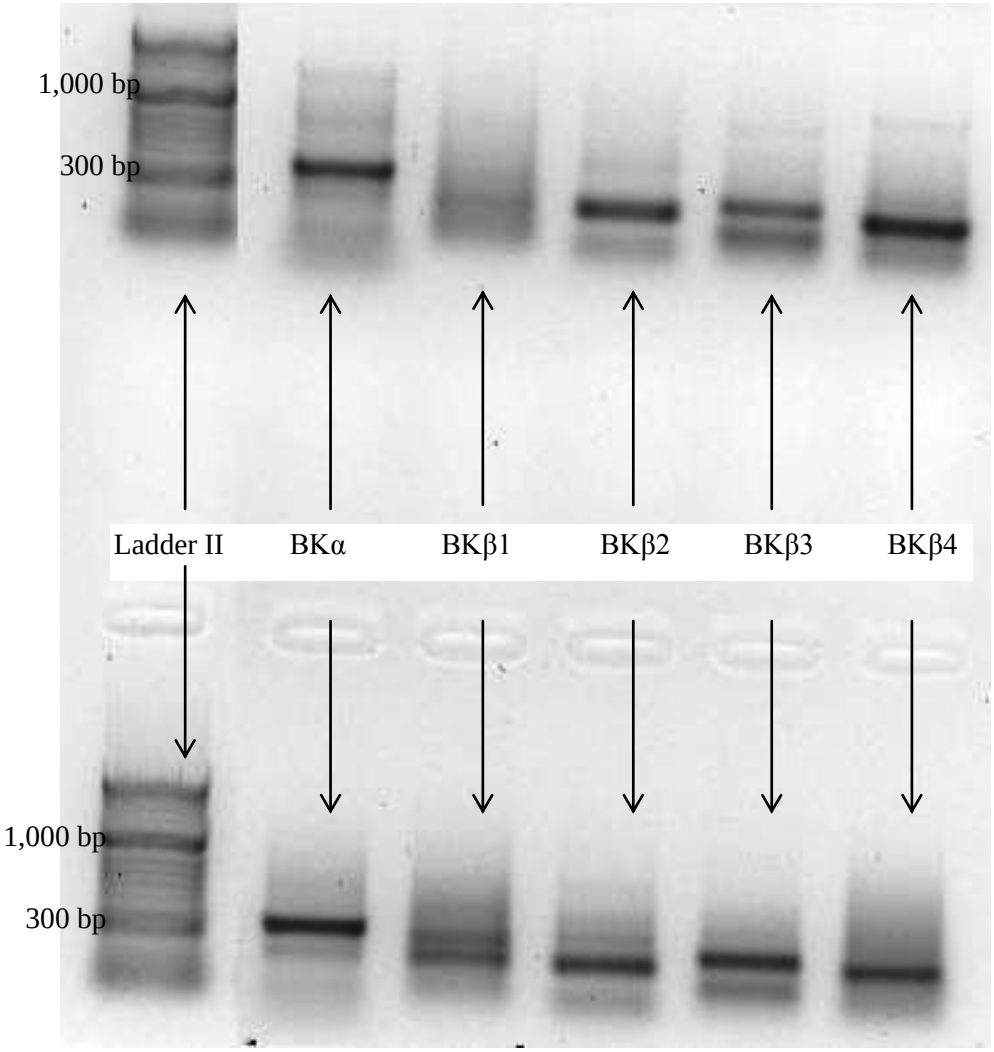

Fig. 6.10 BK channel subunits in undifferentiated (above) and differentiated (bottom) SH-SY5Y cells. There were messages for all the five BK subunits in both undifferentiated and differentiated SH-SY5Y cells.

6.3.4 Electrophysiology

Raw data from a typical inside out patch recording in an undifferentiated SH-SY5Y cell is shown below in Fig. 6.11:

From Fig. 6.11a, it can be seen that the open probability of this channel was voltage dependent, with high activity in high Ca^{2+} which is a feature of BK

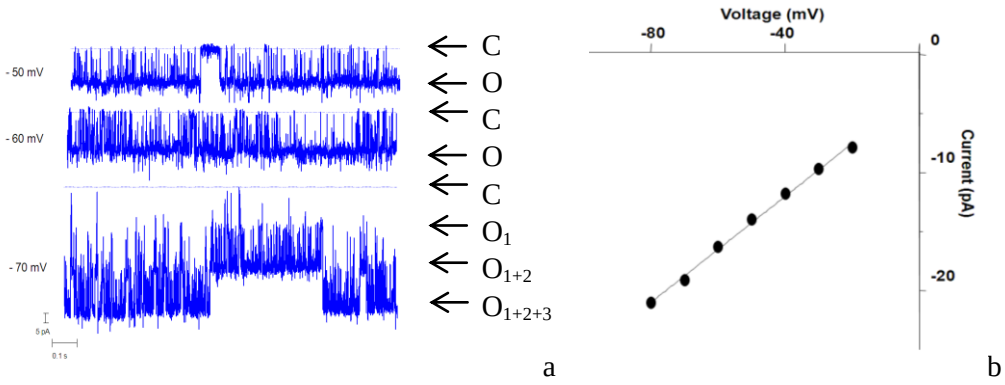

Figure 6.11 Illustration of BK channel activity in an SH-SY5Y inside-out patch with asymmetrical reverse gradient 140 mM $[K^+]_o$ / 3 mM $[K^+]_i$. a: raw records illustrating effect of voltage on BK, and b: I – V relationship.

channel. From Fig. 6.11b, it can be calculated that the conductance, which is the slope of the linear trend line, was about 222 pS. Hence, it can be concluded that the ion channel being patched was a voltage – dependent, Ca^{2+}-activated K^+ channel with a large conductance, which is likely to be a BK channel. After the BK channel was confirmed to exist and to be functional in the SH-SY5Y cell line, BK modulators were then tested.

6.3.5 BK openers effect on H_2O_2 insult

Two BK openers, NS1619 and IPA, were tested here, on the H_2O_2 insult models established in Section 4.

Firstly, the possible effect, if any, of NS1619 was tested on the SH-SY5Y cell line, and the dose – response curves are shown in Fig. 6.12:

As was discussed in Section 4.3.2, differentiated SH-SY5Y cells were more

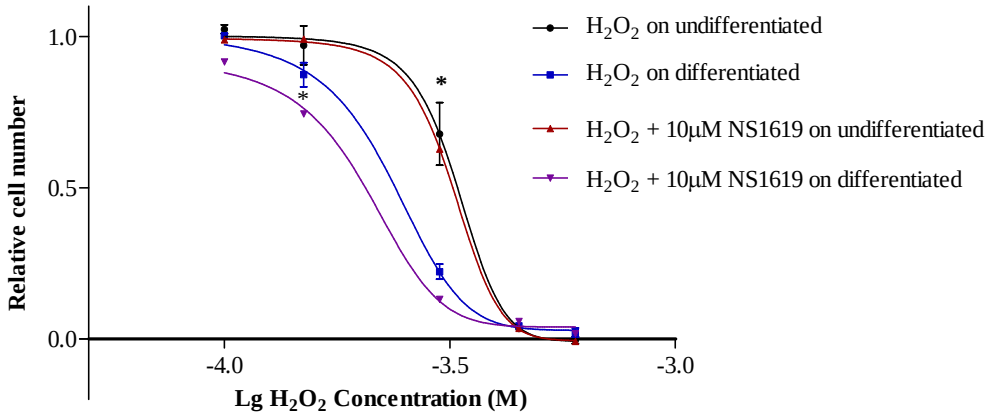

Figure 6.12 Dose – response curve for H_2O_2 in both undifferentiated and differentiated SH-SY5Y cells, with or without NS1619. Data points are the means of 3.

sensitive to the H_2O_2 insult than undifferentiated SH-SY5Y cells. The relative cell number in the differentiated cells was lower than the counterpart in the undifferentiated cells at 300 μM H_2O_2 insult.

In Fig. 6.12, it can be seen that 10 μM NS1619, in combination with H_2O_2 insult, has not markely changed the relative cell number from H_2O_2 alone in undifferentiated SH-SY5Y cells. The difference in the relative cell number between the H_2O_2 alone and H_2O_2 + NS1619 was not significant at the same dose of H_2O_2 insult. Thus, it can be concluded that 10 μM NS1619 did not protect the undifferentiated SH-SY5Y cells from H_2O_2 insult.

However, 10 μM NS1619, in combination with H_2O_2, has reduced the relative cell number from H_2O_2 alone in differentiated SH-SY5Y cells. A one way ANOVA test for all the groups in differentiated SH-SY5Y cells suggested that the difference amongst those groups was significant ($p < 0.001$), and the

Tukey's post test (comparing every two groups) indicated that the relative cell numbers were significantly different between H_2O_2 + NS1619 and H_2O_2 alone at 150 µM H_2O_2 ($p < 0.05$). Furthermore, t tests also indicated that NS1619 in combination with H_2O_2 caused a significant reduction in the relative cell number from the same doses of H_2O_2 alone at 100 µM and 300 µM H_2O_2 ($p < 0.001$ and $p < 0.05$ respectively). Hence, it can be concluded that 10 µM NS1619 did not protect the differentiated SH-SY5Y cells from H_2O_2 insult, and somehow had aggravated the insult of oxidative stress.

Another BK opener, isopimaric acid (IPA) was also tested in the SH-SY5Y cell line. A single dose of IPA, 10 µM, was tested against the H_2O_2 insult in undifferentiated SH-SY5Y cells and the results are shown in Fig. 6.13.

A one way ANOVA test for all the groups in Fig. 6.13 suggested that the difference amongst those groups was significant ($p < 0.01$), but the Bonferroni's post test (comparing every two groups) did not indicate any significant difference in the relative cell numbers between H_2O_2 alone and H_2O_2 + IPA. Hence, it can be concluded that 10 µM IPA did not protect the undifferentiated SH-SY5Y cells from H_2O_2 insult.

IPA was also tested in the presence of H_2O_2 insult in differentiated SH-SY5Y cells, and the results are shown in Fig. 6.14.

A one way ANOVA test for all the groups in Fig. 6.14 suggested that the

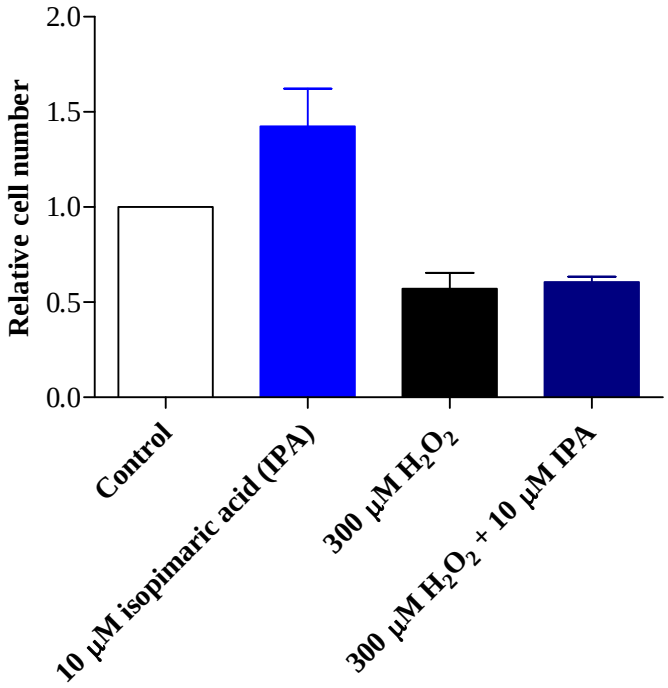

Figure 6.13 The effect of isopimaric acid (IPA, 10 µM) in combination with an EC_{50} of H_2O_2 (300 µM) in undifferentiated SH-SY5Y cells. The results are the means of 6 for IPA alone and the control, and 3 for H_2O_2 alone and H_2O_2 + IPA.

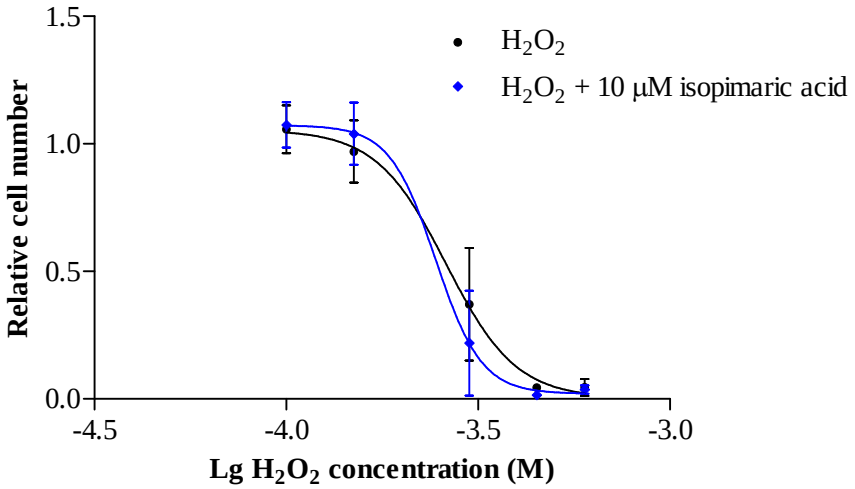

Figure 6.14 Dose – response curve of H_2O_2 insult with or without isopimaric acid (IPA, 10 µM) in differentiated SH-SY5Y cells. Data points are the means of 6 for H_2O_2 alone and 3 for H_2O_2 + IPA.

difference amongst those groups was significant ($p < 0.001$). In addition, a t test indicated that IPA in combination with H_2O_2 caused a significant reduction in the relative cell number from H_2O_2 alone at 450 µM H_2O_2 ($p < 0.01$). Hence, it can be suggested that IPA did not protect the differentiated SH-SY5Y cells from H_2O_2 insult, and may even aggravate the insult.

6.3.6 BK openers against a $CoCl_2$ insult

In addition to oxidative stress induced by H_2O_2, the possible effect of BK openers, if any, was also tested on the hypoxia mimetic effect induced by $CoCl_2$ in both undifferentiated and differentiated SH-SY5Y cells.

Firstly, NS1619, in combination with an EC_{50} of $CoCl_2$ insult, was tested in undifferentiated SH-SY5Y cells and the results are shown in Fig. 6.15.

A one way ANOVA test for all the groups in Fig. 6.15 suggested that the difference amongst those groups was significant ($p < 0.001$), and the Bonferroni's post test (comparing every two groups) indicated that $CoCl_2$ alone caused a significant reduction in the relative cell number from the control ($p < 0.001$), NS1619 alone also had a significant effect on the relative cell number from the control ($p < 0.001$), but NS1619 in combination with $CoCl_2$ caused a significant reduction in the relative cell number from the same dose of $CoCl_2$ alone ($p < 0.01$).

Then, NS1619 in combination with $CoCl_2$ insult was also tested in

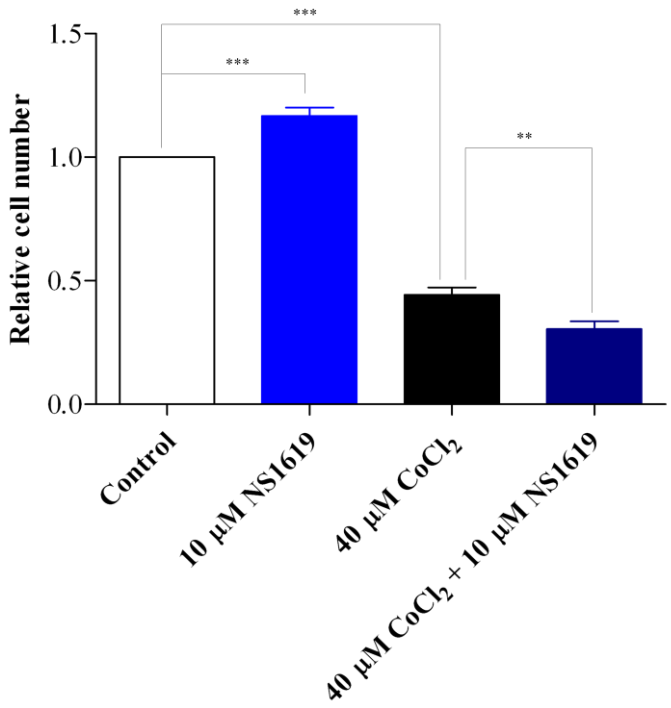

Figure 6.15 The effect of NS1619 (10 μM) in combination with an EC_{50} of $CoCl_2$ (40 μM) in undifferentiated SH-SY5Y cells. The results are the means of 3.

differentiated SH-SY5Y cells and the results are shown in Fig. 6.16.

A one way ANOVA test for all the groups in Fig. 6.16 suggested that the difference amongst those groups was significant ($p < 0.01$), and the Dunnett's post test (comparing each group with 30 μM $CoCl_2$ alone) indicated that $CoCl_2$ alone caused a significant reduction in the relative cell number from the control ($p < 0.001$) and NS1619 in combination with $CoCl_2$ also had a significant effect on the relative cell number from the same dose of $CoCl_2$ alone ($p < 0.05$).

To summarise the results shown in Fig. 6.15 and Fig. 6.16, it can be suggested that 10 μM NS1619 protects neither undifferentiated nor differentiated SH-SY5Y cells from $CoCl_2$ insult and aggravates the insult by further reducing the

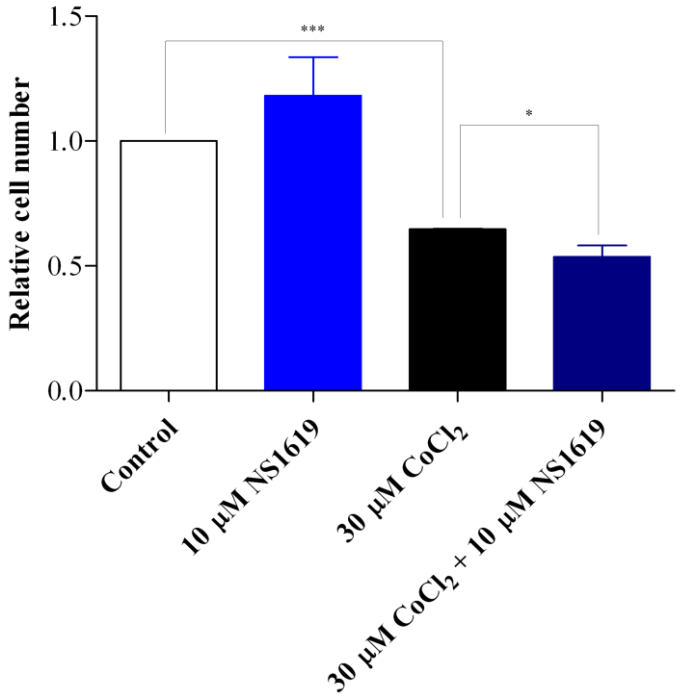

Fig. 6.16 The effect of NS1619 (10 μM) in combination with an EC_{50} of $CoCl_2$ insult (30 μM) in differentiated SH-SY5Y cells. The results are the means of 3.

relative cell number from $CoCl_2$ alone. In addition, despite NS1619 alone increasing the relative cell number in undifferentiated SH-SY5Y cells (see Fig. 6.15), it can be seen that NS1619 potentiats the $CoCl_2$ insult in undifferentiated SH-SY5Y cells.

Besides NS1619, another BK opener, IPA, was also tested on the $CoCl_2$ insult in the SH-SY5Y cell line. The results in undifferentiated SH-SY5Y cells are shown in Fig. 6.17.

A one way ANOVA test for all the groups in Fig. 6.17 suggested that the difference amongst those groups was significant ($p < 0.001$), and the Dunnett's

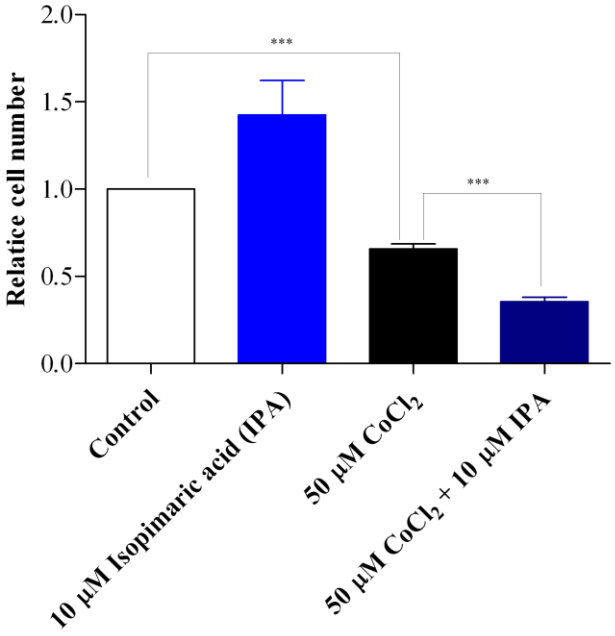

Figure 6.17 The effect of isopimaric acid (IPA, 10 μM) in combination with $CoCl_2$ insult (50 μM) in undifferentiated SH-SY5Y cells. The results are the means of 3.

post test (comparing each group with $CoCl_2$ alone) indicated that $CoCl_2$ alone had a significant effect on the relative cell number from the control ($p < 0.001$) and IPA in combination with $CoCl_2$ caused a significant reduction in the relative cell number from $CoCl_2$ alone ($p < 0.001$).

IPA was then tested on the $CoCl_2$ insult in differentiated SH-SY5Y cells. The results are shown in Fig. 6.18.

A one way ANOVA test for all the groups in Fig. 6.18 suggested that the difference amongst those groups was significant ($p < 0.001$), and the Bonferroni's post test (comparing every two groups) indicated that $CoCl_2$ alone caused a significant reduction in the relative cell number from the control ($p <$

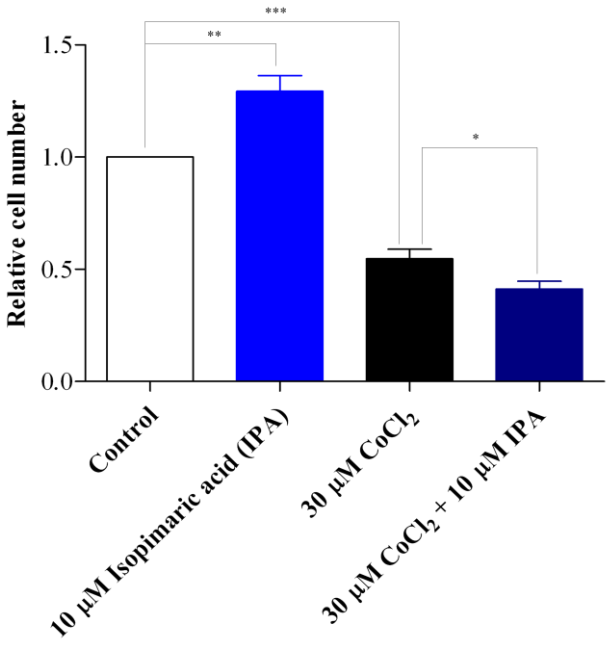

Fig. 6.18 The effect of isopimaric acid (IPA, 10 µM) in combination with an EC_{50} of $CoCl_2$ (30 µM) in differentiated SH-SY5Y cells. The results are the means of 3.

0.001), and IPA also had a significant effect on the relative cell number from the control ($p < 0.01$): but the Dunnett's post test (comparing each group with $CoCl_2$ alone) indicated that IPA in combination with $CoCl_2$ caused a significant reduction in the relative cell number from the same dose of $CoCl_2$ alone ($p < 0.05$).

To summarise the results shown in Fig. 6.17 and Fig. 6.18, it can be concluded that IPA did not protect SH-SY5Y cells, either undifferentiated or differentiated, from a $CoCl_2$ insult, and even aggravates this insult by further reducing the relative cell number from $CoCl_2$ alone. Furthermore, since IPA alone increases the relative cell number from the control in differentiated SH-SY5Y cells, it can also be concluded that IPA may potentiate the $CoCl_2$ insult in differentiated SH-SY5Y cells.

To summarise the results of BK activators, it can be seen that neither NS1619 nor IPA can protect SH-SY5Y cells from the $CoCl_2$ insult, and, both of these may even potentiate the $CoCl_2$ insult since NS1619 or IPA alone increases, or at least tend to increase, the cell proliferation in SH-SY5Y cells. Therefore, in the case of both insults, the oxidative stress induced by H_2O_2, and the hypoxia mimetic effect induced by $CoCl_2$, neither of the two BK openers has shown any neuroprotective effect. Hence, the K^+ channel blockers were then tested to see whether they might have any effects.

6.3.7 K^+ channel blockers effect on $CoCl_2$ insult

As introduced in Section 6.2.3, the three blockers tested here are generic K^+ blockers TEA, and the BK blocker tetrandrine and IbTX. Firstly, the results of TEA in combination with a $CoCl_2$ insult in undifferentiated SH-SY5Y cells are shown in Fig. 6.19.

A one way ANOVA test for all the groups in Fig. 6.19 suggested that the difference amongst those groups was significant ($p < 0.001$) and the Bonferroni's post test (comparing every two groups) indicated that $CoCl_2$ alone caused a significant reduction in the relative cell number from the control ($p < 0.001$) and TEA alone also had a significant effect on the relative cell number from the control ($p < 0.01$). TEA in combination with a $CoCl_2$ insult tended to increase the relative cell number from $CoCl_2$ alone, although not significantly. But, the protective effect of TEA in the presence of $CoCl_2$ insult was

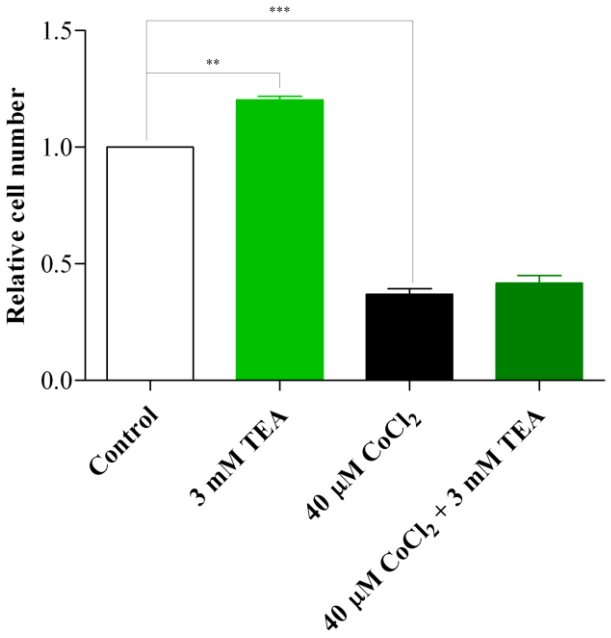

Figure 6.19 The effect of TEA (3 mM) in combination with an EC_{50} of $CoCl_2$ (40 µM) in undifferentiated SH-SY5Y cells. The results are the means of 3.

significant at a higher dose of $CoCl_2$, and the results are shown in Fig. 6.20.

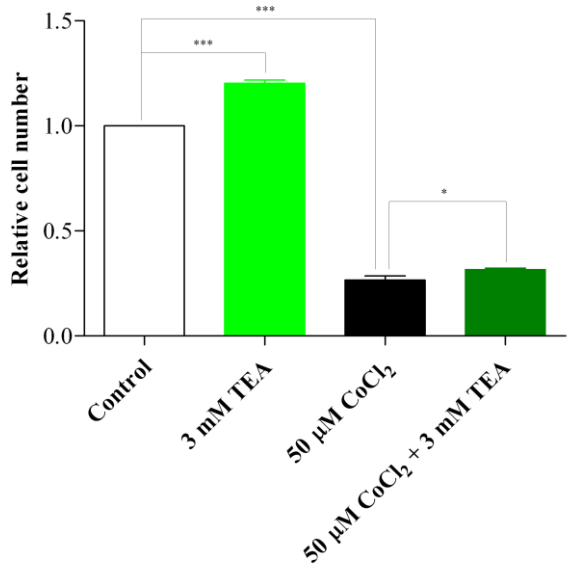

Fig. 6.20 The effect of TEA (3 mM) in combination with 50 µM $CoCl_2$ in undifferentiated SH-SY5Y cells. The results are the means of 3.

A one way ANOVA test for all the groups in Fig. 6.20 suggested that the difference amongst those groups was significant ($p < 0.001$), the Bonferroni's post test (comparing every two groups) indicated that $CoCl_2$ alone caused a significant reduction in the relative cell number from the control ($p < 0.001$), TEA alone also had a significant effect on the relative cell number from the control ($p < 0.001$), and the Dunnett's post test (comparing each group with the $CoCl_2$ alone) indicated that TEA in combination with $CoCl_2$ insult caused a significant increase in the relative cell number from the same dose of $CoCl_2$ alone ($p < 0.05$).

TEA was then tested on the $CoCl_2$ insult in differentiated SH-SY5Y cells. The results are shown in Fig. 6.21.

A one way ANOVA test for all the groups in Fig. 6.21 suggested that the difference amongst those groups was significant ($p < 0.001$), the Bonferroni's post test (comparing every two groups) indicated that $CoCl_2$ alone caused a significant reduction in the relative cell number from the control ($p < 0.001$), TEA alone also had a significant effect on the relative cell number from the control ($p < 0.01$), and the Dunnett's post test (comparing each group with the $CoCl_2$ alone) indicated that TEA in combination with $CoCl_2$ insult caused a significant increase in the relative cell number from the same dose of $CoCl_2$ alone ($p < 0.05$). Hence, 3 mM TEA protects the differentiated SH-SY5Y from an EC_{50} of $CoCl_2$ insult.

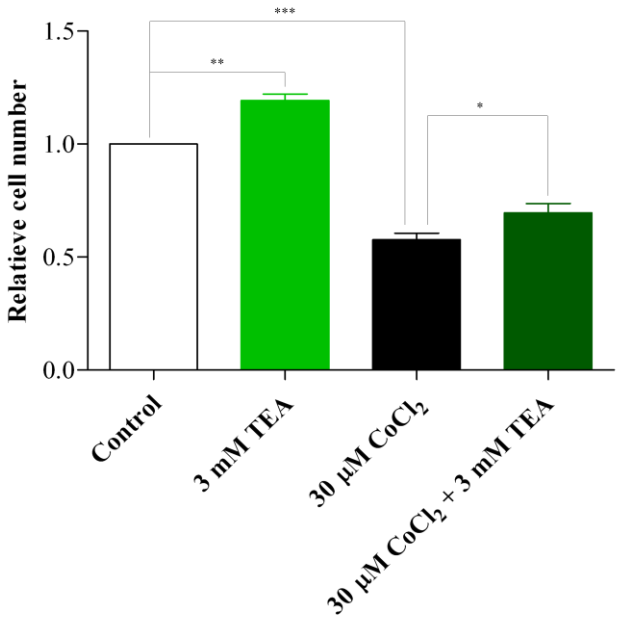

Fig. 6.21 The effect of TEA (3 mM) in combination with an EC_{50} of $CoCl_2$ (30 µM) in differentiated SH-SY5Y cells. The results are the means of 3.

In addition to TEA, another K^+ channel blocker, tetrandrine, was also tested on the $CoCl_2$ insult in differentiated SH-SY5Y cells. The results are shown in Fig. 6.22.

A one way ANOVA test for all the groups in Fig. 6.22 suggested that the difference amongst those groups was significant ($p < 0.001$), and the Bonferroni's post test (comparing every two groups) indicated that $CoCl_2$ alone caused a significant reduction in the relative cell number from the control ($p < 0.001$), tetrandrine also had a significant effect on the relative cell number from the control ($p < 0.001$), and tetrandrine in combination with a $CoCl_2$ insult caused a significant increase in the relative cell number from the same dose of $CoCl_2$ alone ($p < 0.001$). It can then be concluded that 1 µM tetrandrine protects differentiated SH-SY5Y cells from 40 µM $CoCl_2$.

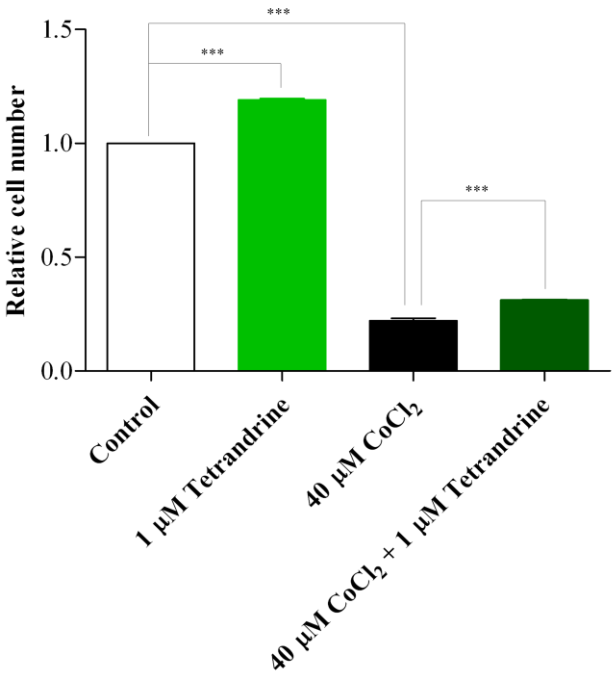

Figure 6.22 The effect of tetrandrine (1 μM) in combination with $CoCl_2$ insult (40 μM) in differentiated SH-SY5Y cells. The results are means of 3.

To summarise the results in Fig. 6.19 to Fig. 6.22, it may be concluded that K^+ channel blockers, TEA and tetrandrine, may protect differentiated SH-SY5Y cells from a $CoCl_2$ insult. In addition to TEA and tetrandrine, a selective BK channel blocker, IbTX, was also tested on a $CoCl_2$ insult in the SH-SY5Y cell line. The results in undifferentiated SH-SY5Y cells are shown in Fig. 6.23.

A one way ANOVA test for all the groups in Fig. 6.23 suggested that the difference amongst those groups was significant ($p < 0.001$), and the Bonferroni's post test (comparing every two groups) indicated that $CoCl_2$ alone caused a significant reduction in the relative cell number from the control ($p < 0.01$), but the difference in the relative cell numbers between $CoCl_2$ alone and $CoCl_2$ + IbTX was not significant.

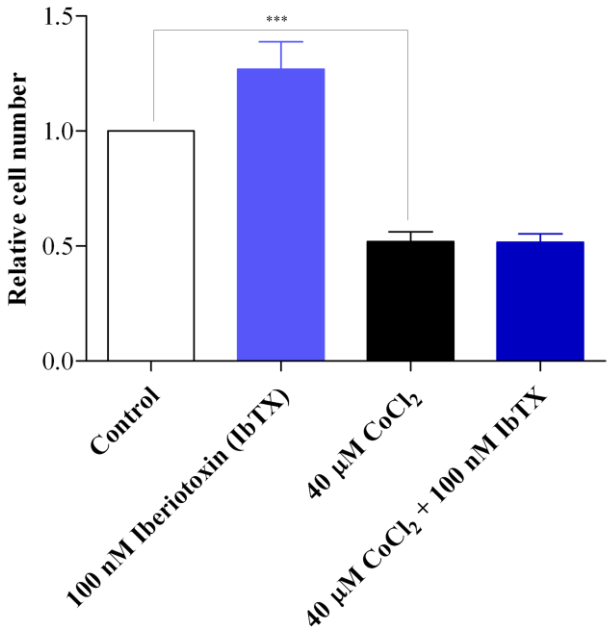

Figure 6.23 The effect of iberiotoxin (IbTX, 100 nM) in combination with an EC_{50} of $CoCl_2$ (40 μM) in undifferentiated SH-SY5Y cells. The results are the means of 3.

IbTX was also tested on the differentiated SH-SY5Y cells and the results are shown in Fig. 6.24.

A one way ANOVA test for all the groups in Fig. 6.24 showed that the difference amongst those groups was significant ($p < 0.001$), and the Bonferroni's post test (comparing every two groups) indicated that $CoCl_2$ alone caused a significant reduction in the relative cell number from the control, IbTX alone also had a significant effect on the relative cell number, but the difference in the relative cell numbers between $CoCl_2$ alone and $CoCl_2$ + IbTX was not significant.

Hence, it can be seen from the results in Figs. 6.23 and 6.24, the BK blocker,

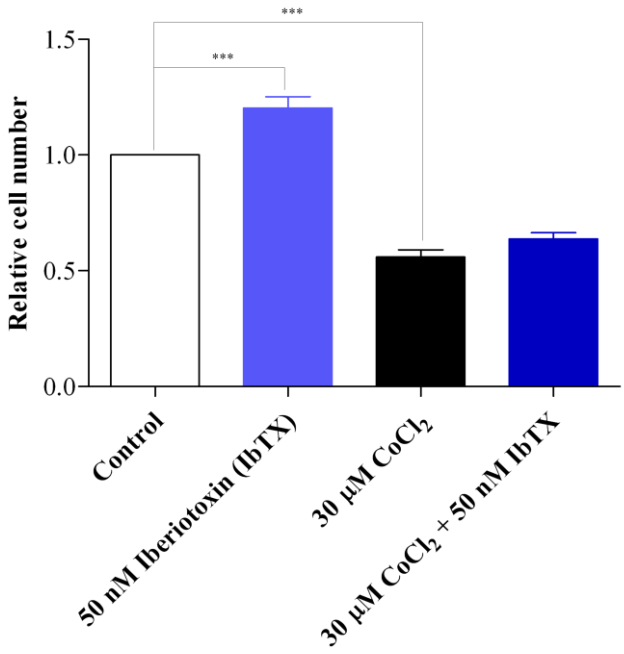

Fig. 6.24 The effect of iberiotoxin (IbTX, 50 nM) in combination with an EC_{50} of $CoCl_2$ (30 μM) in differentiated SH-SY5Y cells. The results are the means of 6.

IbTX, cannot protect SH-SY5Y cells, either undifferentiated or differentiated, from a $CoCl_2$ insult.

6.4 Discussion

To summarise those cell proliferation MTS assays results above, the following considerations are presented.

6.4.1 BK activators cannot protect the cells from the established insults

From the results shown in section 6.3.5 and 6.3.6, it can be seen that NS1619 alone increases cell proliferation in undifferentiated SH-SY5Y cells, but cannot

protect the cells from the established insults, and may even potentiate the $CoCl_2$ insult. NS1619 also aggravates the insults of H_2O_2 and $CoCl_2$ in differentiated SH-SY5Y cells. IPA cannot protect undifferentiated SH-SY5Y cells either and aggravates the insult of $CoCl_2$ at high $CoCl_2$ dose (50 μM). In differentiated SH-SY5Y cells, IPA alone may increase cell proliferation but IPA may potentiate the insults of H_2O_2 and $CoCl_2$.

Therefore, to summarise BK activators, NS1619 and IPA, cannot protect the SH-SY5Y cells from either oxidative stress or a hypoxia mimetic effect, although the modulators alone may increase cell proliferation. The negative results might be due to the different selectivity for different BKβ subunits of the BK modulators, since the BK channel coassembled with certain β subunit(s) might be resistant to some BK modulators (see Section 6.4.3). However, both NS1619 and IPA bind to the BKα subunit, which is the functional and essential part of BK channel (Wulff and Zhorov, 2008). The messages of BKα subunit are present in both undifferentiated and differentiated SH-SY5Y cells in RT-PCR (see Section 6.3.3) and the BK channel has also been shown to be functional in SH-SY5Y cell line in patch recordings (see Section 6.3.4). Hence, the negative results with NS1619 and IPA are not because of the resistance or lack of presence of the BK channel in the SH-SY5Y cell line.

The BK activators potentiated the effects of the insults in some cases above, and this has been discussed in previous studies already. As discussed in the introduction (see Section 1.4.2.1), the BK channel is activated by intracellular

Ca^{2+}. Both of the insults, H_2O_2 and $CoCl_2$, increase $[Ca^{2+}]_i$ (see Section 4.1), in which case, the BK channel in the cells would have been activated already when the cells were treated with the insults. Thus, if the BK channel was further opened with BK channel openers, the K^+ efflux would be further increased, possibly resulting in undesirable cell shrinkage and death (see Fig. 6.25) (Burg et al., 2006).

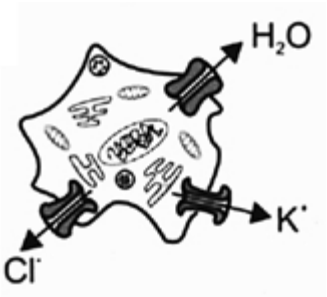

Figure 6.25 K^+ efflux and cell shrinkage (Burg et al., 2006).

Nevertheless, these negative results with BK activators are not exactly in contradiction to previous studies which suggested a neuroprotective role of the BK channel. As introduced in Section 6.1, the activation of the BK channel may protect neurones by reducing Ca^{2+} influx from an extracellular source. Obviously, the entry of extracellular of Ca^{2+} is not the only source to increase the $[Ca^{2+}]_i$. The intracellular Ca^{2+} release channel on the ER, such as the RyR which has been discussed before, is also responsible for any increase of $[Ca^{2+}]_i$ (Stutzmann and Mattson, 2011).

6.4.2 K^+ channel blockers can be neuroprotective against $CoCl_2$ insult

Since the BK activators, NS1619 and IPA, cannot protect the cells from either H_2O_2 or $CoCl_2$ insult, some K^+ channel blockers, such as TEA and tetrandrine, have been tested in this Thesis.

From the results shown in Section 6.3.7, interestingly it can be seen that TEA alone increases cell proliferation in both undifferentiated and differentiated SH-SY5Y cells, and it protects the cells from $CoCl_2$ insult. Tetrandrine also increases cell proliferation in differentiated SH-SY5Y cells and additionally protects the cells.

The neuroprotective effect of the K^+ channel blocker, TEA, has been studied previously. One study in 1998 has shown that 100 μM to 5 mM TEA significantly reduces the neuronal death induced by $A\beta_{25-35}$ in 24 – 48 h (Yu et al., 1998). The results from that study are shown below in Fig. 6.26.

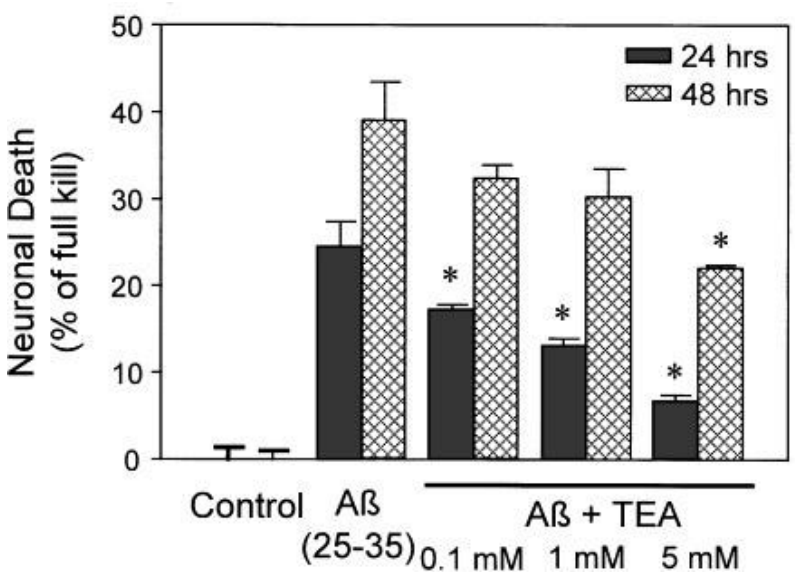

Figure 6.26 TEA can reduce the neuronal death induced by $A\beta_{25-35}$ (Yu et al., 1998).

Thus, the results in this chapter were consistent with those from previous studies. But, whether the neuroprotective effect presented by TEA is because of the blockade of BK channel or not is still uncertain. So, more work should be done with selective BK blockers, rather than generic K^+ channel blockers, to see whether the blockade of the BK channel, rather than any other K^+ channel, would be neuroprotective or not.

6.4.3 Selectivity in respect of the BKβ subunits for BK blocker

The potential neuroprotective effect of K^+ channel blockers might be argued against by the negative results with IbTX (see Fig. 6.23 and Fig. 6.24), which is a selective BK channel blocker. From those results, it can be seen that 50 nM IbTX increases cell proliferation in differentiated SH-SY5Y cells, but 50 – 100 nM IbTX did not protect either undifferentiated or differentiated SH-SY5Y cells from $CoCl_2$ insult.

Actually, these negative results might be explained by the selectivity in respect of BKβ subunits for BK blockers. A review has suggested that β1 enhances the toxin binding but complexes with β4 with BK are resistant to IbTX (Wulff and Zhorov, 2008). According to the PCR results shown in section 6.3.3, there was certainly the message for the BKβ4 subunit in both undifferentiated and differentiated SH-SY5Y cells. That might explain why IbTX has shown a negative effect in both undifferentiated and differentiated SH-SY5Y cells.

Therefore, in future work, blockers which are generic for all BKβ subunits, such as paxilline, should be tested on the established insults, including both oxidative stress and hypoxia mimetic effects, to see whether they would be neuroprotective or not. If the BK blockers afford neuronal protection, a future strategy could be working on the features of BKβ subunits to develop, if possible, selective BK blockers which would target neuronal cells only. This kind of selective BK blocker could be the BK strategy for any drug development against neurodegeneration.

6.5 Conclusions

Based on all of the results and discussions above, the findings here can be summarised:

a. The BK channel exists and is functional in the SH-SY5Y cell line. Additionally, the messages for all the 4 BKβ subunits exist in the mRNA of both undifferentiated and differentiated SH-SY5Y cells.
b. BK activators, NS1619 and IPA, cannot protect either undifferentiated or differentiated cells. Furthermore, the activators alone may increase cell proliferation. When applied in combination however with either H_2O_2 or $CoCl_2$, they may aggravate the insults by further reducing relative cell number.
c. K^+ channel blockers, TEA and tetrandrine, can be neuroprotective. Both TEA and tetrandrine protect the differentiated SH-SY5Y cells from a

$CoCl_2$ insult, and TEA may also protect the undifferentiated SH-SY5Y cells from a $CoCl_2$ insult at a high dose of $CoCl_2$.

d. IbTX, which is a selective BK blocker, cannot protect either undifferentiated or differentiated SH-SY5Y cells from the insult of hypoxia induced by $CoCl_2$. This negative result is probably due to the existence of the BKβ4 subunit in the SH-SY5Y cell line.

7. Consideration of Other K^+ Channels

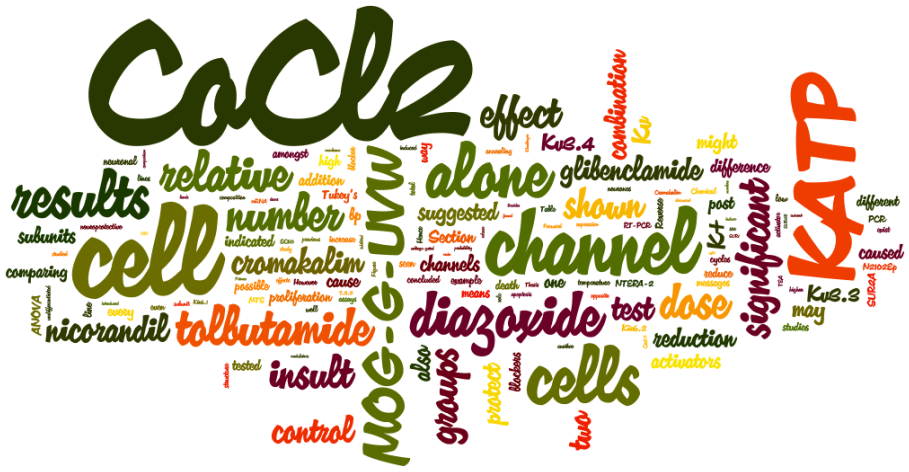

7. Consideration of Other K^+ Channels

7.1 Introduction

As discussed in Section 1.4.2, other K^+ channels may also be implicated in neuronal death and therefore afford a neuroprotective property. For example a mutation in a voltage-gated K^+ channel, $K_v3.3$, can cause degenerative and developmental central nervous system phenotypes (Waters et al., 2006). Another voltage-gated K^+ channel, $K_v3.4$, was found to be up-regulated in the early stages of AD (Angulo et al., 2004). K_{ATP} was also suggested to be neuroprotective (Yamada et al., 2001, Héron-Milhavet et al., 2004, Sun et al., 2006) (see Section, 1.4.2.2). Hence, some work has also been done on K_{ATP}, $K_v3.3$ and $K_v3.4$ channels in this Thesis and this is introduced here.

7.1.1 K_{ATP} channel

As introduced in the introduction (see Section 1.4.2.2), two opposite opinions have been put forward for the possible role of K_{ATP} channel in neuronal death. For example, one study suggested that diazoxide, a K_{ATP} opener, treatment in neurones could reduce neuronal death from insults of $A\beta_{25-35}$ or hypoxia induced by $FeSO_4$ (Goodman and Mattson, 1996), but another study on rat preadipocytes argued that diazoxide can reduce cell number (Wang et al., 2007).

Hence, the possible role of K_{ATP} channel in cells was studied in this Thesis with PCR, and cell proliferation MTS assays using K_{ATP} modulators. The K_{ATP} channel activators used here were cromakalim, diazoxide, nicorandil, and the blockers were glibenclamide, tolbutamide.

In previous studies, 10 µM levcromakalim evoked a hyperpolarisation under current clamp, and this effect of levcromakalim can be inhibited by glibenclamide with an EC_{50} of 55 nM. 10 µM glibenclamide alone depolarises the neurones (Hogg and Adams, 2001). For diazoxide, 200 – 500 µM can increase the channel opening probability by 480 ± 120% (Allen and Brown, 2003). For the K_{ATP} blocker, it has been found in previous studies that the K_{ATP} channel current (I_{KATP}) can be inhibited reversibly by tolbutamide with an EC_{50} at 34.1 µM, and can be inhibited irreversibly by 0.3 – 3 nM glibenclamide (Allen and Brown, 2003). The inhibitory effect of tolbutamide was confirmed in a current clamp experiment suggesting that 100 µM tolbutamide depolarises the neurones (Hogg and Adams, 2001). An irreversible effect of glibenclamide was argued by another study which suggested that the dose of glibenclamide to induce half-maximal inhibitory effect was increased from 9.1 µM to only 10.6 µM by 1 mM nicorandil (Obata and Yamanaka, 2000). The chemical structures of those modulators above are shown below:

7.1.2 K_v channels

In addition to BK and K_{ATP} channels, voltage-gated K^+ (K_v) channel were also

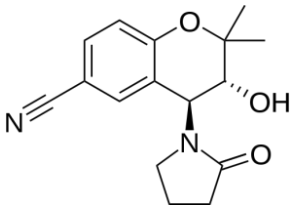

Chemical structure of cromakalim

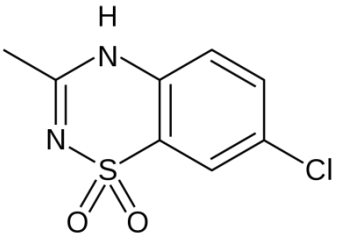

Chemical structure of diazoxide

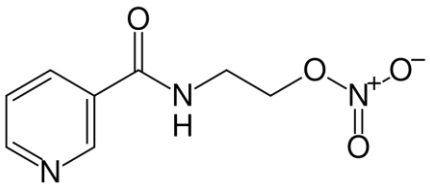

Chemical structure of nicorandil

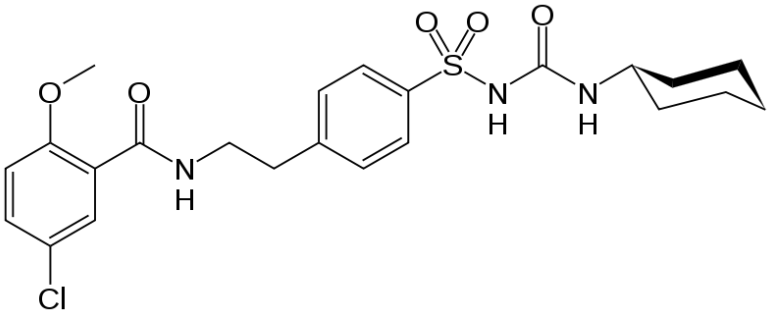

Chemical structure of glibenclamide

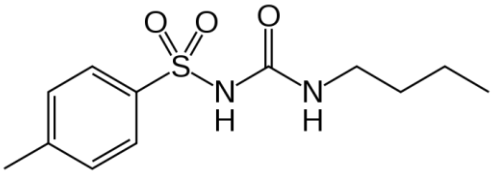

Chemical structure of tolbutamide

studied here, such as $K_v3.3$ and $K_v3.4$.

The K_v channel is known to be involved in the regulation of cell volume, for example the cell shrinkage caused by K^+ efflux, and hence may contribute to cell death. Besides, pro-apoptotic agents, such as staurosporine etc., can enhance the sensitivity of K_v channel to its blockers like TEA and 4-aminopyridine (4-AP). In pulmonary artery smooth muscle cells, the function and expression of K_v channel was up-regulated by mitochondrial oxidative phosphorylation, and a K_v channel was activated during nitric oxide (NO) – induced cell apoptosis. In addition, the Fas- and ceramide-mediated apoptosis was believed to be induced by tyrosine kinase inhibition caused by an enhancement of the K_v channel activity. For neuronal cells, previous studies have believed that apoptosis was accompanied by the increase of K^+ conductance via K_v channel (Burg et al., 2006). In addition to the role of K_v channel in cell death, some other studies have also linked K_v channel with neurodegeneration (Angulo et al., 2004, Waters et al., 2006) (see Section 1.4.2.3).

In this study, the messages of $K_v3.3$ and $K_v3.4$ in neuronal cells were studied with RT-PCR and the possible effect of K_v channel activity is discussed in Section 7.4.

7.2 Methods and materials

7.2.1 Methods

The messages of K_{ATP} subunits were tested by RT-PCR in the mRNA of MOG-G-UVW cells and two different PCR conditions were applied: 55 °C as the annealing temperature for 30 cycles and 58 °C as the annealing temperature for 40 cycles. In addition, the messages of $K_v3.3$ and $K_v3.4$ channel were tested for in N2102Ep and NTERA-2 cell lines. The PCR condition was 60 °C as the annealing temperature for 30 cycles.

Besides PCR, cell proliferation MTS assays were applied to test the possible effects, if any, of K_{ATP} modulators in MOG-G-UVW cells. In the MTS assays here, the cell density was 3,000 cells per well in 96 well plates, unless specific information was given (Khudheyer, 2010).

7.2.2 Drug solutions

Cromakalim, diazoxide, nicorandil and tolbutamide are from Sigma-Aldrich, and glibenclamide is from Tocris. Cromakalim, diazoxide and glibenclamide were dissolved in DMSO at 10 mM for stock. Nicorandil and tolbutamide were dissolved in C_2H_5OH at 10 mM for stock. Diazoxide and nicorandil stocks were stored at -20 °C. Cromakalim, glibenclamide and tolbutamide stocks were stored at 4 °C.

7.3 Results

7.3.1 Primer design

The primers for K_{ATP} channel are listed in Table 7.1:

Table 7.1 Primers for K_{ATP} subunits

Primer		Sequence	Location
$K_{ir}6.1$	Forward	5'-CATCTTTACCATGTCCTTCC-3'	560 – 893 bp in total
NM_004982	Reverse	5'-GTGAGCCTGAGCTGTTTTCA-3'	3,281 bp
$K_{ir}6.2$	Forward	5'-ACTCCAAGTTTGGCAACACC-3'	1,197 – 1,550 bp in
D50582	Reverse	5'-CTGCTGAGGCCAGAAATAGC-3'	total 1,635 bp
SUR1	Forward	5'-ATGAGGAAGAGGAGGAAGAG-3'	2,941 – 3,433 bp in
L78207	Reverse	5'-GCGATGGTGTTACAGTCAGA-3'	total 4,892 bp
SUR2A	Forward	5'-GGCCTTTGCTTCACTGTCTC-3'	1,730 – 1,939 bp in
NM_005691.2	Reverse	5'-TTTGGCTGAACTCCAGTGTG-3'	total 4,670 bp
SUR2B	Forward	5'-TGGGAACACATTTTCTGCAA-3'	1,528 – 1,677 bp in
NM_020297	Reverse	5'-CGCATGGGTCACAAATGTAG-3'	total 4,650 bp

The primers of $K_v3.3$ and $K_v3.4$ channel are shown in Table 7.2.

Table 7.2 Primers for K_v channels

Channel	Primer	Sequence
Kv3.3, KCNC3	Forward	5'-GCTCTTCGAGGACCCCTACT-3'
	Reverse	5'-ACCTCCACGTTGGTGATGTT-3'
Kv3.4, KCNC4	Forward	5'-CTCTTCGAGGATCCCTACTC-3'
	Reverse	5'-TGTGAACCACAGCACACATA-3'

7.3.2 RT-PCR

Two annealing temperatures, 55 °C and 58 °C, have been trialled on the amplification of K_{ATP} subunits in MOG-G-UVW cell line. The figures are

shown in Figs. 7.1 and 7.2.

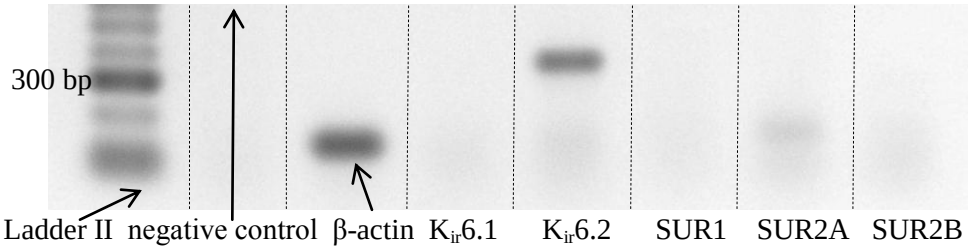

Fig. 7.1 K_{ATP} subunits in MOG-G-UVW, 55 °C, 30 cycles.

Figure 7.2 K_{ATP} subunits in MOG-G-UVW, 58 °C, 40 cycles. The bands are unspecific.

From the two figures, it can be seen that higher annealing temperature with more amplification cycles make the bands for K_{ir}6.1, SUR1 and SUR2B visible and make the SUR2A band clearer, but this condition also causes the bands to be unspecific. From Fig. 7.1, it may also be noticed that K_{ir}6.2 with SUR2A might be the main subunit composition of K_{ATP} channel in MOG-G-UVW cells, but the existence of K_{ir}6.1, SUR1 and SUR2B cannot be eliminated.

The messages of Kv3.3 and Kv3.4 have been identified for in the mRNA samples from both N2102Ep and undifferentiated NTERA-2 cell lines in RT-PCR. The results are shown in Figs. 7.3 and 7.4.

Figure 7.3 K_v3.3 and K_v3.4 in N2102Ep

Figure 7.4 K_v3.3 and K_v3.4 in undifferentiated NTERA-2 cell line.

From those figures, it can be seen that the messages of both K_v3.3 and K_v3.4 channels exist in both N2102Ep and undifferentiated NTERA-2 cell lines.

7.3.3 K_{ATP} activators effect against $CoCl_2$ insult

Firstly, the possible effect, if any, of diazoxide alone on the cell proliferation was tested in MOG-G-UVW cells. The results are shown in Fig. 7.5.

A one way ANOVA test for all the groups in Fig. 7.5 suggested that the difference amongst those groups was significant ($p < 0.05$), and the Dunnett's post test (comparing each group with the control) indicated that 125 μM diazoxide caused a significant reduction in the relative cell number from the control ($p < 0.01$): the vehicle, DMSO, and 100 μM diazoxide did not have any significant effect on the relative cell number. It can be concluded that diazoxide cannot induce cell death in MOG-G-UVW cells at concentrations of 100 μM or lower.

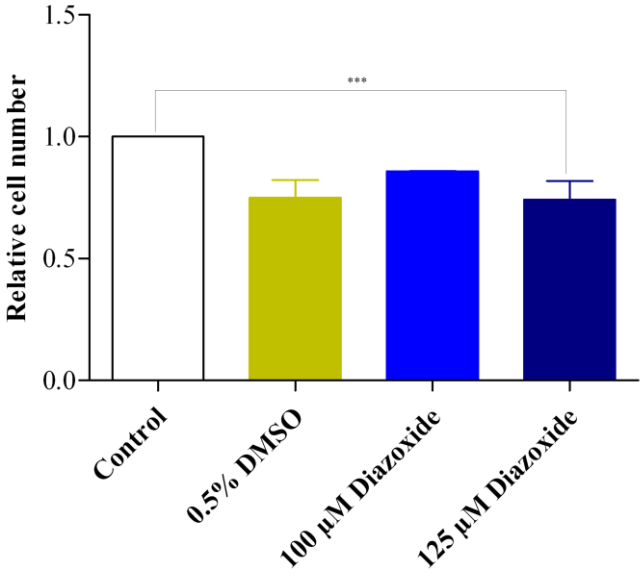

Figure 7.5 The effect of diazoxide alone in MOG-G-UVW cells. The results were the means of 9 for 125 µM diazoxide and the control, and 3 for DMSO vehicle and 100 µM diazoxide.

Diazoxide was then tested against two different doses of $CoCl_2$ in MOG-G-VUW cells. The results are shown in Fig. 7.6.

For the results shown in Fig. 7.6A, a one way ANOVA test for all the groups showed that the difference amongst those groups was significant ($p < 0.001$), and the Tukey's post test (comparing every two groups) indicated that 65 µM $CoCl_2$ caused a significant reduction in the relative cell number from the control ($p < 0.001$). A one tail t test suggested that 100 µM diazoxide in combination with 65 µM $CoCl_2$ had a significant effect on the relative cell number from the same dose of $CoCl_2$ alone ($p < 0.05$).

Interestingly, the opposite effect can be seen with a high dose of $CoCl_2$. From

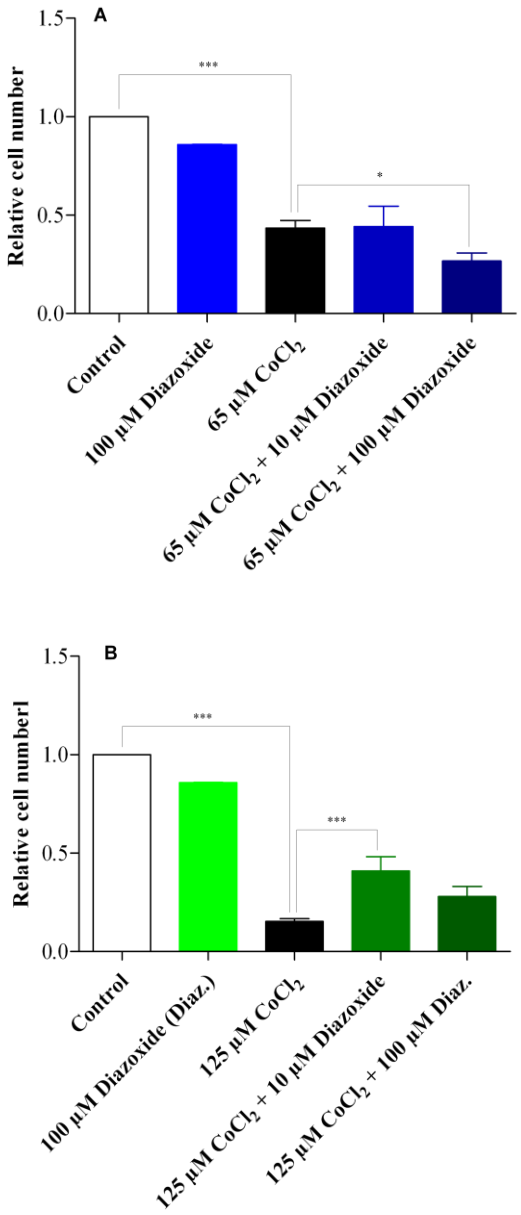

Fig. 7.6 The effect of diazoxide (diaz.) in combination with $CoCl_2$ insult in MOG-G-UVW cells. A: 65 µM $CoCl_2$, the results are the means of 30 for $CoCl_2$ alone and the control, 9 for $CoCl_2$ + 10 µM diazoxide, 6 for $CoCl_2$ + 100 µM diazoxide, and 3 for diazoxide alone. And B: 125 µM $CoCl_2$, the results are the means of 12 for $CoCl_2$ alone and the control, 9 for $CoCl_2$ + 10 µM diazoxide, 6 for $CoCl_2$ + 100 µM diazoxide, and 3 for diazoxide alone.

the results shown in Fig. 7.6B, a one way ANOVA test for all the groups suggested that the difference amongst those groups was significant ($p < 0.001$),

and the Tukey's post test (comparing every two groups) indicated that 125 μM $CoCl_2$ alone caused a significant reduction in the relative cell number from the control ($p < 0.001$), and 10 μM diazoxide in combination with 125 μM $CoCl_2$ also had a significant effect on the relative cell number in comparison with the same dose of $CoCl_2$ alone ($p < 0.001$).

Thus, it can be concluded that diazoxide cannot protect MOG-G-UVW cells from a low dose of $CoCl_2$ (65 μM), and may even further reduce the relative cell number from $CoCl_2$ alone. However, in the presence of a high dose of $CoCl_2$ (125 μM), 10 μM diazoxide can paradoxically protect the cells.

Besides diazoxide, another K_{ATP} activator, nicorandil was also tested on the $CoCl_2$ insult in MOG-G-UVW cells. The results are shown in Fig. 7.7.

For the results shown in Fig. 7.7A, a one way ANOVA test for all the groups showed that the difference amongst all the groups was significant ($p < 0.001$), and the Tukey's post test (comparing every two groups) indicated that 65 μM $CoCl_2$ caused a significant reduction in the relative cell number from the control. However the difference in the relative cell numbers between $CoCl_2$ + nicorandil and $CoCl_2$ alone was not significant.

For the results shown in Fig. 7.7B, a one way ANOVA test for all the groups suggested that the difference amongst those groups was significant ($p < 0.001$), and the Tukey's post test (comparing every two groups) indicated that 125 μM

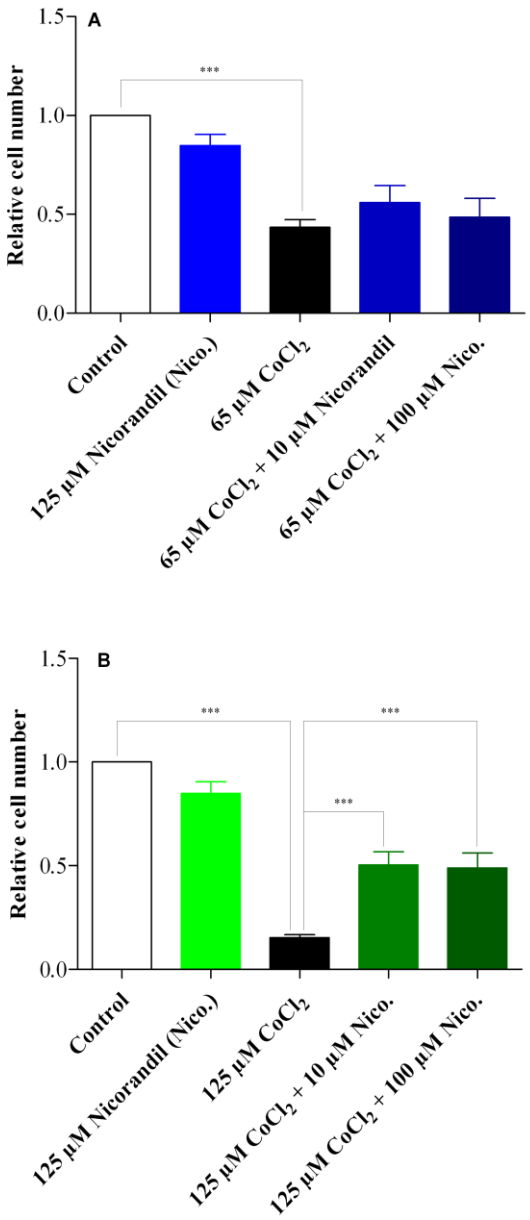

Fig. 7.7 The effect of nicorandil (nico.) in combination with $CoCl_2$ insult in MOG-G-UVW cells. A: 65 μM $CoCl_2$, the results are the means of 30 for 65 μM $CoCl_2$ alone and the control, and 9 for 125 μM nicorandil alone, 65 μM $CoCl_2$ + 10 μM nicorandil and 65 μM $CoCl_2$ + 100 μM nicorandil. And B: 125 μM $CoCl_2$, the results are the means of 12 for $CoCl_2$ alone and the control, and 9 for 125 μM nicorandil alone, 125 μM $CoCl_2$ + 10 μM nicorandil and 125 μM $CoCl_2$ + 100 μM nicorandil.

$CoCl_2$ caused a significant reduction in the relative cell number from the control, and 10 μM or 100 μM nicorandil in combination with 125 μM $CoCl_2$

also had a significant effect on the relative cell number in comparison with the same dose of $CoCl_2$ alone.

Thus, it can be concluded that nicorandil cannot protect MOG-G-UVW cells against a low dose of $CoCl_2$ (65 μM), but protects the cells against a high dose of $CoCl_2$ (125 μM). This property is similar to the effect of diazoxide on $CoCl_2$ in MOG-G-UVW cells.

In addition to diazoxide and nicorandil, the third K_{ATP} activator, cromakalim, was also tested against the same doses of $CoCl_2$ in MOG-G-UVW cells. The results are shown in Fig. 7.8.

For the results shown in Fig. 7.8A, a one way ANOVA test for all the groups suggested that the difference amongst those groups was significant ($p < 0.001$), and the Tukey's post test (comparing every two groups) indicated that 65 μM $CoCl_2$ caused a significant reduction in the relative cell number from the control ($p < 0.001$), but 10 – 100 μM cromakalim in combination with 65 μM $CoCl_2$ did not have any significant effect on the relative cell number from the same dose of $CoCl_2$ alone.

From the results shown in Fig. 7.8B, it can be seen that cromakalim did not protect the cells from a high dose of $CoCl_2$ (125 μM) either. A one way ANOVA test for all the groups suggested that the difference amongst those groups was significant ($p < 0.001$), the Tukey's post test (comparing every two

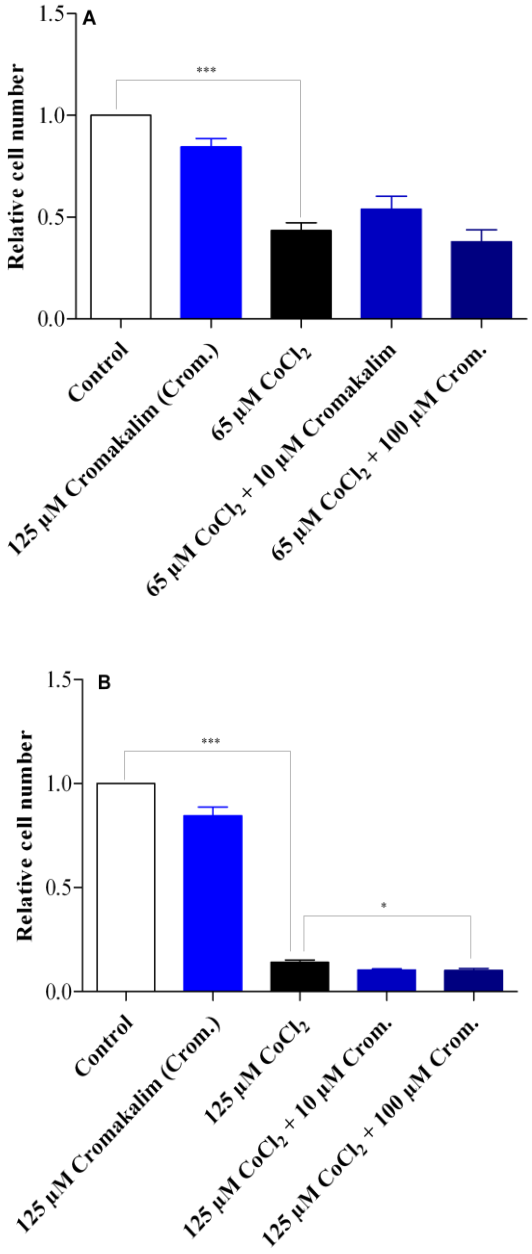

Fig. 7.8 The effect of cromakalim (crom.) in combination with $CoCl_2$ in MOG-G-UVW cells. A: 65 µM $CoCl_2$, the results are the means of 30 for 65 µM $CoCl_2$ alone and the control, and 6 for 125 µM cromakalim alone, 65 µM $CoCl_2$ + 10 µM cromakalim and 65 µM $CoCl_2$ + 100 µM cromakalim. And B: 125 µM $CoCl_2$, the results are the means of 21 for 125 µM $CoCl_2$ alone and the control, and 6 for 125 µM cromakalim alone, 125 µM $CoCl_2$ + 10 µM cromakalim and 125 µM $CoCl_2$ + 100 µM cromakalim.

groups) indicated that 125 µM $CoCl_2$ alone caused a significant reduction in

the relative cell number from the control ($p < 0.001$), and the Dunnett's post test (comparing each group with the $CoCl_2$ alone) indicated that 100 μM cromakalim in combination with 125 μM $CoCl_2$ also had a significant effect on the relative cell number from the same dose of $CoCl_2$ alone ($p < 0.05$).

To summarise the cell proliferation MTS assays results on K_{ATP} activators, it can be reported that none of them can protect MOG-G-UVW cells against a low dose of $CoCl_2$ (65 μM). However, against a high dose of $CoCl_2$ (125 μM), diazoxide and nicorandil protect MOG-G-UVW cells, and cromakalim has the opposite effect by further reducing the relative cell number from 125 μM $CoCl_2$ alone.

7.3.4 K_{ATP} blockers effect on $CoCl_2$ insult

In addition to K_{ATP} activators, the blockers, tolbutamide and glibenclamide, were also tested in MOG-G-UVW cells. The results of tolbutamide in combination with $CoCl_2$ insult are shown in Fig. 7.9.

For the results shown in Fig. 7.9A, a one way ANOVA test for all the groups suggested that the difference amongst those groups was significant ($p < 0.001$), and the Tukey's post test (comparing every two groups) indicated that both 65 μM $CoCl_2$ alone and 100 μM tolbutamide alone caused significant reductions in the relative cell numbers from the control ($p < 0.001$ for both), and 10 μM or 100 μM tolbutamide in combination with 65 μM $CoCl_2$ also had a significant

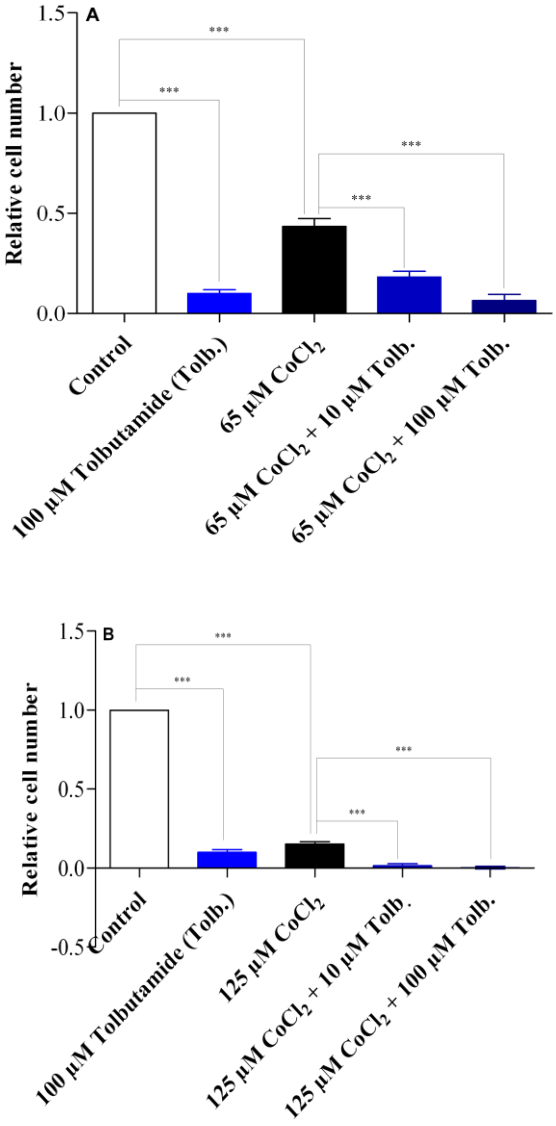

Fig. 7.9 The effect of tolbutamide (tolb.) in combination with $CoCl_2$ in MOG-G-UVW cells. A: 65 µM $CoCl_2$, the results are the means of 30 for 65 µM $CoCl_2$ alone and the control, and 6 for 100 µM tolbutamide alone, 65 µM $CoCl_2$ + 10 µM tolbutamide and 65 µM $CoCl_2$ + 100 µM tolbutamide. And B: 125 µM $CoCl_2$, the results are the means of 12 for 125 µM $CoCl_2$ alone and the control, and 6 for 100 µM tolbutamide, 125 µM $CoCl_2$ + 10 µM tolbutamide and 125 µM $CoCl_2$ + 100 µM tolbutamide.

effect on the relative cell number in comparison to the same dose of $CoCl_2$ alone ($p < 0.001$ for both).

Similar effects can be seen with a higher dose of $CoCl_2$ (125 μM). The Tukey's post test (comparing every two groups) for all the groups in Fig. 7.9B indicated that 10 μM or 100 μM tolbutamide in combination with 125 μM $CoCl_2$ caused a significant reduction in the relative cell number from the same dose of $CoCl_2$ alone ($p < 0.001$). Therefore, it can be concluded that 100 μM tolbutamide alone reduces the relative cell number, and 10 μM – 100 μM tolbutamide cannot protect MOG-G-UVW cells from either a low dose (65 μM) or a high dose (125 μM) of $CoCl_2$, and may in fact further reduce the relative cell number from the same of dose of $CoCl_2$ alone.

In addition to tolbutamide, another K_{ATP} blocker, glibenclamide, has also been tested, but only negative results were achieved (Khudheyer, 2010). The cell density was 5,000 per well in 24 well plates here. The dose – response for the $CoCl_2$ insult in MOG-G-UVW cells was different from the one shown in Section 4.3.1 and the EC_{50} of $CoCl_2$ in these experiments was estimated at about 500 μM. The glibenclamide results are shown in Table 7.3.

Table 7.3 The effect of glibenclamide in combination with an EC_{50} of $CoCl_2$ insult in MOG-G-UVW cells (n = 2)

Glibenclamide concentration (in combination with 500 μM $CoCl_2$)	Relative cell number
10 μM	0.621
50 μM	0.568
100 μM	0.428
500 μM	0.348

[Data from: (Khudheyer, 2010)]

The Bonferronni's post test (comparing every two groups) did not suggest any significant difference in the relative cell number. Hence, it can be concluded that glibenclamide cannot protect MOG-G-UVW cells from a $CoCl_2$ insult.

Therefore, to summarise the results of the K_{ATP} channel blockers against the $CoCl_2$ insult, it can be concluded that neither tolbutamide nor glibenclamide was protective. In addition, tolbutamide in combination with $CoCl_2$ insult may even further reduce the relative cell number compared to the same dose of $CoCl_2$.

7.4 Discussion

7.4.1 K_{ATP} channel

From the PCR results shown in section 7.3.2, it can be seen that the messages of K_{ATP} subunits exist in the MOG-G-UVW cell line, and the subunit composition of K_{ATP} channel in MOG-G-UVW cell line might (tentatively) be $K_{ir}6.2$ with SUR2A.

For the possible role, if any, of the K_{ATP} channel in cell death, previous studies have reached different conclusions, as discussed in Section 7.1. Some studies believe that the activation of K_{ATP} channel can induce cell death when there was no insult applied to the cells, for example both diazoxide and cromakalim can cause a reduction in cell numbers (Wang et al., 2007, Burg et al., 2006),

and the blockade of K_{ATP} channel, with for example glibenclamide, may increase cell proliferation (Wang et al., 2007). However, in combination with insults, such as hypoxia and Aβ, a K_{ATP} channel activator like diazoxide might then be neuroprotective (Goodman and Mattson, 1996).

Interestingly, the results in this Thesis did not exactly concur with those studies above. K_{ATP} channel activators alone, such as diazoxide, nicorandil and cromakalim, tended to cause a reduction in the relative cell number from the control, but not significantly. Only 125 μM diazoxide alone caused a significant reduction in the relative cell number compared to the control, and, K_{ATP} channel activators, like diazoxide and nicorandil, protected the cells from a high dose of $CoCl_2$ (125 μM), although the results were negative in the case of a low dose of insult (65 μM). In addition, K_{ATP} channel blockers, for example tolbutamide and glibenclamide, cannot protect the cells from $CoCl_2$ insult, and tolbutamide in combination with $CoCl_2$ insult may even cause a further reduction in the relative cell number from the same dose of $CoCl_2$ alone.

From the results shown in Section 7.3.3 and 7.3.4, a K_{ATP} channel blocker alone, such as tolbutamide, cannot increase cell proliferation in MOG-G-UVW cells, but causes a reduction in the relative cell number from the control. Additionally, not all K_{ATP} channel activators may protect the cells from $CoCl_2$ insult. Cromakalim may somehow aggravate the insult of a high dose of $CoCl_2$ (125 μM).

These results might be explained by considering the balance of $[Ca^{2+}]_i$ or K^+ release from the cell. K_{ATP} channel activator would reduce the open probability of Ca^{2+} channels on both ER membrane and cell membrane (Brini, 2003). In normal conditions without any insult, such an effect might lower the $[Ca^{2+}]_i$ to below a "normal" physiological level. On the other hand, as introduced in Section 7.1, a K_{ATP} channel blocker might reduce cellular K^+ release and might cause the mitochondrial membrane hyperpolarisation.

In the hypoxia environment, such as exists with a $CoCl_2$ insult, two opposite results might follow the activation of the K_{ATP} channel. It can reduce the open probability of Ca^{2+} channels, but can also cause a K^+ release or even efflux. Hence, whether the K_{ATP} channel activator is neuroprotective or not may depend on the balance of those two opposing effects.

In addition, the difference in the effects of cromakalim and the other two K_{ATP} channel activators might be explained by the selectivity to different K_{ATP} subunits. From the RT-PCR results shown in Section 7.3.2, it can be seen that, in MOG-G-UVW cell line, the expression of $K_{ir}6.2$ is higher than that of $K_{ir}6.1$, and the expression of SUR2A is higher than that of the other two SUR subunits. If there is any possible selectivity with respect to the different K_{ATP} channel subunits in the activators, it might explain the negative results shown by cromakalim.

7.4.2 $K_v3.3$ and $K_v3.4$ channels

From the PCR results shown in Section 7.3.2, it can be concluded that $K_v3.3$ and $K_v3.4$, exist in the neuronal cell lines, such as N2102Ep and NTERA-2.

Previous studies have found that K_v channels can be activated during cell apoptosis induced by NO, and the activation of K_v channels would cause K^+ efflux and cell shrinkage (Burg et al., 2006). In this Thesis, the results shown in Section 6.3 have suggested that the generic K^+ channel blocker, such as TEA, may protect the cells from $CoCl_2$ insult.

7.5 Conclusions and future work

To summarise all the results and discussion in this chapter, it may be suggested that:

a. The messages of K_{ATP} channel subunits exist in the mRNA of MOG-G-UVW cell line, and the main subunit composition of the K_{ATP} channel in this cell line might be $K_{ir}6.2$ with SUR2A.
b. The messages of $K_v3.3$ and $K_v3.4$ channels exist in the mRNA of neuronal cell lines, such as N2102Ep and undifferentiated NTERA-2.
c. K_{ATP} activators, such as diazoxide, nicorandil and cromakalim, cannot increase the cell proliferation of MOG-G-UVW cells and cannot protect the cells from a low dose of $CoCl_2$ (65 μM). However, with a high dose of $CoCl_2$ (125 μM), diazoxide and nicorandil protect the MOG-G-UVW cells, but cromakalim causes a further reduction in the relative cell

number from $CoCl_2$ alone.

d. K_{ATP} channel blockers, such as tolbutamide and glibenclamide, cannot increase cell proliferation in MOG-G-UVW cells, and tolbutamide alone may even cause a reduction in the relative cell number. Neither of the two blockers can protect MOG-G-UVW cells from $CoCl_2$ insult, and tolbutamide may even cause a further reduction in the relative cell number from the same dose of $CoCl_2$ alone.

For the future work on K_{ATP} channel, the possible selectivity, if any, for different K_{ATP} subunits in the activators should be investigated to find out whether this is the reason for cromakalim to be different from the other two activators. If this is the case, the expression of different K_{ATP} subunits in neurones can be studied with Q-PCR to find out what the main subunit composition of K_{ATP} channel in neurones is. Furthermore, the K_{ATP} channel activators which can target those subunits, for example $K_{ir}6.2$ and/or SUR2A, might point the way to a K^+ channel strategy for neuroprotection.

And as for the K_v channels, although TEA, a generic K^+ channel blocker, may have a neuroprotective effect, it is uncertain which K^+ channel(s) exactly TEA targets when it protects the cells. Hence, selective K_v channel blockers, such as dendrotoxin (Harvey and Robertson, 2004), should be tested on those established cell insult models in cell proliferation MTS assays to see whether more selective ligands may protect the cells or not.

8. General Discussion, Conclusion and Future Work

8. General Discussion, Conclusion and Future Work

8.1 General discussion

8.1.1 $[Ca^{2+}]_i$ pathogenesis in neurodegeneration and neuronal death

In the general introduction (see Section 1.1), it has been argued that an overload of $[Ca^{2+}]_i$ could be one of the key pathogenesis in neuronal death (Berridge, 2010). The causes of $[Ca^{2+}]_i$ overload might be different in different neurodegenerative diseases: for example, it has been suggested that the $[Ca^{2+}]_i$ overload and neuronal death in AD is probably because of the deposition of Aβ plaque on the cell membrane and the subsequent formation of a Ca^{2+} channel (Arispe et al., 2007).

In this Thesis, the cell death induced by Aβ was confirmed in cell proliferation MTS assays in both undifferentiated and differentiated SH-SY5Y cells (see Section 4.3.4). In addition, another two cell insults which were suggested to increase the $[Ca^{2+}]_i$ in previous studies, the hypoxia mimetic effect induced by $CoCl_2$ and oxidative stress induced by H_2O_2 (Krebs et al., 2007), were also established in the cell lines used here, and were confirmed to be toxic to both astrocytoma (MOG-G-UVW) and neuronal (SH-SY5Y and NTERA-2) cell lines (see Section 4.3). Both of these insults were presumed to be related to $[Ca^{2+}]_i$ overload causing neurodegeneration. The hypoxia mimetic effect induced by $CoCl_2$ was applied as a model of ischemic stroke and has also been

found to increase the generation of Aβ (Zhu et al., 2009). Oxidative stress induced by H_2O_2 was also linked with, and applied as a model of neurodegeneration, for example AD, in previous studies (Lin and Beal, 2006, Floyd, 1999, Floyd and Hensley, 2002), and has been suggested to increase the Ca^{2+} channel open probability on the sarcoplasmic reticulum (SR, the smooth ER found in smooth and striated muscle cells) by possibly targeting the ryanodine receptor (Boraso and Williams, 1994) which is one of the key targets in this Thesis.

Based on those previous studies mentioned above, it has been proposed that an increase of $[Ca^{2+}]_i$ may induce cell death. Thus, those insults, $CoCl_2$, H_2O_2 and Aβ, were then selected to establish the cell insult models in this Thesis to induce the neuronal death.

According to previous studies on Aβ, this insult would be the model which is closest to the real circumstances in the neuronal cell death in AD. But, as discussed before in Section 4.4.3 and Section 4.4.4, the Aβ peptide is not easily controllable. It has to be incubated at 37 °C for one week for aggregation, and the length of the aggregated $Aβ_{1-42}$ was quite variable, which meant some of the amyloid was aggregated to long fibres whereas some others still formed only short peptides. Different lengths of $Aβ_{1-42}$ after incubation can be found in TEM photos from the work presented here (see Section 4.3.3 and Section 4.4.3). As the toxic effects of aggregated and non-aggregated amyloid are different, the cell proliferation MTS assays results with $Aβ_{1-42}$ were very

variable and there was little statistical significance to be found. Hence, $A\beta_{1-42}$ insult was not good enough to establish a reliable cell insult model for further cell proliferation MTS assays, although it might be agreed that it mimics the neuronal cell death environment in AD best.

Thus several other insult models, which can also increase $[Ca^{2+}]_i$, were established here, such as hypoxia mimetic effect induced by $CoCl_2$, oxidative stress induced by H_2O_2, and glutamate cytotoxicity via NMDA receptor binding and activation. As discussed in Chapters 1 and 4, they have been used in previous studies as models of neurodegeneration and have been shown to increase $[Ca^{2+}]_i$. Nevertheless, whether the $[Ca^{2+}]_i$ was significantly increased or not by those insults has not been directly tested in this study. Although $CoCl_2$, H_2O_2 and glutamate induce neuronal death in cell proliferation MTS assays, the $[Ca^{2+}]_i$, which is the key issue in neuronal death in this study, has not been tested in any measurement. Future work should undertake Ca^{2+} imaging when the cells were under insult to determine directly whether $[Ca^{2+}]_i$ was increased or not. Based on the results from cell proliferation MTS assays, $CoCl_2$ and H_2O_2 induce reliably cell death, and such an effect is repeatable and statistically significant. Thus, apart from glutamate which cannot induce cell death until a high dose (mM), $CoCl_2$ and H_2O_2 were adopted in this Thesis and established as neuronal insult models for further experiments.

8.1.2 Cell differentiation

Besides the manoeuvres adopted to induce cell death, another issue which has been of concern in this study was the cell lines used. Two cell lines were required to be differentiated in this study, SH-SY5Y and NTERA-2. As discussed in Section 2.2, undifferentiated SH-SY5Y and NTERA-2 cells are neuroblastoma and pluripotent embryonal carcinoma respectively before differentiation. They are not human neurones unless they have been differentiated with retinoic acid. In this Thesis, both cell lines have been differentiated with retinoic acid following standard protocols and the morphology of the cells were examined, but it was still always an issue on how to evaluate a successful differentiation.

As discussed in Section 3.4, some neuronal markers have been suggested in previous studies, although their effects might be arguable, such as PCR of GAP-43 (Laifenfeld et al., 2002) and western blot for transglutaminase (T-Gase) (Joshi et al., 2007). In this study, both of these have been deployed to test the differentiation of SH-SY5Y cells. The results were however not consistent in different experiments. Such PCR results are shown in Fig. 8.1.

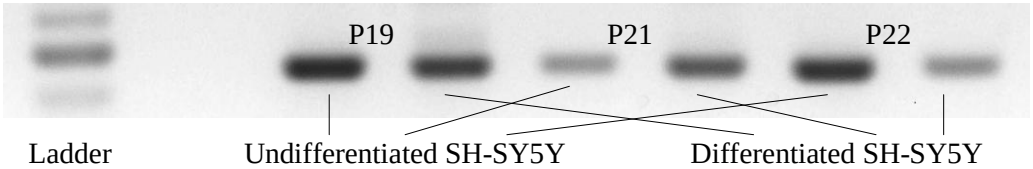

Fig 8.1 PCR of GAP-43 in both undifferentiated and differentiated SH-SY5Y cell lines. Here "P" represents the passage number.

From Fig. 8.1, it can be seen that the GAP-43 message expression was not always up-regulated after differentiation. Its expression was up-regulated at

P21, but was down-regulated at P19 and P22.

In addition to the PCR of GAP-43, western blot for T-Gase was also tested, but there was no overt difference observed between the undifferentiated and differentiated SH-SY5Y cells. Therefore, a change in morphology was selected to evaluate the differentiation in this Thesis. As discussed in section 3.4, morphology was not ideal to evaluate the differentiation since the change in cell morphology might not be always obvious. Even in some previous studies which have used a change in morphology to confirm a successful differentiation, the difference in cell morphology between undifferentiated and differentiated SH-SY5Y cells was not obviously noticeable (see Fig. 3.36) (Lovat et al., 1997).

Besides GAP-43 and T-Gase, other neuronal markers have also been utilised to evaluate the differentiation of a neuroblastoma cell line, for example neurites for the differentiation of C1300, a rat neuroblastoma cell line (Freshney, 1994). Antibodies which are specific for neurones have also been suggested, but whether they might have similar effects on neuroblastoma cell lines is not certain. Therefore, future work could seek to establish a reliable neuronal marker to evaluate the differentiation of SH-SY5Y and NTERA-2 cells.

8.1.3 Ryanodine receptor function in neuronal cell death

The main target in the cell lines used here is the RyR. As introduced earlier

(see Section 1.2.2), the RyR is a CICR channel on the ER membrane (Berridge, 2010). It can be activated by cytosolic Ca^{2+} at μM level (Alexander et al., 2009) and releases further Ca^{2+} from the ER which may cause $[Ca^{2+}]_i$ overload. Since the overload of $[Ca^{2+}]_i$ was found in neuronal death in neurodegeneration, it is worthwhile to study the possible effect, if any, of the RyR in neuronal death. Significantly a previous study has already described the up-regulation of RyRIII in a transgenic mouse model of AD, and tried to link its up-regulation with an increase in $[Ca^{2+}]_i$ (Supnet et al., 2006).

8.1.3.1 RyRIII expression and cell sensitivity to the insults

Considering the results from Chapters 3 and 4, it can be seen that the increased RyRIII message in differentiated SH-SY5Y cells was accompanied with an increased sensitivity to insults which might increase $[Ca^{2+}]_i$, including both the hypoxia mimetic effect induced by $CoCl_2$ and oxidative stress induced by H_2O_2. For possible pathogenesis, it can be proposed that $[Ca^{2+}]_i$ was firstly increased by the insults, either $CoCl_2$ or H_2O_2, and the RyR on the ER membrane was then activated by the increased $[Ca^{2+}]_i$. The activated RyR channel can release more Ca^{2+} from the ER and further increase $[Ca^{2+}]_i$. The more RyR there is on the ER membrane, the more Ca^{2+} could be released through RyR channel. Thus, it may be suggested that the cells with a higher expression of RyR would be more sensitive to the insults which may cause an initial increase of $[Ca^{2+}]_i$. This proposed pathogenesis is briefly summarised in Fig. 8.2.

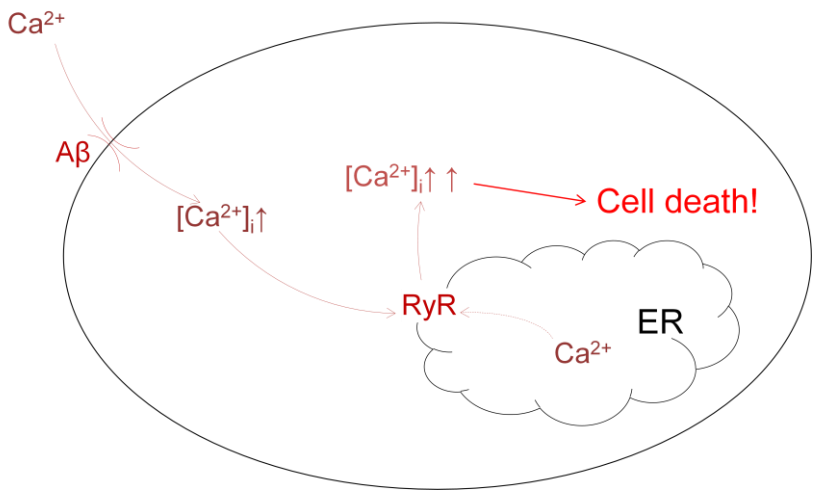

Fig. 8.2 Ca^{2+} induced Ca^{2+} release (CICR) route via the ryanodine receptor (RyR).

Nevertheless, as discussed in Section 3.4, there is still one concern in concluding that a higher expression of RyR might increase cell sensitivity to insults. From the Q-PCR result of RyRIII expression shown in Section 3.3.6, it can be found that the RyRIII message in differentiated SH-SY5Y cells was about 6 fold higher than the undifferentiated counterpart. But, from the cell proliferation MTS assays results of $CoCl_2$ insult (see Section 4.3.1), the differences in cell sensitivity to $CoCl_2$ between undifferentiated and differentiated SH-SY5Y cells were not marked, although statistically significant. Thus, it might be considered debatable that the different sensitivity to insult was caused solely by different RyR expression. Other factors may thus contribute to the different sensitivity to these stressors. In addition, the expression of RyRIII message was only tested by PCR, but no western blot was carried out. Therefore, there were no data available to quantitatively conclude how many RyRs were present at a protein level in this cell line.

As introduced in Section 1.2, RyR is not the only one receptor which can

modulate $[Ca^{2+}]_i$. IP_3R, PS1, CALHM1 and SERCA etc. are also involved in the Ca^{2+} release from ER and the modulation of $[Ca^{2+}]_i$. IP_3R is located on the ER membrane and can be activated by $[Ca^{2+}]_i$ (< 300 nM) to further release Ca^{2+} from ER (Stutzmann and Mattson, 2011). While the RyRIII message was increased in SH-SY5Y cell line after differentiation, what changes in IP_3R expression there might have been, was not investigated in this study.

In addition, the increase of $[Ca^{2+}]_i$ can induce both activation and inhibitory effects on the RyR according to different $[Ca^{2+}]_i$. μM levels of $[Ca^{2+}]_i$ can activate RyR but mM levels of $[Ca^{2+}]_i$ may inhibit it (Alexander et al., 2009). Such a difference is based on different binding sites and affinity of Ca^{2+} for the RyR (Laver, 2007) (see Fig. 8.3). The same considerations apply to the IP_3R also. Low concentrations of Ca^{2+} (< 300 nM) can activate the channel but high Ca^{2+} concentrations can inhibit the channel opening (Stutzmann and Mattson, 2011). Although it is known, from previous studies, that both a hypoxia mimetic insult and oxidative stress can increase $[Ca^{2+}]_i$, the $[Ca^{2+}]_i$ was not quantitatively measured in this study. Hence, it is difficult to tell quantitatively how many RyR and/or IP_3Rs have been activated or inhibited.

To summarise, even if how important the role of RyR is in neuronal cell death is debatable, one conclusion stands. According to the results in this Thesis, the higher expression of RyRIII message is associated with a higher sensitivity of neuronal cells to insults which increase $[Ca^{2+}]_i$, such as a hypoxia mimetic effect and oxidative stress.

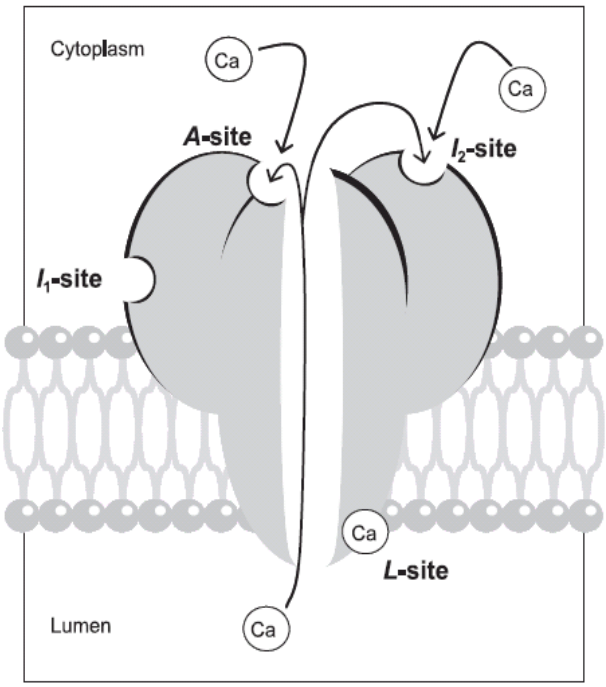

Fig. 8.3 Ca^{2+} binding sites on RyR. A-site: activation site, I_1-site: inhibition site, I_2-site: inactivation site, and L-site: luminal activation site. (Laver, 2007)

8.1.3.2 RyR isoforms and blockade

As introduced in Section 1.2.2, there are 3 different isoforms of RyR. RyRI is mainly located in skeletal muscle, RyRII is mainly found in cardiac cells, and RyRIII, which is the most important target in this Thesis, is mainly observed in brain neurones (Sorrentino, 1995). The RT-PCR results of RyRs in MG-63 cells, an osteosarcoma cell line which is not neuronal, are consistent with previous studies since the message of RyRIII was absent in the MG-63 cell line (see Section3.3.4).

Based on the findings from previous studies and the Q-PCR in this Thesis, blockade of the RyR was then tested to see whether the cells could be protected

or not. From the results presented in Chapter 5, it can be seen that ruthenium red, a generic RyR blocker for the 3 isoforms, protects both astrocytoma (MOG-G-UVW) and neuronal (SH-SY5Y and NTERA-2) cells against a $CoCl_2$ insult, and tended to protect the cells against $A\beta_{1-42}$ insult, although not significantly. The generic activation of RyR with caffeine or ryanodine (nM – μM) aggravates the insult by further reducing the cell numbers. Hence, it may be concluded that blockade of RyR is potentially neuroprotective.

Obviously, one key question was how to identify the relevant isoforms of RyR. As mentioned in Section 5.1, there is no selective RyRIII blocker available, therefore, the idea here was to use other selective RyR modulators to narrow down the possible target. According to the results in Chapter 5, dantrolene, a selective RyRI and RyRIII blocker also protects both MOG-G-UVW and SH-SY5Y cells from $CoCl_2$ insult. But, procaine and ryanodine (100 μM), selective RyRI and RyRII blockers, cannot protect the cells from the insult. Thus, it was concluded that RyRI and RyRII may not be important targets for neuroprotection, but that the RyRIII, the target of ruthenium red and dantrolene, may offer protection to the cells.

Assuming this as a potential possible target, the drug design question then becomes how to selectively block the RyRIII for a neuroprotective end point. RyRI and RyRII are widely distributed in skeletal and cardiac cells. A generic RyR blocker like ruthenium red would therefore cause significant and serious side effects, even if there is any neuroprotective benefit. The selective binding

domains for RyRIII blockers require to be investigated. From the previous limited studies on RyRIII binding domains, a simple idea can be proposed here. Previous studies have pointed out that the selective binding domain of ruthenium red on RyRIII is region 6b and 12a located at 1,861 – 2,094 and 3,657 – 3,776 respectively in the amino acid sequence (Chen and MacLennan, 1994). Another study has also suggested that the domain between cytoplasmic and transmembrane domains (3,722 – 4,610 in the amino acid sequence) could be the relevant binding domain of RyR (George et al., 2004), which partly overlaps with the selective RyRIII binding domain 12a. Thus the area between the cytoplasmic and transmembrane part of RyRIII may be the selective binding domain of RyRIII. Future work studying RyRIII blockade should involve an investigation on the structure of this binding domain with computer based modelling system to determine the requirements of a selective RyRIII blocker.

8.1.4 K^+ channels and neuroprotection

In addition to the RyR, K^+ channels are another important membrane target considered in this Thesis. As previously discussed (see Section 1.4.2) different considerations were raised in previous studies on the possible effects of K^+ channels in neuronal death and neuroprotection. Some studies claimed that Ca^{2+}-activated K^+ channels are relevant to a neurodegeneration model and/or neuroprotection (Coles et al., 2008, Liao et al., 2010), while some others disagree (Yu et al., 1998, Burg et al., 2006). And, different opinions have also

been discussed on the role of K_{ATP} channel: for example some studies suggest that K_{ATP} activators may protect cells from the insults of Aβ and a hypoxia mimetic effect (Goodman and Mattson, 1996) but some others claimed that K_{ATP} blockers increase cell proliferation (Wang et al., 2007). Hence, the possible effect, if any, of BK and K_{ATP} channels were tested here in the cell lines in cell proliferation MTS assays.

8.1.4.1 BK channel

Firstly, the BK channel was identified in undifferentiated SH-SY5Y cells in both RT-PCR and patch clamp recording, which means it exists and is active in this neuronal cell line.

The activation of BK channel, with NS1619 and IPA, increased cell proliferation in both undifferentiated and differentiated SH-SY5Y cells. Neither of the two activators has shown any neuroprotective effect. As shown in Section 6.3.6, both NS1619 and IPA had a negative effect against the insult of H_2O_2 in the undifferentiated SH-SY5Y cells and have potentiated the toxic effect of the insult in the differentiated SH-SY5Y cells. In the presence of a hypoxia mimetic effect induced by $CoCl_2$, both NS1619 and IPA have potentiated the toxic effect of $CoCl_2$ in both undifferentiated and differentiated SH-SY5Y cells.

For the negative results shown by the two activators, increased K^+ efflux was

considered as a possible explanation. BK channel has been activated already in the presence of insults since both insults can increase the $[Ca^{2+}]_i$ which is an activator of BK channel. Further activation with BK activators may induce an additional K^+ efflux and cell shrinkage, as well as cell death (Burg et al., 2006). If this is the case, K^+ channel blockers might be neuroprotective. From the results shown in Section 6.3.7, K^+ channel blockers, TEA and tetrandrine, protect or tended to protect SH-SY5Y cells from a $CoCl_2$ insult. Nevertheless, K^+ channel blockers have not been tested in the presence of BK activators to see whether the blocker might reverse the effect of activator. That would be obvious future work.

The proposed neuroprotective effect of BK blockade, if any, is still uncertain. Both TEA and tetrandrine are non selective BK blockers and some other K^+ channels have also been suggested to have a protective role, such as K_v channels. Additionally, a selective BK blocker, IbTX, presented a negative result in this study, although that might be explained by the resistance of the BK channel with a β4 subunit.

8.1.4.2 K_{ATP} channel

In addition to the BK channel, another K^+ channel, the K_{ATP} channel was also studied in this Thesis. RT-PCR results indicated that there are K_{ATP} subunits in the MOG-G-UVW cell line and the main subunit composition might be $K_{ir}6.2$ and SUR2A (see Section 7.3).

The possible role of K_{ATP} channel in neuroprotection was tested in cell proliferation MTS assays in the presence of a $CoCl_2$ insult. From the results shown in Section 7.3.4, it can be concluded that K_{ATP} blockers tolbutamide and glibenclamide were not protective. In fact tolbutamide alone reduces the cell number, and it may also aggravate the insult of $CoCl_2$.

That does not necessarily mean however that K_{ATP} activators are protective. From the results shown in section 7.3.3, it can be seen that different K_{ATP} activators may present different effects. K_{ATP} channel activators alone cannot increase the cell number, and both diazoxide and cromakalim alone may even reduce the cell number. In addition, K_{ATP} channel activators cannot protect the cells against $CoCl_2$ insult at a low dose of $CoCl_2$, and diazoxide may even aggravate the insult by further reducing the relative cell number. However, in the presence of a high dose of $CoCl_2$, both diazoxide and nicorandil protect the cells by increasing the relative cell number from the same dose of $CoCl_2$ alone. But the third activator, cromakalim, aggravated the insult by further reducing the relative cell number.

To summarise the results from K_{ATP} modulators, it can be concluded that K_{ATP} channel blocker can aggravate the insult of a hypoxia mimetic effect, and the K_{ATP} channel activators cannot protect the cells against a low dose of $CoCl_2$ either. Nevertheless, whether a K_{ATP} activator strategy can be protective against a high dose of $CoCl_2$ is uncertain since unfortunately different activators have shown different effects. In addition, K_{ATP} activators have not

been tested in the presence of K_{ATP} blockers to see whether the activator might reverse the effect of the blockers or not. That is for future work.

To summarise the effects of K^+ channels in neuroprotection, it can be concluded that BK activation and K_{ATP} blockade were not protective, and may probably potentiate or aggravate the insults by further reducing the cell number. On the contrary, generic K^+ blockers, TEA and tetrandrine, were protective or tended to be protective against the $CoCl_2$ insult. Activation of the K_{ATP} channel was not protective against a low dose of $CoCl_2$ but was sometimes, although cromakalim was an exception, protective against a high dose of $CoCl_2$.

8.2 Conclusions

The principal findings of the Thesis are as follows:

a. The RyRIII message exists in the neuronal cell lines, but is absent in MG-63 cells. Its expression was up-regulated in SH-SY5Y cell line when the cells were differentiated from neuroblastoma to human neurones.
b. The cells with higher RyRIII expression, such as differentiated SH-SY5Y cells, were more sensitive than those with lower expression, such as undifferentiated SH-SY5Y cells, to insults, including a hypoxia mimetic effect induced by $CoCl_2$ and oxidative stress induced by H_2O_2.
c. Blockade of RyR, with ruthenium red or dantrolene, was

neuroprotective against $CoCl_2$. Such an effect has been found in both astrocytoma (MOG-G-UVW) and neuronal (undifferentiated NTERA-2, undifferentiated SH-SY5Y and differentiated SH-SY5Y) cell lines. Ruthenium red tended to be protective against an $A\beta_{1-42}$ insult as well in undifferentiated SH-SY5Y cells. In addition, RyR activation, with caffeine or ryanodine (nM – μM), can aggravate the insults of $CoCl_2$ by further reducing the relative cell number.

d. Selective blockade of RyRI and RyRII, with procaine or ryanodine (100 μM) cannot protect the cells against $CoCl_2$. Hence, it is suggested that selective blockade of RyRIII, rather than the other 2 isoforms, can be potentially neuroprotective.

e. The BK channel exists and is functional in a neuronal cell line, such as SH-SY5Y cells.

f. BK openers, like NS1619 and IPA, potentiate the insults of H_2O_2 and $CoCl_2$. Generic K^+ channel blockers, such as TEA and tetrandrine, can protect the cells against $CoCl_2$. The negative results of IbTX might probably indicate a selectivity of BK blockers towards different β subunits.

g. K_{ATP} activators, including diazoxide, nicorandil and cromakalim, cannot protect the cells against a low dose of $CoCl_2$, but might be protective against a high dose of $CoCl_2$. K_{ATP} blockers, such as tolbutamide and glibenclamide, cannot protect the cells against $CoCl_2$ and may even aggravate the insult.

8.3 Future work

For future work, the following ideas might be worth investigating to firm up the conclusions above.

a. To confirm the expression of RyRs, especially RyRIII, in neuronal cell lines with western blotting.
b. To find a neuronal marker to determine whether the cells, such as NTERA-2 and SH-SY5Y, have been successfully differentiated or not.
c. To apply Ca^{2+} imaging technique in the presence of cell insults, such as hypoxia mimetic or oxidative stress, to see whether the $[Ca^{2+}]_i$ was increased, and to quantify how much the $[Ca^{2+}]_i$ is increased.
d. To use a computer based modelling system to find out the selective binding domain(s) of RyRIII and probably to develop selective RyRIII blocker(s).
e. To further study the K_{ATP} and K_v channels with patch recording, pharmacology and cell proliferation MTS assays on other insult models or in other cell lines to determine their possible roles, if any, in neuronal death and neuroprotection.
f. To test cell viability in trypan blue assays and to measure cell apoptosis with fluorescence-activated cell sorting (FACS) to determine how insults may induce cell death and to test how modulators protect the cells from neuronal death or apoptosis.

Abbreviations and Symbols

%	percent
°C	centigrade
Å	angstrom, 10^{-10} m
$(CH_3)_2CHOH$	isopropyl alcohol
$[Ca^{2+}]_i$	intracellular Ca^{2+} concentration
$[Mg^{2+}]$	Mg^{2+} concentration
ι	tau
μg	micro gram, 10^{-6} g
μg/mL	micro gram per millitre
μm	micro meter, 10^{-6} m
μL	micro litre, 10^{-6} L
μM	micromole, 10^{-6} M
μm	micrometre, 10^{-6} m
A	adenine
Ach	acetylcholine
AD	Alzheimer's disease
ALS	amyotrophic lateral sclerosis
ANOVA	analysis of variance
APP	amyloid precursor protein
ATP	adenosine-5'-triphosphate
Aβ	beta amyloid
BK	large conductance Ca^{2+}-activated K^+ channel
bp	base pair(s)
C	cytosine
C_2H_5OH	ethanol
Ca^{2+}	calcium
$CaCl_2$	calcium chloride
$CaCl_2 \cdot 2H_2O$	calcium chloride dehydrate
CALHM1	Ca^{2+} homeostasis modulator 1
CH_3COOH	acetic acid
CH_3COONa	sodium acetate
CHAPS	3-[(3-cholamidoprophl)dimethylammonio]-1-propanesulfonic acid

$CHCl_3$	chloroform
CICR	Ca^{2+} induced Ca^{2+} release
cm^2	square centimetre
CO_2	carbon dioxide
$CoCl_2$	cobalt (II) chloride
CTX	charybdotoxin
Cu	copper
Cu^+	copper I
$CuSO_4 \cdot 5H_2O$	copper (II) sulphate
dATP	deoxyadenosine triphosphate
dCTP	deoxycytidine triphosphate
dGTP	deoxyguanosine triphosphate
DMEM	Dulbeceo's modified Eagle medium
DMSO	dimethyl sulfoxide
DNA	deoxyribonucleic acid
dUTP	deoxyuridine triphosphate
EB	ethidium bromide
EC_{50}	half maximal effective concentration
EDTA	ethylenediaminetetraacetic acid, $(HOOCCH_2)_2NCH_2CH_2N(CH_2COOH)$
EGTA	ethylene glycol-bis(2-aminoethyl-ether)-N,N,N',N'-tetraacetic acid, $C_{14}H_{24}N_2O_{10}$
EMEM	minimum essential medium Eagle
ER	endoplasmic reticulum
F10	nutrient mixture F10 ham
F12	nutrient mixture F12 ham
FACS	fluorescence – activated cell sorting
FBS	foetal bovine serum
Fe^{2+}	ferrous
$FeSO_4$	ferrous sulphate
g	gram, 10^{-3} kg
G	guanine
g/cm^2	gram per square centimetre
GΩ	giga ohm, 10^{12} Ω
GAP-43	growth-associated-protein

GC%	percentage of C and G
h	hour
H_2O	water
H_2O_2	hydrogen peroxide
HCl	hydrochloride acid
HD	Huntington's disease
Hz	hertz
I-V	current – voltage
IbTX	iberiotoxin
IP_3	inositol 1,4,5-trisphosphate
IP_3R	IP_3 receptor
IPA	isopimaric acid
IR	inward rectifier
K^+	potassium
K_{ATP}	ATP-sensitive K^+ channel
KCl	potassium chloride
K_{ir}	inward rectifier subunit
K_v	voltage gated K^+ channel
M	mole
mg/mL	milligram per millilitre
Mg^{2+}	magnesium
$MgCl_2$	magnesium (II) chloride
min	minute
mL	millilitre, 10^{-3} L
mM	milli mole, 10^{-3} M
mm	millimetre
MTS	3-(4,5-dimethylthiazol-2-yl)-5-(3-carboxymethoxyphenyl)-2-(4-sulfophenyl)-2H-tetrazolium, inner salt
mV	milli volt, 10^{-3} V
N_2	nitrogen
Na^+	sodium
NaCl	sodium chloride
NaOH	sodium hydroxide
NEAA	MEM non-essential amino acid solution
nm	nano metre, 10^{-9} m

nM	nanomole, 10^{-9} M
NMDA	N-Methyl-D-aspartate
NO	nitric oxide
No.	number
NS1619	1-(2'-hydroxy-5'-trifluoromethylphenyl)-5-trifluoromethyl-2(3H)benzimidazolone
$O^{\cdot-}$	superoxide
pA	pico ampere, 10^{-12} A
pg	pico gram, 10^{-12} g
P/S	penicillin-streptomycin mixture
PBS	phosphate-buffered saline
PCR	polymerase chain react
PD	Parkinson's disease
PIPES	1,4-piperazinediethanesulfonic acid
PMS	phenazine methosulfate
P_o	open probability
pS	pico simens, 10^{-12} S
PS1	presenilin 1
Q-PCR	quantitative PCR
r/min	round per min
RNA	ribonucleic acid
RR	ruthenium red
RT	reverse transcription
RyR	ryanodine receptor
s	second
SERCA	sarcoplasmic-endoplasmic reticulum Ca^{2+} ATPase
SOD	superoxide dismutase
SR	sarcoplasmic reticulum
SUR	sulfonylurea receptor
T	thymine
T-Gase	transglutaminase
TEA	tetraethylammonium
TEM	transmission electron microscope
T_m	melting temperature
u	unit

UDG	uracil DNA glycosylase
UV	ultroviolet
v/v	volume to volume
v/w	volume to weight
W	watt
w/v	weight to volume
WHO	World Health Organisation
Zn	zinc

Appendix

A. mRNA sequence of RyRIII (data from pubmed)

mRNA sequence (with primer sequences shown)

```
   1 cgcacgccga gcggctgccg ggggaagcag aggcgccgga ggctggggca ccgccgacgc
  61 ctcgggagcc atggccgaag ggggagaagg aggcgaggac gagatccagt ttctgaggac
 121 tgaggatgaa gtggtactcc agtgcatcgc caccattcat aaggagcaga ggaagttctg
 181 cctggcagcc gagggacttg ggaatcgcct gtgcttcttg gaacccactt cagaagccaa
 241 gtacattcct ccagatctct gcgtctgcaa ttttgtgctg gaacagtccc tatctgtcag
 301 agccctgcag gaaatgcttg ccaacacagg tgaaaatggc ggcgaagggg cagcacaagg
 361 aggtggccac aggaccctgt tatacggcca tgcagttctc ctgaggcact ctttcagcgg
 421 aatgtatcta acatgcttga ctacatcaag atcccagaca gacaaacttg cctttgatgt
 481 aggtctacgg gaacatgcca caggagaagc ctgttggtgg actatacatc ctgcttccaa
 541 acagaggtcc gaaggagaga aagttcgaat tggcgatgac ctcatcctcg tcagcgtgtc
 601 ctctgaaaga taccttcatc tctcagtatc aaatggtaac atacaagtgg atgcctcctt
 661 tatgcaaaca ctctggaatg tacatcctac gtgctcagga agtagcatcg aagaaggata
 721 cctacttggt gggcatgtag tacgtctttt ccatggtcat gatgaatgtt tgacgatacc
 781 atctacagac cagaatgatt cccagcacag gaggatattc tacgaagctg ggggagctgg
 841 gactcgagcc aggtctcttt ggagagtgga acccccttcgg ataagctgga gtggcagtaa
 901 catcagatgg ggccaggctt tccgactccg gcatctcacc acaggccact acctggcctt
 961 gacagaagac caaggcctta tactgcaaga ccgggcaaag tcagacacca agtccacagc
1021 tttctctttc cgggcatcaa aggaactcaa ggagaaatta gactccagtc acaagcgaga
1081 catagaaggc atgggagttc cagaaatcaa gtatggagat tctgtctgct ttgtgcagca
1141 tatagccagt ggtctgtggg tgacctacaa agcacaagac gccaaaactt cccgcctggg
1201 acctctaaaa agaaaggtca tactccatca ggaaggccac atggatgatg gattaacact
1261 gcagagatgc cagcgtgagg agtcccaggc tgctcggatc atccggaaca ctacagcctt
1321 attcagccag tttgtcagcg gaaacaatcg cacagctgcc cccatcaccc tgcctataga
1381 agaagtcctg cagaccctac aggacttgat cgcctacttc cagcccccag aggaggagat
1441 gcgacatgaa gacaagcaga acaagctccg ctcactcaaa aacagacaaa atcttttcaa
1501 ggaagaggga atgttggccc ttgtcttaaa ttgcattgac cgcttaaatg tctacaatag
1561 cgtagcacac tttgcaggga ttgcaaggga agagagtggc atggcctgga aagaaattct
1621 gaacctcctc tacaaattgc tggctgctct cattcgcgga aacagaaaca attgcgctca
1681 attctccaat aaccttgatt ggctcatcag taaattggac agactagaat cttcctcagg
1741 tatcttggaa gttttgcact gcatcttaac tgaaagccca gaagccttaa atctgatagc
1801 ggagggccac atcaagtcga tcatctccct gttggataag cacgggcgga atcacaaggt
1861 tctggatatc ctgtgctccc tctgtctctg caatggggtt gcagtgagag ccaaccagaa
1921 tctgatctgt gacaacttgc tgccccggag aaacctactc ctgcagacac gactgattaa
1981 cgatgtaacc agtatccggc caaacatctt cctgggagtc gcggagggct cagcccagta
2041 caagaagtgg tacttcgagc tgattatcga ccaggtggac cccttcctaa cagcagagcc
2101 cacacatctg cgggtgggct gggcctcttc ttcaggctat gccccatacc caggaggtgg
2161 agaaggatgg ggaggcaatg gtgttggtga cgacctgtac tcctatggct ttgatggact
2221 tcacctttgg tcaggccgga tacccagagc tgtggcttcc atcaaccagc acctcctgag
2281 atcggatgac gtggtaagct gctgcctgga cctcggggtg cccagcatct cattccgcat
2341 caatgggcag cccgtgcagg ggatgtttga gaacttcaac acagacgggc tcttcttccc
2401 tgtgatgagc ttttcagcag gtgtcaaagt acgtttcctg atgggtggac gtcatggaga
```

2461 gtttaagttc ctgcctccct ctggctatgc cccttgctat gaagccttac ttccaaaaga
2521 gaagatgaga ttggagcctg tcaaagaata taaacgtgat gctgatggca ttagagatct
2581 cttgggtacc acccagttcc tctcccaagc ctctttcatc ccatgccccg tagacaccag
2641 tcaggttatt ttgccacctc acctagaaaa gatccgagac agactagctg aaaacatcca
2701 tgagctttgg ggaatgaata aaatagaact tggctggact ttcggcaaga tacgagatga
2761 caataaaaga caacaccctt gccttgtgga gttttcaaag ctcccagaaa ctgagaagaa
2821 ctataacctg caaatgtcaa ctgaaacctt aaaaaccctc ttggccctgg ggtgccacat
2881 tgctcatgtt aacccagctg ctgaggagga tctcaagaag gtcaaactgc ccaaaaacta
2941 tatgatgtcc aacggctata agccagcccc tttggatttg tctgatgtga agctgttacc
3001 tcctcaagaa attttagtgg ataagcttgc agaaaatgca cacaatgttt gggcaaaaga
3061 cagaataaaa caaggatgga cctatggcat ccaacaggat ttgaagaaca aaagaaatcc
3121 ccgtctggtg ccatatgcat tactggatga gcgtaccaag aagtcaaaca gggacagcct
3181 gcgggaagct gtgcgcactt ttgttggtta cgggtataac attgagccat cagaccaaga
3241 actagctgac tcggctgtgg agaaggtcag catagacaag atccgatttt tccgggtaga
3301 gcgatcttat gcagtgagat ctggaaagtg gtattttgag tttgaagtgg tgactggagg
3361 agacatgcga gtcggctggg cgaggccagg ctgtcgacct gatgtcgagc tgggggccga
3421 tgaccaagcc tttgtgtttg aaggcaacag gggccagcgt tggcatcaag gaagtgggta
3481 ttttgggcgt acctggcagc caggggatgt ggtcggatgt atgattaacc tggatgatgc
3541 ttcaatgatc ttcacactga atggggagct gctgatcacc aacaaaggct ctgaacttgc
3601 cttcgctgac tacgagattg agaatggctt cgtgcccatc tgctgtctgg gtctatctca
3661 gatcggccgc atgaatctcg ggacagatgc cagtaccttc aagttttata ccatgtgcgg
3721 tctccaagag ggctttgagc cttttgctgt caacatgaac agagatgttg ctatgtggtt
3781 cagcaagcgc ctcccgacgt ttgtcaacgt gccaaaggat catccacaca tagaggtcat
3841 gaggattgat ggcaccatgg acagccctcc gtgtctcaag gtgacgcata agacatttgg
3901 cacacagaat agcaatgccg acatgatcta ttgccgcttg agcatgcctg tcgagtgcca
3961 ctcctccttc agccacagcc cctgtctgga cagtgaagct ttccagaaaa ggaaacagat
4021 gcaagaaata ctctctcata caacaacaca gtgctactac gccatccgca tctttgctgg
4081 acaggatcca tcctgtgtct gggtcggatg ggtgactcca gactatcact tgtacagtga
4141 aaagtttgac ctgaataaaa actgcacagt gactgtcacc ctaggggatg aaagaggccg
4201 ggtccat***gaa agtgtgaaac gcagcaa***ctg ctacatggtc tggggtggag acattgtagc
4261 cagttcccag agatcaaatc ggagcaacgt ggacctggag atcggctgtc tcgtggatct
4321 ggccatgggc atgttgtcct tctcagccaa tggaaaggaa ctgggcacct gctaccaggt
4381 ggagcctaat accaaagt***gt ttccagcagt cttcctgc***ag cctacaagta cttctttgtt
4441 tcagtttgaa cttggaaagc tgaagaacgc aatgcccctg tcagcggcca tattcaggag
4501 tgaagagaag aacccagtcc cacagtgtcc acctcggctg gacgtccaaa ccatccagcc
4561 cgtgctctgg agccgcatgc ccaacagctt cctgaaggtg gagaccgagc gtgtgagcga
4621 gcgccacggc tgggtggtgc agtgcctgga gcccctgcag atgatggcgc tccacatccc
4681 cgaggagaac aggtgtgtgg atatcctgga gctctgtgag caggaggacc tgatgcggtt
4741 ccattaccac acgctgaggc tctacagcgc ggtgtgcgcc ctgggaaaca gccgcgtggc
4801 ctacgccctg tgcagccacg tggacctctc ccagctcttc tatgccattg acaacaagta
4861 cctccccggc ctccttcgat ctggtttcta tgacctgctc atcagcatcc acctggccag
4921 cgccaaggag aggaagctga tgatgaagaa cgagtacatc atccccatta ccagcaccac
4981 caggaatatc cgcctcttcc cggacgagtc caagaggcat ggactgcctg gggtgggcct
5041 gagaacatgt ctcaagcccg ggttcaggtt ctccaccccct tgctttgttg tgactggtga
5101 ggatcaccaa aagcagagcc ccgagattcc cttggagagt ctcaggacga aggctctgag
5161 tatgctgaca gaggcagtgc agtgcagcgg ggcccacatc cgagaccctg taggggggtc
5221 tgtggagttc cagtttgtgc ctgtgctgaa actcattgga accctgctgg tcatgggcgt
5281 gtttgatgat gatgatgttc ggcagatcct cctcctgatt gatccctctg tgtttgggga
5341 gcatagtgcg gggacagagg agggagcaga aaaggaggaa gtgacccagg tggaggagaa

```
5401 ggctgtggag gctggggaga aggccggcaa ggaggctcct gtcaaaggct tgttgcagac
5461 tcgattaccc gaatccgtca agctgcagat gtgtgagctc ctcagctatc tctgcgactg
5521 tgagctgcag caccgagtgg aggccattgt ggcatttggt gacatttatg tctccaagct
5581 gcaggcaaat cagaagttcc gctacaatga gctcatgcag gccctgaaca tgtctgcggc
5641 cctgactgcc cggaagacca aggagttccg ctcaccccca caggagcaga tcaacatgct
5701 gcttaacttt caactgggag agaactgccc ctgcccagag gagattcggg aggagctgta
5761 tgatttccat gaggaccttc tccttcactg tggggttcct ttggaagaag aggaagagga
5821 ggaggaggac acctcctgga caggaaaact ctgtgccttg gtttacaaaa tcaaaggccc
5881 acccaagcca gagaaggagc agccgacgga ggaggaggag agatgcccca caacattgaa
5941 ggaactcatc tcacagacga tgatctgctg ggcccaggag gaccagatcc aggattcaga
6001 gctggtccga atgatgttca acctcctccg gaggcagtat gacagcattg gggagctgct
6061 gcaggcgctg cggaagacct acaccatcag ccacacctct gtaagcgaca ccatcaacct
6121 gctggctgcc ctgggccaaa tccgctccct cctcagtgtc aggatgggca aggaagagga
6181 gttgctcatg atcaatgggc tgggagacat aatgaacaac aaggtgtttt accagcatcc
6241 caacctcatg agagtcctgg gcatgcacga gacggtgatg gaggtgatgg tgaacgtgtt
6301 gggtacagag aaatctcaga ttgcatttcc aaagatggtt gctagctgct gccgtttcct
6361 ttgctatttc tgtcgaatta gccggcaaaa tcagaaggcc atgtttgagc atctgagtta
6421 tcttctggag aatagcagtg ttggcctagc ctccccgtcg atgaggggat ccaccccgct
6481 ggatgtggca gcttcctctg tgatggacaa caatgagtta gcgctgagct tagaggaacc
6541 agacctcgag aaggtggtga cctacttggc aggctgtggc ctacagagct gccccatgct
6601 tctggccaaa ggataccctg atgtcggctg gaaccccatt gaaggggaac gctacctgtc
6661 cttcctgagg tttgctgtct tcgtgaacag tgagagtgtg gaagaaaacg ccagcgttgt
6721 ggtcaagctg ctcatcagac gcccagagtg cttcggcccg gccctgcggg gtgaggggag
6781 aaacgggctc ttggcagcca tgcagggtgc cattaagatc tctgagaacc cagcgctcga
6841 cctcccctct caaggataca aaagagaagt cagcacgggg gacgatgaag aggaagaaga
6901 aatcgtgcat atgggcaatg caattatgtc attttattcg gcccttatag atctactggg
6961 ccgctgtgct cctgaaatgc acctcatcca gacaggaaag ggggaagcca tccgcatcag
7021 gtccatcctg cgctccctgg tccccacaga agacctggtt gggatcatca gcatcccctt
7081 gaaactgccc tccctcaaca aagatgggtc ggtcagtgag ccagatatgg cggccaattt
7141 ctgccctgac cacaaggcac ctatggtgct gttcttggac cgcgtttatg gcattaagga
7201 tcaaactttt ctgctccact tgctggaggt tggattttta cctgacctaa gagcttctgc
7261 ctctctagat acagtttccc taagcaccac agaggctgcg cttgcactaa ataggtatat
7321 atgttctgct gtgctcccgc tcctcacaag atgtgcccct ctctttgccg gaacagaaca
7381 ctgcacctct ctgattgatt ccacactgca gacaatatac aggctatcca agggacgttc
7441 cctcaccaaa gcacaaaggg acactataga agaatgtttg cttgccattt gcaatcactt
7501 gaggccttcc atgttacagc aactcctgcg acgcctcgtt tttgatgtgc cgcaactcaa
7561 tgaatactgc aaaatgcctc tcaagcttct gacgaatcac tatgaacagt gttggaagta
7621 ttactgcctg ccttcaggat gggggagcta cgggctagct gtggaagaag agctgcacct
7681 aacggagaag cttttctggg ggatttttga ctcgctctcc cataagaaat atgacccaga
7741 tcttttccga atggccctgc cttgtctcag tgctatagct ggggccttgc caccagatta
7801 tttagatacc agaatcacag ccacgttgga gaaacagatc tcagtggatg cggatggcaa
7861 ctttgaccca aaacctatta acaccatgaa tttttccttg cctgaaaaat tggaatacat
7921 cgtcaccaag tatgctgagc attcacatga taaatgggcc tgtgacaaga gtcagagtgg
7981 atggaaatat gggatttccc tggatgaaaa tgtgaagacc cacccactga taaggccttt
8041 caagacatta acggagaagg agaaggaaat ttatcgctgg cctgcgcgag agtccctgaa
8101 aaccatgctg gctgtgggct ggactgtgga gaggaccaaa gagggagaag ctttggttca
8161 acagcgggaa aatgagaagc ttcgaagtgt gtcccaggcc aaccagggca acagctacag
8221 tcctgctccc ctcgacctct caaacgttgt gctctccaga gagctccagg gaatggtgga
8281 ggtcgtggct gagaactatc acaatatctg ggccaagaag aagaagctgg agctggagag
```

```
 8341 caaaggtggt ggcagccacc ctcttctggt accatatgac accttgactg ccaaggaaaa
 8401 gttcaaggac cgggagaagg cacaggacct gtttaagttc ctccaagtga atggcatcat
 8461 agtttccagg ggtatgaagg atatggagct ggatgcctcc tccatggaga agaggtttgc
 8521 ctataagttc ttgaagaaga tcctgaaata cgttgattct gctcaagaat ttattgccca
 8581 tttagaagcc attgtcagca gtgggaaaac tgaaaagtct ccccgtgacc aggagatcaa
 8641 attctttgcc aaagttctcc tcccgctggt tgaccagtac ttcaccagtc attgcctcta
 8701 cttcttgtca tcccctctga agccccttag cagcagcgga tatgcctccc ataaggagaa
 8761 agaaatggtg gccggcctgt tctgcaaact tgccgctctc gttagacaca gaatttccct
 8821 ctttggtagt gattctacta caatggtgag ctgtcttcac atcttagctc agacacttga
 8881 cacaaggact gtcatgaagt caggctcaga gctggtgaag gctgggttac gagcattctt
 8941 tgaaaatgct gcagaagatt tggagaagac ttcagaaaac ctgaaacttg ggaagttcac
 9001 ccattcccga acgcagatta aaggcgtttc tcagaatatt aactacacta cagtggctct
 9061 gctccccatc ctgacgtcca tctttgagca cgtcactcag catcagtttg gaatggatct
 9121 actcttgggt gatgtgcaga tttcatgcta ccacatactg tgcagcctct actcccttgg
 9181 gacgggaaag aacatttatg ttgaaaggca acgccctgcc cttggagaat gtctggcctc
 9241 gctggcagct gccataccag tggcattcct ggagcccacc cttaatcgct acaatccact
 9301 ctcggtcttc aacaccaaaa cccccaggga gaggtctatt ctggggatgc cagacacggt
 9361 agaagacatg tgtcctgaca tcccccagct ggaaggcctg atgaaggaaa tcaacgacct
 9421 ggccgagtca ggggcccggt acacagagat gccccatgtc atcgaggtga tcttacccat
 9481 gctctgcaac tacttgtcct actggtggga gcggggtcct gagaacctgc cccccagcac
 9541 agggccatgc tgcaccaagg tcacctctga acacctcagt ctcatcctgg gcaacattct
 9601 gaaaatcatc aacaacaacc tgggcatcga tgaggcctcc tggatgaagc gcattgcagt
 9661 gtatgcacag cccatcatca gcaaagccag gcccgacctg ctgagaagcc acttcatccc
 9721 aactctggag aagctgaaga aaaaggctgt caagacggtg caggaggagg agcagttgaa
 9781 agccgatggc aaaggggaca cccaggaggc agaactcctc atcctggacg agttcgcggt
 9841 cctctgcaga gatctctatg ccttctaccc catgctgatc cgctacgtgg acaacaacag
 9901 atctaactgg ctgaaaagtc ctgatgctga ttctgaccag ctcttccgca tggtggcaga
 9961 agtcttcatt ctgtggtgta aatctcataa cttcaagaga gaagagcaaa attttgtgat
10021 tcagaatgaa attaataatt tggcattttt aactggagac agcaaaagca agatgtcaaa
10081 agccatgcaa gtaaagtctg gaggacaaga ccaggagcgg aagaagacaa agcggcgggg
10141 agacttgtat tccatccaga cctccctcat cgtggctgca ctcaagaaaa tgctgcccat
10201 tggtttgaat atgtgtactc caggcgacca ggagctgatc tccctcgcaa aatcgcgata
10261 cagccatagg gacacagatg aagaggtcag agaacatctg cggaacaact tgcacttgca
10321 ggaaaagtct gatgacccag ctgtaaaatg gcaactgaac ctctacaagg atgttctgaa
10381 gagtgaagaa cctttcaatc cggaaaagac agtggagcgt gtgcagagaa tttcagcagc
10441 tgtcttccac ctggaacagg tggaacagcc tttgaggtcc aagaaggccg tctggcacaa
10501 actgttatca aagcaacgga aacgggcagt ggtggcctgt ttcaggatgg cccctctcta
10561 caacctgccc aggcaccgct ctattaacct cttcctccat ggctatcaga gattttggat
10621 agaaacagag gagtattcct ttgaagagaa actagtacag gatttggcta aatctccaaa
10681 ggtggaagag gaggaggagg aagagacaga aaaacaacct gacccactac atcagatcat
10741 tctctatttt agccgcaacg ctctcacgga gaggagcaaa ttggaagacg acccctttgta
10801 cacctcctat tccagcatga tggccaagag ttgtcaaagt ggtgaggatg aagaagaaga
10861 tgaagacaag gaaaaaacat tcgaagagaa agagatggag aagcaaaaaa ccctctatca
10921 gcaagctcgg ctgcatgagc gtggtgctgc agagatggtc cttcagatga taagcgctag
10981 caaaggtgag atgagcccca tggtggttga gacgctgaag ctggggatcg ccattctgaa
11041 cggaggcaat gctggtgtgc aacagaaaat gctagattac ctaaaggaga aaaaggatgc
11101 tggattcttt caaagccttt ctggtcttat gcagtcttgc agtgtccttg atttgaatgc
11161 atttgagagg cagaataaag ctgaaggcct ggggatggtg actgaagaag gaacactcat
11221 tgttcgggaa cgtggtgaaa aagtactcca gaatgacgag ttcacgcgtg atctctttag
```

```
11281 attcctacag ttactttgtg agggacataa cagtgacttt cagaacttcc tgcggactca
11341 gatgggcaac accaccaccg tgaatgtcat catcagcact gtggactacc ttctgcgtct
11401 gcaggaatca atcagtgatt tctactggta ttattcaggg aaggacatca ttgatgaatc
11461 tggacagcac aatttttcca aagctctggc agtcaccaag cagattttca attctcttac
11521 agaatacatc cagggccctt gcattggtaa tcaacagagc ctggctcaca gcaggctgtg
11581 ggacgcagtg gttggcttcc tccatgtctt tgctaatatg cagatgaaac tctctcagga
11641 ttccagtcag atcgagctgc tgaaggaact cttggatctc cttcaggaca tggtggtgat
11701 gcttctgtcc ctcctggaag ggaatgtggt aaatggcacc attggcaagc agatggttga
11761 cacactggta gaatcatcta ccaatgtaga aatgatcttg aaattctttg acatgttctt
11821 gaaacttaaa gacttaacca gctcagacac cttcaaagaa tatgacccag atggtaaagg
11881 aattatctcc aaaaaagaat tccagaaggc catggaaggg caaaaacagt acacgcagtc
11941 agagattgac tttctcctgt cgtgtgcaga agctgatgag aatgacatgt ttaattacgt
12001 tgattttgta gaccggttcc atgagccagc caaggacata gggtttaatg tggctgtgtt
12061 attgacaaat ctttctgaac acatgccaaa cgattcccgc ctgaagtgtc tgttggaccc
12121 agcagaaagt gtgctaaatt acttcgaacc ctacctagga cgcatcgaga tcatgggtgg
12181 ggccaagaag attgagcgtg tttattttga gatcagtgaa tccagtcgca ctcagtggga
12241 gaagccccag gtgaaggaat ctaagcgaca gttcattttt gatgttgtca atgaaggtgg
12301 ggagcaggaa aagatggagc tgtttgtgaa cttctgtgag gacaccatct ttgaaatgca
12361 gttagcatct cagatctctg aatccgattc agctgacagg ccagaagagg aggaagaaga
12421 tgaagattct tcttacgtgt tagaaattgc gggtgaagag gaagaagacg ggtctcttga
12481 gccggcctct gcatttgcta tggcctgtgc ctctgtgaag aggaatgtca ccgacttcct
12541 gaagagagca accctgaaga acctcaggaa gcagtacagg aacgtgaaaa agatgactgc
12601 gaaggagctg gtgaaggtgc tcttctcctt tttctggatg ctgttcgtgg ggctattcca
12661 gttgctcttc accatcctgg gaggaatctt tcagatcctc tggagcacag tgtttggagg
12721 gggcctggta gaaggggcaa agaacatcag agtgaccaag atcctgggtg acatgcctga
12781 cccaacccaa tttggtatcc atgatgacac tatggaggct gagagggcag aggtgatgga
12841 gccaggtatc accactgaac tagtacactt cataaagggg gagaagggag atacagatat
12901 catgtcagac ctctttggac tccacccaaa gaaagagggc agcttaaagc atgggcctga
12961 agtgggtttg ggtgacctct cagaaattat tggcaaggat gaacccccta cattagagag
13021 tactgtacag aagaagagga aagctcaggc agcagaaatg aaagcagcaa atgaagcaga
13081 aggaaaagta gaatccgaga aggcagacat ggaagatgga gagaaggaag acaaagacaa
13141 agaagaggag caagctgagt acctgtggac agaagtgaca aaaaagaaga agcggcggtg
13201 tggtcagaag gttgagaagc cggaagcttt cacagccaat ttctttaaag ggctggaaat
13261 ctatcagacc aagttactgc attacctggc caggaatttc tacaacctga ggttccttgc
13321 tctgtttgta gccttcgcta tcaacttcat cctgcttttt tataaggtca ctgaagaacc
13381 tttagaagaa gagacagagg atgttgcaaa cctatggaat tcctttaatg acgaggaaga
13441 ggaagaagcg atggtattct ttgtccttca ggagagcacc gggtatatgg caccaaccct
13501 gcgtgccctg gccatcatcc ataccatcat ctctctagtc tgtgtggtgg gctactactg
13561 cctgaaggtg cctttggtgg ttttcaaaag ggaaaaagaa atcgccagga agctggagtt
13621 tgatggccta tatatcaccg aacagccatc tgaagatgac atcaaggggc agtgggaccg
13681 cttggtgatc aacacaccat cttttcctaa taactactgg gacaagtttg taaagagaaa
13741 ggtgatcaac aagtatggag atctctacgg agcagaacgc attgctgaac ttctgggttt
13801 ggacaaaaat gctcttgact ttagcccagt agaagagacc aaagcagaag cggcttctct
13861 ggtgtcatgg ctaagttcca tagacatgaa gtaccatatc tggaagcttg gagttgtttt
13921 tactgacaac tcctttctct accttgcctg gtatacaacc atgtcagtcc tgggccacta
13981 caataacttc ttctttgctg ctcacctatt ggacatcgca atgggcttca agacactgag
14041 gaccattctg tcatctgtaa ctcacaatgg caaacagttg gttctgactg tcggtctcct
14101 ggccgtggtg gtttatctct atactgtggt ggctttcaac ttcttccgca agttctacaa
14161 caaaagcgaa gacgatgacg agcccgatat gaagtgcgac gacatgatga cgtgttacct
```

```
14221 tttccacatg tacgtgggag tgagagcagg aggtggcatt ggtgatgaaa ttgaagaccc
14281 tgctggtgat ccttatgaaa tgtatcgcat tgtctttgac attacctttt tcttcttcgt
14341 cattgtcatc ttgctggcca tcattcaagg tcttattatt gatgctttcg gagagctaag
14401 agaccagcag gaacaagtac gagaagatat ggagactaaa tgtttcatct gtgggattgg
14461 caatgactac tttgacacaa cccctcatgg ttttgaaaca catacattac aagagcacaa
14521 cttagccaac tacttgttct ttctgatgta tttgattaat aaagatgaaa cagagcacac
14581 gggtcaggaa tcttatgtct ggaagatgta ccaagaaagg tgttgggatt tcttcccagc
14641 cggtgactgc tttcgtaaac aatatgaaga tcagcttgga taaatctgaa tcaaagaagc
14701 gcgacaattc tggacagtca acttcccatg aaataaagtc ccctttttac agttctgcaa
14761 catatctgaa atgtgacatt ttctaaatgc ctcccttaaa aaaaaaactg ctgaaaatct
14821 gtgctatttt gaaattgatt tggctttttg tgcctaatgg acatacactg tgggagagaa
14881 cctgtcaaaa tgtcgaagaa ggaaggcgaa gaatcaagta atctctaggc aaatgccttc
14941 aagttttcca gttctgaggt aactagttca gtttgttggg atggaagcat gaaggaaagg
15001 gctagagaag tatgaaatct cgaatgtgta atacctgaaa atttaaacac ttgaatgtca
15061 tcatggtatc caacttgtga ctcatagggt ctgaactcac tccaaaagat aataactgca
15121 gtctaatttt tcccatggta cttgctagtg actgtatcca gaaaagcttt aagcagttaa
15181 agaaacagaa aaaaaccgac actttgtcga cactgaaata tcgattaagt gccttaaaac
15241 ctctttagac atagctatgc aagtttttta tgtttgtgtt ccagaaggac agttccattc
15301 attagttgtg atcttccgtc ttactttatg aaactgcact tgaaggttat tcatacaagt
15361 ttttttagta acagctgtca gtcaactgct gttattagaa gaaaagtact gtactgaaaa
15421 ttcagaaaaa aaatctcaac cttatgccaa aatggagtaa tgctttatgg tcccttgtaa
15481 gtagtggagc tgctctgttt aggtgaatct cctcaaatac aatgaagtgc ccactgcaat
15541 aaagtaatac gtaccaataa aaa
```

B. Amino acid sequence of RyRIII (data from pubmed)

MAEGGEGGEDEIQFLRTEDEVVLQCIATIHKEQRKFCLAAEGLGNRLCFLEPT
SEAKYIPPDLCVCNFVLEQSLSVRALQEMLANTGENGGEGAAQGGGHRTLLY
GHAVLLRHSFSGMYLTCLTTSRSQTDKLAFDVGLREHATGEACWWTIHPASK
QRSEGEKVRIGDDLILVSVSSERYLHLSVSNGNIQVDASFMQTLWNVHPTCSG
SSIEEGYLLGGHVVRLFHGHDECLTIPSTDQNDSQHRRIFYEAGGAGTRASSL
WRVEPLRISWSGSNIRWGQAFRLRHLTTGHYLALTEDQGLILQDRAKSDTKST
AFSFRASKELKEKLDSSHKRDIEGMGVPEIKYGDSVCFVQHIASGLWVTYKAQ
DAKTSRLGPLKRKVILHQEGHMDDGLTLQRCQREESQAARIIRNTTALFSQFV
SGNNRTAAPITLPIEEVLQTLQDLIAYFQPPEEEMRHEDKQNKLRSLKNRQNLF
KEEGMLALVLNCIDRLNIYNSVAHFAGIAREESGMAWKEILNLLYKLLAALIR
GNRNNCAQFSNNLDWLISKLDRLESSSGILEVLHCILTESPEALNLIAEGHIKSII
SLLDKHGRNHKVLDILCSLCLCNGVAVRANQNLICDNLLPRRNLLLQTRLIND
VTSIRPNIFLGVAEGSAQYKKWYFELIIDQVDPFLTAEPTHLRVGWASSSGYAP
CPGGGEGWGGNGVGDDLYSYGFDGLHLWSGRIPRAVASVNQHLLRSDDVVS
CCLDLGVPSISFRINGQPVQGMFENFNTDGLFFPVMSFSAGVKVRFLMGGRHG
EFKFLPPSGYAPCYEALLPKEKMRLEPVKEYKRDADGIRDLLGTTQFLSQASFI

PCPVDTSQVILPPHLEKIRDRLAENIHELWGMNKIELGWTFGKIRDDNKRQHP
CLVEFSKLPETEKNYNLQMSTETLKTLLALGCHIAHVNPAAEEDLKKVKLPK
NYMMSNGYKPAPLDLSDVKLLPPQEILVDKLAENAHNVWAKDRIKQGWTYG
IQQDLKNKRNPRLVPYALLDERTKKSNRDSLREAVRTFVGYGYNIEPSDQELA
DSAVEKVSIDKIRFFRVERSYAVRSGKWYFEFEVVTGGDMRVGWARPGCRPD
VELGADDQAFVFEGNRGQRWHQGSGYFGRTWQPGDVVGCMINLDDASMIFT
LNGELLITNKGSELAFADYEIENGFVPICCLGLSQIGRMNLGTDASTFKFYTMC
GLQEGFEPFAVNMNRDVAMWFSKRLPTFVNVPKDHPHIEVMRIDGTMDSPPC
LKVTHKTFGTQNSNADMIYCRLSMPVECHSSFSHSPCLDSEAFQKRKQMQEIL
SHTTTQCYYAIRIFAGQDPSCVWVGWVTPDYHLYSEKFDLNKNCTVTVTLGD
ERGRVHESVKRSNCYMVWGGDIVASSQRSNRSNVDLEIGCLVDLAMGMLSF
SANGKELGTCYQVEPNTKVFPAVFLQPTSTSLFQFELGKLKNAMPLSAAIFRSE
EKNPVPQCPPRLDVQTIQPVLWSRMPNSFLKVETERVSERHGWVVQCLEPLQ
MMALHIPEENRCVDILELCEQEDLMRFHYHTLRLYSAVCALGNSRVAYALCS
HVDLSQLFYAIDNKYLPGLLRSGFYDLLISIHLASAKERKLMMKNEYIIPITSTT
RNICLFPDESKRHGLPGVGLRTCLKPGFRFSTPCFVVTGEDHQKQSPEIPLESLR
TKALSMLTEAVQCSGAHIRDPVGGSVEFQFVPVLKLIGTLLVMGVFDDDDVR
QILLLIDPSVFGEHSAGTEEGAEKEEVTQVEEKAVEAGEKAGKEAPVKGLLQT
RLPESVKLQMCELLSYLCDCELQHRVEAIVAFGDIYVSKLQANQKFRYNELM
QALNMSAALTARKTKEFRSPPQEQINMLLNFQLGENCPCPEEIREELYDFHED
LLLHCGVPLEEEEEEEEDTSWTGKLCALVYKIKGPPKPEKEQPTEEEERCPTTL
KELISQTMICWAQEDQIQDSELVRMMFNLLRRQYDSIGELLQALRKTYTISHT
SVSDTINLLAALGQIRSLLSVRMGKEEELLMINGLGDIMNNKVFYQHPNLMRV
LGMHETVMEVMVNVLGTEKSQIAFPKMVASCCRFLCYFCRISRQNQKAMFE
HLSYLLENSSVGLASPSMRGSTPLDVAASSVMDNNELALSLEEPDLEKVVTYL
AGCGLQSCPMLLAKGYPDVGWNPIEGERYLSFLRFAVFVNSESVEENASVVV
KLLIRRPECFGPALRGEGGNGLLAAMQGAIKISENPALDLPSQGYKREVSTED
DEEEEEIVHMGNAIMSFYSALIDLLGRCAPEMHLIQTGKGEAIRIRSILRSLVPT
EDLVGIISIPLKLPSLNKDGSVSEPDMAANFCPDHKAPMVLFLDRVYGIKDQTF
LLHLLEVGFLPDLRASASLDTVSLSTTEAALALNRYICSAVLPLLTRCAPLFAG
TEHCTSLIDSTLQTIYRLSKGRSLTKAQRDTIEECLLAICNHLRPSMLQQLLRRL
VFDVPQLNEYCKMPLKLLTNHYEQCWKYYCLPSGWGSYGLAVEEELHLTEK
LFWGIFDSLSHKKYDPDLFRMALPCLSAIAGALPPDYLDTRITATLEKQISVDA
DGNFDPKPINTMNFSLPEKLEYIVTKYAEHSHDKWACDKSQSGWKYGISLDE
NVKTHPLIRPFKTLTEKEKEIYRWPARESLKTMLAVGWTVERTKEGEALVQQ

RENEKLRSVSQANQGNSYSPAPLDLSNVVLSRELQGMVEVVAENYHNIWAK
KKKLELESKGGGSHPLLVPYDTLTAKEKFKDREKAQDLFKFLQVNGIIVSRGM
KDMELDASSMEKRFAYKFLKKILKYVDSAQEFIAHLEAIVSSGKTEKSPRDQEI
KFFAKVLLPLVDQYFTSHCLYFLSSPLKPLSSSGYASHKEKEMVAGLFCKLAA
LVRHRISLFGSDSTTMVSCLHILAQTLDTRTVMKSGSELVKAGLRAFFENAAE
DLEKTSENLKLGKFTHSRTQIKGVSQNINYTTVALLPILTSIFEHVTQHQFGMD
LLLGDVQISCYHILCSLYSLGTGKNIYVERQRPALGECLASLAAAIPVAFLEPTL
NRYNPLSVFNTKTPRERSILGMPDTVEDMCPDIPQLEGLMKEINDLAESGARY
TEMPHVIEVILPMLCNYLSYWWERGPENLPPSTGPCCTKVTSEHLSLILGNILKI
INNNLGIDEASWMKRIAVYAQPIISKARPDLLRSHFIPTLEKLKKKAVKTVQEE
EQLKADGKGDTQEAELLILDEFAVLCRDLYAFYPMLIRYVDNNRSNWLKSPD
ADSDQLFRMVAEVFILWCKSHNFKREEQNFVIQNEINNLAFLTGDSKSKMSK
AMQVKSGGQDQERKKTKRRGDLYSIQTSLIVAALKKMLPIGLNMCTPGDQEL
ISLAKSRYSHRDTDEEVREHLRNNLHLQEKSDDPAVKWQLNLYKDVLKSEEP
FNPEKTVERVQRISAAVFHLEQVEQPLRSKKAVWHKLLSKQRKRAVVACFR
MAPLYNLPRHRSINLFLHGYQRFWIETEEYSFEEKLVQDLAKSPKVEEEEEEET
EKQPDPLHQIILYFSRNALTERSKLEDDPLYTSYSSMMAKSCQSGEDEEEDED
KEKTFEEKEMEKQKTLYQQARLHERGAAEMVLQMISASKGEMSPMVVETLK
LGIAILNGGNAGVQQKMLDYLKEKKDAGFFQSLSGLMQSCSVLDLNAFERQN
KAEGLGMVTEEGTLIVRERGEKVLQNDEFTRDLFRFLQLLCEGHNSDFQNFLR
TQMGNTTTVNVIISTVDYLLRLQESISDFYWYYSGKDIIDESGQHNFSKALAVT
KQIFNSLTEYIQGPCIGNQQSLAHSRLWDAVVGFLHVFANMQMKLSQDSSQIE
LLKELLDLLQDMVVMLLSLLEGNVVNGTIGKQMVDTLVESSTNVEMILKFFD
MFLKLKDLTSSDTFKEYDPDGKGIISKKEFQKAMEGQKQYTQSEIDFLLSCAE
ADENDMFNYVDFVDRFHEPAKDIGFNVAVLLTNLSEHMPNDSRLKCLLDPAE
SVLNYFEPYLGRIEIMGGAKKIERVYFEISESSRTQWEKPQVKESKRQFIFDVV
NEGGEQEKMELFVNFCEDTIFEMQLASQISESDSADRPEEEEEDEDSSYVLEIA
GEEEEDGSLEPASAFAMACASVKRNVTDFLKRATLKNLRKQYRNVKKMTAK
ELVKVLFSFFWMLFVGLFQLLFTILGGIFQILWSTVFGGGLVEGAKNIRVTKIL
GDMPDPTQFGIHDDTMEAERAEVMEPGITTELVHFIKGEKGDTDIMSDLFGLH
PKKEGSLKHGPEVGLGDLSEIIGKDEPPTLESTVQKKRKAQAAEMKAANEAE
GKVESEKADMEDGEKEDKDKEEEQAEYLWTEVTKKKKRRCGQKVEKPEAFT
ANFFKGLEIYQTKLLHYLARNFYNLRFLALFVAFAINFILLFYKVTEEPLEEETE
DVANLWNSFNDEEEEEAMVFFVLQESTGYMAPTLRALAIIHTIISLVCVVGYY
CLKVPLVVFKREKEIARKLEFDGLYITEQPSEDDIKGQWDRLVINTPSFPNNY

WDKFVKRKVINKYGDLYGAERIAELLGLDKNALDFSPVEETKAEAASLVSWL
SSIDMKYHIWKLGVVFTDNSFLYLAWYTTMSVLGHYNNFFFAAHLLDIAMGF
KTLRTILSSVTHNGKQLVLTVGLLAVVVYLYTVVAFNFFRKFYNKSEDDDEP
DMKCDDMMTCYLFHMYVGVRAGGGIGDEIEDPAGDPYEMYRIVFDITFFFFV
IVILLAIIQGLIIDAFGELRDQQEQVREDMETKCFICGIGNDYFDTTPHGFETHTL
QEHNLANYLFFLMYLINKDETEHTGQESYVWKMYQERCWDFFPAGDCFRKQ
YEDQLG

References

Akita T & Kuba K (2000). Functional triads consisting of ryanodine receptors, Ca^{2+} channels, and Ca^{2+}-activated K^+ channels in bullfrog sympathetic neurons - plastic modulation of action potential. J. Gen. Physiol., 116**,** 697 - 720.

Alarcón JM, Brito JA, Hermosilla T, Atwater I, Mears D & Rojas E (2006). Ion channel formation by Alzheimer's disease amyloid β-peptide (aβ40) in unilamellar liposomes is determined by anionic phospholipids. Piptides, 27**,** 95 - 104.

Alexander SPH, Mathie A & Peter JA (2009). Guide to receptors and channels (GRAC). Br. J. Pharmacol., 158**,** 1 - 254.

Alford S, Frenguelli BG, Schofield JG & Collingridge GL (1993). Characterization of Ca^{2+} signals induced in hippocampal ca1 neurones by the synaptic activation of nmda receptors. J. Physiol. (Lond). 469**,** 693 - 716.

Allen TGJ & Brown DA (2003). Modulation of the excitability of cholinergic basal forebrain neurones by K_{ATP} channels. The Journal of Physiology, 554**,** 353 - 370.

Andrews PW (1984). Retinoic acid induces neuronal differentiation of a cloned human embryonal carcinoma cell line in vitro. Dev. Biol., 103**,** 285 - 293.

Angulo E, Noé V, Casadó V, Mallol J, Gomez-Isla T, Lluis C, *et al.* (2004). Up-regulation of the $K_v3.4$ potassium channel subunit in early stages of Alzheimer's disease. J. Neurochem., 91**,** 547 - 557.

Ankarcrona M, Dypbukt JM, Bonfoco E, Zhivotovsky B, Orrenius S, Lipton SA, *et al.* (1995). Glutamate-induced neuronal death: A succession of necrosis or apoptosis depending on mitochondrial function. Neuron, 15**,** 961 - 973.

Arispe N, Diaz JC & Simakova O (2007). Aβ ion channels. Prospects for treating Alzheimer's disease with Aβ channel blockers. Biochim. Biophys. Acta, 1768**,** 1952 - 1965.

Barltrop JA, Owen TC, Cory AH & Cory JG (1991). 5-(3-carboxymethoxyphenyl)-2-(4,5-dimenthylthiazolyl)-3-(4-sulfophenyl) tetrazolium, inner salt (MTS) and related analogs of 3-(4,5-dimenthylthiazolyl)-2,5-diphenyltetrazolium bromide (MTT) reducing to purple water-soluble formazans as cell-viability indicators. Bioorganic & Medicinal Chemistry Letters, 1(11): 611-614.

Bautista L, Castro MJ, López-Barneo J & Castellano A (2009). Hypoxia inducible factor-2α stabilization and maxi-K^+ channel β_1-subunit gene repression by

hypoxia in cardiac myocytes. Circ. Res., 104**,** 1364 - 1372.

Bazan NG, Palacios-Pelaez R & Lukiw WJ (2002). Hypoxia signaling to genes - significance in Alzheimer's disease. Mol. Neurobiol., 26**,** 283 - 298.

Berridge MJ (2010). Calcium hypothesis of Alzheimer's disease. Pflügers Arch - European Journal of Physiology, 459**,** 441 - 449.

Bezprozvanny I (2005). The inositol 1,4,5-trisphosphate receptors. Cell Calcium, 38**,** 261-272.

Bhat MB & Ma J (2002). The transmembrane segment of ryanodine receptor contains an intracellular membrane retention signal for Ca^{2+} release channel. The Journal of Biological Chemistry, 277**,** 8597 - 8601.

Bickler PE, Fahlman CS, Gray J & Mckleroy W (2009). Inositol 1,4,5-triphosphate receptors and NAD(P)H mediate $Ca(^{2+})$ signaling required for hypoxic preconditioning of hippocampal neurons. Neuroscience, 160**,** 51-60.

Boraso A & Williams AJ (1994). Modification of gating of the cardiac sarcoplasmic reticulum Ca^{2+}-release channel by H_2O_2 and dithiothreitol. Am. J. Physiol., 267**,** H1010 - H1016.

Brini M (2003). Ca^{2+} signalling in mitochondria: Mechanism and role in physiology and pathology. Cell Calcium, 34**,** 399 - 405.

Burg ED, Remillard CV & Yuan JX-J (2006). K^+ channels in apoptosis. The Journal of Membrane Biology, 209**,** 3 - 20.

Burgos C, Carrodeguas JA, Moreno C, Sánchez AC, Tarrafeta L, Barcelona JA, *et al.* (2005). A real time PCR (RT-PCR) alternative assay to detect the t/c mutation in position 1843 of the ryanodine receptor gene. Meat Science, 70**,** 395 - 398.

Calabrese EJ, Bachmann KA, Bailer AJ, Bolger PM, Borak J, Cai L, *et al.* (2007). Biological stress response terminology: Integrating the concepts of adaptive response and preconditioning stress within a hormetic dose-response framework. Toxicol. Appl. Pharmacol., 222**,** 122-128.

Chapman H, Piggot C, Andrews PW & Wann KT (2007). Characterisation of large-conductance calcium-activated potassium channels (BK_{ca}) in human NT2-N cells. Brain Res., 1129**,** 15 - 25.

Chen SRW & Maclennan DH (1994). Identification of calmodulin-, Ca^{2+}-, and ruthenium red-binding domains in the Ca^{2+} release channel (ryanodine receptor) of rabbit skeletal muscle sarcoplasmic reticulum. The Journal of Biological Chemistry, 269**,** 22698 - 22704.

Chen X, Wu J, Lvovskaya S, Herndon E, Supnet C & Bezprozvanny I (2011).

Dantrolene is neuroprotective in Huntington's disease transgenic mouse model. Molecular Neurodegeneration, 6**,** 1 - 12.

Chong ZZ, Li F & Maiese K (2007). Cellular demise and inflammatory microglial activation during β-amyloid toxicity are governed by wnt1 and canonical signaling pathways. Cell. Signal., 19**,** 1150 - 1162.

Coles B, Wilton LaK, Good M, Chapman PF & Wann KT (2008). Potassium channels in hippocampal neurones are absent in a transgenic but not in a chemical model of Alzheimer's disease. Brain Res., 1190 1 - 14.

Dolga A, Terpolilli N, Kepura F, Nijholt I, Knaus H-G, D'orsi B, *et al.* (2011). $K_{ca}2$ channels activation prevents $[Ca^{2+}]_i$ deregulation and reduces neuronal death following glutamate toxicity and cerebral ischemia. Cell Death and Disease, 2**,** 1 - 10.

Dreses-Werringloer U, Lambert J-C, Vingtdeux V, Zhao H, Vais H, Siebert A, *et al.* (2008). A polymorphism in calhm1 influences Ca^{2+} homeostasis, Aβ levels, and Alzheimer's disease risk. Cell, 133**,** 1149 - 1161.

Egea J, Rosa AO, Cuadrado A, García AG & López MG (2007). Nicotinic receptor activation by epibatidine induces heme oxygenase-1 and protects chromaffin cells against oxidative stress. J. Neurochem., 102**,** 1842 - 1852.

Endo M (1977). Calcium release from the sarcoplasmic reticulum. Physiol. Rev., 57**,** 71 - 108.

Fernyhough P & Calcutt NA (2010). Abnormal calcium homeostasis in peripheral neuropathies. Cell Calcium, 47**,** 130-139.

Floyd RA (1999). Antioxidants, oxidative stress and degenerative neurological disorders. Exp. Biol. Med., 222**,** 236 - 245.

Floyd RA & Hensley K (2002). Oxidative stress in brain aging implications for therapeutics of neurodegenerative diseases. Neurobiol. Aging, 23**,** 795 - 807.

Folin M, Baiguera S, Tommasini M, Guidolin D, Conconi MT, Decarlo E, *et al.* (2005). Effects of β-amyloid on rat neuromicrovascular endothelial cells cultured in vitro. Int. J. Mol. Med., 15**,** 929 - 935.

Foskett JK, White C, Cheung K-H & Mak D-OD (2007). Inositol trisphosphate receptor Ca^{2+} release channels. Physiol. Rev., 87**,** 593-658.

Freshney RI 1994. *Culture of animal cells,* New York, Wiley-Liss, Inc.

Fülöp L, Zarándi M, Datki Z, Soós K & Penke B (2004). B-amyloid-derived pentapeptide $riigl_a$ inhibits $A\beta_{1-42}$ aggregation and toxicity. Biochem. Biophys. Res. Commun., 324**,** 64 - 69.

Furuichi T, Furutama D, Hakamata Y, Nakai J, Takeshima H & Mikoshiba K (1994). Multiple types of ryanodine receptor/Ca^{2+} release channels are differentially expressed in rabbit brain. The Journal of Neuroscience, 14**,** 4794 - 4805.

Garaschuk O, Yaari Y & Konnerth A (1997). Release and sequestration of calcium by ryanodine-sensitive stores in rat hippocampal neurones. J. Physiol. (Lond). 502**,** 13 - 30.

Gasperi RD, Sosa MaG, Dracheva S & Elder GA (2010). Presenilin-1 regulates induction of hypoxia inducible factor-1α: Altered activation by a mutation associated with familial Alzheimer's disease. Molecular Neurodegeneration, 5**,** 1 - 20.

George CH, Jundi H, Thomas NL, Scoote M, Walters N, Williams AJ, *et al.* (2004). Ryanodine receptor regulation by intramolecular interaction between cytoplasmic and transmembrane domains. Mol. Biol. Cell, 15**,** 2627 - 2638.

Giannini G, Conti A, Mammarella S, Scrobogna M & Sorrentino V (1995). The ryanodine receptor/calcium channel genes are widely and differentially expressed in murine brain and peripheral tissues. The Journal of Cell Biology, 128**,** 893 - 904.

Good TA & Murphy RM (1996). Effect of β-amyloid block of the fast-inactivating K^+ channel on intracellular Ca^{2+} and excitability in a modeled neuron. Proc. Natl. Acad. Sci. USA, 93**,** 15130 - 15135.

Goodman Y & Mattson MP (1996). K^+ channel openers protect hippocampal neurons against oxidative injury and amyloid β-peptide toxicity. Brain Res., 706**,** 328 - 332.

Green KN, Demuro A, Akbari Y, Hitt BD, Smith IF, Parker I, *et al.* (2008). Serca pump activity is physiologycally regulated by presenilin and regulates amyloid β production. J. Cell Biol., 181**,** 1107 - 1116.

Gribkoff VK, Lum-Ragan JT, Boissard CG, Post-Munson DJ, Meanwell NA, Starrettjr JE, *et al.* (1996). Effects of channel modulators on cloned large-conductance calcium-activated potassium channels. Mol. Pharmacol., 50**,** 506 - 217.

Gribkoff VK, Starrettjr JE, Dworetzky SI, Hewawasam P, Boissard CG, Cook DA, *et al.* (2001). Targeting acute ischemic stroke with a calcium-sensitive opener of maxi-K potassium channels. Nat. Med., 7**,** 471 - 477.

Grievink H & Stowell KM (2008). Identification of ryanodine receptor 1 single-nucleotide polymorphisms by high-resolution melting using the lightcycler

480 system. Anal. Biochem., 374**,** 396 - 404.

Gustavsson A, Svensson M, Jacobi F, Allgulander C, Alonso J, Beghi E, *et al.* (2011). Cost of disorders of the brain in europe 2010. Eur. Neuropsychopharmacol., 21**,** 718 - 779.

Hakamata Y, Nakai J, Takeshima H & Imoto K (1992). Primary structure and distribution of a novel ryanodine receptor/calcium release channel from rabbit brain. FEBS Lett., 312**,** 229 - 235.

Harvey AL & Robertson B (2004). Dendrotoxins: Structure-activity relationships and effects on potassium ion channels. Curr. Med. Chem., 11**,** 3065-3072.

Henney NC. 2008. *The expression and characteristics of ion channels in osteoblasts: Putative roles for TRP and K^+ channels.* Philosophiæ Doctor, Cardiff University.

Henney NC, Li B, Elford C, Reviriego P, Campbell AK, Wann KT, *et al.* (2009). A large-conductance (BK) potassium channel subtype affects both growth and mineralization of human osteoblasts. Am. J. Physiolo. Cell Physiol., 297**,** 1397 - 1408.

Héron-Milhavet L, Xue-Jun Y, Vannucci SJ, Wood TL, Willing LB, Stannard B, *et al.* (2004). Protection against hypoxic-ischemic injury in transgenic mice overexpressing $K_{ir}6.2$ channel pore in forebrain. Mol. Cell. Neurosci., 25**,** 585 - 593.

Ho K, Nichols CG, Lederer WJ, Lytton J, Vassilev PM, Kanazirska MV, *et al.* (1993). Cloning and expression of an inwardly retifying ATP-regulated potassium channel. Nature, 362**,** 31 - 38.

Hogg RC & Adams DJ (2001). An ATP-sensitive K^+ conductance in dissociated neurones from adult rat intracardiac ganglia. J. Physiol. (Lond). 534**,** 713 - 720.

Hohenegger M, Suko J, Gscheidlinger R, Drobny H & Zidar A (2002). Nicotinic acid-adenine dinucleotide phosphate activates the skeletal muscle ryanodine receptor. Biochem. J., 367**,** 423 - 431.

Holtzman DM (2004). In vivo effects of apoe and clusterin an amyloid-β metabolism and neuropathology. J. Mol. Neurosci., 23**,** 247 - 254.

Hosoi E, Nishizaki C, Gallagher KL, Wyre HW, Matsuo Y & Sei Y (2001). Expression of the ryanodine receptor isofirms in immune cells. The Journal of Immunology, 167**,** 4887 - 4894.

Humerickhouse RA, Besch HR, Gerzon K, Ruest L, Sutko JL & Emmick JT (1993).

Differential activating and deactivating effects of natural ryanodine congeners on the calcium release channel of sarcoplasmic reticulum: Evidence for separation of effects at functionally distinct sites. Mol. Pharmacol., 44**,** 412 - 421.

Humerickhouse RA, Bidasee KR, Gerzon K, Emmick JT, Kwon S, Sutko JL, *et al.* (1994). High affinity C_{10}-O_{eq} ester derivatives of ryanodine - activator-selective agonists of the sarcoplasmic reticulum calcium release channel. The Journal of Biological Chemistry, 269**,** 30243 - 30253.

Hunya Á, Földi I, Szegedi V, Soós K, Zarándi M, Szabó A, *et al.* (2008). Difference between normal and alpha-synuclein overexpressing SH-SY5Y neuroblastoma cells after Aβ(1-42) and nac treatment. Brain Res. Bull., 75**,** 648 - 654.

Ishimura A, Ishige K, Taira T, Shimba S, Ono S-I, Ariga H, *et al.* (2008). Comparative study of hydrogen peroxide- and 4-hydroxy-2-nonenal-induced cell death in HT22 cells. Neurochem. Int., 52**,** 776 - 785.

Jämsä A, Hasslund K, Cowburn RF, Bäckström A & Vasänge M (2004). The retinoic acid and brain-derived neurotrophic factor differentiated SH-SY5Y cell line as a model for Alzheimer's disease-like tau phosphorylation. Biochem. Biophys. Res. Commun., 319**,** 993 - 1000.

Jang H, Arce FT, Ramachandran S, Capone R, Azimova R, Kagan BL, *et al.* (2010). Truncated β-amyloid peptide channels provide an alternative mechanism for Alzheimer's disease and Down syndrome. PNAS, 107**,** 6538 - 6543.

Jolly-Tornetta C, Gao Z-Y, Lee VM-Y & Wolf BA (1998). Regulation of amyloid precursor protein secretion by glutamate receptors in human NTera 2 neurons (NT2N). The Journal of Biological Chemistry, 273**,** 14015 - 14021.

Joshi S, Guleria RS, Pan J, Dipette D & Singh US (2007). Heterogeneity in retinoic acid signaling in neuroblastomas: Role of matrix metalloproteinases in retinoic acid-induced differentiation. Biochim. Biophys. Acta, 1772**,** 1093 - 1102.

Kagan BL, Hirakura Y, Azimov R, Azimova R & Lin M-C (2002). The channel hypothesis of Alzheimer's disease: Current status. Peptides, 23**,** 1311 - 1315.

Kajkowski EM, Lo CF, Ning X, Walker S, Sofia HJ, Wang W, *et al.* (2001). B-amyloid peptide-induced apoptosis regulated by a novel protein containing a G protein activation module. The Journal of Biological Chemistry, 276**,** 18748 - 18756.

Kanichai M, Ferguson D, Prendergast PJ & Campbell VA (2008). Hypoxia promotes

chondrogenesis in rat mesenchymal stem cells: A role for akt and hypoxia-inducible factor (HIF)-1α. J. Cell. Physiol., 216**,** 708 - 715.

Kar S (2002). Role of amyloid beta peptides in the regulation of central cholinergic function and its relevance to Alzheimer's disease pathology. Drug Dev. Res., 56**,** 248-263.

Kar S, Issa AM, Seto D, Auld DS, Collier B & Quirion R (1998). Amyloid beta-peptide inhibits high-affinity choline uptake and acetylcholine release in rat hippocampal slices. J. Neurochem., 70**,** 2179-2187.

Kato BM & Rubel EW (1999). Glutamate regulates IP_3-type and CICR stores in the avian cochlear nucleus. J. Neurophysiol., 81**,** 1587 - 1596.

Kelliher M, Fastbom J, Cowburn RF, Bonkale W, Ohm TG, Ravid R, *et al.* (1999). Alterations in the ryanodine receptor calcium release channel correlate with Alzheimer's disease neurofibrillary and β-amyloid pathologies. Neuroscience, 92**,** 499 - 513.

Khudheyer M. 2010. *A comparative study of the effects of cellular stresses on astrocyte and neuronal cell survival.* Master of Pharmacy, Cardiff University.

Kimball BC, Yule DI & Mulholland MW (1996). Caffeine- and ryanodine-sensitive Ca^{2+} stores in cultured guinea pig myenteric neurons. Am. J. Physiol., 270**,** G594 - G603.

Krebs B, Wiebelitz A, Balitzki-Korte B, Vassallo N, Paluch S, Mitteregger G, *et al.* (2007). Cellular prion protein modulates the intracellular calcium response to hydrogen peroxide. J. Neurochem., 100**,** 358 - 367.

Kruman, Ii, Pedersen WA, Springer JE & Mattson MP (1999). Als-linked Cu/Zn-SOD mutation increases vulnerability of motor neurons to excitotoxicity by a mechanism involving increased oxidative stress and perturbed calcium homeostasis. Exp. Neurol., 160**,** 28-39.

Lafon-Cazal M, Pietri S, Culcasi M & Bockaert J (1993). NMDA-dependent superoxide production and neurotoxicity. Nature, 364**,** 535 - 537.

Laifenfeld D, Klein E & Ben-Shachar D (2002). Norepinephrine alters the expression of genes involved in neuronal sprouting and differentiation: Relevance for major depression and antidepressant mechanisms. J. Neurochem., 83**,** 1054 - 1064.

Lal R, Lin H & Quist AP (2007). Amyloid beta ion channel: 3D structure and relevance to amyloid channel paradigm. Biochim. Biophys. Acta, 1768**,** 1966 - 1975.

Laver DR (2007). Ca^{2+} stores regulate ryanodine receptor Ca^{2+} release channels via luminal and cytosolic Ca^{2+} sites. Clin. Exp. Pharmacol. Physiol., 34**,** 889 - 896.

Lee EB, Skovronsky DM, Abtahian F, Doms RW & Lee VM-Y (2003). Secretion and intracellular generation of truncated Aβ in β-site amyloid-β precursor protein-cleaving enzyme expressing human neurons. The Journal of Biological Chemistry, 278**,** 4458 - 4466.

Lessard CB, Lussier MP, Cayouette S, Bourque G & Boulay G (2005). The overexpression of presenilin2 and Alzheimer's-disease-linked presenilin2 variants influences TRPC6-enhanced Ca^{2+} entry into HEK293 cells. Cell. Signal., 17**,** 437 - 445.

Liao Y, Kristiansen A-M, Oksvold CP, Tuvnes FA, Gu N, Rundén-Pran E, *et al.* (2010). Neuronal Ca^{2+}-activated K^{+} channels limit brain infarction and promote survival. PLoS ONE, 5**,** 1 - 8.

Lin H, Bhatia R & Lal R (2001). Amyloid β protein forms ion channels: Implications for Alzheimer's disease pathophysiology. The FASEB Journal, 15**,** 2433 - 2444.

Lin MT & Beal MF (2006). Mitochondrial dysfunction and oxidative stress in neurodegenerative diseases. Nature, 443**,** 787 - 795.

Liu D, Lu C, Wan R, Auyeung WW & Mattson MP (2002). Activation of mitochondrial ATP-dependent potassium channels protects neurons against ischemia-induced death by a mechanism involving suppression of bax translocation and cytochrome c release. J. Cereb. Blood Flow Metab., 22**,** 431 - 443.

Liu D, Slevin JR, Lu CB, Chan SL, Hansson M, Elmer E, *et al.* (2003). Involvement of mitochondrial K^{+} release and cellular efflux in ischemic and apoptotic neuronal death. J. Neurochem., 86**,** 966-979.

Lovat PE, Irving H, Margherita, Annicchiarico-Petruzzelli, Bernassola F, Malcolm AJ, *et al.* (1997). Apoptosis of N-type neuroblastoma cells after differentiation with 9-cis-retinoic acid and subsequent washout. Journal of National Cancer Institute, 89**,** 446 - 452.

Macdonald JF, Xiong ZG & Jackson MF (2006). Paradox of Ca^{2+} signaling, cell death and stroke. Trends Neurosci., 29**,** 75-81.

Mak DOD, Mcbride S & Foskett JK (1998). Inositol 1,4,5-tris-phosphate activation of inositol tris-phosphate receptor Ca^{2+} channel by ligand tuning of Ca^{2+} inhibition. Proc. Natl. Acad. Sci. U. S. A., 95**,** 15821-15825.

Makarewicz D, Ziemińska E & Łazarewicz JW (2003). Dantrolene inhibits nmda-induced ^{45}Ca uptake in cultured cerebellar granule neurons. Neurochem. Int., 43**,** 273 - 278.

Manunta MDI. 2000. *Functional properties of RyR3 - Ca^{2+} release channel, of native, expressed and tagged isoforms.* Doktors der Naturwissenschaften Dissertation, Johannes Kepler Universität.

Mattson MP (1989). Acetylcholine potentiates glutamate-induced neurodegeneration incultured hippocampal neurons. Brain Res., 497**,** 402 - 406.

Mattson MP (2003). Excitotoxic and excitoprotective mechanisms - abundant targets for the prevention and treatment of neurodegenerative disorders. Neuromolecular Med., 3**,** 65-94.

Mattson MP (2007). Calcium and neurodegeneration. Aging Cell, 6**,** 337 - 350.

Mattson MP, Gleichmann M & Cheng A (2008). Mitochondria in neuroplasticity and neurological disorders. Neuron, 60**,** 748-766.

Mattson MP & Kater SB (1989). Development and selective neurodegeneration in cell cultures from different hippocampal regions. Brain Res., 490**,** 110 - 125.

Mattson MP & Magnus T (2006). Ageing and neuronal vulnerability. Nature Reviews Neuroscience, 7**,** 278-294.

Matyash M, Matyash V, Nolte C, Sorrentino V & Kettenmann H (2002). Requirement of functional ryanodine receptor type 3 for astrocyte migration. The FASEB Journal, 16**,** 84 - 86.

Meera P, Wallner M & Toro L (2000). A neuronal β subunit (KCNMB4) makes the large conductance, voltage- and Ca^{2+}-activated K^+ channel resistant to charybdotoxin and iberiotoxin. PNAS, 97**,** 5562 - 5567.

Mori F, Okada M, Tomiyama M, Kaneko S & Wakabayashi K (2005). Effects of ryanodine receptor activation on neurotransmitter release and neuronal cell death following kainic acid-induced status epilepticus. Epilepsy Res., 65**,** 59 - 70.

Mulder J, Berghuis P, Cate BT & Luiten PGM 2003. Improved method to investigate β-amyloid toxicity in rat primary cholinergic culture. *In:* NEUROSCIENCE, S. O. (ed.) *33rd Annual Meeting of the Society of Neuroscience.* New Orleans, LA, USA: Society for Neuroscience Abstract View and Itinery Planner.

Nixon RA (2003). The calpains in aging and aging-related diseases. Ageing Research Reviews, 2**,** 407 - 418.

Obata T & Yamanaka Y (2000). Block of cardiac atp-sensitive K^+ channels reduces

hydroxyl radicals in the rat myocardium. Arch. Biochem. Biophys., 378**,** 195 - 200.

Olesen S-P, Munch E, Moldt P & Drejer J (1994). Selective activation of Ca^{2+}-dependent K^+ channels by novel benzimidazolone. Eur. J. Pharmacol., 251**,** 53 - 59.

Orio P, Rojas P, Ferreira G & Latorre R (2002). New disguises for an old channel: Maxik channel β-subunits. News Physiol. Sci., 17**,** 156 - 161.

Papassotiriou J, Köhler R, Prenen J, Krause H, Akbar M, Eggermont J, *et al.* (2000). Endothelial K^+ channel lacks the Ca^{2+} sensitivity-regulating β subunit. The FASEB Journal, 14**,** 885 - 894.

Parker I, Choi J & Yao Y (1996). Elementary events of InsP(3)-induced Ca^{2+} liberation in xenopus oocytes: Hot spots, puffs and blips. Cell Calcium, 20**,** 105-121.

Parri HR & Crunelli V (2003). The role of Ca^{2+} in the generation of spontaneous astrocytic Ca^{2+} oscillations. Neuroscience, 120**,** 979 - 992.

Plant LD, Boyle JP, Smith IF, Peer C & Pearson HA (2003). The production of amyloid β peptide is a critical requirement for the viability of central neurons. The Journal of Neuroscience, 23**,** 5531 - 5535.

Prilipko L 2004. Neurological atlas. *Country resources for neurological disorders.* Geneva: World Health Organisation, World Federation Neurology.

Pugh N, Mead-Savery FC, Coadwell WJ, Rossi D, Sorrentino V & Williams AJ (2005). Probing luminal negative charge in the type 3 ryanodine receptor. Biochem. Biophys. Res. Commun., 337**,** 1072 - 1079.

Qahwash IM, Boire A, Lanning J, Krausz T, Pytel P & Meredith SC (2007). Site-specific effects of peptide lipidation on β-amyloid aggregation and cytotoxicity. The Journal of Biological Chemistry, 282**,** 36987 - 36997.

Reviriego P. 2009. *Engineering aequorin as an indicator of calcium signals near the BK channel.* Philosophiae Doctor, Cardiff University.

Robitaille R & Charlton MP (1992). Presynaptic calcium signals and transmitter release are modulated by calcium-activated potassium channels. The Journal of Neuroscience, 12**,** 297 - 305.

Rogers EF, Koniuszy FR, Shavel J & Folkers K (1948). Plant insecticides. I. Ryanodine, a new alkaloid from ryania speciosa vahl. J. Am. Chem. Soc., 70**,** 3086 - 3088.

Roher AE, Palmer KC, Yurewicz EC, Ball MJ & Greenberg BD (1993).

Morphological and biochemical analyses of amyloid plaque core proteins purified from Alzheimer's dissease brain tissue. J. Neurochem., 61**,** 1916 - 1928.

Rong Y-P, Aromolaran AS, Bultynck G, Zhong F, Li X, Mccoll K, *et al.* (2008). Targeting Bcl-2-IP_3 receptor interaction to reverse Bcl-2's inhibition of apoptotic calcium signals. Mol. Cell, 31**,** 255 - 265.

Rootwelt T, Dunn M, Yudkoff M, Itoh T, Almaas R & Pleasure D (1998). Hypoxic cell death in human NT2-N neurons: Involvement of nmda and non-NMDA glutamate receptors. Joournal of Neurochemistry, 71**,** 1544 - 1553.

Rosa R, Sanfeliu C, Rodríguez-Farré E, Frandsen A, Schousboe A & Suñol C (1997). Properties of ryanodine receptor in cultured cerebellar granule neurons: Effects of hexachlorocyclohexane isomers and calcium. J. Neurosci. Res., 47**,** 27 - 33.

Ross RA, Spengler BA & Biedler JL (1983). Coordinate morphological and biochemical interconversion of human neuroblastoma cells. J. Natl. Cancer Inst., 71**,** 741 - 747.

Rybalchenko V, Hwang S-Y, Rybalchenko N & Koulen P (2008). The cytosolic N-terminus of presenilin-1 potentiates mouse ryanodine receptro single channel activity. The International Journal of Biochemistry & Cell Biology, 40**,** 84 - 97.

Samsó M, Wagenknecht T & Allen PD (2005). Internal structure and visualization of transmembrane domains of the RyR1 calcium release channel by cryo-EM. Nat. Struct. Mol. Biol., 12**,** 539 - 544.

Sharma MR, Jeyakumar LH, Fleischer S & Wagenknecht T (2000). Three-dimensional structure of ryanodine receptor isoform three in two conformational states as visualized by cryo-electron microscopy. The Journal of Biological Chemistry, 275**,** 9485 - 9491.

Sheehan JP, Swerdlow RH, Parker WD, Miller SW, Davis RE & Tuttle JB (1997). Altered calcium homeostasis in cells transformed by mitochondria from individuals with Parkinson's disease. J. Neurochem., 68**,** 1221-1233.

Shoshan-Barmatz V, Orr I, Martin C & Vardi N (2005). Novel ryanodine-binding properties in mammalian retina. The International Journal of Biochemistry & Cell Biology, 37**,** 1681 - 1695.

Silva HaD, Aronson JK, Grahame-Smith DG, Jobst KA & Smith AD (1998). Abnormal function of potassium channels in platelets of patients with

Alzheimer's disease. Lancet, 352.

Smith IF, Hitt B, Green KN, Oddo S & Laferla FM (2005). Enhanced caffeine-induced Ca^{2+} release in the 3xTg-AD mouse model of Alzheimer's disease. J. Neurochem., 94**,** 1711 - 1718.

Sorrentino V (1995). The ryanodine receptor family of intracellular calcium release channels. Adv. Pharmacol., 33**,** 67 - 90.

Spillantini MG 2011. Inflammation, astrocytes and tau related neurodegeneration. *In:* BRAIN REPAIR CENTRE, U. O. C. (ed.) *Cambridge Centre for Brain Repair Spring School.* Cambridge, UK.

Stutzmann GE & Mattson MP (2011). Endoplasmic reticulum Ca^{2+} handling in excitable cells in health and disease. Pharmacol. Rev., 63**,** 700 - 727.

Stutzmann GE, Smith I, Caccamo A, Oddo S, Laferla FM & Parker I (2006a). Enhanced ryanodine receptor recruitment contributes to Ca^{2+} disruptions in yound, adult, and aged Alzheimer's disease mice. The Journal of Neuroscience, 26**,** 5180 - 5189.

Stutzmann GE, Smith I, Caccamo A, Oddo S, Parker I & Laferla F 2006b. Enhanced ryanodine-mediated calcium release in mutant PS1-expressing Alzheimer's mouse models. *Meeting on Imaging and the Aging Brain.* New York, NY, USA: New York Academy of Sciences.

Sun H-S, Feng Z-P, Miki T, Seino S & French RJ (2006). Enhanced neuronal damage after ischemic insults in mice lacking $K_{ir}6.2$-containing atp-sensitive K^+ channels. J. Neurophysiol., 95**,** 2590 - 2601.

Supnet C, Grant J, Kong H, Westaway D & Mayne M (2006). Amyloid-β-(1-42) increases ryanodine receptor-3 expression and function in neurons of TgCRND8 mice. The Journal of Biological Chemistry, 281**,** 38440 - 38447.

Szewczyk A, Kajma A, Malinska D, Wrzosek A, Bednarczyk P, Zablocka B, *et al.* (2010). Pharmacology of mitochondrial potassium channels: Dark side of the field. FEBS Lett., 584**,** 2063 - 2069.

Tieu K, Zuo DM & Yu PH (1999). Differential effects of staurosporine and retinoic acid on the vulnerability of the SH-SY5Y neuroblastoma cells: Involvement of Bcl-2 and P53 proteins. J. Neurosci. Res., 58**,** 426 - 435.

Tilgen N, Zorzato F, Halliger-Keller B, Muntoni F, Sewry C, Palmucci LM, *et al.* (2001). Identification of four novel mutations in the C-terminal membrane spanning domain of the ryanodine receptor 1: Association with central core disease and alteration of calcium homeostasis. Hum. Mol. Genet., 10**,** 2879 -

2887.

Tokuhiro S, Tomita T, Iwata H, Kosaka T, Saido TC, Maruyama K, *et al.* (1998). The presenilin 1 mutation (M146V) linked to familial Alzheimer's disease attenuates the neuronal differentiation of NTERA 2 cells. Biochem. Biophys. Res. Commun., 244**,** 751 - 755.

Torp R, Head E, Milgram NW, Hahn F, Ottersen OP & Cotman CW (2000). Ultrastructural evidence of fibrillar β-amyloid associated with neuronal membranes in behaviorally characterized aged dog brains. Neuroscience, 96**,** 495 - 506.

Tu H, Nelson O, Bezproavanny A, Wang Z, Lee S-F, Hao Y-H, *et al.* (2006). Presenilins form ER Ca^{2+} leak channels, a function disrupted by familial Alzheimer's disease-linked mutations. Cell, 126**,** 981 - 993.

Tweedie D, Brossi A, Chen D, Ge Y-W, Bailey J, Yu Q-S, *et al.* (2006). Neurien, an acetylcholine autolysis product, elevates secreted amyloid-β protein precursor and amyloid-β peptide levels, and lowers neuronal cell viability in culture: A role in Alzheimer's disease. J. Alzheimer's Dis., 10**,** 9 - 16.

Ueda T, Nagata M, Monji A, Yoshida I, Tashiro N & Imoto T (2002). Effect of sucrose on formation of the β-amyloid fibrils and D-aspartic acids in $A\beta_{1-42}$. Biol. Pharm. Bull., 25**,** 375 - 378.

Usachev Y, Shmigol A, Pronchuk N, Kostyuk P & Verkhratsky A (1993). Caffeine-induced calcium release from internal stores in cultured rat sensory neurons. Neuroscience, 57**,** 845 - 859.

Vanterpool CK, Vanterpool EA, Pearce WJ & Buchholz JN (2006). Advancing age alters the expression of the ryanodine receptor 3 isoform in adult rat superior cervical ganglia. J. Appl. Physiol., 101**,** 392 - 400.

Vaucher E, Aumont N, Pearson D, Rowe W, Poirier J & Kar S (2001). Amyloid beta peptide levels and its effects on hippocampal acetylcholine release in aged, cognitively-impaired and -unimpaired rats. J. Chem. Neuroanat., 21**,** 323-329.

Wang G & Lemos JR (1995). Tetrandrine: A new ligand to block voltage-dependent Ca^{2+} and Ca^{2+}-activated K^{+} channels. Life Sci., 56**,** 295 - 306.

Wang G, Lemos JR & Iadecola C (2004). Herbal alkaloid tetrandrine: From an ion channel blocker to inhibitor of tumor proliferation. Trends Pharmacol. Sci., 25**,** 120 - 123.

Wang HY, Lee DHS, D'andrea MR, Peterson PA, Shank RP & Reitz AB (2000). Beta-amyloid(1-42) binds to alpha 7 nicotinic acetylcholine receptor with high

affinity - implications for Alzheimer's disease pathology. J. Biol. Chem., 275**,** 5626-5632.

Wang Y-H, Zheng H-Y, Qin N-L, Yu S-B & Liu S-Y (2007). Involvement of atp-sensitive potassium channels in proliferation and differentiation of rat preadipocytes. Acta Physiologica Sinica, 59**,** 8 - 12.

Waters MF, Minassian NA, Stevanin G, Figueroa KP, Bannister JPA, Nolte D, *et al.* (2006). Mutations in voltage-gated potassium channel KCNC3 cause degenerative and developmental central nervous system phenotypes. Nat. Genet., 38**,** 447 - 451.

Wulff H & Zhorov BS (2008). K^+ channel modulators for the treatment of neurological disorders and autoimmune diseases. Chem. Rev., 108**,** 1744 - 1773.

Xu WH, Liu YG, Wang S, Mcdonald T, Van Eyk JE, Sidor A, *et al.* (2002). Cytoprotective role of Ca^{2+}-activated K^+ channels in the cardiac inner mitochondrial membrane. Science, 298**,** 1029-1033.

Yamada K & Inagaki N (2005). Neuroprotection by K_{ATP} channels. J. Mol. Cell. Cardiol., 38**,** 945 - 949.

Yamada K, Ji JJ, Yuan H, Miki T, Sato S, Horimoto N, *et al.* (2001). Protective role of ATP-sensitive potassium channels in hypoxia-induced generalized seizure. Science, 292**,** 1543 - 1546.

Yamaguchi N, Xu L, Evans EE, Pasek DA & Meissner G (2004). Different regions in skeletal and cardiac muscle ryanodine receptor are involved in transducting the functional effects of calmodulin. The Journal of Biological Chemistry, 279**,** 36433 - 36439.

Yao Z-X, Han Z, Xu J, Greeson J, Lecanu L & Papadopoulos V (2007). 22R-hydroxycholesterol induces differentiation of human NT2 precursor (NTERA2/D1 teratocarcinoma) cells. Neuroscience, 148**,** 441 - 453.

Yu SP, Farhangrazi ZS, Ying HS, Yeh C-H & Choi DW (1998). Enhancement of outward potassium current may participate in β-amyloid peptide-induced cortical neuronal death. Neurobiol. Dis., 5**,** 81 - 88.

Yu SP, Yeh CH, Sensi SL, Gwag BJ, Canzoniero LMT, Farhangrazi ZS, *et al.* (1997). Mediation of neuronal apoptosis by enhancement of outward potassium current. Science, 278**,** 114-117.

Zahradníková A & Palade P (1993). Procaine effects on single sarcoplasmic reticulum Ca^{2+} release channels. Biophys. J., 64**,** 991 - 1003.

Zhang W, Jin H-W & Wang X-L (2004). Effects of presenilins and β-amyloid precursor protein on delayed rectifier potassium channels in cultured rat hippocampal neurons. Acta Pharmacol. Sin., 25**,** 181 - 185.

Zhu X, Zhou W, Cui Y, Zhu L, Li J, Xia Z, *et al.* (2009). Muscarinic activation attenuates abnormal processing of β-amyloid precursor protein induced by cobalt chloride-mimetic hypoxia in retinal ganglion cells. Biochem. Biophys. Res. Commun., 384**,** 110 - 113.

Acknowledgements

By the end of my PhD, it is my pleasure to acknowledge all those people who have provided me with support and encouragement during these four years.

Firstly my supervisors. Prof. Kenneth T. Wann has supported me very much on my research planning, results analysis, thesis writing and attendance in both internal and international conference presentations. And, Prof. Wann always encourages me to generate my idea and to try my idea in experiments. That has not only improved my understanding of the research topic I am working on, but also enhanced my research skills and abilities which I believe will benefit my future career a lot. In addition, I very much appreciate the support from Prof. Wann, as well as my other supervisor Prof. Gary F. Baxter, the Head of school, foy my living costs in my final year and funding applications.

Secondly, I much appreciate the sources of funding. Particularly, my family, Prof. Zhang Cheng-Zhi and Prof. Wang Ai-Qin, have supported my tuition fee and bench fee for three years, as well as some living costs, which is something more than £60,000 in total. I know it is unusual, in acknowledgement, to put funding or family before any other help from colleagues, but I believe everybody that may have some ideas of the average salary for a Professor in China will absolutely acknowledge their unvaluable support and forgive me my preference for this acknowledgement priority. That support, as well as all of their encouragement, has shown their love for me; I would like to say that

nothing is possible in this PhD without that. Besides, I also thank the funding from Great Britain – China Centre (£4,000) and Henry Lester Trust (£2,500).

Thirdly, I much appreciate all the help from my colleagues in Cardiff University. My thanks to Dr. Dwaine Burley, Dr. Neil C. Henney, Dr. Pablo Reviriego, Mr. Charles D. Cox and Miss Nassrin Vassel in my lab for their demonstration of experimental techniques and suggestions on my research, especially when I was sometimes puzzled. I also thank Dr. Bronwen Evans in the School of Medicine, Dr. Rhian Thomas and the Tenovas group in School of Pharmacy and Pharmaceutical Sciences for their kind offer of their research facilities, as well as the discussion of relevant data, to support my research. In addition, I thank all the Erasmus students and project students who worked with me, including Miss. Elisabetta Asson, Miss Jasmin Nowak, Miss Marwa Khudheyer, Miss Emily Knight and Mr. Mohamedameer Pirmohamed, for their efforts in research and their ideas which have inspired me several times. I also thank all the administrative staff in this school, especially Mrs. Lynne Terrett, Mrs. Sarah Davis and Mrs. Wendy Davies, for their kind help which has guranteed a good research environment in the school.

Last but not least, I also much appreciate the other colleagues and friends in the department, the school and all over the university. I am very glad for having shared 4 years of a happy time, which is fortunately not only lab work, and that has encouraged me to hold a positive attitude and being sunshine into both my research and life.